ROBUST CAPILLARY ELECTROPHORESIS METHODS FOR BIOMARKER DISCOVERY AND ROUTINE MEASUREMENTS IN CLINICAL AND EPIDEMIOLOGICAL APPLICATIONS

ROBUST CAPILLARY ELECTROPHORESIS METHODS FOR BIOMARKER DISCOVERY AND ROUTINE MEASUREMENTS IN CLINICAL AND EPIDEMIOLOGICAL APPLICATIONS

By ADRIANA NORI DE MACEDO, M.Sc.

A Thesis Submitted to the School of Graduate Studies in Partial Fulfilment of the Requirements for the Degree

Doctor of Philosophy

March 2017

DOCTOR OF PHILOSOPHY (2017) McMaster University

(Chemistry and Chemical Biology) Hamilton, ON

TITLE: Robust capillary electrophoresis methods for biomarker discovery and routine measurements in clinical and epidemiological applications

AUTHOR: Adriana Nori de Macedo, M.Sc. (University of São Paulo)

SUPERVISOR: Professor Dr. Philip Britz-McKibbin

PAGES: xx, 208

Abstract

Biochemical markers (*i.e.*, biomarkers) are of key importance to guide clinical decisions and public health policies by enabling early detection, accurate diagnosis and/or prevention of human diseases. However, major challenges remain due to the limited clinical utility of many biomarkers and the lack of robust analytical methods for their reliable measurements in a routine clinical setting that is also suitable to large-scale epidemiological studies. This thesis includes two major research themes involving the analysis of known biomarkers that lack appropriate methods, and the discovery of new biomarkers for complex disease conditions. In particular, this thesis describes the (1) development and validation of robust analytical methods based on capillary electrophoresis (CE) with photometric detection for the measurement of inorganic anions in volume-restricted biofluids; and (2) characterization of the sweat metabolome in infants and identification of sweat biomarkers in asymptomatic cystic fibrosis (CF) infants using multisegment injection-capillary electrophoresis-mass spectrometry (MSI-CE-MS). *Chapter II* introduces a simple CE assay that is remarkably selective for the analysis of sulfate, sulfite and chloride, which was applied in a pilot study to investigate the role of urinary sulfate as a biomarker for kidney stone risk assessment in children. *Chapter III* introduces a novel CE method for assessing iodine nutrition, which is followed by an inter-method comparison with inductively coupled plasma-mass spectrometry as described in *Chapter IV*. This led to the development of a fully validated CE method for monitoring the prevalence of iodine deficiency on a population level as required for global health initiatives. *Chapter V* demonstrates that more than 64 endogenous and exogenous compounds are present in the sweat of screen-positive CF infants, including a panel of differentiating metabolites that are associated with CF status, as well as treatment responsivity to nutritional and/or drug intervention. In summary, this thesis has contributed novel analytical methods suitable for routine biomarker analysis, in addition to the first non-targeted characterization of the sweat metabolome from infants, which require further studies to evaluate their clinical utility as biomarkers that allow for improved diagnosis, prognosis and treatment monitoring of the highly variable CF disease spectrum.

Acknowledgements

First, I would like to express my deepest gratitude to my supervisor, Dr. Philip Britz-McKibbin, for giving me the opportunity to be part of his group and for his continuous support and motivation during my Ph.D. studies. His guidance, patience and optimism were essential to overcome the problems along the way and make me see the importance of taking one step at a time. I really appreciate his time, ideas, and attention in numerous discussions that have made this Ph.D. productive and gratifying. I also would like to thank my committee members Dr. Giuseppe Melacini and Dr. Stephen Hill for their feedback, suggestions and encouragement during my committee meetings, including the hard questions that helped me realize what I needed to study more.

The Britz's group has been an immense source of collaborative work, good advice and friendship. I am extremely grateful for the fun and enjoyable working environment created by my past and current labmates: Meera Shanmuganathan, Nadine Wellington, Alicia DiBattista, Karen Lam, Naomi Kuehnbaum, Michelle Saoi, Mai Yamamoto, Stellena Mathiaparanam, Ritchie Ly, Sandy Azab and Jennifer Wild, including also several undergraduate thesis and summer students.

I sincerely thank all the collaborators involved in the studies described in this thesis for their time and precious advice. In especial, I thank Dr. Joseph Macri for the generous donation of a CE instrument used in most of my experiments, and for his crucial contribution in the iodine inter-laboratory method comparison. Additionally, this work would not have been possible without the precious help from Dr. Stephen Hill, who contributed so many aspects, from submitting REB applications to coordinating meetings and samples storage, de-identification, and compilation of patient information together with Lauren Brick and Dr. Linda Pedder. I also want to acknowledge the collaboration of Dr. Tanja Gonska and Katherine Keenan, who provided sweat samples from Sick Kids, as well as Dr. Andrew Mente, who introduced me to SPSS and some basic concepts of statistics applied to epidemiology. I also gratefully acknowledge funding support from the Province of Ontario that provided me an Ontario Trillium Scholarship for 4 years.

My time at McMaster was more enjoyable by the presence of my friends and roommates, who became my family away from home. I am grateful for the time spent together, for the trips around the city, bike ridings, dinners, and long conversations that enriched my experience in Canada and resulted in memorable moments and friendships that I will cherish for the rest of my life.

I also would like to thank three especial mentors who have greatly inspired my professional decisions: Marta Santos, my high school Chemistry teacher, who gave me essential support when going to university; Dr. Silvia H. G. Brondi, my undergraduate supervisor, who first introduced me to the research in separation science; and Dr. Eny M. Vieira, my Master's supervisor, a dedicated instructor who has markedly shaped my view of university education. I really appreciate their continuous mentorship that has lasted many years and contributed to my excitement for research and teaching. In addition, I want to thank Dr. Emanuel Carrilho for his help when trying to find a graduate supervisor abroad. Even without knowing me well, he gave me invaluable advice and also introduced me to Dr. Philip Britz-McKibbin.

Lastly, I am sincerely grateful to my parents and sisters for their endless love and encouragement that are so important to me. I also thank my boyfriend of almost a decade, and now fiancé, Thiago for his continuous support and for always being by my side, making my life happier and long distances shorter. Most of all, I thank God for all the conditions to complete this work, for giving me focus, perseverance and for so many important people around me who immensely contributed to this pursuit.

Table of Contents

List of Figures

Supporting Figures

List of Tables

Supporting Tables

List of Abbreviations and Symbols

$[M+H]^+$	Protonated molecule
$[M-H]^-$	Deprotonated molecule
μ_A	Electrophoretic mobility of the analyte
$\mu_{ep,AC}$	Electrophorectic mobility of the complex (iodide:α-CD)
μ_{LE}	Electrophoretic mobility of the leading electrolyte
μ_{TE}	Electrophoretic mobility of the terminating electrolyte
^{129}I	Iodine isotope with atomic mass 129
^{130}Te	Tellurium isotope with atomic mass 130
^{187}Re	Rhenium isotope with atomic mass 187
^{1}H-NMR	Proton nuclear magnetic resonance
AgI	Silver iodide
ANN	Artificial neural networks
Arg	*L*-Arginine
As(III)	Arsenic III
Asn	*L*-Asparagine
AUC	Area under the curve
BALF	Brochoalveolar lavage fluid
BGE	Background electrolyte
BMI	Body mass index
C	Concentration of ligand (α-CD)
CDC	Centers for Disease Control and Prevention
CE	Capillary electrophoresis
Ce(III)	Cerium III
Ce(IV)	Cerium IV
CE-MS	Capillary electrophoresis-mass spectrometry
CE-UV	Capillary electrophoresis with UV detection
CF	Cystic fibrosis
CF-SPID	Cystic fibrosis positive inconclusive diagnosis

CFTR	Cystic fibrosis transmembrane conductance regulator
CI	Confidence interval
CLSI	Clinical and Laboratory Standards Institute
Cl-Tyr	3-Chloro-*L*-tyrosine
CMS	Centers for Medicare and Medicaid Services
CV	Coefficient of variance
DEHP	Bis(2-ethylhexyl) phthalate
DI-MS	Direct injection-mass spectrometry
EDR	Extended dynamic range
EDTA	Ethylenediaminetetraacetic acid
EIE	Extracted ion electropherogram
EI-MS	Electron impact ionization-mass spectrometry
EMA	European Medicines Agency
EOF	Electroosmotic flow
EQUIP	Ensuring the Quality of Iodine Procedures
ESI	Electrospray ionization
ESI-MS	Electrospray ionization-mass spectrometry
ESI-MS/MS	Electrospray ionization-tandem mass spectrometry
FA	Formic acid
FDA	Food and Drug Administration
FDR	False discovery rate
FEV_1	Forced expiratory volume in 1 second
FVC	Forced expiratory vital capacity
GC	Gas chromatography
GC-MS	Gas chromatography-mass spectrometry
Gln	*L*-Glutamine
Gly-His	Glycylhistidine
HHS	Department of Health and Human Services
Hi Res	High resolution

HILIC	Hydrophilic interaction liquid chromatography
I_0	Current for BGE without ligand (α-CD)
ICP-MS	Inductively coupled plasma-mass spectrometry
ICP-MS	Inductively coupled plasma-mass spectrometry
IDD	Iodine deficiency disorder
I_i	Current for BGE with *i* concentration of ligand (α-CD)
IQR	Interquartile range
IRT	Immunoreactive trypsinogen
IUPAC	International Union of Pure and Applied Chemistry
K_b	Binding constant
KNN	k-Nearest neighbor
LC	Liquid chromatography
LC-MS	Liquid chromatography-mass spectrometry
LC-MS/MS	Liquid chromatography-tandem mass spectrometry
LE	Leading electrolyte
LOD	Limit of detection
LOQ	Limit of quantification
m/z	Mass-to-charge ratio
MEHP	Mono(2-ethylhexyl)phthalic acid
MFE	Molecular Feature Extractor
MS	Mass spectrometry
MS/MS	Tandem mass spectrometry
MSI-CE-MS	Multisegment injection-capillary electrophoresis-mass spectrometry
MT	Migration time
NBS	Newborn screening
ND	Not detected
NDS	1,5-Naphthalene disulfonate
NHANES	US National Health and Nutrition Examination Survey
NIH	National Institutes of Health

NIST	National Institute of Standards and Technology
NMS	2-Naphthalenesulfonate
NSO	Newborn Screening Ontario
NTS	1,3(6,7)-Naphthalene trisulfonate
OPLS-DA	Orthogonal partial least squares-discriminant analysis
PA	Pilocarpic acid
PALCAN	Program of Accreditation of Laboratories
PCA	Principal component analysis
Phe	*L*-Phenylalanine
PKU	Phenylketonuria
PLS-DA	Partial least squares-discriminant analysis
POC	Point-of-care
PON	Paraoxonase
PQN	Probabilistic quotient normalization
PURE	Prospective Urban and Rural Epidemiological
PVC	Polyvinyl chloride
QC	Quality control
QTOF	Quadrupole time-of-flight
R^2	Coefficient of determination
RF	Random forest
RMT	Relative migration time
ROC	Receiver-operating characteristic
RPA	Relative peak area
R_S	Resolution
RSD	Relative standard deviation
RT	Retention time
S/N	Signal-to-noise ratio
SD	Standard deviation
S-K	Sandell-Kolthoff

SRM	Standard reference material
$t_{1/2}$	Half-life
T4	*L*-Thyroxine
TE	Terminating electrolyte
tITP	Transient isotachophoresis
TMAO	Trimethylamine *N*-oxide
TriHOME	Trihydroxyoctadecenoic acid
Tyr	*L*-Tyrosine
UPLC-MS	Ultra-performance liquid chromatography-mass spectrometry
WHO	World Health Organization
α-CD	α-Cyclodextrin
Σ%RE	Percentage relative error
$\nu\mu_{ep,A}$	Viscosity-corrected apparent electrophoretic mobility of analytes
$\nu\mu_i$	Viscosity-corrected electrophoretic mobility of analytes

Declaration of Academic Achievement

The following material has been previously published and is reprinted with written permission:

Chapter II. Reprinted and adapted from Macedo, A. N.; Jiwa, M. I. Y.; Macri, J.; Belostotsky, V.; Hill, S.; Britz-McKibbin, P. Strong Anion Determination in Biological Fluids by Capillary Electrophoresis for Clinical Diagnosis. *Anal. Chem.* **85**, 11112-11120, 2013. Copyright (2013) American Chemical Society.

Chapter III. Reprinted and adapted from Macedo, A. N.; Teo, K.; Mente, A.; McQueen, M. J.; Zeidler, J.; Poirier, P.; Lear, S. A.; Wielgosz, A.; Britz-McKibiin, P. A Robust Method for Iodine Status Determination in Epidemiological Studies by Capillary Electrophoresis. *Anal. Chem.* **86**, 10010-10015, 2014. Copyright (2014) American Chemical Society.

The following material has been accepted for publication:

Chapter IV. Macedo, A. N.; Macri, J.; Macri, J.; Hudecki, P.; Saoi, M.; McQueen, M. J.; Britz-McKibbin, P. Validation of a Capillary Electrophoresis Assay for Monitoring Iodine Nutrition in Populations for Prevention of Iodine Deficiency: An Inter-Laboratory Method Comparison. JALM, 2016, American Association for Clinical Chemistry.

Chapter I

Introduction to Biomarker Discovery and Biomarker Measurements for Clinical Medicine

Chapter I: Introduction to Biomarker Discovery and Biomarker Measurements for Clinical Medicine

1.1 Introduction to biomarkers in clinical medicine

The term biochemical marker or "biomarker" first appeared in the literature about 40 years ago with the advent of molecular biology and genomics/proteomics research.[1] However, the use of biomarkers to determine health conditions that are not clearly discernible based on symptoms alone has been associated with medical practice across diverse cultures throughout history.[2] For instance, in the fourth century BC, Hippocrates looked for bubbles on the surface of fresh urine as an indicator of kidney problems, which is now known to be associated with proteins in urine (*i.e.*, proteinuria) that stabilize bubbles by reducing surface tension at the water-air interface.[3] Ancient physicians also related urine sweetness (determined by noting specimens that attracted ants or even by taste testing) to the occurrence of a disease that was later named diabetes mellitus.[4] Those and other apparent bulk properties of urine (*e.g.*, colour, smell, volume) were commonly used in ancient and medieval times,[4] although diagnostic information in this case was not always reliable, resulting in biased interpretation and abusive practice of urinalysis for profit, as highlighted by Thomas Brian in his book "Pisse Prophet", published in 1637.[3] The recognition that simple characterization of the physical appearance of biological fluids was inadequate for reliable diagnostics lead to a slow transition towards more detailed chemical analysis of the composition of human biological specimens over the next centuries.[5] In modern medicine, biomarkers are objectively quantified by analytical techniques and instrumental methods available in clinical laboratories that provide adequate selectivity, sensitivity and robustness for reliable measurements. According to the National Institutes of Health (NIH) Biomarkers Definitions Workgroup, a biomarker is defined as "a characteristic that is objectively measured and evaluated as an indicator of normal biological processes, pathogenic processes, or pharmacologic

responses to a therapeutic intervention".[6] The International Programme on Chemical Safety, a joint effort of the World Health Organization (WHO), United Nations, and the International Labour Organization, defined a biomarker as "any substance, structure, or process that can be measured in the body or its products and influence or predict the incidence of outcome or disease".[7] Other definitions also define indicators of environmental exposure and dietary intake under the concept of biomarkers.[8,9]

Indeed, the majority of common clinical tests used in modern medicine are based on biomarkers, including physiological measures (*e.g.*, blood pressure) and, increasingly, molecular compounds in biological fluids (*e.g.*, fasting plasma glucose).[10] Biochemical biomarkers include DNA, RNA, proteins, metabolites, electrolytes, and any substances present in biological fluids, tissues or cells, which are measured using specialized instrumentation in clinical laboratories, and point-of-care (POC) devices for routine testing at home.[1,11] Biomarkers can be used for a variety of clinical applications as described in **Table 1.1**. For instance, 24 h urine testing is commonly used to diagnose probable pathogenic causes of recurrent kidney stones. In this case, urine volume, pH, uric acid, calcium, phosphate, oxalate and other ions are evaluated in combination and compared to their reference levels within a healthy population. This is done in order to guide dietary recommendations and treatment options which are dependent on the knowledge of the chemical composition of kidney stone.[12] Another example comes from universal newborn screening (NBS) programs, which enable early diagnosis of rare yet treatable genetic diseases. Although symptoms are often absent at birth, diseases included in NBS can lead to sudden death or serious lifelong morbidities (*i.e.*, cognitive impairment) if not treated within the first weeks of life.[13] In the province of Ontario, newborns are currently screened for 29 diseases using dried blood spot samples collected from a heel prick a few days after birth.[13] For instance, early diagnosis of phenylketonuria (PKU) in NBS using

Table 1.1. Common roles of biomarkers in medicine. Adapted from Puntmann.[10]

Role	Description	Example
Antecedent	Identifying the risk of developing a disease	High blood pressure as a risk factors for cardiovascular disease[14]
Screening	Screening for subclinical diseases (*i.e.*, no apparent symptoms)	Elevated phenylalanine in dried blood spot samples from newborn screening as an indicator of phenylketonuria[15]
Diagnostic	Recognizing overt diseases	Elevated fasting plasma glucose or 2 h plasma glucose after oral glucose load for diagnosis of diabetes[16]
Staging / stratifying	Categorizing disease severity/development stage	Expression of hormone receptors, protein HER2 and antigen Ki67 in breast cancer cells for disease classification[17]
Prognostic	Predicting future disease development and/or response to treatment	Level of serum CA125 antigen to predict survival after chemotherapy for advanced stages of ovarian cancer[18]

L-phenylalanine (Phe) or the *L*-phenylalanine to *L*-tyrosine ratio (Phe/Tyr) as biomarker(s) can prevent severe and permanent brain damage by early intervention with a phenylalanine-restricted diet in conjunction with tetrahydrobiopterin therapy.[19]

Independent of its clinical context, in order to be useful for medical applications, a biomarker must: (1) demonstrate a significant association to a clinical outcome or disease; (2) be present in biological specimens (*e.g.*, urine, blood, saliva, feces etc.), which can be easily collected without invasive interventions; and (3) be reliably analyzed by a rapid, simple, accurate, robust yet cost-effective analytical method suitable for laboratory medicine.[1] Thousands of publications about biomarkers have been reported in the literature in the last few

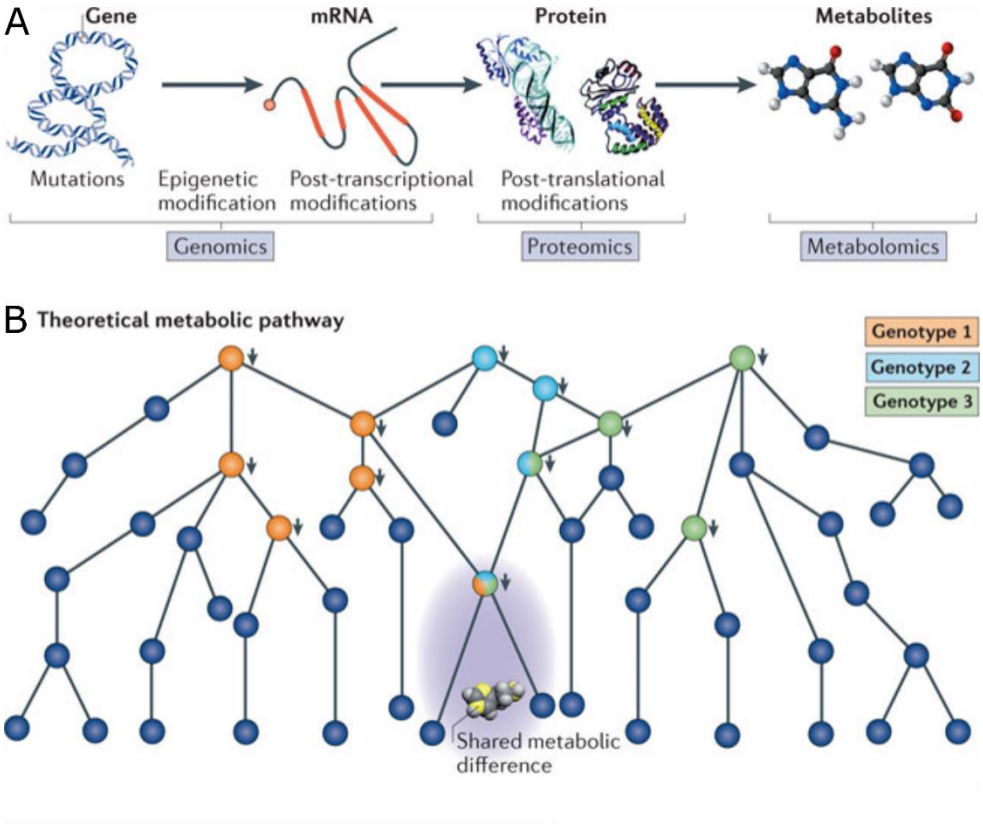

Figure 1.1. The "-omics" cascade and a scheme of a theoretical metabolic pathway. **(A)** Genes are susceptible to regulatory epigenetic processes, whereas RNAs and proteins are subject to post-translational modifications. In contrast, metabolites are downstream biochemical products that reflect epigenetic and post-translational modifications, representing more closely the phenotype. **(B)** Enzymes that are affected by different genotypes can produce a cascade of alterations in metabolites and metabolic pathways, including common metabolites that are altered by multiple genotypes and may be associated to phenotype perturbations not always apparent based on genomics or proteomics alone.[20]

decades. These high numbers are related to advances in analytical instrumentation and bioinformatics applied in untargeted "-omics" approaches for biomarker discovery, including genomics, transcriptomics, proteomics and metabolomics (**Figure 1.1**). Indeed, new biomarkers can offer invaluable information to guide clinical decisions, improve individual patient and/or population health outcomes, while also providing new insights into underlying disease mechanisms.[21] However, only a limited number of biomarker candidates have been translated

from "-omics" technologies into clinical practice.[22,23] This is mainly due to major obstacles associated with replication of pilot studies that are prone to false discoveries, as well as the lengthy and rigorous processes needed for biomarker validation/qualification, and challenges related to implementing robust analytical platforms for reliable analysis of new biomarkers within a clinical laboratory setting.[21,24] In fact, the overwhelming majority of candidate biomarkers reported in the literature often lack statistical power without adequate validation in follow-up studies among different cohorts to confirm their suitability for clinical practice, which has led to major criticism of biomarker research.[25–27] Nevertheless, the potential utility of biomarkers in clinical medicine is well-recognized and recent efforts have been made to improve the scientific research quality, including recommendations related to study design,[28,29] standards for reporting results,[30,31] and required phases for biomarker development.[32] Additionally, growing interest in biomarker discovery has expanded with the advent of precision (or personalized) medicine,[33–35] which aims to combine clinical data (*e.g.*, symptoms, histology, medical history) to biomarker measurements on a population level. This is being done in order to support the development of more customized and efficacious treatments for individual patients while reducing adverse effects with emphasis on chronic disease prevention.[33]

1.2 Phases and challenges of biomarker discovery in metabolomics

Traditionally, biomarkers have been discovered by means of clinical observations or insights into disease pathophysiology that inspired subsequent hypothesis-driven studies.[10] For instance, the sweat chloride test, which represents the current gold standard for cystic fibrosis (CF) diagnosis, was originally developed after Dorothy H. Andersen observed several CF patients with heat prostration *(i.e.,* hyperthermia) during the particularly intense summer of 1949.[36] Working with Andersen, Paul di Sant'Agnese hypothesized and demonstrated that severe

dehydration and salt loss were related to the problem.[37] Their observations were replicated by other groups in the following years and resulted in the introduction of sweat chloride as a diagnostic test for CF a decade later. This test has remained in practice since then[38] despite the discovery that mutations in the CF transmembrane regulator (*CFTR*) gene are the primary cause of CF.[39] Another example of traditional biomarker discovery can be seen with the introduction of population-based screening of PKU. The disease was first reported in 1934 by Dr. Asbjorn Folling, after a mother insistently asked for an explanation in the case of her two mentally disabled children. At a time when there was no clinical laboratory in the hospital, Dr. Folling used his previous training in classical chemistry to investigate an unusual substance present in the children's urine, which was subsequently identified as phenylpyruvic acid, a by-product of Phe metabolism. In follow-up collaborative experiments, he found that a group of patients with the same symptoms had very high levels of blood Phe.[40] Horst Bickel and colleagues later reported that PKU patients can be successfully treated using a low Phe diet, which was more effective if affected individuals were identified early in life.[41] The introduction of a simple bacterial inhibition assay for Phe in dried blood spots collected on filter cards in 1963 by Robert Guthrie and Ada Susi[42] revolutionized clinical medicine by introducing a practical means for population-based screening of neonates for pre-symptomatic diagnosis and early treatment of PKU. This was later adapted to other in-born errors of metabolism, such as maple syrup urine disease and galactosemia.[43] Nowadays, with the development of "-omics" approaches that allow the identification of putative biomarkers of human diseases among hundreds or even thousands of molecular features (*e.g.*, genes, proteins, metabolites) measurable in biological specimens, biomarkers have increasingly become independent of previous clinical observations or knowledge about their biological role in specific health conditions. This has given rise to an era of data-driven, hypothesis-generating biomarker research.[10]

Metabolites are a chemically diverse class of small molecules or ions (< 1500 Da) present in the body as by-products of host metabolism and precursors to biopolymer synthesis (*e.g.*, nucleotides, sugars, amino acids, peptides, organic acids, lipids, electrolytes) and also derived from exogenous sources, including diet, drugs, gut microbiome and lifelong environmental exposures.[44,45] Considered as "direct signatures of biochemical activity",[20] metabolites can provide valuable information for understanding biological systems since biochemical changes are closely associated with phenotype and importantly clinical outcomes (**Figure 1.1**).[20,44] Metabolomics is a field dedicated to the comprehensive and untargeted characterization of metabolites in biological samples, including biofluids, tissues and cells,[20] which offers a promising approach for the discovery of new biomarkers related to aberrant metabolic pathways that may also provide new insights into the underlying mechanisms of disease pathogenesis.[46] For example, Wang *et al.*[47] used metabolomics to identify five branched-chain and aromatic amino acids (*i.e.*, leucine, isoleucine, valine, phenylalanine and tyrosine) in fasting plasma as predictive biomarkers associated with increased risk for type 2 diabetes up to 12 years *before* disease occurrence. As a result, elevated levels of these circulating amino acids can help to identify individuals at risk for diabetes much earlier than hyperglycemia or changes in insulin sensitivity, allowing timely interventions for delaying or preventing disease onset. Additionally, their results helped to support previous findings indicating the role of some amino acids as essential nutrients that serve as biochemical modulators of insulin secretion.[47] Similarly, Wang *et al.*[48] used metabolomics to identify trimethylamine *N*-oxide (TMAO) as a plasma biomarker to predict risk for atherosclerosis and cardiovascular disease, which is derived from dietary phospholipid intake in association with gut microflora activity and host liver metabolism. In this case, TMAO provides a novel "meta-organismal" pathway that links the effects of diet and gut microflora on cardiovascular disease risk that is independent of insulin resistance and other conventional risk factors (*e.g.*, obesity), including insights

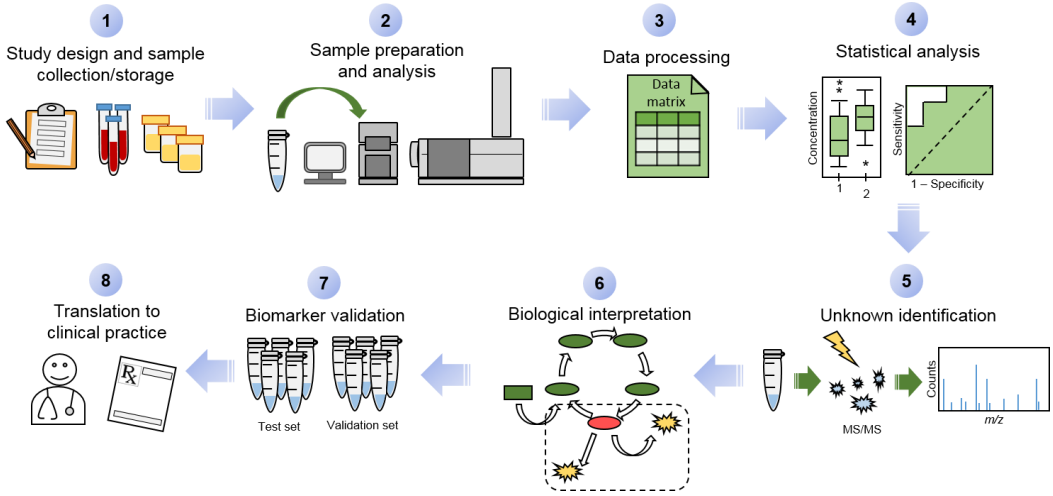

Figure 1.2. Scheme depicting the major steps and data workflow involved in the process of biomarker discovery in clinical medicine when using MS-based metabolomic studies.

into potential lifestyle modifications for chronic disease prevention using probiotics.[48]

Establishing robust associations between metabolites and disease states constitutes a lengthy and multi-step process that is prone to bias,[49,50] as shown in **Figure 1.2**, which summarizes the basic workflow involved in biomarker discovery by metabolomics. Untargeted metabolomics aims to characterize as many metabolites as possible, in contrast to targeted metabolomics (*i.e.*, metabolite profiling), which the focus is on selected metabolites belonging to specific classes or known pathways.[20] In terms of the workflow for biomarker discovery, untargeted mass spectrometry (MS)-based metabolomics has an extra step related to the identification of the chemical structure of unknown compounds that is required for interpreting the biological significance of the biomarker from a differentiating molecular feature. Major challenges present within each step have hindered the translation of potential biomarkers into clinical applications, including improper standardization of sample collection and storage conditions,

lack of quality controls for assessing instrumental drift, poor study designs and inadequate statistical power, and lack of follow-up validation that is replicated within an independent cohort and representative population.[51] Although researchers can not always avoid all these problems, there are recommendations to minimize their contribution to study bias thereby reducing false discoveries such that putative biomarker(s) will proceed to the next phases of clinical translation.[52] In fact, even pilot studies with limited external validation can be perfectly suitable to establish "proof-of-principle" if well-designed and conducted to provide adequate foundation to subsequent larger-scale studies.[28]

1.2.1 Study design and sample collection/storage

Study design in metabolomics follows the same basic principles as other medical and epidemiological research fields.[53] In many cases, two or more groups are compared (*e.g.*, healthy *vs.* disease, treatment *vs.* placebo) in order to identify differentiating metabolites. When designing studies, it is important to avoid unbalanced characteristics (*e.g.*, sex, age, ethnicity), which can cause bias due to confounding factors that require adjustment.[28] In addition, an adequate sample size helps to avoid false negatives attributed to low statistical power. In reality, researchers do not always have complete control over the study design, due to limited resources and time, studies involving rare diseases or invasive sample collection procedures.[53] Power calculation may also be challenging, especially in untargeted metabolomics, when the number of authentic metabolites is still unknown.[45] In this case, it is recommended to clearly report the study limitations and their possible impact on the results.[28] Other pre-analytical variables, including sample collection, handling and storage have major impact on downstream analysis.[54] For example, blood plasma or serum is often used in metabolomics due to homeostatic control that results in less biological variability in healthy individuals, compared to urine, for example.[55] However, the choice of blood collection tube, fasting state, time of collection, processing time, and storage

conditions can affect the reliability of the results.[56,57] For instance, blood collection tubes can introduce interference from the rubber stoppers, stopper lubricants, anticoagulants (for plasma), clot activators (for serum), separator gels, and surfactants, which vary depending on the tube supplier.[56] Townsend *et al*.[57] reported median differences of up to 58% for bile acids and vitamins in blood when comparing fasting states, although most metabolites were not considerably affected, with median differences under 15% when analyzing 166 compounds in 423 individuals by liquid chromatography-tandem mass spectrometry (LC-MS/MS). Metabolites that are both chemically stable and subject to less biological variation (*i.e.*, diet, diurnal cycle, sex etc.) yet are associated with early disease pathogenesis represent promising predictive biomarkers for clinical application in the context of preventative medicine. In general, study design and procedures to keep sample integrity should be optimized as much as possible to avoid non-biological variability, a process that should be recorded in detail and reported along with the study results.[58]

1.2.2 Sample preparation and untargeted metabolite profiling

No single analytical platform can achieve full coverage of the metabolome, due to the large number of metabolites, their chemical diversity in terms of physicochemical properties (*e.g.*, polarity, molecular weight, solubility, volatility, stability), as well as concentration ranges that can vary up to 10^9-fold.[50,59] Currently, more than 4,200 metabolites have been annotated in human serum[60] and more than 2,600 have been reported in human urine, which are likely underestimates of the human metabolome due to limitations in sensitivity, dynamic range and resolution.[61] In order to improve metabolome coverage, orthogonal analytical platforms can be applied in parallel, provided that adequate sample volume is available.[60,61] The relative strengths and limitations of the main analytical techniques used in metabolomics are summarized in **Table 1.2**, including nuclear magnetic resonance (^{1}H-NMR), as well as MS techniques often

Table 1.2. Most common analytical platforms used in metabolomics. Adapted from Holmes *et al.*[49] and Wishart.[35]

Platform	Relative strengths	Relative limitations
Nuclear magnetic resonance (NMR)	High reproducibility Non-destructive Minimal reagent use Minimal sample preparation Allow absolute quantification Rapid (10-15 min/sample) High linear dynamic range Wide range of chemical structures and molecular sizes	Relatively insensitive (mitigated by cryoprobes and high magnetic fields) Large sample volume requirement (~500 µL, mitigated by low-volume microprobes requiring ~60 µL) High installation cost Large instrument footprint Overlap of metabolites in 1D spectra (mitigated by ≥2D methods)
Direct infusion mass spectrometry (DI-MS)	Rapid acquisition (1-3 min/sample) High sensitivity No solvents or reagents Allow fragmentation for metabolite identification Low sample volume (5-10 µL)	Issues with specificity and reproducibility Inability to separate isobaric species Challenges with spectral alignment Differential ionization with potential error in quantification (mitigated by stable-isotope labelled internal standards)
Liquid chromatography mass spectrometry (LC-MS)	Simple sample preparation (protein precipitation or dilution) High sensitivity Relatively rapid (1-20 min) Wide range of compounds using appropriate columns	Variations in retention times Incomplete metabolite databases Variations between MS instruments Instrument drift over time (susceptible to batch effect, not very quantitative) Relatively large solvent consumption
Gas chromatography mass spectrometry (GC-MS)	High sensitivity High reproducibility Extensive database available Mature technology Excellent for volatile compounds	Derivatization required in most cases (time-consuming, costly reagents) Environmentally unfriendly solvents Run times relatively long (30-60 min)
Capillary electrophoresis mass spectrometry (CE-MS)	Excellent for polar/ionizable compounds with simple sample workup Low sample volume (~5 µL) Low operating costs	Issues with long term method robustness and limited sensitivity Variations in migration times Metabolite identification databases are not extensive

coupled to various separation methods.[49] Although MS-based metabolomics can be done using direct injection (DI-MS), this approach is susceptible to ion suppression and low specificity due to isobaric/isomeric interferences.[59] These problems can be minimized by coupling MS analysis to high efficiency

separations that improve overall method specificity and MS spectral quality as required for unambiguous metabolite identification, including gas chromatography (GC), liquid chromatography (LC), and capillary electrophoresis (CE).[58]

Sample preparation follows different protocols depending on the biological specimen, class of metabolite being studied (*e.g.*, polar/ionic, non-polar) and the analytical method selected for metabolomics. For example, GC-MS requires a number of steps involving sample deproteinization, extraction and chemical derivatization, whereas LC-MS and CE-MS often require only deproteinization and sample dilution for serum or plasma samples.[62,63] In some cases, the chemical stability of metabolites is dependent on sample workup conditions that affect their recovery, including buffer pH, temperature and/or light exposure. In general, sample preparation for untargeted metabolomics should balance low selectivity to ensure broader metabolite coverage with adequate clean-up to minimize degradation of analytical performance due to other sample matrix components.[50] Simple, rapid and automated procedures are ideal to reduce inadvertent chemical degradation while consuming small amounts of sample notably for volume-limited bio-banked specimens.[50] Batch randomization is also recommended during sample preparation and analysis, as a way to reduce the bias associated with the order of preparation or analysis.[64] MS-based instruments are susceptible to performance variation over time, which is related to the accumulation of sample constituents in the instrument parts or drift in electronic components. This problem can be minimized by routine preventative maintenance, including cleaning instrument components (*e.g.*, electrospray ion source) together with periodic tuning and calibration of the mass analyzer.[64] Instrument drifts can be monitored by analyzing quality control (QC) samples intermittently during analysis of randomized sample batches. A challenge related to untargeted analysis consists in the preparation of truly representative QCs. Ideally, QCs should be prepared as pools of the study samples for each group, in

order to increase the chances that all metabolites detected in the samples would have an associated signal and variability estimate from the QCs. However, when sample volumes are restricted or difficult to homogenize (*e.g.*, tissues, cells), surrogate samples may have to be used instead.[65] The consistent use of QCs throughout an experiment helps to identify changes in instrument response for sample batches analyzed in different points in time. These changes may still occur despite careful instrument maintenance and calibration while working under standard operating protocols.[62] In this case, QC samples can be used to detect batch effects while also applying algorithms for batch correction when comparing data across multiple analytical batches.[66]

1.2.3 Data processing and statistical analysis

Once data acquisition has been completed for randomized batches of samples with the inclusion of appropriate blank and QC runs, a large amount of data needs to be converted into a suitable data matrix for subsequent data analysis. This may include data transformation, pattern recognition or dimensionality reduction in conjunction with various univariate or multivariate statistical analysis methods. Data processing and analysis constitute a major bottleneck in the data workflow for biomarker discovery in MS-based metabolomics.[50,67] In general, MS-based raw data requires the use of an initial sequence of operations, including: (1) filtering (*i.e.*, removal of background ions), (2) peak picking (*i.e.*, detection of measured ions from the background signal, peak integration and normalization using internal standards), and (3) time alignment (*i.e.*, clustering peaks to correct for retention time drift from sample to sample), which can be performed using proprietary software developed by instrument vendors or open-access web-based data processing tools developed by the scientific community, such as XCMS Online and MZmine2.[45,50,67] However, significant differences in peak intensity and ion assignment have been demonstrated for molecular feature detection when processing the same raw data using different software tools and/or different

parameters.[68] At this stage, QC samples are also processed and often used to exclude features that have unusually high variation, with a relative standard deviation (RSD) of 30% usually adopted as a threshold,[45,62] although QC filtering may not be recommended in some specific cases (*e.g.*, when QCs are not representative of the groups under comparison in the study).[65] Adducts, dimers and in-source fragments can contribute to redundant features in the data matrix, especially when using electrospray ionization (ESI). Those secondary features should be filtered out as much as possible in order to avoid the impact of repeated variables in the statistical analysis (*e.g.,* collinearity, data overfitting) and to help streamline unknown identification.[50,69] Knowledge about common adduct and in-source fragments,[70,71] as well as correlation analysis[72] and computational tools[73] can help to identify and filter out those unwanted features. However, this process is still challenging, especially for species derived from unknown compounds. Missing values are usually replaced by a non-zero value to allow more robust multivariate analysis. Several missing value imputation techniques have been used in metabolomics, including small value replacement, mean or median replacement, k-nearest neighbour (KNN) and others.[74,75] Currently, there is no consensus recommendation about which technique to use for missing data imputation, which may also depend on the analytical platform used to generate the data, as well as the statistical methods intended for data analysis.[74]

Further data transformation may be required depending on the biological sample and the statistical test intended. For instance, metabolite concentrations in urine are highly dependent on hydration status,[76] especially in randomly collected single spot urine samples. As a result, there is a need to correct for sample dilution effects in order to minimize biological variability. In this case, creatinine, osmolality, specific gravity or the total integrated MS signal (*i.e.*, total intensity of compounds that are common to all the samples) are often used to correct for hydration status.[77] Another option is given by the probabilistic quotient normalization (PQN), which uses a reference spectrum to calculate the most

probable distribution factor.[78] Although this normalization method was first developed and applied in NMR-based metabolomics,[78,79] it has also been used to reduce variations due to dilution of biological samples in MS data sets.[80,81] Additional data pretreatment may be required prior to multivariate analysis, including dried mass or total protein normalization (*e.g.*, tissue biospecimens), as well as log-transformation, auto-scaling, Pareto scaling, centering and power transformation, among other methods.[82] The choice of transformation method can have a significant effect on overall data variance and the ranking of metabolites that are found to be significant, depending on properties of the data set and the kind of statistical method used.[75,82]

In biomarker discovery, statistical analysis is primarily used to identify differential metabolites in two or more groups under investigation while correcting for confounding effects. Multivariate statistical analysis is often chosen in metabolomics to facilitate handling large data sets containing hundreds or even thousands of metabolites, which allows for efficient noise filtering and data dimensionality reduction for pattern recognition.[83] A number of multivariate statistical methods have been developed for distinct applications, including, for example, principal component analysis (PCA) for unsupervised data exploration. PCA is useful to evaluate the overall variability within QCs and study groups, while also helping to identify potential outliers.[84] Identification of differentiating metabolites can be performed by partial least squares-discriminant analysis (PLS-DA) or orthogonal PLS-DA (OPLS-DA), as well as machine learning algorithms based on artificial neural networks (ANN), and random forest (RF) among other supervised multivariate statistical methods.[23] Despite their versatility and convenience, multivariate statistics are especially prone to bias due to data overfitting and false discoveries. Avoiding this bias requires careful validation using independent samples (*i.e.*, holdout sample set), or at a minimum a cross-validation step (*i.e.*, leave-one-out cross validation) and permutation testing as a way to check the robustness of the model to correctly assign samples randomly

withheld from training data set.[28] For example, Lawton *et al.*[85] have reported that about 100 out of 300 metabolites analyzed in human plasma from 269 healthy subjects were associated with age, while a smaller number was associated to sex and body mass index (BMI). Even though balanced conditions should be aimed when developing a study design, conditions are not always known or directly controllable. Univariate analysis can also be used in metabolomics as a classical statistical approach to evaluate one variable at a time and provide clear visualization of differentiating metabolites when using an appropriate adjusted *p*-value to correct for multi-hypothesis testing.[86,87] In fact, the combined use of multivariate and univariate methods is recommended to increase the chances of identifying statistically significant yet consistent molecular features for subsequent characterization and validation.[88]

Simple comparison between groups can be performed using parametric or nonparametric univariate statistical analysis (*e.g.*, Student's t test, ANOVA, Mann-Whitney U test), depending on study design, whether the data is normally distributed, shows homogeneity of variances, has a large fraction of missing or skewed data or has observations that are independent from each order.[88] Broadhurst and Kell[86] recommend reporting scatter plots, frequency plots (histograms), boxplots, and receiver-operating characteristic (ROC) curves in metabolomics studies, in order to provide adequate data visualization for identifying and ranking differentiating metabolites in two or more groups. Despite the widespread use of *p*-value to indicate the probability that there are significant differences between the groups based on an specific variable, this measure is very dependent on the sample size and can mislead decisions if not considered in combination with other statistical parameters (*e.g.*, effect size and fold-change).[86,88] Indeed, numerous papers have discussed the prevailing misuse and misinterpretation of p-values in the medical and scientific literature in general,[89–92] including the insightful paper by Ioannidis,[93] entitled "Why most published research findings are false". In the case of metabolomics, when several variables

are tested in parallel, the significance threshold should be modified to correct for multiple hypothesis testing, which can be done using several available methods, most commonly Bonferroni correction or false discovery rate (FDR).[88] Bonferroni correction is the most conservative approach for multiple hypothesis test correction, which minimizes false positive results (Type I error) while increasing the risk for false negatives (Type II error). This approach is recommended by some authors for being easy to understand and implement, while giving more confidence that putative biomarkers are not only statistically significant, but likely more robust as discriminating molecular features such that they can be replicated in independent sample cohorts.[86] On the other hand, FDR is reported as a less conservative method that can minimize the premature rejection of candidate compounds, especially due to metabolite collinearity, which makes the tests not completely independent in metabolomics.[84]

According to Xia *et al.*,[23] ROC curves were mentioned in less than 2% of publications involving metabolomics and biomarkers in a 10-year period, which is surprising, given their broad recognition as one of the best ways to describe the performance of binary classifications that is routinely used as part of validation of biomarkers for use in clinical laboratories.[86,94] ROC curves combine measurements of clinical sensitivity (*i.e.*, true positive rate or detection of a condition when the condition is truly present) and 1-specificity (*i.e.*, false positive rate or failure to identify the absence of a condition when the condition is truly absent), while also providing a single numeric measure of clinical accuracy through the area under the curve (AUC). Unlike some other metrics, ROC curves are robust to non-normally distributed data, independent of disease prevalence, and allow overlaying two or more variables as a way to compare their performances.[23,95] When reporting results for ROC curves, it is important to include confidence intervals (CIs) for the AUC to allow more meaningful interpretation of the variable performance, a parameter that is missing in many research publications.[96] Moreover, the objective of the study should also be

considered, as ROC curves are extremely valuable for diagnostic purposes, but limited efficiency may be observed when evaluating biomarkers for disease prognosis or risk factor identification (*i.e.*, antecedent biomarker).[97]

Overall, most of the challenges associated with statistical analysis in biomarker discovery are related to a failure to correct for multiple hypothesis testing, lack of independent validation or even cross-validation to assess model overfitting and robustness, as well as inappropriate selection of statistical tests that are not optimal for the study design and underlying data distribution.[86] In this context, expertise in chemometrics/bioinformatics is critical to obtain high quality outcomes, which can minimize the number of potential biomarkers reported in the literature that have no chance for successful translation into clinical practice.[51] Moreover, as highlighted by Xia *et al.*,[23] the metabolomics community should start "speaking the same language" as clinicians and clinical chemists in order to effectively communicate their finding to the major audience involved in biomarker validation or qualification. For example, although data normalization, scaling or centering algorithms that involve population parameters or measurement of numerous metabolites may be useful during statistical analysis in the discovery phase, those transformations are often not applicable in real-world applications, and thus constitute an obstacle in later translation stages.[23] Additionally, an understanding of the biological variability of a putative biomarker in a population, as well as its inherent chemical stability are critical when evaluating its usefulness in routine clinical laboratory testing in order to positively impact decision making with improved health outcomes for patients.

1.2.4 Unknown identification

In untargeted MS-based metabolomics, a large fraction of metabolites analyzed are unknown and thus require structural elucidation in order to provide biological knowledge into their function and origin, including likely protein/genes,

microflora, diet and/or environmental exposures associated with their regulation. This labour-intensive step is often highlighted as a major bottleneck in discovery-based metabolomics research.[69,98] Four levels of metabolite identification have been defined by the Chemical Analysis Working Group of the Metabolomics Standards Initiative, as presented in **Table 1.3**.[98] The use of properly calibrated mass spectrometers with high resolution (resolving power > 10,000) enables accurate mass measurements (< 5 ppm) as required for reliably measuring isotopic formula (or elemental composition) – the first critical step towards the identification of an unknown compound by MS.[69] However, a molecular formula is often associated with dozens to hundreds of known chemical structures, thus fragmentation spectra based on electron impact ionization (EI)-MS or collisional-induced dissociation MS/MS experiments when using ESI-MS are essential to assist in structural elucidation. As a result, open-access compound databases are extremely useful to identify putative molecular structures, allowing searches based on *m/z*, monoisotopic mass, molecular formula, and/or fragment ions.[98] However, currently available databases are far from complete and unknown metabolites that are not listed require *de novo* structural elucidation based on gas-phase ion chemistry.[45] In this case, fragment spectral interpretation is still heavily based on manual peak assignment, which is time-consuming and often challenging due to the wide chemical diversity of metabolites and high sensitivity and resolution needed to obtain high quality fragmentation spectra for low abundance metabolites without co-eluting or isobaric interferences.[50] Moreover, the presence of adducts and in-source fragments in ESI that may further complicate unknown identification by increasing the number of apparent unknowns and misleading molecular mass assignment.[69] For instance, Brown *et al.*[99] have found that 14-33% of the features detected in a range of biological samples by ultra-performance LC (UPLC)-MS were multiplicities of the same compound, whereas Xu *et al.*[71] reported that 16% of the detected ions in yeast metabolome by LC-MS were related to in-source fragments that could lead to

Table 1.3. Levels of metabolite identification defined according to the Metabolomics Standard Initiative. Adapted from Dunn *et al*.[98]

Level	Confidence	Evidence	Example
1	*Confidently identified compounds*	Comparison of two or more orthogonal properties with an authentic chemical standard analyzed under identical analytical conditions	Same RT/MT, *m/z* and/or fragmentation spectrum as a standard analyzed using the same instrument in the same laboratory
2	*Putatively annotated compounds*	Based upon physicochemical properties and/or spectral similarity with public/commercial spectral libraries, without reference to authentic chemical standards	Similar RT/MT, *m/z* and/or fragmentation spectrum as a compound present in a database
3	*Putatively annotated compound classes*	Based upon characteristic physicochemical properties of a chemical class of compounds, or by spectral similarity to known compounds of a chemical class	RT/MT, *m/z* and/or fragmentation spectrum that are comparable with expected properties of certain chemical classes
4	*Unknown compounds*	Although unidentified and unclassified, these metabolites can still be differentiated and quantified based upon spectral data	RT/MT, *m/z* and/or fragmentation spectrum with no clear matches or indication of chemical class

RT = retention time; MT = migration time; *m/z* = mass-to-charge ratio

misannotation. Moreover, a major fraction of detectable signals in ESI-MS are associated with spurious signals and background ions from solvent/buffer that require rigorous filtering.

Although it is largely recognized that MS-based metabolomics still lacks appropriate tools for rapid unknown identification as needed when handling extensive compound lists, new approaches have been developed recently that can

assist metabolite annotation.[69] For instance, separation modeling can assist in the identification of unknown compounds or filtering out unlikely isobaric or isomeric candidates. Separation modeling is complimentary to high resolution, accurate MS and MS/MS based on physicochemical properties that affect the retention or electromigration behaviour of solutes in GC, LC and CE.[50,69] For instance, the retention time index has been used for many years in GC-MS to greatly improve precision when comparing solute retention behaviour between different instrument platforms that better tolerate changes in experimental conditions, also accounting with recent improvement geared towards metabolomics applications.[100] Despite more difficult standardization due to strong dependence on instrumental conditions and mobile phase composition in LC-MS, promising efforts have been reported in retention time prediction using hydrophilic interaction LC (HILIC).[101] Similarly, computational models can be used in CE-MS to predict the apparent electrophoretic mobility or relative migration time of an ion that is dependent on the molecular volume and its effective charge (pK_a) under the buffer conditions used for the separation.[102,103] In addition, public accessible compound spectral databases (*e.g.*, Metlin, HMDB, Mass Bank) are constantly being updated to facilitate comparison with fragmentation spectra generated by different instrumental platforms and facilities.[69] While lack of reproducibility is known to affect direct comparison of spectra generated by ESI-MS/MS, those libraries are still a valuable resource for putative metabolite identification.[104] For instance, unlike standardized EI-MS spectra (70 eV) for GC-MS, ESI-MS/MS spectral matching in LC-MS or CE-MS is far more challenging since fragmentation spectra are acquired under different collisional energies (*e.g.*, 10, 20, 40 V) due to differences in the intrinsic chemical stability of a precursor ion. In addition, the relative intensity of product ions is often dependent on the specific instrument configuration used to acquire reference spectra (*i.e.,* ion optic configurations), whereas coelution of isobaric ions in real complex samples can hinder reliable MS/MS spectral matches with databases

acquired with commercial standards. Moreover, computational approaches for *in silico* prediction of fragmentation spectra can improve the level of confidence in unknown identification, even when reference standards or entries in spectral libraries are not available.[69] For example, the Competitive Fragmentation Modeling for Metabolite Identification (CFM-ID) is a practical online tool for spectrum prediction at multiple collision energies, peak assignment, and putative unknown identification.[105] Nevertheless, confirmation with authentic standards analyzed under the same analytical conditions is ultimately necessary for unambiguous unknown identification (*i.e.,* level 1 identification from **Table 1.3**), which can be another challenge when the putative compound is not available or requires a complicated multi-step synthesis and purification.[69,106] In some cases, partial characterization of an unknown chemical (*i.e.,* level 2 or 3 from **Table 1.3**) is only feasible based on characteristic elements (*e.g.,* sulfur isotope) or functional group assignment (*e.g.,* neutral loss of trimethylamine). In all cases, two independent descriptors for a molecular feature (*e.g., m/z* and retention or migration time) are required as minimum reporting standards in metabolomic investigations (*i.e.,* level 4 from **Table 1.3**). Otherwise, classical and hypothesis-driven approaches for compound identification are required. These include chemical reactivity tests, enzyme transformations and purification methods for compound isolation, as well as enrichment and/or characterization by MS/MS and NMR.

1.2.5 Biological interpretation

Many biomarkers currently used in medicine do not necessarily have a well-understood biochemical pathway and established role in disease pathophysiology. In fact, some authors indicate that a complete understanding of the biological relationship between biomarker and phenotype is usually a challenging long-term pursuit that involves effort from multiple research groups, and should not be required for biomarker approval.[6,23] However, some degree of

plausible biological interpretation can greatly increase confidence that a compound may be a relevant biomarker that is causally involved in disease pathogenesis and its later progression.[23,52] Additionally, insights into disease mechanisms may provide meaningful information to guide disease management, including treatment responses to therapy.[107] Koulman *et al.*[107] highlight that literature search beyond the scope of an individual disease of interest can be indicative of potential clinical specificity, mentioning the example of phospholipids and ceramides, which have been reported as differentiating metabolites in five studies covering totally different diseases and organisms. Literature search and metabolite databases (*e.g.*, HMDB) can provide complementary information about expected concentrations and biological variation previously reported by other researchers.[107] Computational tools to identify underlying biochemical pathways (*e.g.*, Metabolic Pathway Analysis on MetaboAnalyst)[108] are another option to facilitate visualization of meaningful known pathways that may relate to one or more metabolites of interest and help to identify interactions with associated enzymes and genes.[46] Thus, even small changes in individual metabolites measured between groups (*i.e.*, case-control) may provide deeper insight into the developmental origins of health and disease when considering metabolites linked to common or coupled metabolic biochemical pathway(s).[108]

1.2.6 Translation to clinical practice

As mentioned by Goodsaid *et al.*,[109] "although publications of the experimental data in the peer-reviewed scientific literature is important and provides a way to validate and disseminate scientific data, publication alone does not qualify a biomarker for a specific use or purpose in a regulatory setting". Once a candidate biomarker is discovered and validated in the original study, a series of other phases should be followed for biomarker qualification or evaluation, which constitute a long-term process and usually involves effort from different groups

Table 1.4. Major stages involved in the evaluation of screening biomarkers. Adapted from Pepe *et al.*[32]

Phase	Description
I	***Preclinical/exploratory studies:*** potentially useful markers are identified in control vs. disease samples (discovery phase)
II	***Clinical assay development and validation:*** clinical test to assess the biomarker ability to distinguish control vs. disease is performed using non-invasive samples; a simple and reproducible assay is developed and validated; factors that can be associated to the biomarker status (*e.g.*, gender, age, smoking) are evaluated to identify the need for subpopulation screening thresholds
III	***Retrospective longitudinal repository studies:*** test to detect disease in early stages as a function of time before it becomes clinically diagnosed is performed using samples from repositories; criteria for screen positive test are determined
IV	***Prospective screening studies:*** stage and nature of disease detected by the test and false positive rates are determined; practical feasibility of implementing the screening program are evaluated; preliminary effect of screening on disease outcomes are assessed; diseases that are clinically identified but not detected by screening (false negatives) are monitored
V	***Control studies:*** impact of screening on improving clinical outcomes in the population is quantified; information about cost, treatment and compliance with screening are obtained; screening protocols and treatment approaches for positive screen individuals are compared; impact of overdiagnosis is evaluated

and contributors with different expertise, including clinicians, biostatisticians, chemists, clinical biochemists, technicians and industry.[25,110] The term "evaluation" is preferred by the NIH Biomarkers Definitions Working Group in order to avoid confusion with "validation" since the latter term is already used to address analytical performance and initial reproducibility of differentiating metabolites.[6] **Table 1.4** shows the phases generally required in the evaluation process of biomarkers used for the screening of human diseases. The phases are

ordered according to strength of evidence, also considering that results from previous phases are often needed to design the next ones. The phases are recognized as a guiding structure to facilitate coherent and efficient biomarker development, rather than a rigorous path.[32] On the other hand, the term "qualification" is used by regulatory agencies, including the Food and Drug Administration (FDA) and the European Medicines Agency (EMA), to describe the the formal process of submission and evaluation of a candidate biomarker before approval for clinical usage.[52,111] A collaborative effort between FDA and EMA also created a voluntary exploratory data submission program in 2004, which helps to improve communication between the regulatory agencies and biomarker developers (*e.g.*, academic researchers, pharmaceutical companies and technology providers), even during early stages of biomarker exploratory analysis. This program aims to facilitate scientific progress towards biomarker translation to clinical practice or drug response applications, with no direct regulatory intents, yet increasing the chances of subsequent regulatory applications.[25,109] Importantly, biomarker approval must be accompanied by the implementation of validated analytical methods for reliable yet routine measurements of new biomarkers in a clinical laboratory setting, as well as adequate training on results interpretation for health care providers.[110]

1.3 Method validation and quality assurance practices for biomarkers in clinical and epidemiological studies

The availability of simple, reliable, and cost-effective analytical methods is essential to support the use of biomarkers in clinical medicine at the individual and population levels.[112] Unreliable results can greatly affect decision-making by health care providers, potentially leading to incorrect or delayed diagnosis, unnecessary medical interventions, ineffective or adverse treatments, and/or misleading medical recommendations.[113,114] For this reason, quality of the results provided is one of the biggest concerns of clinical laboratories, which is largely

dependent on adequate method validation, including effective quality control protocols and participation in quality assurance programs, such as proficiency and round robin testing.[115] Various organizations, including the Clinical and Laboratory Standards Institute (CLSI), the Centers for Disease Control and Prevention (CDC) in the US, and the Program of Accreditation of Laboratories (PALCAN) in Canada provide guidelines for method validation and quality control, coordinate proficiency programs, and are involved in assessing the quality of laboratory services, which has greatly contributed to decrease the occurrence of laboratory errors directly related to the analytical methods.[115]

Method validation can be described as "the process of defining an analytical requirement, and confirming that the method under consideration has performance capabilities consistent with what the application requires".[116] The extent of the validation depends on the intended use of the method. For instance, clinical laboratories often adopt new methods that have been previously developed and validated in another institution. In this case, a short validation, also called verification, may be enough to confirm that the method performs in accordance with specifications under the conditions present in the clinical laboratory (*e.g.*, changes in temperature or humidity, different analyst). In contrast, new methods internally developed or modified require a full validation.[117,118] **Table 1.5** summarizes the validation/verification parameters required in each case, which are useful to establish the expected performance of the analytical method, as well as required quality control procedures for timely identification of possible problems during analysis. These criteria will also depend on whether the assay in a clinical laboratory is applied to measure one or more biomarkers for screening (*i.e.,* presumptive diagnosis) or confirmatory testing (*i.e.*, unambiguous diagnosis).

Recommended procedures to determine validation parameters are available in guidelines from the FDA,[119] International Union of Pure and Applied Chemistry (IUPAC),[120] CLSI, and Eurachem,[116] among others institutions.

Table 1.5. General guidelines for method validation in clinical laboratories, based on recommendations from the CDC, Centers for Medicare and Medicaid Services (CMS) and Department of Health and Human Services (HHS).[117]

Method	Required validation/verification parameters
New method previously validated in another laboratory/institution: Determine comparable performance (verification or partial validation)	1. Precision 2. Accuracy 3. Reportable range 4. Reference interval
New method developed or modified by the laboratory: Determine all validation parameters (full validation)	1. Precision 2. Accuracy 3. Analytical sensitivity 4. Calibration and quality control procedures 5. Analytical specificity, including interferences 6. Reportable range 7. Reference interval 8. Other performance characteristics

Fortunately, most protocols overlap to a considerable extent, although there are some differences in terminologies and specific requirements.[121] For example, **Table 1.6** summarizes recommendations related to method precision according to different guidelines. Although their definitions are very similar, the terms used to specify levels of precision are slightly different. Additionally, the type of requirements for bioanalytical methods in general (*i.e.*, FDA, IUPAC, Eurachem) is less specific, in order to accommodate the needs of different bioanalytical applications. On the other hand, the CLSI has a more defined protocol for clinical method validation in terms of number of replicates, batches, concentration levels and long-term performance. In many cases, the literature in method development does not report validation parameters up to the clinical level, even when the method is intended for clinical application. While it is not a general requirement for publication, initial demonstration that the method performs well under the

Table 1.6. Recommended terminology and protocol for precision determination according to different method validation guidelines.

Aspect	FDA[119]	IUPAC[120]	CLSI[125]	Eurachem[116]
Definition	Closeness of individual measures of an analyte repeated for multiple aliquots of a biological matrix	Closeness of agreement between independent test results obtained under stipulated conditions	Closeness of agreement between independent test/measurement results obtained under stipulated conditions	Measure of how close results are to one another
Classification	- Within-run, intra-batch - Between-run, inter-batch - Reproducibility	- Within-run, repeatability - Run-to-run, between-run - Reproducibility	- Total within-laboratory precision - Reproducibility	- Repeatability - Intermediate precision - Reproducibility
Protocol	Minimum 3 concentrations, 5 replicates, no further specification for between-run precision	Minimum 2 concentrations, 6 replicates, representative of likely routine conditions	Minimum 2 concentrations, 2 replicates, 2 batches/day analyzed at least 2 h apart, over 20 days	Minimum 2 concentrations, 6-15 replicates, one-way ANOVA to estimate intermediate precision
Criteria	RSD ≤ 15% or ≤ 20% for low limit of quantification	Dependent on the test	Dependent on the test	Dependent on the test

CLSI recommendations can be an advantage when clinical laboratories are selecting new methods to be implemented in their routine workflow.

The interpretation of a number of clinical tests for diseases with non-specific symptoms relies on predefined thresholds or acceptable ranges that determine disease diagnosis or drug dosage recommendations. In this case, the performance of analytical tests, especially in terms of calibration, accuracy, and interferences may have a critical impact on medical decisions.[114,122] Hormone tests are an example of clinical results that are critically important for decision-making at the clinic, yet susceptible to considerable impact of interferences in immunoassay tests. Immunoassay still remain in use in many clinical laboratories,

due to relatively low cost, adequate sensitivity, easy automation and high sample throughput.[123] Hawley *et al.*[124] have recently reported considerable bias (> 10%) in serum cortisol when analyzing patient samples using different routine immunoassays in comparison to a candidate reference method based on LC-MS/MS. In this case, interferences from elevated cortisol-binding globulin in a pregnant cohort resulted in underestimated cortisol level for most assays tested, whereas consistently overestimated levels were found in patients undergoing treatment for adrenal insufficiency or Cushing syndrome.[124] Another example is given by a report from the National Institute of Standards and Technology (NIST),[122] which highlights the impact of calibration error in medical decision making and health care costs, exemplified by reported problems in hypercalcemia diagnostics based on serum total calcium levels. According to the report, factors affecting the result are mainly related to lot-to-lot variation in reagent and calibrants due to homogeneity issues, as well as matrix effects in spectrophotometric and atomic spectroscopy methods.[122] An additional example is the need for recalibration of Jaffe and enzymatic assays used to measure serum creatinine in comparison with a more selective methods based on stable-isotope dilution LC-MS, which helps to improve agreement between results obtained by different methods across multiple laboratories.[126] In this case, accurate creatinine determination is required for reliable estimation of glomerular filtration rate, which is used to assess need for dialysis, severity of renal failure, and success of kidney transplantation.[126]

In this context, assay accuracy tests are essential to assist the identification of sources of bias that may affect the quality of results provided. Although spike-recovery experiments and analysis of reference material are useful, this does not necessarily reflect the range of interferences present in patient samples. Therefore, a proper assessment of the accuracy of these tests should be accompanied by method comparison studies using authentic patient samples and proficiency tests, which give a better estimate of bias, important interferences, and adequacy of

calibration.[94,114] Proficiency tests indicate how well each participant laboratory compares with others, allowing a better route to identify the occurrence of bias over time.[116] Given its importance as a tool to monitor analytical performance and avoid reporting erroneous results, clinical laboratories are often required to participate in proficiency tests by regulatory agencies.[117,127] Method comparison studies usually involve the analysis of a selected set of authentic patient samples (n = 40-100), which are also analyzed by a reference method.[94] Correlation between methods can be examined using Passing-Bablok or Deming regression, which are more appropriate than least squares regression when both variables are susceptible to imprecision. Additionally, those models are more robust to outliers and non-normally distributed data, which are common in real-world clinical applications.[94,128] The most recommended approach to evaluate agreement between methods rely on Bland-Altman plots, which show the differences or percentage differences between the methods as a function of their mean concentration, including limits of agreements and their 95% CI.[94,128] Acceptable bias between methods depends on the intended application and the nature of the analyte. Additional information about expected biological variation and current desirable limits for bias can be found in a database hosted by Westgard[129] for most biochemical analyses currently performed in clinical laboratories.

1.4 Thesis motivation and objectives: Biomarker analysis for clinical and epidemiological applications

Biomarkers have a fundamental role in guiding medical decisions and public health policies. Although great progress has been made in the last decades with the development of high performance analytical platforms and computational tools, challenges remain in the data workflow in metabolomics for biomarker discovery and its subsequent validation and application in clinical and epidemiological studies. Moreover, many biomarkers currently used in decision making in the clinic have major limitations in terms of clinical utility (*i.e.*,

specificity) or rely on costly and/or poorly performing analytical assays. In this context, the work in this thesis contributes to two main aspects of biomarker research. The first involves developing and rigorously validating targeted CE assays for reliable determination of biomarkers in human biofluids used in epidemiological and clinical applications, including two inorganic anions of relevance to human health and chronic disease risk, namely sulfate (*Chapter II*) and iodide (*Chapter III*) that also includes a rigorous inter-method validation study after correcting for a source of bias not detected in the original assay (*Chapter IV*). The second involves characterizing the sweat metabolome of CF-screen positive infants by non-targeted metabolite profiling using CE-MS. This also involved evaluating metabolic changes associated with CF that can identify potential new biomarkers to complement the current sweat chloride test (as a third inorganic anion of relevance to clinical diagnostics) and improve CF diagnosis, prognosis and treatment monitoring (*Chapter V*).

1.4.1 Urinary sulfate and risk assessment of kidney stone formation

Sulfur, one of the most abundant minerals in the human body, is mainly derived from dietary intake of the sulfur-containing amino acids, methionine and cysteine, which are involved in the production of several essential metabolic intermediates, sulfation pathways for detoxification of exogenous agents, as well as gut microflora activity by sulfate-reducing bacteria.[130,131] Sulfate is the major end-product of sulfur metabolism, which is considered an indicator of protein intake and plays a fundamental role in human health. Although it is not directly present in the composition of kidney stones, sulfate is a primary contributor to urinary ionic strength, which affects supersaturation and thus the solubility of stone-forming ions.[12] Several studies have demonstrated that higher sulfate excretion is associated with positive health outcomes in patients with renal diseases.[132,133] However, reduced protein intake that concomitantly results in lower sulfate, remains a common medical dietary recommendation to prevent stone recurrence,

despite conflicting results obtained in different clinical trials.[12] Therefore, further studies are needed to evaluate the role of sulfate in stone formation. Currently, assays for sulfate determination are not available in most clinical laboratories, due to lack of reliable and simple methods that are selective for sulfate analysis in complex matrices without complicated/long sample pre-treatment protocols. *Chapter II* of this thesis focuses on the development and careful validation of a simple yet selective CE method with indirect UV detection for sulfate determination in urine and other biofluids without interferences (plasma, sweat), which also allows simultaneous analysis of chloride and the redox-active reactive intermediate of sulfur metabolism, sulfite.[134] Additionally, a pilot study was conducted to evaluate sulfate levels in single-spot urine samples collected from a pediatric population. Preliminary findings indicate significantly lower sulfate levels in stone forming patients compared to non-stone forming children controls while also allowing for unambiguous diagnosis of the rare yet fatal in-born error of metabolism, sulfite oxidase deficiency.[135]

1.4.2 Iodine nutrition determination for epidemiological studies

Urinary iodide is a well-established biomarker of dietary iodine intake as recommended by the WHO to determine the iodine nutritional status in a population.[136] Although urinary iodine is highly variable on an individual level, those differences even out when considering median urinary iodine concentrations when evaluating the prevalence of iodine deficiency on a population level.[136] Despite successful implementation of table salt iodization programs in several countries, lack of consistent monitoring of iodine intake coupled with recent changes in diet and lifestyle has led to the recurrence of mild to moderate iodine deficiency in regions that had been previously considered iodine sufficient. This can seriously impact public health, especially cognitive development and impaired learning in young children.[137] Methods currently available for urinary iodine analysis involve time-consuming sample pretreatment, toxic reagents,

costly infrastructure and operation while suffering from poor selectivity. In *Chapter III*, a new method for urinary iodide analysis is introduced as a simple and affordable option to evaluate population iodine nutrition in epidemiological studies using CE with direct UV detection.[138] Separation conditions were optimized to quantify sub-micromolar iodide levels by using an online sample preconcentration technique based on sample self-stacking that relied upon dynamic complexation of iodide with α-cyclodextrin as a buffer additive. Internal method validation demonstrated good method performance, however, a considerable positive bias was observed when using external reference samples, which could impact proper iodine nutritional classification based on the categories proposed by WHO.[136] As a result, *Chapter IV* describes a subsequent inter-laboratory method comparison for rigorous validation of the CE assay, which helped to identify and correct sources of bias in the original method. In this case, sulfate was found to interfere with the sample self-stacking process due to its similar electrophoretic mobility to iodide, which resulted in a lowering of the signal response for iodide as measured in authentic urine samples and calibrants solutions containing sulfate salts. The optimized CE method overcame this matrix interference following further optimization of separation conditions, which resulted in consistent results with the reference method based on inductively coupled plasma mass spectrometry (ICP-MS) that is suitable for iodine nutritional assessment in large-scale population studies. Inter-method validation was performed in collaboration with colleagues at Hamilton General Hospital and the CDC in support of their world-wide program for Ensuring Quality in Urinary Iodine Procedures (EQUIP).

1.4.3 Sweat metabolome characterization in screen-positive CF infants

Quality of life and life expectancy can be greatly improved for CF patients with pre-symptomatic diagnosis early in life through NBS.[139] Due to a high rate of false-positives for CF in NBS programs, a confirmatory sweat chloride test using

a chloridometer is required for unambiguous diagnosis of screen-positive infants.[140] Despite being simple, non-invasive and the foremost option for CF diagnosis currently available, the sweat chloride test still has limitations, especially when chloride levels are intermediate/borderline (30-59 mM). These cases are classified as CF-screen positive inconclusive diagnosis (CF-SPID) cases.[140] Additionally, sweat chloride levels do not allow clear assessment of variable disease phenotypes in CF, notably in cases of *CFTR* mutations comprising compound heterozygote patients. Therefore, there is growing interest in new biomarkers to complement the sweat chloride test for better decision-making in the clinic, including differential diagnosis, patient stratification and treatment monitoring. However, the sweat metabolome remains largely uncharacterized to date and there have been only few recent studies reported to date, which do not involve infants or authentic CF cases.[141–145] In this context, *Chapter V* describes the first rigorous characterization of volume-restricted sweat specimens in CF-screen positive infants by untargeted metabolite profiling, including unaffected infants with less than two *CFTR* mutations and low sweat chloride (< 30 mM), as well as affected CF cases involving two disease-causing *CFTR* mutations with high sweat chloride (≥ 60 mM). In this study, multisegment injection (MSI)-CE-MS[146] was used as a high throughput platform for the resolution and detection of 64 polar/ionic metabolites present in residual pilocarpine-stimulated sweat samples. Amino acids, organic acids, dipeptides, amino acid derivatives and various exogenous compounds were among the metabolites identified in infant sweat specimens. Unknown metabolites were tentatively identified by high resolution, accurate MS/MS and confirmed by comparing with authentic standards whenever possible. A preliminary comparison between metabolite levels in sweat from CF affected and non-affected infants collected from two CF clinics in Ontario (McMaster Children's Hospital and The Hospital for Sick Children) demonstrated the presence of some consistent differentiating metabolites independent of study site. To the best of our

knowledge, this work represents the first report involving the characterization of the sweat metabolome in infants (< 3 months), as well as the first tentative identification of differentiating sweat metabolites for CF status beyond common inorganic electrolytes, such as chloride or sodium. Moreover, preliminary studies were also performed on changes in the sweat metabolome of a CF patient with a G551D mutation undergoing nutritional therapy followed by drug intervention using the CFTR-potentiator, ivacaftor that has been shown to improve lung function, promote weight gain, and reduce pulmonary exacerbation rate.[147] Importantly, several sweat metabolites were found to respond selectively to nutritional interventions and/or drug therapy when analyzing repeat sweat specimens over time, which offers a promising approach to evaluate treatment responsivity on an individual level for orphan diseases, including nutritional supplementation, physiotherapy and genotype-specific pharmacological intervention.

1.5 References

(1) Jain, K. K. In *The handbook of biomarkers*; Springer: Totowa (NJ), 2010; pp 1–21.

(2) Strimbu, K.; Tavel, J. A. *Curr. Opin. HIV AIDS* **2011**, *5*, 463–466.

(3) Armstrong, J. A. *Kidney Int.* **2007**, *71*, 384–387.

(4) Strasinger, S. K.; Di Lorenzo, M. S. *Urinalysis and body fluids*, 5th ed.; F. A. Davis Company: Philadelphia (PA), 2008.

(5) Haber, M. H. *Clin. Lab. Med.* **1988**, *8*, 415–430.

(6) Biomarkers Definitions Working Group. *Clin. Pharmacol. Ther.* **2001**, *69*, 89–95.

(7) WHO International Programme on Chemical Safety. *Biomarkers in risk assessment: Validity and validation*; Geneva, 2001.

(8) O'Gorman, A.; Gibbons, H.; Brennan, L. *Comput. Struct. Biotechnol. J.* **2013**, *4*, e201301004.

(9) Wild, C. P. *Cancer Epidemiol. Biomarkers Prev.* **2005**, *14*, 1847–1850.

(10) Puntmann, V. O. *Postgrad. Med. J.* **2009**, *85*, 538–545.

(11) Price, C. P.; Kricka, L. J. *Clin. Chem.* **2007**, *53*, 1665–1675.

(12) Worcester, E. M.; Coe, F. L. *N. Engl. J. Med.* **2010**, *363*, 954–963.

(13) Newborn Screening Ontario. *Newborn screening manual: A guide for newborn care providers*; Ottawa (ON); 2015.

(14) Eckel, R. H.; Jakicic, J. M.; Ard, J. D.; De Jesus, J. M.; Houston Miller, N.; Hubbard, V. S.; Lee, I. M.; Lichtenstein, A. H.; Loria, C. M.; Millen, B. E.; Nonas, C. A.; Sacks, F. M.; Smith, S. C.; Svetkey, L. P.; Wadden, T. A.; Yanovski, S. Z. *J. Am. Coll. Cardiol.* **2014**, *63*, 2960–2984.

(15) van Spronsen, F. J. *Nat. Rev. Endocrinol.* **2010**, *6*, 509–514.

(16) World Health Organization. *Definition and diagnosis of diabetes mellitus and intermediate hyperglycemia*; 2006.

(17) Viale, G. *Ann. Oncol.* **2012**, *23*, x207–x210.

(18) Gupta, D.; Lis, C. G. *J. Ovarian Res.* **2009**, *2*, 13.

(19) Aldámiz-Echevarría, L.; Bueno, M. A.; Couce, M. L.; Lage, S.; Dalmau, J.; Vitoria, I.; Andrade, F.; Llarena, M.; Blasco, J.; Alcalde, C.; Gil, D.; García, M. C.; González-Lamuño, D.; Ruiz, M.; Ruiz, M. A.; González, D.; Sánchez-Valverde, F. *Mol. Genet. Metab.* **2013**, *109*, 331–338.

(20) Patti, G. J.; Yanes, O.; Siuzdak, G. *Nat. Rev. Mol. Cell Biol.* **2012**, *13*, 263–269.

(21) Ptolemy, A. S.; Rifai, N. *Scand. J. Clin. Lab. Invest.* **2010**, *S242*, 6–14.

(22) Anderson, N. L. *Clin. Chem.* **2010**, *56*, 177–185.

(23) Xia, J.; Broadhurst, D. I.; Wilson, M.; Wishart, D. S. *Metabolomics* **2013**, *9*, 280–299.

(24) Ransohoff, D. F. *J. Clin. Epidemiol.* **2007**, *60*, 1205–1219.

(25) Drucker, E.; Krapfenbauer, K. *EPMA J.* **2013**, *4*, 7.

(26) Poste, G. *Trends Mol. Med.* **2012**, *18*, 717–722.

(27) Ransohoff, D. F. *Gastroenterology* **2003**, *125*, 290.

(28) Ransohoff, D. F. *Nat. Rev. Cancer* **2005**, *5*, 142–149.

(29) Pepe, M. S.; Li, C. I.; Feng, Z. *Cancer Epidemiol. Biomarkers Prev.* **2015**, *24*, 944–950.

(30) Castle, A. L.; Fiehn, O.; Kaddurah-Daouk, R.; Lindon, J. C. *Brief. Bioinform.* **2006**, *7*, 159–165.

(31) Bossuyt, P. M.; Reitsma, J. B.; Bruns, D. E.; Gatsonis, C. A.; Glasziou, P. P.; Irwig, L. M.; Lijmer, J. G.; Moher, D.; Rennie, D.; de Vet, H. C. W.; STARD steering group. *Clin. Chem.* **2003**, *49*, 1–6.

(32) Pepe, M. S.; Etzioni, R.; Feng, Z.; Potter, J. D.; Thompson, M. Lou; Thornquist, M.; Winget, M.; Yasui, Y. *J. Natl. Cancer Inst.* **2001**, *93*, 1054–1061.

(33) Vargas, A. J.; Harris, C. C. *Nat. Rev. Cancer* **2016**, *16*, 525–537.

(34) National Research Council. *Toward precision medicine: Building a knowledge network for biomedical research and a new taxonomy of disease*; The National Academies Press: Washington (WA), 2011.

(35) Wishart, D. S. *Nat. Rev. Drug Discov.* **2016**, *9*, 473–484.

(36) Kessler, W. R.; Andersen, D. H. *Pediatrics* **1951**, *8*, 648–655.

(37) Darling, R. C.; di Sant'Agnese, P. A.; Perera, G. A.; Andersen, D. H. *Am. J. Med. Sci.* **1953**, *225*, 67–70.

(38) Quinton, P. M. *Physiology* **2007**, *22*, 212–225.

(39) Rommens, J. M.; Iannuzzi, M. C.; Kerem, B.; Drumm, M. L.; Melmer, G.; Dean, M.; Rozmahel, R.; Cole, J. L.; Kennedy, D.; Hidaka, N. *Science* **1989**, *245*, 1059–1065.

(40) Folling, I. *Acta Paediatr.* **1994**, *S407*, 4–10.

(41) Bickel, H.; Gerrard, J.; Hickmans, E. M. *Acta Paediatr.* **1954**, *43*, 64–77.

(42) Guthrie, R.; Susi, A. *Pediatrics* **1963**, *32*, 338–343.

(43) Scriver, C. R. *Hum. Mutat.* **2007**, *28*, 831–845.

(44) Milne, S. B.; Mathews, T. P.; Myers, D. S.; Ivanova, P. T.; Brown, H. A. *Biochemistry* **2013**, *52*, 3829–3840.

(45) Tzoulaki, I.; Ebbels, T. M. D.; Valdes, A.; Elliott, P.; Ioannidis, J. P. A. *Am. J. Epidemiol.* **2014**, *180*, 129–139.

(46) Baumgartner, C.; Osl, M.; Netzer, M.; Baumgartner, D. *J. Clin. Bioinforma.* **2011**, *1*, 2.

(47) Wang, T. J.; Larson, M. G.; Vasan, R. S.; Cheng, S.; Rhee, E. P.; McCabe, E.; Lewis, G. D.; Fox, C. S.; Jacques, P. F.; Fernandez, C.; O'Donnell, C. J.; Carr, S. A.; Mootha, V. K.; Florez, J. C.; Souza, A.; Melander, O.; Clish, C. B.; Gerszten, R. E. *Nat. Med.* **2011**, *17*, 448–453.

(48) Wang, Z.; Klipfell, E.; Bennett, B. J.; Koeth, R.; Levison, B. S.; Dugar, B.; Feldstein, A. E.; Britt, E. B.; Fu, X.; Chung, Y.-M.; Wu, Y.; Schauer, P.; Smith, J. D.; Allayee, H.; Tang, W. H. W.; DiDonato, J. A.; Lusis, A. J.; Hazen, S. L. *Nature* **2011**, *472*, 57–63.

(49) Holmes, E.; Wijeyesekera, A.; Taylor-Robinson, S. D.; K, N. J. *Nat. Rev. Gastroenterol. Hepatol.* **2015**, *12*, 458–471.

(50) Courant, F.; Antignac, J. P.; Dervilly-Pinel, G.; Le Bizec, B. *Proteomics* **2014**, *14*, 2369–2388.

(51) Poste, G. *Nature* **2011**, *469*, 156–157.

(52) Beger, R. D.; Colatsky, T. *Metabolomics* **2012**, *8*, 2–7.

(53) Brown, M.; Dunn, W. B.; Ellis, D. I.; Goodacre, R.; Handl, J.; Knowles, J. D.; O'Hagan, S.; Spasić, I.; Kell, D. B. *Metabolomics* **2005**, *1*, 39–51.

(54) Ellervik, C.; Vaught, J. *Clin. Chem.* **2015**, *61*, 914–934.

(55) Álvarez-Sánchez, B.; Priego-Capote, F.; Luque de Castro, M. D. *Trends Anal. Chem.* **2010**, *29*, 111–119.

(56) Bowen, R. A. R.; Remaley, A. T. *Biochem. Medica* **2014**, *24*, 31–44.

(57) Townsend, M. K.; Bao, Y.; Poole, E. M.; Bertrand, K. A.; Kraft, P.; Wolpin, B. M.; Clish, C. B.; Tworoger, S. S. *Cancer Epidemiol. Biomarkers Prev.* **2016**, *25*, 823–829.

(58) Barnes, S.; Benton, H. P.; Casazza, K.; Cooper, S. J.; Cui, X.; Du, X.; Engler, J.; Kabarowski, J. H.; Li, S.; Pathmasiri, W.; Prasain, J. K.; Renfrow, M. B.; Tiwari, H. K. *J. Mass Spectrom.* **2016**, *51*, 461–475.

(59) Dunn, W. B.; Ellis, D. I. *Trends Anal. Chem.* **2005**, *24*, 285–294.

(60) Psychogios, N.; Hau, D. D.; Peng, J.; Guo, A. C.; Mandal, R.; Bouatra, S.; Sinelnikov, I.; Krishnamurthy, R.; Eisner, R.; Gautam, B.; Young, N.; Xia, J.; Knox, C.; Dong, E.; Huang, P.; Hollander, Z.; Pedersen, T. L.; Smith, S. R.; Bamforth, F.; Greiner, R.; McManus, B.; Newman, J. W.; Goodfriend, T.; Wishart, D. S. *PLoS One* **2011**, *6*, e16957.

(61) Bouatra, S.; Aziat, F.; Mandal, R.; Guo, A. C.; Wilson, M. R.; Knox, C.; Bjorndahl, T. C.; Krishnamurthy, R.; Saleem, F.; Liu, P.; Dame, Z. T.; Poelzer, J.; Huynh, J.; Yallou, F. S.; Psychogios, N.; Dong, E.; Bogumil, R.; Roehring, C.; Wishart, D. S. *PLoS One* **2013**, *8*, e73076.

(62) Dunn, W.; Broadhurst, D.; Begley, P.; Zelena, E.; Francis-McIntyre, S.; Anderson, N.; Brown, M.; Knowles, J. D.; Halsall, A.; Haselden, J. N.; Nicholls, A. W.; Wilson, I. D.; Kell, D. B.; Goodacre, R.; The Human Serum Metabolome (HUSERMET) Consortium. *Nat. Protoc.* **2011**, *6*, 1060–1083.

(63) Ramautar, R.; Demirci, A.; Jong, G. J. d. *Trends Anal. Chem.* **2006**, *25*, 455–466.

(64) Dunn, W. B.; Wilson, I. D.; Nicholls, A. W.; Broadhurst, D. *Bioanalysis* **2012**, *4*, 2249–2264.

(65) Godzien, J.; Alonso-Herranz, V.; Barbas, C.; Armitage, E. G. *Metabolomics* **2015**, *11*, 518–528.

(66) Johnson, W. E.; Li, C.; Rabinovic, A. *Biostatistics* **2007**, *8*, 118–127.

(67) Katajamaa, M.; Orešič, M. *J. Chromatogr. A* **2007**, *1158*, 318–328.

(68) Sugimoto, M.; Kawakami, M.; Robert, M.; Soga, T.; Tomita, M. *Curr. Bioinform.* **2012**, *7*, 96–108.

(69) Junot, C.; Fenaille, F.; Colsch, B.; Bécher, F. *Mass Spectrom. Rev.* **2014**, *33*, 471–500.

(70) Huang, N.; Siegel, M. M.; Kruppa, G. H.; Laukien, F. H. *J. Am. Soc. Mass Spectrom.* **1999**, *10*, 1166–1173.

(71) Xu, Y.-F.; Lu, W.; Rabinowitz, J. D. *Anal. Chem.* **2015**, *87*, 2273–2281.

(72) Godzien, J.; Armitage, E. G.; Angulo, S.; Martinez-Alcazar, M. P.; Alonso-Herranz, V.; Otero, A.; Lopez-Gonzalvez, A.; Barbas, C. *Electrophoresis* **2015**, *36*, 2188–2195.

(73) Kuhl, C.; Tautenhahn, R.; Böttcher, C.; Larson, T. R.; Neumann, S. *Anal. Chem.* **2012**, *84*, 283–289.

(74) Hrydziuszko, O.; Viant, M. R. *Metabolomics* **2012**, *8*, S161–S174.

(75) Di Guida, R.; Engel, J.; Allwood, J. W.; Weber, R. J. M.; Jones, M. R.; Sommer, U.; Viant, M. R.; Dunn, W. B. *Metabolomics* **2016**, *12*, 93.

(76) Armstrong, L. E. *Nutr. Rev.* **2005**, *63*, S40–S54.

(77) Chetwynd, A. J.; Abdul-Sada, A.; Holt, S. G.; Hill, E. M. *J. Chromatogr. A* **2016**, *1431*, 103–110.

(78) Dieterle, F.; Ross, A.; Schlotterbeck, G.; Senn, H. *Anal. Chem.* **2006**, *78*, 4281–4290.

(79) Ragan, T. J.; Bailey, A. P.; Gould, A. P.; Driscoll, P. C. *Anal. Chem.* **2013**, *85*, 12046–12054.

(80) Kirwan, J. A.; Weber, R. J. M.; Broadhurst, D. I.; Viant, M. R. *Sci. Data* **2014**, *1*, 140012.

(81) Davies, S. K.; Ang, J. E.; Revell, V. L.; Holmes, B.; Mann, A.; Robertson, F. P.; Cui, N.; Middleton, B.; Ackermann, K.; Kayser, M.; Thumser, A. E.; Raynaud, F. I.; Skene, D. J. *Proc. Natl. Acad. Sci. U. S. A.* **2014**, *111*, 10761–10766.

(82) van den Berg, R. a; Hoefsloot, H. C. J.; Westerhuis, J. a; Smilde, A. K.; van der Werf, M. J. *BMC Genomics* **2006**, *7*, 142.

(83) Liland, K. H. *Trends Anal. Chem.* **2011**, *30*, 827–841.

(84) Alonso, A.; Marsal, S.; Julià, A. *Front. Bioeng. Biotechnol.* **2015**, *3*, 23.

(85) Lawton, K. A.; Berger, A.; Mitchell, M.; Milgram, K. E.; Evans, A. M.; Guo, L.; Lawton, K. A.; Berger, A.; Mitchell, M.; Milgram, K. E.; Evans, A. M.; Guo, L.; Richard, W.; Kalhan, S. C.; Ryals, J. A.; Milburn, M. V. *Pharmacogenomics* **2008**, *9*, 383–397.

(86) Broadhurst, D. I.; Kell, D. B. *Metabolomics* **2006**, *2*, 171–196.

(87) Goodacre, R.; Broadhurst, D.; Smilde, A. K.; Kristal, B. S.; Baker, J. D.; Beger, R.; Bessant, C.; Connor, S.; Capuani, G.; Craig, A.; Ebbels, T.; Kell, D. B.; Manetti, C.; Newton, J.; Paternostro, G.; Somorjai, R.; Sjöström, M.; Trygg, J.; Wulfert, F. *Metabolomics* **2007**, *3*, 231–241.

(88) Vinaixa, M.; Samino, S.; Saez, I.; Duran, J.; Guinovart, J. J.; Yanes, O. *Metabolites* **2012**, *2*, 775–795.

(89) Ludwig, D. A. *Aviat. Sp. Environ. Med.* **2005**, *76*, 675–680.

(90) Wasserstein, R. L.; Lazar, N. A. *Am. Stat.* **2016**, *70*, 129–133.

(91) Colquhoun, D. *R. Soc. Open Sci.* **2014**, *1*, 140216.

(92) Austin, P. C.; Mamdani, M. M.; Juurlink, D. N.; Hux, J. E. *J. Clin. Epidemiol.* **2006**, *59*, 964–969.

(93) Ioannidis, J. P. A. *PLOS Med.* **2005**, *2*, e124.

(94) Henderson, M. P. A.; Cotten, S. W.; Rogers, M. W.; Willis, M. S.; McCudden, C. R. In *Clinical chemistry: Principles, techniques, and correlations*; Bishop, M. L., Fody, E. P., Schoeff, L. E., Eds.; Wolters Klumer Health / Lippincott Williams & Wilkins: Philadelphia (PA), 2013; pp 52–89.

(95) Zweig, M. H.; Campbell, G. *Clin. Chem.* **1993**, *39*, 561–577.

(96) Obuchowski, N. A.; Lieber, M. L.; Wians, F. H. *Clin. Chem.* **2004**, *50*, 1118–1125.

(97) Cook, N. R. *Clin. Chem.* **2008**, *54*, 17–23.

(98) Dunn, W. B.; Erban, A.; Weber, R. J. M.; Creek, D. J.; Brown, M.; Breitling, R.; Hankemeier, T.; Goodacre, R.; Neumann, S.; Kopka, J.; Viant, M. R. *Metabolomics* **2013**, *9*, S44–S66.

(99) Brown, M.; Dunn, W. B.; Dobson, P.; Patel, Y.; Winder, C. L.; Francis-McIntyre, S.; Begley, P.; Carroll, K.; Broadhurst, D. I.; Tseng, A.; Swainston, N.; Spasic, I.; Goodacre, R.; Kell, D. B. *Analyst* **2009**, *134*, 1322–1332.

(100) Kind, T.; Wohlgemuth, G.; Lee, D. Y.; Lu, Y.; Palazoglu, M.; Shahbaz, S.; Fiehn, O. *Anal. Chem.* **2009**, *81*, 10038–10048.

(101) Creek, D. J.; Jankevics, A.; Breitling, R.; Watson, D. G.; Barrett, M. P.; Burgess, K. E. V. *Anal. Chem.* **2011**, *83*, 8703–8710.

(102) Sugimoto, M.; Kikuchi, S.; Arita, M.; Soga, T.; Nishioka, T.; Tomita, M. *Anal. Chem.* **2005**, *77*, 78–84.

(103) D'Agostino, L. A.; Lam, K. P.; Lee, R.; Britz-McKibbin, P. *J. Proteome Res.* **2011**, *10*, 592–603.

(104) Oberacher, H.; Pavlic, M.; Libiseller, K.; Schubert, B.; Sulyok, M.; Schuhmacher, R.; Csaszar, E.; Köfeler, H. C. *J. Mass Spectrom.* **2009**, *44*, 485–493.

(105) Allen, F.; Pon, A.; Wilson, M.; Greiner, R.; Wishart, D. *Nucleic Acids Res.* **2014**, *42*, 1–6.

(106) Bowen, B. P.; Northen, T. R. *J. Am. Soc. Mass Spectrom.* **2010**, *21*, 1471–1476.

(107) Koulman, A.; Lane, G. A.; Harrison, S. J.; Volmer, D. A. *Anal. Bioanal. Chem.* **2009**, *394*, 663–670.

(108) Xia, J.; Wishart, D. S.; Valencia, A. *Bioinformatics* **2011**, *27*, 2342–2344.

(109) Goodsaid, F. M.; Amur, S.; Aubrecht, J.; Burczynski, M. E.; Carl, K.; Catalano, J.; Charlab, R.; Close, S.; Cornu-Artis, C.; Essioux, L.; Fornace, A. J.; Hinman, L.; Hong, H.; Hunt, I.; Jacobson-Kram, D.; Jawaid, A.; Laurie, D.; Lesko, L. J.; Li, H.-H.; Lindpaintner, K.; Mayne, J.; Morrow, P.; Papaluca-Amati, M.; Robison, T. W.; Roth, J.; Schuppe-Koistinen, I.; Shi, L.; Spleiss, O.; Tong, W.; Truter, S. L.; Vonderscher, J.; Westelinck, A.; Zhang, L.; Zineh, I. *Nat. Rev. Drug Discov.* **2010**, *9*, 435–445.

(110) Zaninotto, M.; Mion, M. M.; Novello, E.; Altinier, S.; Plebani, M. *Clin. Chim. Acta* **2007**, *381*, 14–20.

(111) Goodsaid, F. M.; Mendrick, D. L. *Sci. Transl. Med.* **2010**, *2*, 47ps44.

(112) The Lewin Group. *Laboratory medicine: A national status report*; 2008.

(113) The Lewin Group. *The Value of laboratory screening and diagnostic tests for prevention and health care improvement*; 2009.

(114) Plebani, M. *Clin. Chem. Lab. Med.* **2006**, *44*, 750–759.

(115) Agarwal, R. *Lab. Med.* **2014**, *45*, 80–88.

(116) Magnusson, B.; Örnemark, U. *Eurachem guide: The fitness for purpose of analytical methods - A laboratory guide to method validation and related topics*, 2nd ed.; 2014.

(117) Centers for Disease Control and Prevention; Centers for Medicare and Medicaid Services; Health and Human Services. *Fed. Regist.* **2003**, *68*, 3639–3714.

(118) Standards Council of Canada. *PALCAN guidance for the validation of test methods (CAN-P-1629)*; Ottawa, 2006.

(119) Food and Drug Administration. *Guidance for industry: Bioanalytical method validation*; 2001.

(120) Thompson, M.; Ellison, S. L. R.; Wood, R. *Pure Appl. Chem.* **2002**, *74*, 835–855.

(121) Peters, F. T.; Maurer, H. H. *Accredit. Qual. Assur.* **2002**, *7*, 441–449.

(122) Gallaher, M.; Mobley, L.; Klee, G.; Schryver, P. *The impact of calibration error in medical decision making*; 2004.

(123) Krasowski, M. D.; Drees, D.; Morris, C. S.; Maakestad, J.; Blau, J. L.; Ekins, S. *BMC Clin. Pathol.* **2014**, *14*, 33.

(124) Hawley, J. M.; Owen, L. J.; Lockhart, S. J.; Monaghan, P. J.; Armston, A.; Chadwick, C. A.; Wilshaw, H.; Freire, M.; Perry, L.; Keevil, B. G. *Clin. Chem.* **2016**, *62*, 1220–1229.

(125) Chesher, D. *Clin. Biochem. Rev.* **2008**, *29*, S23–S26.

(126) Peake, M.; Whiting, M. *Clin. Biochem. Rev.* **2006**, *27*, 173–184.

(127) Standards Council of Canada. *Program requirements for applicant and accredited medical laboratories (CAN-P-1569:2014)*; Ottawa, 2014.

(128) Giavarina, D. *Biochem. Medica* **2015**, *25*, 141–151.

(129) Westgard, Q. C. Quality requirements: Desirable biological variation database specifications https://www.westgard.com/biodatabase1.htm (accessed Nov 24, 2016).

(130) Nimni, M. E.; Han, B.; Cordoba, F. *Nutr. Metab.* **2007**, *4*, 24.

(131) Carbonero, F.; Benefiel, A. C.; Alizadeh-Ghamsari, A. H.; Gaskins, H. R. *Front. Physiol.* **2012**, *3*, 448.

(132) van den Born, J. C.; Frenay, A.-R. S.; Bakker, S. J. L.; Pasch, A.; Hillebrands, J.-L.; Lambers Heerspink, H. J.; van Goor, H. *Nitric Oxide* **2016**, *55–56*, 18–24.

(133) van den Berg, E.; Pasch, A.; Westendorp, W. H.; Navis, G.; Brink, E. J.; Gans, R. O. B.; van Goor, H.; Bakker, S. J. L. *J. Am. Soc. Nephrol.* **2014**, *25*, 1303–1312.

(134) Macedo, A. N.; Jiwa, M. I. Y.; Macri, J.; Belostotsky, V.; Hill, S.; Britz-McKibbin, P. *Anal. Chem.* **2013**, *85*, 11112–11120.

(135) Tan, W.-H.; Eichler, F. S.; Hoda, S.; Lee, M. S.; Baris, H.; Hanley, C. A.; Grant, P. E.; Krishnamoorthy, K. S.; Shih, V. E. *Pediatrics* **2005**, *116*, 757–766.

(136) World Health Organization. *Assessment of iodine deficiency disorders and monitoring their elimination: a guide for programme managers*, 3rd ed.; WHO: Geneva, 2007.

(137) Li, M.; Eastman, C. J. *Nat. Rev. Endocrinol.* **2012**, *8*, 434–440.

(138) Macedo, A. N.; Teo, K.; Mente, A.; McQueen, M. J.; Zeidler, J.; Poirier, P.; Lear, S. A.; Wielgosz, A.; Britz-McKibbin, P. *Anal. Chem.* **2014**, *86*, 10010–10015.

(139) Mak, D. Y.; Stephenson, A. L.; Lands, L. C. *J. Cyst. Fibros.* **2016**, *15*, 302–308.

(140) Munck, A.; Mayell, S. J.; Winters, V.; Shawcross, A.; Derichs, N.; Parad, R.; Barben, J.; Southern, K. W. *J. Cyst. Fibros.* **2015**, *14*, 706–713.

(141) Kutyshenko, V. P.; Molchanov, M.; Beskaravayny, P.; Uversky, V. N.; Timchenko, M. A. *PLoS One* **2011**, *6*, e28824.

(142) Calderón-Santiago, M.; Priego-Capote, F.; Jurado-Gámez, B.; Luque de Castro, M. D. *J. Chromatogr. A* **2014**, *1333*, 70–78.

(143) Calderón-Santiago, M.; Priego-Capote, F.; Turck, N.; Robin, X.; Jurado-Gámez, B.; Sanchez, J. C.; Luque De Castro, M. D. *Anal. Bioanal. Chem.* **2015**, *407*, 5381–5392.

(144) Delgado-Povedano, M. M.; Calderón-Santigao, M.; Priego-capote, F.; Luque de Castro, M. D. *Anal. Chim.* **2016**, *905*, 115–125.

(145) Hooton, K.; Han, W.; Li, L. *Anal. Chem.* **2016**, *88*, 7378–7386.

(146) Kuehnbaum, N. L.; Kormendi, A.; Britz-Mckibbin, P. *Anal. Chem.* **2013**, *85*, 10664–10669.

(147) Davies, J. C.; Wainwright, C. E.; Canny, G. J.; Chilvers, M. A.; Howenstine, M. S.; Munck, A.; Mainz, J. G.; Rodriguez, S.; Li, H.; Yen, K.; Ordoñez, C. L.; Ahrens, R. *Am. J. Respir. Crit. Care Med.* **2013**, *187*, 1219–1225.

Chapter II

Strong Anion Determination in Biological Fluids by Capillary Electrophoresis with Indirect UV Detection for Clinical Diagnostics

Authors of this work are Adriana Nori de Macedo, Mohammad Irfan Yasin Jiwa, Joseph Macri, Vladimir Belostotsky, Stephen Hill, and Philip Britz-McKibbin.

Anal. Chem. **85**, 11112-11120, 2013.

I conducted most of the experiments for optimization and validation of the method, performed the sulfate analysis in pediatric urine samples, and did most of the data analysis, as well as wrote an initial manuscript draft used for publication. Other co-authors played roles in patient recruitment, specimen collection, and provided feedback on the manuscript draft.

Chapter II: Strong Anion Determination in Biological Fluids by Capillary Electrophoresis with Indirect UV Detection for Clinical Diagnostics

2.1 Abstract

New methods for quantitative analysis of strong anions are required for diagnostic testing of human diseases. Current techniques suffer from poor selectivity and/or long analysis times that are not amenable for labile anions in high-saline or volume-restricted samples. We introduce a rapid assay (<5 min) based on capillary electrophoresis (CE) with indirect UV detection for simultaneous analysis of sulfate, sulfite, and chloride in human urine, plasma, and sweat specimens. Remarkable selectivity for strong anions is achieved by using an acidic background electrolyte under reversed polarity that results in electrokinetic rejection of matrix interferences at the capillary inlet. A dual co-ion probe system consisting of 5 mM naphthalene disulfonate (NDS) and 5 mM naphthalene trisulfonate (NTS) in 0.4 M formic acid, pH 2.0 is developed for detection of UV transparent anions ($S/N \approx 3$, 60 μM with a 25 μm inner diameter fused-silica capillary) with good peak symmetry and baseline stability. Due to the chemical reactivity of sulfite, dilute formaldehyde is used as a reagent to form an acid-stable hydroxymethylsulfonate adduct. Method validation confirmed excellent linearity ($R^2 > 0.999$), good accuracy (mean bias ≈ 7%), and acceptable long-term reproducibility ($CV < 10\%$) over 20 days. The assay allows for artifact-free determination of sulfate and sulfite with consistent results for chloride when compared to standard electrochemical methods ($R^2 > 0.975$). Preliminary data suggest that kidney-stone formers have lower urinary sulfate excretion relative to non-kidney-stone patient controls ($p = 0.0261$). CE offers a selective yet robust platform for routine analysis of strong anions that is needed for confirmatory testing of cystic fibrosis, sulfite oxidase deficiency, urolithiasis, and other disorders of sulfur metabolism and/or anion transport.

2.2 Introduction

Sulfate is a major end-product in the metabolism of sulfur-containing amino acids, and its homeostasis is regulated by dietary intake and urine excretion.[1] Inorganic sulfate plays important roles in human health, including secondary metabolism, xenobiotic detoxification and colonic microflora activity involving sulfate-reducing bacteria.[2] Although sulfate is not directly involved in kidney stone formation, it influences urine supersaturation and thus the solubility of ions that form kidney stones,[3] while also serving as a marker of protein intake, renal insufficiency and other kidney disorders.[4] The reactive intermediate of sulfur metabolism, sulfite is normally not detectable in healthy individuals, but specific conditions that impair the activity of sulfite oxidase result in elevated levels of this neurotoxic anion. For instance, sulfite oxidase deficiency is a rare genetic disorder that causes toxic accumulation of sulfite triggering severe seizures and neurological impairment.[5] Problems related to sulfite are also reported in cases of molybdenum deficiency and allergies due to hypersensitivity to sulfite-preserved foods/drugs.[6] Despite the many roles of sulfur metabolism in gene expression and cell redox status, current dietary guidelines recommend a daily intake that may be inadequate for optimum human health.[7] Chloride represents a major anion interference in assays for sulfate and/or sulfite that is measured to assess electrolyte balance and hydration status, while also representing the gold standard in diagnostic sweat testing for cystic fibrosis.[8]

Classical methods for sulfate and/or sulfite analysis using turbidimetry[9] or colorimetric test strips[10] are prone to bias due to matrix interferences in biological fluids. Simultaneous analysis of strong anions with improved selectivity is achieved by ion chromatography,[11] but require complicated sample handling protocols and/or long analysis times that are not suitable for routine clinical practice. Capillary electrophoresis (CE) enables high efficiency separations of UV-transparent strong anions when using indirect photometric[12–16] or contactless conductivity detection.[17,18] However, the lack of reliable methods for sulfate

and/or sulfite determination is a major reason why these ions are not measured routinely in most clinical laboratories, which need to satisfy rigorous method validation for diagnostic testing.[19] Robust methods that enable direct analysis of multiple strong anions with minimal sample handling while also being compatible to volume-restricted specimens (< 10 µL) from infants are desirable in a clinical setting. Herein, we introduce and validate a new CE assay for sulfate, sulfite and chloride that is relevant for clinical diagnostic testing of several human diseases.

2.3 Experimental Section

2.3.1 Chemicals and reagents

Sodium sulfate decahydrate, sodium thiocyanate, sodium chloride, sodium nitrate, sodium nitrite, oxalic acid, formic acid, perchloric acid, indoxyl-3-sulfate and hydrobromic acid were obtained from Sigma-Aldrich (St. Louis, MO, USA), whereas sodium sulfite was purchased from Alfa-Aesar (Ward Hill, MA, USA). The anionic chromophores 1,3(6,7)-naphthalenetrisulfonic acid trisodium salt hydrate (NTS) and 1,5-naphthalenedisulfonic acid disodium salt hydrate (NDS) were also obtained from Sigma-Aldrich. Concentrated formaldehyde (37% v) was obtained from Caledon Inc. (Georgetown, ON, Canada), and sodium thiosulfate pentahydrate was purchased from EMD Chemicals (Darmstadt, Germany). Stock solutions of sulfate were prepared by dissolving sodium sulfate in de-ionized water using a Barnstead EASYpure II LF system (Dubuque, IA, USA) to obtain a final concentration 500 mM. Stock solutions of chloride, nitrate, nitrite (1.0 M) and thiosulfate (200 mM) were also prepared dissolving their sodium salts in de-ionized water. However, sulfite was prepared fresh daily by dissolution in degassed de-ionized water containing methanol (10% v) to enhance its long-term stability while stored at 4ºC. All other solutions were stored in plastic transparent tubes and kept at room temperature.

2.3.2 Instrumentation

All CE separations were performed in a P/ACE MDQ system equipped with a photodiode array detector from Beckman-Coulter Inc. (Fullerton, CA, USA). Uncoated fused-silica capillaries (Polymicro Technologies Inc., Phoenix, USA) with different internal diameters (75, 50 or 25 µm) but similar outer diameters (360 µm) and total capillary lengths (60 cm) and an effective capillary length to detector (50 cm) were used during assay optimization. All CE separations were performed at 25ºC, where samples are introduced via hydrodynamic injection under 0.5 psi for 10 s unless otherwise stated. CE separations were performed under reversed polarity using an applied voltage of -30 kV (capillary outlet as anode), where indirect UV absorbance is monitored at 214 nm using a reference wavelength at 400 nm to improve baseline stability with a data acquisition rate of 4 Hz. For clarity, the UV absorbance scale is inverted during data collection, such that strong anions in an electropherogram display positive peak responses. New capillaries are conditioned with methanol for 5 min, followed by water for 5 min, and the background electrolyte (BGE) for 20 min (20 psi). Before each separation, the capillary is rinsed with the BGE for 3 min (20 psi). For overnight storage, the capillary is rinsed with de-ionized water for 5 min and left immersed in vials with de-ionized water. Each morning the capillary is flushed of BGE for 15 min. UV absorbance spectra of strong anions and co-ion probes were acquired using a Cary 50 UV-vis spectrophotometer (Varian Inc., Palo Alto, USA).

2.3.3 Sample pretreatment of biological fluids

Sample collection of biological fluids for CE assay validation was approved by the Hamilton Health Science/Faculty of Health Sciences Research Ethics Board. Pooled 24 h human urine samples from children (5-17 years old, n = 20) at McMaster University were collected in sterilized tubes and kept frozen (-80ºC) prior to thawing and sample workup. Also, randomized single-spot urine

specimens (2-17 years old, *n* = 29) were also collected at the Nephrology Clinic at McMaster Children's Hospital from kidney stone formers (*n* = 10, 7 females/3 males) and non-kidney stone controls (*n* = 19, 8 females/11 males) who consisted of a mixture of patients with hypertension, hematuria, proteinuria, anatomical abnormalities or normal function, but with family history of kidney disease or urinary tract infection. Exclusion criteria included ages below two years old and dilute/low volume urine samples with osmolality values below 50 mOsm/kg. Kidney stone cases were confirmed by performing diagnostic kidney ultrasound scans at McMaster Children's Hospital. The chemical composition of isolated kidney stones excreted from patients were confirmed only in some cases (*n* = 5), including calcium oxalate, struvite, and calcium phosphate. An aliquot of 250 µL of urine was transferred to a 0.5 mL tube containing 10 µL of 150 mM perchlorate, 10 µL of 2% v/v formaldehyde, and 230 µL of a buffer composed by 20 mM formic acid, pH 2.6. The mixture was mixed by vortex for 30 s and centrifuged at 6,700 g for 10 min to remove any particulates. A 60 µL aliquot of the supernatant was transferred to another 0.5 mL tube and analyzed by CE with indirect UV detection. Similarly, pooled human plasma samples (*n* = 20) were fractionated from whole blood samples collected in lithium heparin coated tubes and stored frozen (-80ºC). Plasma samples were thawed once and then deproteinized by ultrafiltration using a molecular weight cut-off filter of 3 kDa (Pall Corp., Port Washington, NY, USA) at 14,100 g for 20 min. A 25 µL aliquot of filtered plasma was transferred to a 0.5 mL tube, adding 3 µL of 50 mM perchlorate and 22 µL of 20 mM formic acid buffer, pH 2.6. The mixture was homogenized by vortex for 30 s prior to analysis. Blank samples (de-ionized water) processed with lithium and sodium heparin tubes and ultrafiltration tubes confirmed the lack of detectable levels of sulfate, sulfite and chloride. Stimulated human sweat samples (*n* = 3) were collected from patients at the Cystic Fibrosis Clinic at McMaster University. Sweating was induced by pilocarpine iontophoresis using a Webster Model 3700 Macroduct Sweat Capillary Collection

System (Wescor Inc. Logan, UT, USA) with electrodes composed of solid agar discs containing 0.5% w/w pilocarpine nitrate, which were attached to subjects right forearm for 5 min at 1.5 mA. Sweat samples (> 30 µL) were collected via a spiral capillary tube containing blue dye for visual confirmation prior to storage at -20°C. Chloride measurements for sweat were performed by a chloridometer via coulometric titration with silver ions using a temperature-controlled conductivity cell (Wescor Sweat-Check Model 3120), whereas an Abbott Architect ci4000 ion selective electrode system using integrated chip technology (Abbott Diagnostics Canada, Mississauga, ON, Canada) was used for chloride measurements in human urine. In the case of single-spot urine samples, osmolality and creatinine were also measured by automated freezing point depression (Advanced Micro Osmometer 3300) and Jaffé reaction (ci4100 Abbott Diagnostics) methods, respectively.

2.3.4 Method calibration and assay validation

Calibration standards at seven concentration levels were prepared in triplicate by dilution of the stock solutions in 20 mM formic acid, pH 2.6 using 3 mM perchlorate as an internal standard. Weighted linear least-squares regression was used to calculate the calibration equation, and the linearity was evaluated by the coefficient of determination (R^2), while sensitivity was evaluated using the slope of the calibration curve. Accuracy was evaluated via spike/recovery experiments (n = 3) for pooled human urine, plasma, and sweat samples that were spiked with standard solutions of sulfate, sulfite and chloride at two concentration levels and analyzed in duplicate by CE with indirect UV detection. In addition, method accuracy for chloride in urine and sweat samples was independently assessed using a validated ion selective electrode system and chloridometer, respectively. The limit of detection ($S/N \approx 3$) and limit of quantification ($S/N \approx 10$) were determined from the slope of calibration curve and background noise measured at the migration time of each anion. Intraday precision (repeatability) was evaluated by the coefficient of variation (CV) of the relative peak area (RPA) and relative

migration time (RMT) for ten replicates of pooled urine and plasma samples at two concentration levels for sulfate and sulfite and one concentration level for chloride. Interday precision (reproducibility) was examined over 20 days by analyzing a series of aliquots of pooled urine samples in duplicate each day at two concentration levels with replicate injections separated by at least 2 h. Three different fused-silica capillaries were installed and operated by two analysts during the 20 day validation study for assessment of long-term reproducibility. Each sequence of runs also included two quality controls (QCs), which was a standard mixture of strong anions (50 mM chloride and 3 mM perchlorate or 3mM perchlorate, 8 mM sulfate, 1 mM sulfite as formaldhyde adduct). Due to impurities of sulfate detectable in high concentrations of chloride, QCs and calibrant solutions with chloride and sulfate were analyzed separately. Robustness was assessed by changing the ionic strength of the BGE (± 5%), namely formic acid (380 or 420 mM) and co-ion probes (4.75 or 5.25 mM), since they impact separation and detection performance of the assay. A pooled urine sample spiked with 1 mM sulfite was used in this two factor/two level (2^2) experimental design experiment with triplicate central point in order to evaluate the statistical significance of one- and two-way interactions on measured responses, namely RPA, RMT and peak resolution. Sulfite stability in neutral and acidic pH was evaluated by measuring changes in UV spectra at the peak absorbance for 1.0 mM sulfite solutions prepared in 20 mM phosphate buffer, pH 6.2 (λ_{max} = 195 nm) and 1.8 (λ_{max} = 274 nm). The solutions were kept at room temperature or on ice and the absorbance was measured over time with 10 min intervals up to 2 h after initial solution preparation. Sulfite stability in pooled urine was also examined by spiking 0.1 mM sulfite and then adding dilute formaldehyde at different times intervals up to 5 h, which was performed in triplicate and analyzed by CE with indirect UV detection. Similarly, sulfate and chloride stabilities were tested for a pooled urine sample (n = 6) at room temperature for up to 92 h and after one to three freeze-thaw cycles. In this case, individual aliquots of pooled urine samples

were kept at room temperature (≈ 25ºC) while others were stored in a -80ºC freezer. All samples were analyzed in triplicate, and the stability was evaluated as a function of residence time and storage temperature for strong anions. All data processing, linear regression and non-parametric statistical tests were performed using Igor Pro 5.0 (Wavemetrics Inc., Lake Oswego, OR, USA) and Origin Pro 8 (OriginLab Corporation, Northampton, MA, USA). Box whisker plots depict median values with their 25-75th percentiles, whereas outliers are defined as data beyond 1.5x of interquartile range. Non-parametric statistics are used to compare urine profiles (*p*-values) using a Mann-Whitney U test for single-spot urine samples from pediatric patients.

2.4 Results

2.4.1 Method development and assay optimization

An acidic BGE (0.4-1.0 M formic acid, pH 1.8-2) is used for the separation under reversed polarity in order to achieve high selectivity for strong anions[20] in biological fluids as depicted in **Figure 2.1A**. In this configuration, cationic (*e.g.*, amino acids) and weakly acidic/neutral (*i.e.*, organic acids) metabolites within a sample plug migrate out of the capillary with the electroosmostic flow (EOF). In contrast, only strongly ionic solutes ($pK_a < 2$) possess a high negative mobility to counter the EOF and migrate past the detector. **Figure 2.1B** shows that sulfate is partially ionized ($pK_{a2} \approx 1.9$) with a slower negative mobility than chloride under these conditions due to its lower charge density. Because sulfate and chloride are both UV-transparent anions, a strongly acidic co-ion probe, NTS, is added as a chromophore to the BGE to allow for indirect UV detection.[21] Because sulfite oxidizes spontaneously to sulfate under ambient conditions, all samples were first treated with dilute formaldehyde as a reagent to form a stable yet UV transparent

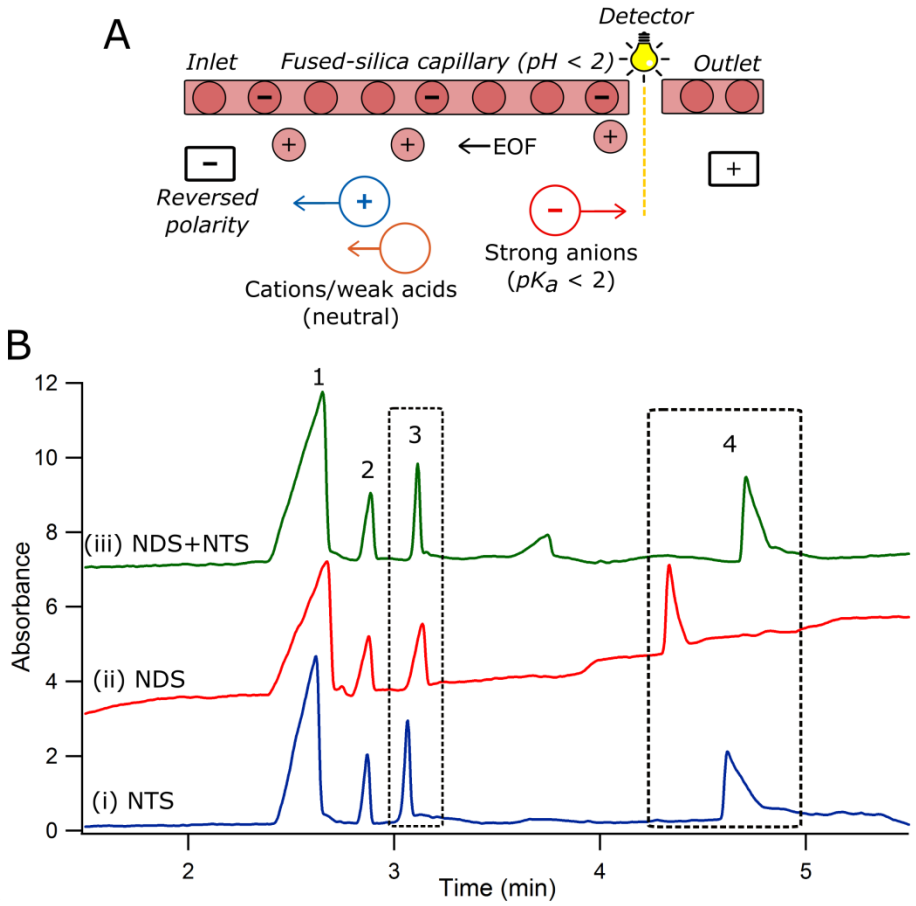

Figure 2.1. (**A**) Assay configuration for selective analysis of strong anions under acidic conditions with reversed polarity by CE, where matrix interferences (cations/neutrals) within sample are electrokinetically rejected at the capillary inlet. (**B**) Electropherogram overlay comparing the impact of one or two naphthalene sulfonates as co-ion probes for indirect detection of UV transparent strong anions, including 100 mM chloride (1), 10 mM perchlorate (2), sulfate (3) and sulfite (4) as its hydroxymethylsulfonate adduct after reaction with dilute formaldehyde. The use of a binary mixture of co-ion probes (NDS+NTS) offers better overall peak symmetry for sulfate and sulfite that differ widely in their intrinsic mobility, where * represents a system peak that arises when using the dual co-ion probe system.

hydroxymethylsulfonate adduct.[22] This reaction occurs rapidly under acidic conditions (pH 2.6) at room temperature, where the sulfite adduct migrates after sulfate due to its larger hydrodynamic volume. A dual co-ion probe system based on an equimolar mixture of NDS and NTS is used as a way to generate sharper and more symmetric peaks for sulfate and sulfite due to mobility matching[23] when

using indirect UV detection (**Figure S2.1** and **Table S2.1**). Perchlorate is used as a convenient internal standard due to its intermediate mobility relative to chloride and sulfate. Despite its shorter optical path length, the use of a narrow fused-silica capillary (25 µm inner diameter) results in a more stable UV baseline with better signal to noise for detection of strong anions (**Figure S2.2**). Other UV absorbing strong anions do not interfere in this method due to their suppressed signal and high detection limits, including iodide, thiosulfate, citrate and nitrate. However, CE with direct UV detection (no co-ion probes in BGE) allows for analysis of nitrate and indoxyl-3-sulfate in pooled urine samples (**Figure S2.3**). Thus, the inherent selectivity of the assay derives from both the unique separation and detection configuration, which enables direct analysis of human biofluids without complicated sample workup or spectral interferences.

2.4.2 Stability tests, method calibration, and biofluid analysis

Reliable diagnostic tests for sulfite[24] are hampered by its intrinsic chemical reactivity that is dependent on solution properties and sample storage conditions. The pH dependent stability of sulfite is first examined by measuring changes in its peak absorbance as a function of time (**Figure 2.2A**). Sulfite oxidation is catalyzed under acidic conditions (pH 1.8) with an 80% loss in response measured within 2 h at room temperature that is not compatible with CE conditions. In contrast, sulfite is stable under weakly acidic/neutral buffer conditions (pH 6.5) characteristic of most human biofluids. However, standard amounts of sulfite spiked into freshly collected urine (pH ≈ 6.5) undergo a loss in signal response over time prior to formaldehyde addition that is attenuated when stored on ice as shown in **Figure 2.2B**. Thus, other matrix components in urine enhance sulfite reactivity. In this case, collection tubes are ideally pre-filled with dilute formaldehyde for rapid capture of sulfite that prevents a negative bias of up to 30%. Although chloride and sulfate are inert anions, co-precipitation may occur

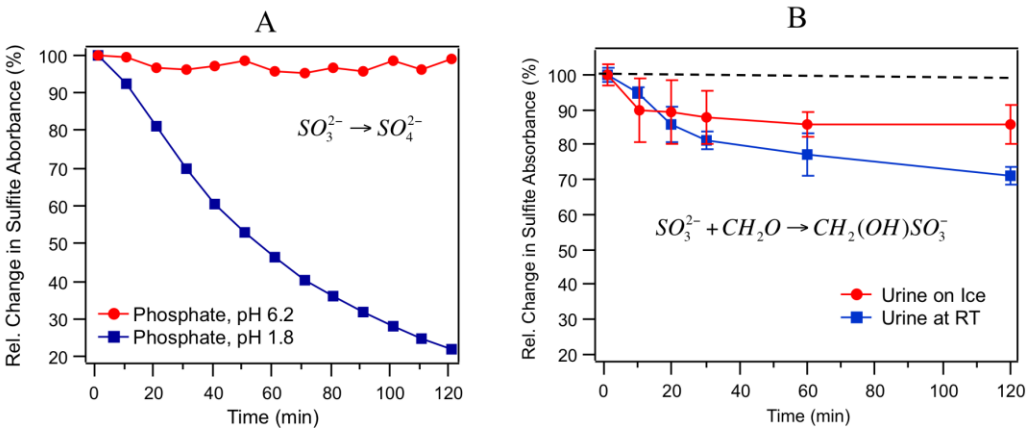

Figure 2.2. (**A**) The pH-stability of sulfite (0.1 mM) that spontaneously oxidizes to sulfate under strongly acidic conditions (pH 1.8) yet it is stable for at least 2 h in weakly acidic/neutral buffer conditions (pH 6.2) at room temperature. (**B**) The stability of sulfite was also examined in a freshly collected urine samples by spiking 1.0 mM sulfite (n = 3, error bars ± 1SD) and then measuring changes in hydroxymethylsulfonate by CE with indirect UV detection. The addition of dilute formaldehyde was varied over time after initial spiking of sulfite into urine at room temperature or when urine is stored on ice. Unlike weakly acidic buffer conditions, sulfite is more unstable in human urine with about a 30% loss within 2 h at room temperature that was attenuated to 15% when stored on ice.

during urine storage; however, minimal bias within ± 4% is demonstrated for chloride and sulfate when urine is analyzed directly by CE relative to aged samples stored for up to 92 h at room temperature or samples undergoing three consecutive freeze/thaw cycles while stored at -80°C (**Table S2.2**).

The analytical performance of the CE assay is assessed in terms of several figures of merit as summarized in **Table 2.1**. Overall, excellent linearity (R^2 > 0.999) over a wide dynamic range (24 to 200-fold concentration) is achieved when using weighted linear regression for calibration curves of chloride, sulfate and sulfite as its formaldehyde adduct (**Figure S2.4**). This linear dynamic range spans biologically relevant concentration levels with detection limits ($S/N \approx 3$) of 60 and 400 µM for sulfate/sulfite and chloride, respectively. In all cases, measured responses correspond to the relative peak area (RPA) ratio of analyte normalized to perchlorate as internal standard. Similarly, migration times for strong anions were normalized to perchlorate in terms of relative migration times

Table 2.1. Figures of merit for quantitative analysis of strong anions by CE with indirect UV detection.

Parameters	Chloride	Sulfate	Sulfite
RMT (± SD)	0.902 ± 0.024	1.085 ± 0.013	1.676 ± 0.012
LOD (mM)	0.40	0.06	0.06
LOQ (mM)	1.0	0.10	0.10
Linear regression			
Slope (± SD)	0.284 ± 0.002	0.750 ± 0.001	1.28 ± 0.01
y-Intercept (± SD)	-0.068 ± 0.014	0.065 ± 0.001	0
Linearity (R^2)	1.000	0.999	0.999
Linear range (mM)	1.0 – 140.0	0.1 – 20.0	0.1 – 2.4

(RMT) as a way to correct for long-term variations in EOF. Intra-day repeatability (n = 10) for strong anions was evaluated at two concentration levels (except for chloride) in pooled human urine and plasma specimens (**Table S2.3**). In general, good precision was measured in terms of quantitation and migration behavior with average *CV* for RPAs and RMTs of 9% and 0.2%, respectively. The analysis of pooled 24 h human urine samples from pediatric subjects (n = 20) confirmed that the method was selective for chloride and sulfate (**Figure 2.3A**) with mean concentration levels of 107 ± 6 mM and 10.9 ± 0.6 mM, respectively. Endogenous sulfite is not detected (< 0.1 mM) in all biological fluids tested; however, sulfite spiked into both urine and plasma confirmed excellent selectivity and resolution with analogous performance compared to standard solutions (**Figure 2.1B**). Although pooled plasma filtrates have similar mean chloride levels of 117 ± 6 mM, sulfate is over an order of magnitude lower than 24 h urine samples at 0.89 ± 0.11 mM as shown in **Figure 2.3B**. Blank filtrate samples revealed no detectable background levels of sulfate, sulfite or chloride derived from blood collection and ultrafiltration devices that avoided pre-washing with de-ionized water (data not shown). **Figure 2.3C** demonstrates that chloride is quantified in small volumes of human sweat (≈ 5 µL) stimulated by pilocarpine

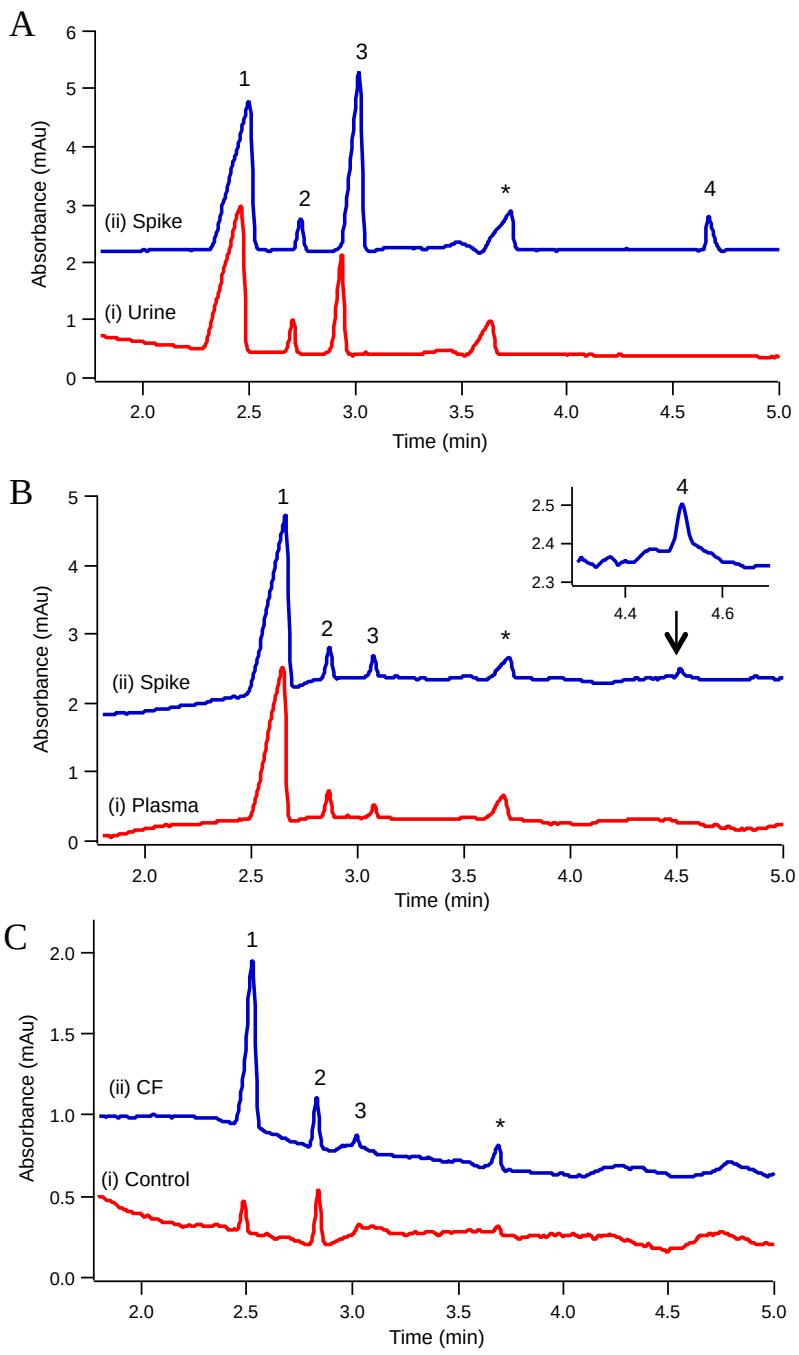

Figure 2.3. Rapid determination of chloride (1), perchlorate (2), sulfate (3) and/or sulfite (4) in human biological fluids by CE with indirect UV detection, including (**A**) pooled urine, (**B**) plasma filtrate and (**C**) sweat samples. Samples were diluted in buffer with internal standard (2) and analyzed directly by CE (i) or spiked with sulfate and sulfite (ii) using 16 and 2 mM, or 0.4 and 0.4 mM for urine and plasma samples, respectively. Sweat samples represent (i) pooled control and (ii) cystic fibrosis (CF) patient with normal (< 30 mM) and elevated (≥ 60 mM) sweat chloride levels. Separation conditions are 0.4 M formic acid, 5 mM NDS, 5 mM NTS, pH 2.0 with indirect UV detection at 214 nm. Analyte peak numbering is the same as Figure 2.1.

ionotophoresis, including normal infants (n = 3) and a cystic fibrosis (CF) patient (n = 1) homozygous with the DF508 mutation.[8] In this case, sweat chloride is over 5-fold more elevated in the CF patient relative to non-CF controls with 71 ± 5 mM and 12.8 ± 0.3 mM, respectively. Confirmatory diagnosis of screen-positive CF patients in newborn screening is indicated by a sweat chloride concentration ≥60 mM.[25] Low micromolar levels of sulfate (≈ 100 µM) are detected in all diluted sweat specimens, however it is not reliably measured since responses are below the limit of quantification (*LOQ*). Sweat sulfate is reported to be differentially expressed in CF patients,[26] as well as subjects with chronic renal failure.[27]

2.4.3 Clinical validation and urinary sulfate in kidney-stone formers

Recovery studies are performed using standard solutions spiked into pooled urine and plasma (sulfate/sulfite), as well as normal sweat (chloride) specimens at two concentration levels, which demonstrate acceptable method accuracy with a mean bias of 7% (**Table S2.4**). Due to the lack of routine methods for sulfate and sulfite determination, external validation of the CE assay was evaluated for chloride in comparison to two validated electrochemical methods used in the clinical laboratory (**Figure S2.5**), namely ion selective electrode (potentiometry) and coloumetric titration (chloridometer). Correlation plots confirmed the high accuracy of the CE assay consistent with spike/recovery experiments as reflected by a coefficient of determination (R^2 = 0.976 and 0.999) and slope close to unity (0.95 and 0.99) for urine and sweat specimens, respectively. Method reproducibility (inter-day precision) is also evaluated based on duplicate injections of pooled urine samples at two concentration levels over 20 days (**Table S2.3**). Overall, long-term precision based on average *CV* derived from RPA (7%) and RMT (1.3%) for strong anions was excellent as shown in **Figure 2.4**. Furthermore, method robustness was also evaluated using a two factor/two level experimental design based on systematic variation of formic acid and probe

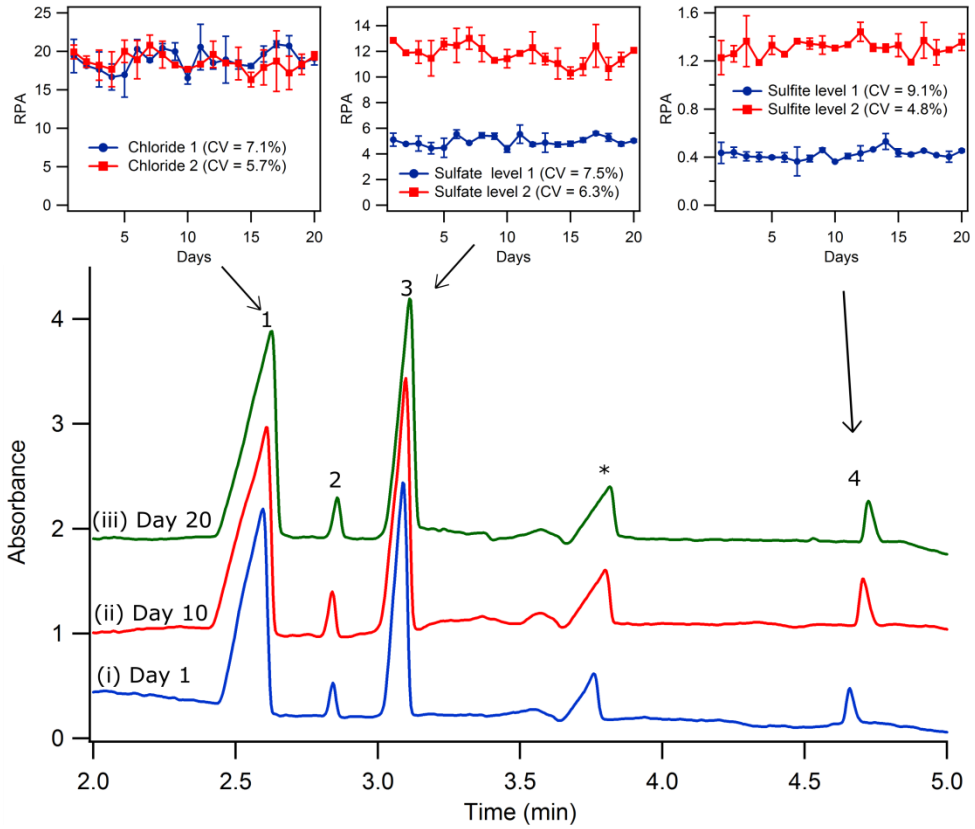

Figure 2.4. Overlay of representative electropherograms highlighting the interday reproducibility of CE assay for reliable analysis of pooled urine samples spiked with sulfite, where insets summarize daily average responses measured for strong anions at two concentration levels (except for chloride) over 20 days. Each sample aliquot was stored frozen and thawed once prior to CE with indirect UV detection in duplicate at two concentration levels. Overall, excellent long-term reproducibility was obtained with an average *CV* of about 7% and 1% for relative peak areas (RPA) and relative migration times (RMT), respectively. Separation conditions and analyte peak numbering similar to Figure 2.3.

co-ion concentrations by ± 5% relative to optimum buffer conditions. Overall, there is no significant impact ($p > 0.05$) of experimental variables on measured responses, including RMT, RPA and resolution (**Table S2.5**).

Given the growing incidence of urolithiasis among children and adolescents due to changing lifestyle and dietary habits,[28] a pilot study was performed to evaluate the differential urinary excretion pattern of sulfate among kidney stone formers.[29] In this case, randomized single-spot urine specimens were collected from pediatric patients during clinic visits, including kidney stone

formers (n = 10) and non-kidney stone patient controls (n = 19). Osmolality levels in single-spot urine samples (n = 27) were found to have lower overall variance (CV = 56%) with more consistent median values and lower interquartile range (730 ± 407 mOsm/kg) across a wide age group unlike creatinine, which is notably elevated in patients above 10 years old (**Figure S2.6**). Overall, there is a significant difference between osmolality-corrected urinary sulfate (p = 0.0459), as well as median sulfate concentration levels (p = 0.0261) between kidney stone formers and patient controls as depicted in box and whisker plots (**Figure S2.7**) with median and inter-quartile ranges of 10.7 ± 4.6 mM and 17.2 ± 8.0 mM, respectively. In contrast, urinary chloride, sulfate/chloride ratio and osmolality-corrected chloride are not statistically different (p > 0.05) due to the high biological variability of random single-spot urine samples. Receiver operating characteristic (ROC) curves also highlight the diagnostic performance of urinary sulfate to differentiate kidney stone formers from a diverse group of patient controls (AUC = 0.763; p = 0.0253) with a lower cutoff of 13.6 mM (**Figure S2.8**).

2.5 Discussion

2.5.1 Assay performance and reliable sulfite determination

The CE assay is simple, fast, selective, and robust and it offers a wide linear dynamic range, good accuracy and acceptable long-term reproducibility for reliable quantification of strong anions. In general, biological fluids are analyzed directly after a simple dilution or filtration step with minimal sample workup. Due to its tendency to spontaneously oxidize to sulfate, sulfite analysis is not performed routinely in clinical laboratories despite its relevance to the diagnosis of sulfite oxidase deficiency,[24] chronic renal failure,[30] acute pneumonia,[31] sulfite-related allergies[32] and other disorders associated with sulfur metabolism and/or molybdenum deficiency. Qualitative urine test strips are used for detection of

sulfite when performing confirmatory testing of sulfite oxidase deficiency.[10] However, they suffer from false-positives due to matrix interferences and false-negatives if samples are not properly stored.[33] As a result, other intermediates of sulfur metabolism need to be measured to confirm diagnosis, such as cystine, thiosulfate and *S*-sulfocysteine.[34] In our work, stability tests demonstrate that sulfite undergoes degradation in freshly collected urine samples that is avoided when using dilute formaldehyde upon sample collection. The sulfite adduct is formed rapidly and is stable when urine is stored in the freezer for up to 20 days, whereas chloride and sulfate require far less stringency. Although sulfite oxidase deficiency is a rare in-born error of metabolism that is likely under-diagnosed because neurological symptoms mimic hypoxic-ischemic insults,[24] unambiguous diagnosis can be achieved by CE via ratiometric sulfite/sulfate measurements in single-spot urine samples. The sensitivity of the current assay ($LOD \approx 60$ µM) is inadequate to quantify serum sulfite at low micromolar levels (≈ 5 µM) in healthy individuals,[32] however reliable measurements are feasible in clinically relevant cases of sulfite oxidase deficiency, where urinary sulfite levels can exceed 10 mM.[35]

2.5.2 Merits of assay for sulfate determination

Due to the lack of ion selective electrode membranes,[36] various methods have been developed for sulfate analysis yet they are not widely used in clinical practice due to their low sample throughput, inadequate selectivity and/or poor robustness.[1] Although largely considered an end-product of sulfur amino acid metabolism, there is growing interest in sulfate transport and regulation mechanisms due to their important roles in human health, including fetal development.[37] Classical methods for sulfate analysis are primarily based on barium precipitation using turbidimetry,[9] and ion chromatography.[11] However, phosphate is a matrix interference for sulfate when using barium for precipitation, whereas complicated sample handling is required to achieve reproducible data.[38]

Ion chromatography enables selective analysis of sulfate, however separation efficiency is poor with long analysis times needed to resolve sulfate from high levels of chloride and phosphate.[11] In our work, chloride and sulfate are resolved within about 3 min after injection of dilute urine, sweat or plasma filtrate samples, whereas matrix interferences are electrokinetically rejected at the capillary inlet (**Figure 2.1A**). The assay is robust as it can tolerate small changes in buffer conditions without major impact on separation performance as supported by long-term precision ($CV \approx 7\%$) over 20 days. Also, consistent results are achieved by CE for chloride quantification in urine and sweat samples when compared to two validated electrochemical methods. However, the use of buffer conditions with pH > 2 results in the co-migration of sulfate with chloride since the former anion becomes increasingly ionized, which is critical for method selectivity.[39] A dual co-ion probe system is used to improve peak symmetry for simultaneous analysis of sulfate and sulfite that are prone to peak fronting/tailing[23] when using a single chromophore alone. Other types of UV-active strong anions ($pK_a < 2$) are not detected with this assay due to signal suppression, however urinary nitrate and indoxyl-3-sulfate can be measured when using a BGE without co-ion probes. The latter anion is a major sulfate ester conjugate and tryptophan metabolite derived from gut microflora that is associated with impaired renal function and higher risk for cardiovascular disease,[40] whereas the former anion is a stable product of nitric oxide metabolism and putative biomarker of pediatric acute kidney injury.[41] This separation configuration is distinct from previous CE methods for sulfate analysis that are prone to spectral interferences, since they require amine or cationic surfactant additives to reverse the EOF under neutral or weakly alkaline conditions.[12,13] Although CE with indirect UV detection offers adequate sensitivity for sulfate and chloride determination in most biofluids, improved sensitivity is still needed for analysis of sweat sulfate, which can be achieved by direct injection of larger sample volumes with online sample preconcentration or when using contactless conductivity detection.[17]

2.5.3 Urinary sulfate for kidney stone risk assessment

Because serum and notably urinary sulfate levels are dependent on dietary intake, age and vitamin D status, reference concentrations in healthy adult subjects are reported to vary from 300-500 µM and 2-66 mM, respectively.[11] These sulfate levels are consistent with data measured in pooled 24 h urine (10.9 ± 0.6 mM), and median single-spot urine samples (15 ± 12 mM), whereas sulfate levels in pooled plasma filtrate samples are higher than the expected range at (0.89 ± 0.11 mM). The latter discrepancy may reflect the pediatric population examined in our study since normal reference levels are still lacking. Moreover, recovery studies and blank samples demonstrate good accuracy without artifacts from plasma ultrafiltration and blood collection. Due to its high abundance, sulfate influences urine supersaturation and the solubility of salts that can form kidney stones, such as calcium oxalate.[42] Preliminary studies indicate that urinary sulfate is significantly lower for kidney stone formers relative to non-kidney stone controls ($p = 0.0261$) who consist of a heterogeneous group of patients with kidney-related disorders, including hematuria, proteinuria, hypertension or anatomical abnormalities (**Figure S2.7**). Biological variability is a concern when analyzing randomized single-spot urine samples yet it represents a convenient surrogate to 24 h urine specimens for children during clinic visits. Creatinine is widely used for hydration status/urine volume correction, however it is not appropriate for pediatric patients ranging from infants to adolescents who have widely different muscle mass and dietary patterns.[43] In this case, osmolality should be used. Chloride concentrations, sulfate/chloride ratio and osmolality-corrected chloride levels are not statistically different between the two sub-groups ($p > 0.05$) unlike urinary sulfate and osmolality-corrected sulfate. In addition, no major differences in median creatinine and osmolality levels are measured between kidney stone formers and controls ($p > 0.05$). To date, there is conflicting data regarding the exact relationship of urinary sulfate and kidney stone risk,[21,38] likely due to inappropriate use of creatinine normalization and the large biological variance

within a pediatric cohort. The pathogenesis of stone formation in children remains poorly understood although urolithiasis is associated with several risk factors, including elevated urinary calcium and oxalate, lower citrate and decreased urine volume.[44] In our case, a urinary sulfate cutoff value of 13.6 mM provides moderate diagnostic performance (AUC = 0.763; sensitivity = 80%; specificity = 74%) when using ROC curves to classify kidney stone formers relative to a diverse patient control group in a nephrology clinic (**Figure S2.8**). However, because no single factor is adequate to characterize urolithiasis given its complex etiology, urine supersaturation has been proposed to assess relative risk as it takes into account the contributions of several major electrolytes involved in kidney stone formation, including sulfate.[45] Future work will examine the performance of sulfate and other major electrolytes associated with urine supersaturation as a way to predict kidney stone recurrence and patient responses to citrate therapy when using 24 h urine specimens corrected for dietary protein intake.

2.6 Conclusion

CE with indirect UV detection offers a robust platform for analysis of strong anions with minimal sample pretreatment. To the best of our knowledge, this is the first reported assay that enables artifact-free determination of sulfate and sulfite in highly saline or volume-restricted biofluids. Rigorous method validation demonstrates excellent selectivity, good accuracy, a wide linear dynamic range with adequate sensitivity for reliable analysis of sulfate, sulfite and chloride in complex biological samples. Since most solutes are electrokinetically rejected at the capillary inlet, strong anions are detected without spectral interferences irrespective of sample matrix, including human urine, plasma, and sweat. Given the growing number of human diseases associated with impaired sulfur metabolism/transport, molybdenum deficiency and/or chloride conduction, this method is suitable for confirmatory testing of cystic fibrosis, sulfite oxidase deficiency, urolithiasis and chronic/acute renal failure. Preliminary data indicates

that kidney stone formers are characterized by lower sulfate excretion that may reduce urine supersaturation with a higher risk for stone formation. Further work is needed to evaluate the significance of the differential excretion of inorganic sulfate and other organic sulfate conjugates within a larger patient cohort as a way to improve clinical practice for the prognosis and/or treatment of idiopathic kidney disorders in children.

2.7 Acknowledgements

P.B.M. wishes to acknowledge funding support from National Science and Engineering Research Council of Canada. A.N.M. also acknowledges generous support in the form of an Ontario Trillium Scholarship. The authors also wish to thank the Hamilton Regional Laboratory Medicine Program for the loan of a capillary electrophoresis instrument.

2.8 References

(1) Cole, D. E. C.; Evrovski, J. *Crit. Rev. Clin. Lab. Sci.* **2000**, *37*, 299–344.

(2) Carbonero, F.; Benefiel, A. C.; Alizadeh-Ghamsari, A. H.; Gaskins, H. R. *Front. Physiol.* **2012**, *3*, 448.

(3) Okonkwo, O. W.; Batwara, R.; Granja, I.; Asplin, J. R.; Goldfarb, D. S. *PLoS One* **2013**, *8*, e60380.

(4) Nakanishi, T.; Otaki, Y.; Hasuike, Y.; Nanami, M.; Itahana, R.; Miyagawa, K.; Nishikage, H.; Izumi, M.; Takamitsu, Y. *Am. J. Kidney Dis.* **2002**, *40*, 909–915.

(5) Bindu, P. S.; Christopher, R.; Mahadevan, A.; Bharath, R. D. *J. Child Neurol.* **2011**, *26*, 1036–1040.

(6) Vally, H.; Misso, N. L. A.; Madan, V. *Clin. Exp. Allergy* **2009**, *39*, 1643–1651.

(7) Tesseraud, S.; Métayer Coustard, S.; Collin, A.; Seiliez, I. *Br. J. Nutr.* **2009**, *101*, 1132–1139.

(8) LeGrys, V. A.; Yankaskas, J. R.; Quittell, L. M.; Marshall, B. C.; Mogayzel, P. J. *J. Pediatr.* **2007**, *151*, 85–89.

(9) Lundquist, P.; Märtensson, J.; Sörbo, B.; Öhman, S. *Clin. Chem.* **1980**, *26*, 1178–1181.

(10) Hoffmann, C.; Ben-Zeev, B.; Anikster, Y.; Nissenkorn, A.; Brand, N.; Kuint, J.; Kushnir, T. *J. Child Neurol.* **2007**, *22*, 1214–1221.

(11) Cole, D. E. C.; Evrovski, J. *J. Chromatogr. A* **1997**, *789*, 221–232.

(12) Muzikář, M.; Havel, J.; Macka, M. *Electrophoresis* **2003**, *24*, 2252–2259.

(13) Sidorova, A. A.; Grigoriev, A. V. *J. Anal. Chem.* **2012**, *67*, 478–485.

(14) Soga, T.; Imaizumi, M. *Electrophoresis* **2001**, *22* (16), 3418–3425.

(15) Kokkonen, R.; Sirén, H.; Kauliomäki, S.; Rovio, S.; Luomanperä, K. *J. Chromatogr. A* **2004**, *1032*, 243–252.

(16) Kubáň, P.; Timerbaev, A. R. *Electrophoresis* **2012**, *33*, 196–210.

(17) Kubáň, P.; Hauser, P. C. *Lab Chip* **2008**, *8*, 1829–1836.

(18) Blanco, G. A.; Nai, Y. H.; Hilder, E. F.; Shellie, R. A.; Dicinoski, G. W.; Haddad, P. R.; Breadmore, M. C. *Anal. Chem.* **2011**, *83*, 9068–9075.

(19) Theodorsson, E. *Bioanalysis* **2012**, *4*, 305–320.

(20) Thornton, M. J.; Fritz, J. S. *J. Chromatogr. A* **1997**, *770*, 301–310.

(21) Shamsi, S. A.; Danielson, N. D. *Anal. Chem.* **1994**, *66*, 3757–3764.

(22) Kiryushov, V. N.; Skyvortsova, L. I. *J. Anal. Chem.* **2010**, *65*, 305–307.

(23) Doble, P.; Macka, M.; Haddad, P. R. *Trends Anal. Chem.* **2000**, *19*, 10–17.

(24) Choong, C. T.; Hart, C.; Tan, E. S.; Goh, D. L. M. *Proc. Singapore Healthc.* **2010**, *19*, 94–100.

(25) Wilschanski, M.; Zielenski, J.; Markiewicz, D.; Tsui, L. C.; Corey, M.; Levison, H.; Durie, P. R. *J. Pediatr.* **1995**, *127*, 705–710.

(26) Cole, D. E. C.; Landry, D. A.; Boucher, M. J.; Gillespie, C. T. *Clin. Chim. Acta* **1986**, *155*, 237–244.

(27) Cole, D. E.; Boucher, M. J. *Nephron* **1986**, *44*, 92–95.

(28) López, M.; Hoppe, B. *Pediatr. Nephrol.* **2010**, *25*, 49–59.

(29) Puche, R. C.; Vaccaro, D.; Sanchez, A.; Gonzalez, A.; Sarano, H. D. *Br. J. Urol.* **1993**, *71*, 523–526.

(30) Kajiyama, H.; Nojima, Y.; Mitsuhashi, H.; Ueki, K.; Tamura, S.; Sekihara, T.; Wakamatsu, R.; Yano, S.; Naruse, T. *J. Am. Soc. Nephrol.* **2000**, *11*, 923–927.

(31) Mitsuhashi, H.; Ikeuchi, H.; Yamashita, S.; Kuroiwa, T.; Kaneko, Y.; Hiromura, K.; Ueki, K.; Nojima, Y. *Shock* **2004**, *21*, 99–102.

(32) Ji, A. J.; Savon, S. R.; Jacobsen, D. W. *Clin. Chem.* **1995**, *41*, 897–903.

(33) Wadman, S. K.; Cats, B. P. *Eur. J. Pediatr.* **1983**, *141*, 62–63.

(34) Tan, W.-H.; Eichler, F. S.; Hoda, S.; Lee, M. S.; Baris, H.; Hanley, C. A.; Grant, P. E.; Krishnamoorthy, K. S.; Shih, V. E. *Pediatrics* **2005**, *116*, 757–766.

(35) van der Klei-van Moorsel, J. M.; Smit, L. M.; Brockstedt, M.; Jakobs, C.; Dorche, C.; Duran, M. *Eur. J. Pediatr.* **1991**, *150*, 196–197.

(36) Sathyapalan, A.; Zhou, A.; Kar, T.; Zhou, F.; Su, H. *Chem. Commun.* **2009**, 325–327.

(37) Dawson, P. A. *Semin. Cell Dev. Biol.* **2011**, *22*, 653–659.

(38) Pascoe, P. J.; Peake, M. J.; Walmsley, R. N. *Clin. Chem.* **1984**, *30*, 275–277.

(39) Jung, B.; Caslavska, J.; Thormann, W. *J. Chromatogr. A* **2008**, *1206*, 26–32.

(40) Lekawanvijit, S.; Kompa, A. R.; Manabe, M.; Wang, B. H.; Langham, R. G.; Nishijima, F.; Kelly, D. J.; Krum, H. *PLoS One* **2012**, *7*, e41281.

(41) Mian, A. I.; Du, Y.; Garg, H. K.; Caviness, A. C.; Goldstein, S. L.; Bryan, N. S. *Pediatr. Res.* **2011**, *70*, 203–207.

(42) Parks, J. H.; Coward, M.; Coe, F. L. *Kidney Int.* **1997**, *51*, 894–900.

(43) Richmond, W.; Colgan, G.; Simon, S.; Stuart-Hilgenfeld, M. *Clin. Nephrol.* **2005**, *64*, 264–270.

(44) Finkielstein, V. A.; Goldfarb, D. S. *CMAJ* **2006**, *174*, 1407–1409.

(45) Milosević, D.; Batinić, D.; Blau, N.; Konjevoda, P.; Stambuk, N.; Votava-Raić, A.; Barbarić, V.; Fumić, K.; Rumenjak, V.; Stavljenić-Rukavina, A.; Nizić, L.; Vrljićak, K. *J. Chem. Inf. Comput. Sci.* **1998**, *38*, 646–650.

2.9 Supporting Information Section

Table S2.1. Comparison of single co-ions probes with a binary mixture for enhancement of peak symmetry/sharpness for sulfate and sulfite adduct detection by CE with indirect UV detection.

Anion	NTS	NDS	NDS + NTS
Sulfate			
Asymmetry factor	0.806	0.677	0.893
Base peak width (min)	0.093	0.126	0.077
Sulfite			
Asymmetry factor	3.54	1.97	2.41
Base peak width (min)	0.228	0.130	0.160

Table S2.2. Stability test for chloride and sulfate in urine kept at room temperature and at -80ºC after 1, 2 or 3 consecutive freeze-thaw cycles relative to the freshly analyzed pooled urine sample.

Room temperature			Freeze/thaw		
Time (h)	**Chloride (% ± SD)**	**Sulfate (% ± SD)**	**Cycle**	**Chloride (% ± SD)**	**Sulfate (% ± SD)**
24	105 ± 9	104 ± 9	1	96 ± 11	96 ± 10
48	108 ± 6	107 ± 5	2	104 ± 6	104 ± 6
92	101 ± 9	99 ± 8	3	105 ± 6	104 ± 5

Table S2.3. Intra and interday precision for strong anions by CE with indirect UV detection based on average relative peak area (RPA) and relative migration time (RMT) measured for 10 replicates of pooled urine and plasma samples (n = 20) at two concentration levels.

Anion	Intraday precision (n = 10)						Interday precision (n = 20 x 2)		
	Urine			Plasma			Urine		
	Conc. (mM)	*CV* (%)		Conc. (mM)	*CV* (%)		Conc. (mM)	*CV* (%)	
		RPA	RMT		RPA	RMT		RPA	RMT
Chloride	119	6.7	0.3	116	6.5	0.3	119	7.1	0.5
Sulfate	11.2	8.5	0.1	0.4	9.2	0.1	11.2	7.5	0.5
	27.2	8.2		1.0	8.7		27.2	6.3	
Sulfite	0.6	9.3	0.3	0.4	20.5	0.2	0.6	9.1	2.7
	2.0	8.0		1.0	5.5		2.0	4.8	

Table S2.4. Accuracy for strong anions by CE with indirect UV detection based on spike-recovery studies in pooled urine (n = 20), plasma (n = 20), and sweat (n = 3) samples measured in triplicate at two concentration levels expressed as percentage recovery (%).

Anions	Urine		Plasma		Sweat	
	Conc. (mM)	Recovery ± SD (%)	Conc. (mM)	Recovery ± SD (%)	Conc. (mM)	Recovery ± SD (%)
Chloride	-	-	-	-	8.0	96 ± 13
	-	-	-	-	80.0	92 ± 9
Sulfate	6.0	118 ± 7	0.4	97 ± 17	-	-
	16.0	107 ± 2	1.0	96 ± 20	-	-
Sulfite	0.6	102 ± 9	0.4	95 ± 12	-	-
	2.0	102 ± 3	1.0	86 ± 8	-	-

Table S2.5. Summary of results in a robustness study expressed as *p*-values when using a 2^2 experimental design with multiple linear regression. Formic acid (FA) and probe co-ion concentration (probes) are two key experimental variables in the BGE that impact assay performance, which were systematically changed by ± 5% in this study from optimum assay conditions (0.4 M formic acid, 5 mM NTS + NDS, pH 2.0). Measured responses included relative peak areas (RPA), relative migration time (RMT) and resolution (R_s) for chloride, sulfate, and sulfite in urine. No significant effects were identified, even when considering two way-interactions of variables (FA x Probes) since all *p*-values were > 0.05.

Responses	FA	Probes	FA x Probes
RPA Cl^-	0.09	0.42	0.13
RPA SO_4^{2-}	0.14	0.76	0.09
RPA SO_3^{2-}	0.33	0.84	0.69
RMT Cl^-	0.99	0.35	0.48
RMT SO_4^{2-}	0.13	0.41	0.92
RMT SO_3^{2-}	0.46	0.73	0.51
R_S Cl^-/IS	0.79	0.77	0.56
R_S IS/ SO_4^{2-}	0.24	0.43	0.46
R_S IS/ SO_3^{2-}	0.33	0.22	0.41

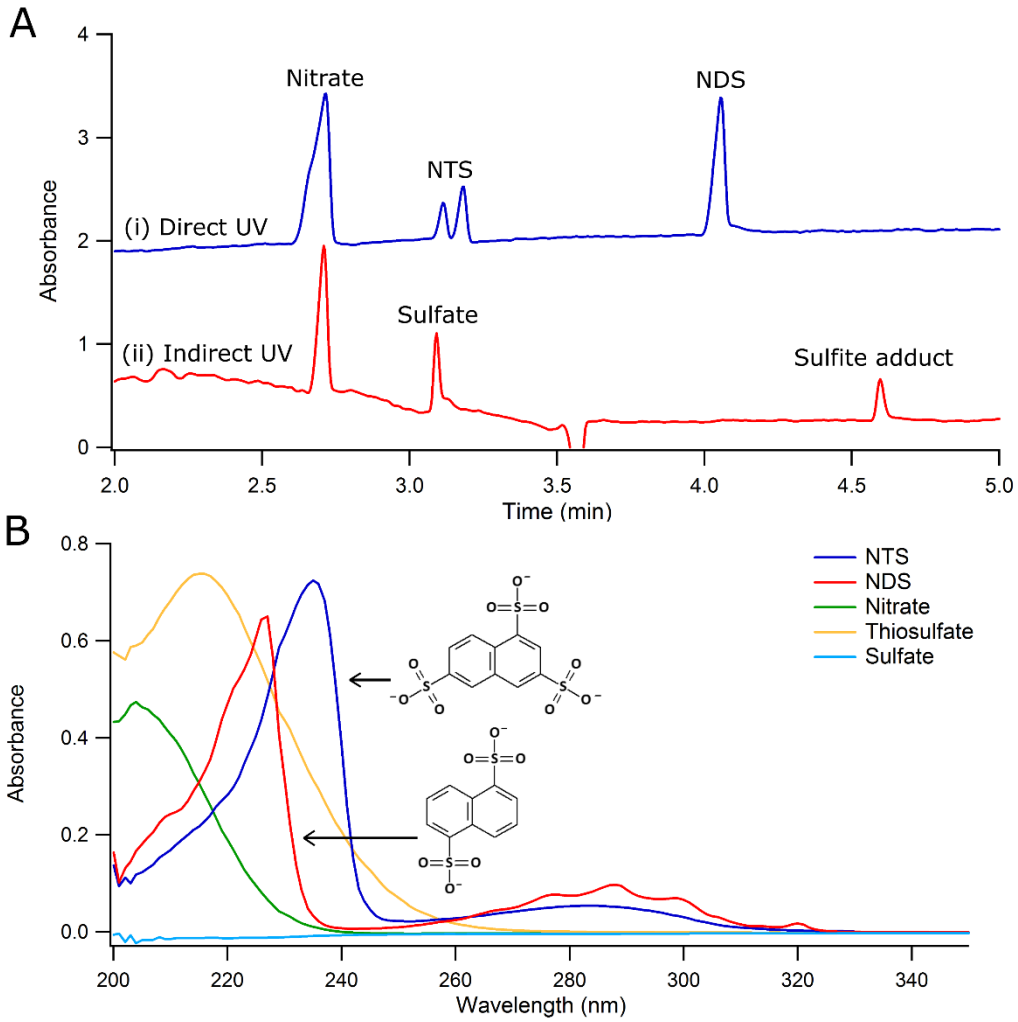

Figure S2.1. (**A**) An electropherogram overlay that compares the migration time of (i) NTS (1 mM) and NDS (1 mM) analyzed by CE with direct UV detection (214 nm) relative to (ii) a standard solution of sulfate (1 mM) and sulfite (1 mM), analyzed by CE with indirect UV detection with co-ion probes in BGE (234 nm). Nitrate (10 mM) was added to the solutions as an internal standard, since it can be detected in both direct (214 nm) and indirect UV (234 nm). The two major NTS isomers have a similar average electrophoretic mobility to sulfate (*i.e.*, mobility match), while NDS has a slower negative mobility that is more comparable to the sulfite adduct. Thus, NTS provides optimal peak symmetry for sulfate, while NDS results in moderately improved peak shape for sulfite, whereas a mixture of probes results in better peak symmetry for both anions. The poorer mobility match of NDS with sulfite results in a lower linear dynamic range and peak tailing occurring at high sulfite concentrations (> 5 mM) in comparison to sulfate. However, a mixture of both co-ion probes results in a better peak symmetry for simultaneous analysis of both sulfate and sulfite as its formaldehyde adduct. (**B**) UV absorbance spectrum overlay for NTS (10 µM), NDS (10 µM), nitrate (50 µM), thiosulfate (25 µM), and sulfate (50 µM).

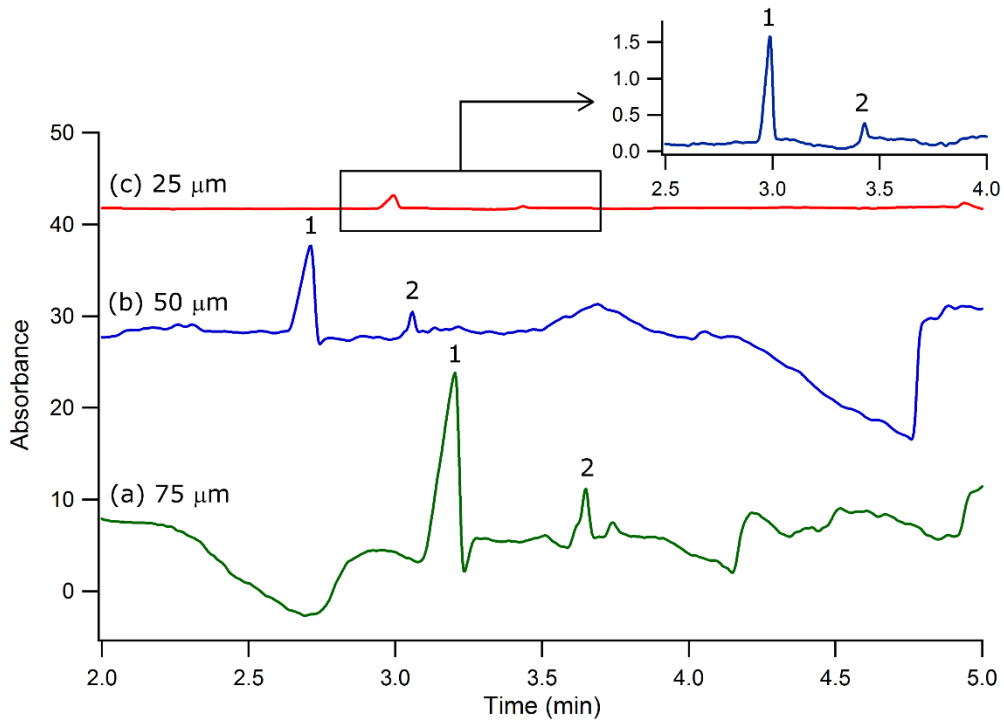

Figure S2.2. Comparison of the impact of fused-silica capillary inner diameter on the separation performance of CE with indirect UV detection for measurement of 10 mM perchlorate (1) and 0.5 mM sulfate (2). Although the use of increasingly narrow capillary diameters reduces absolute signal intensity for strong anions due to its shorter optical path length and lower injection volume, the more effective heat dissipation and lower currents resulted in a more stable baseline and sharper peaks with over a two-fold better signal to noise (*S/N*) for sulfate (*S/N* of 1.8, 2.3 and 4.0 for 75, 50 and 25 µm capillaries, respectively) when using CE with indirect UV detection. Conditions: 1 M formic acid, 5 mM NTS, pH 1.8; 5 s sample injection at 0.5 psi; voltage of -30 kV; total capillary length 60 cm; UV detection at 214 nm.

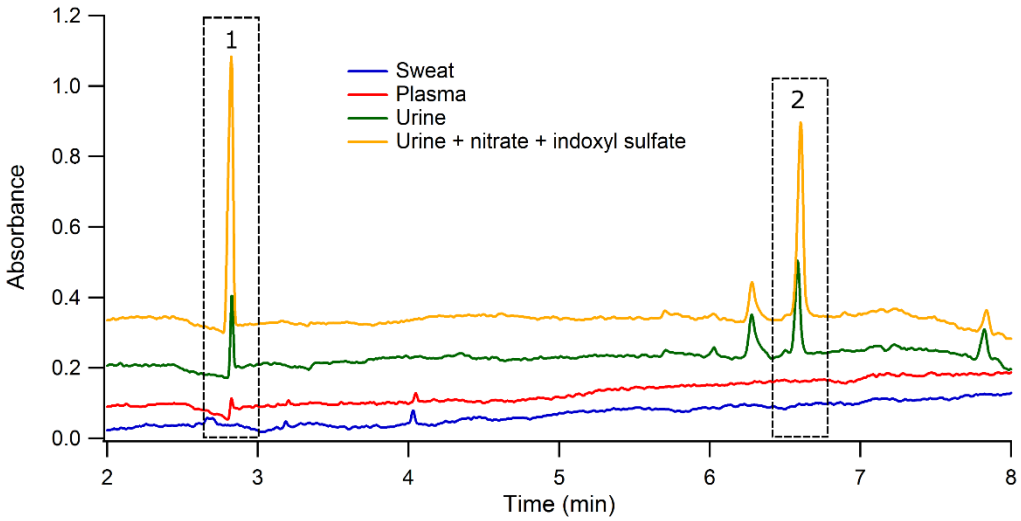

Figure S2.3. An electropherogram overlay that compares the analysis of 2-fold diluted human urine and plasma filtrate, and 4-fold diluted human sweat samples by CE with direct UV absorbance detection (no co-ion probes added to BGE). Under these conditions, only urinary nitrate (1, ≈ 0.4 mM) and indoxyl-3-sulfate (2, ≈ 85 µM) were detected in pooled 24 h human urine along with two unknown metabolites. In the case of both plasma filtrate and sweat samples, no significant peaks were detectable due to the inherent selectivity of the method. Separation conditions were 1 M formic acid, pH 1.8, 15 s injection, -30 kV with direct UV detection at 214 nm.

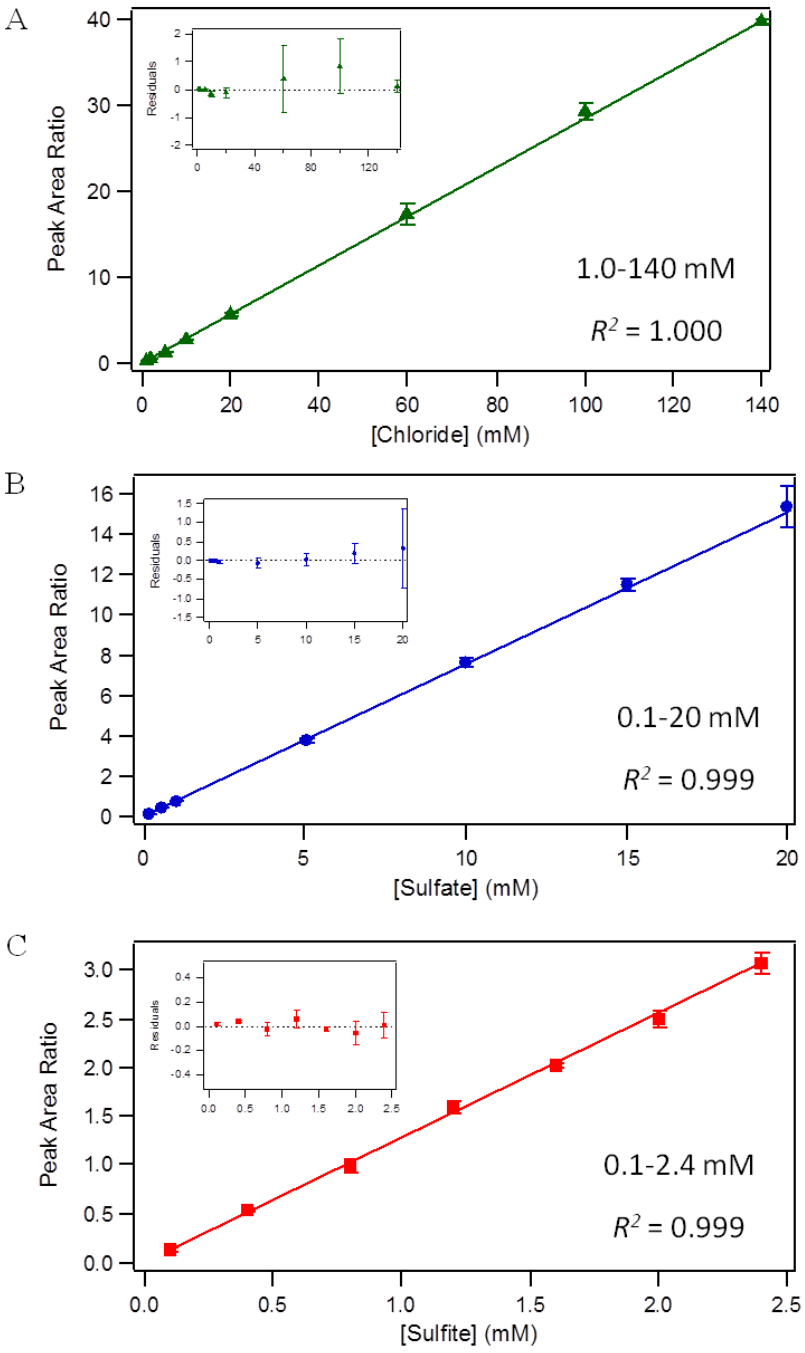

Figure S2.4. Calibration curves and residual plots (insets) for accurate quantification of chloride, sulfate and sulfite by CE with indirect UV detection. Standard solutions were measured in triplicate with error representing (±1SD), whereas weighted linear regression was performed in order to correct for non-constant variance across a wide linear dynamic range (24-200-fold).

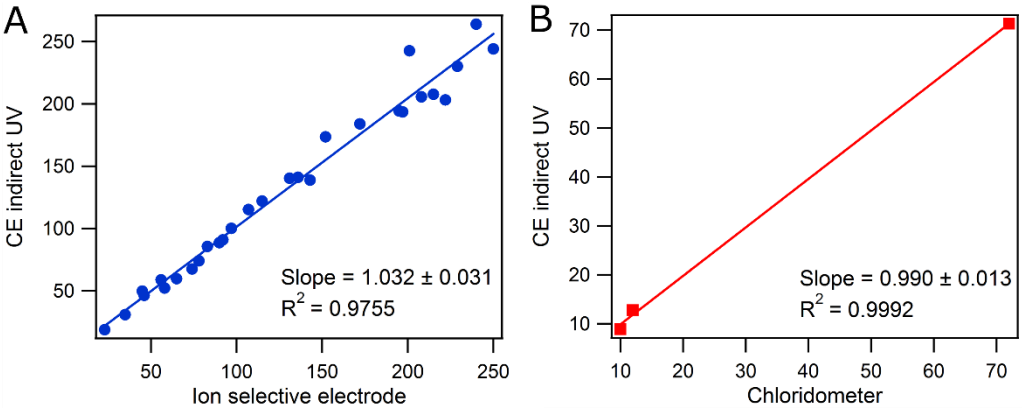

Figure S2.5. Method comparison for chloride (mM) in pooled 24 h human urine (**A**) and stimulated sweat (**B**), using ion selective electrode/potentiometry and chloridometer as reference methods in the clinical laboratory, respectively. The correlation between the two methods is expressed by the determination coefficient (R^2) and the magnitude of the slope that is close to unity.

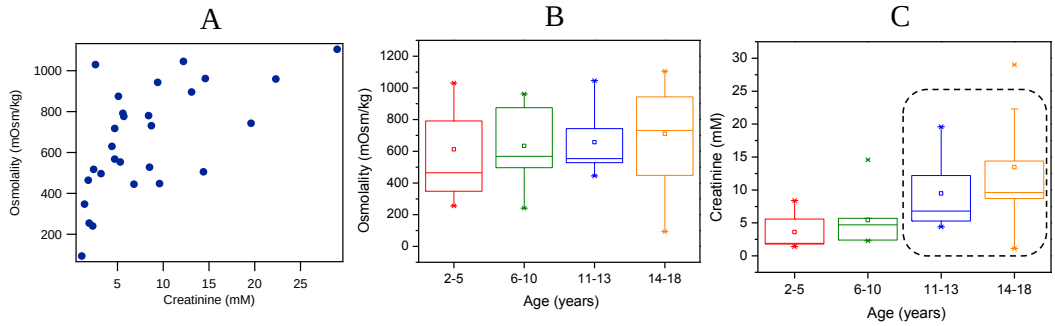

Figure S2.6. (**A**) Comparison of osmolality with creatinine in randomized single spot urine samples collected from a pediatric population (n = 27). A poor correlation (R^2 = 0.344) is found between these two parameters widely used to correct for hydration status, whereas (**B**) median osmolality values obtained for children in different sub-groups was largely consistent over a wide age range, unlike (**C**) urinary creatinine that is significantly elevated in pediatric patients above 10 years old ($p < 0.05$). Similarly, median osmolality (730 ± 407 mOsm/kg) was found to have more than two-fold lower overall variance across all age groups in terms of interquartile range (CV = 56%) relative to median creatinine (5.7 ± 8.0 mM) concentration levels (CV = 140%).

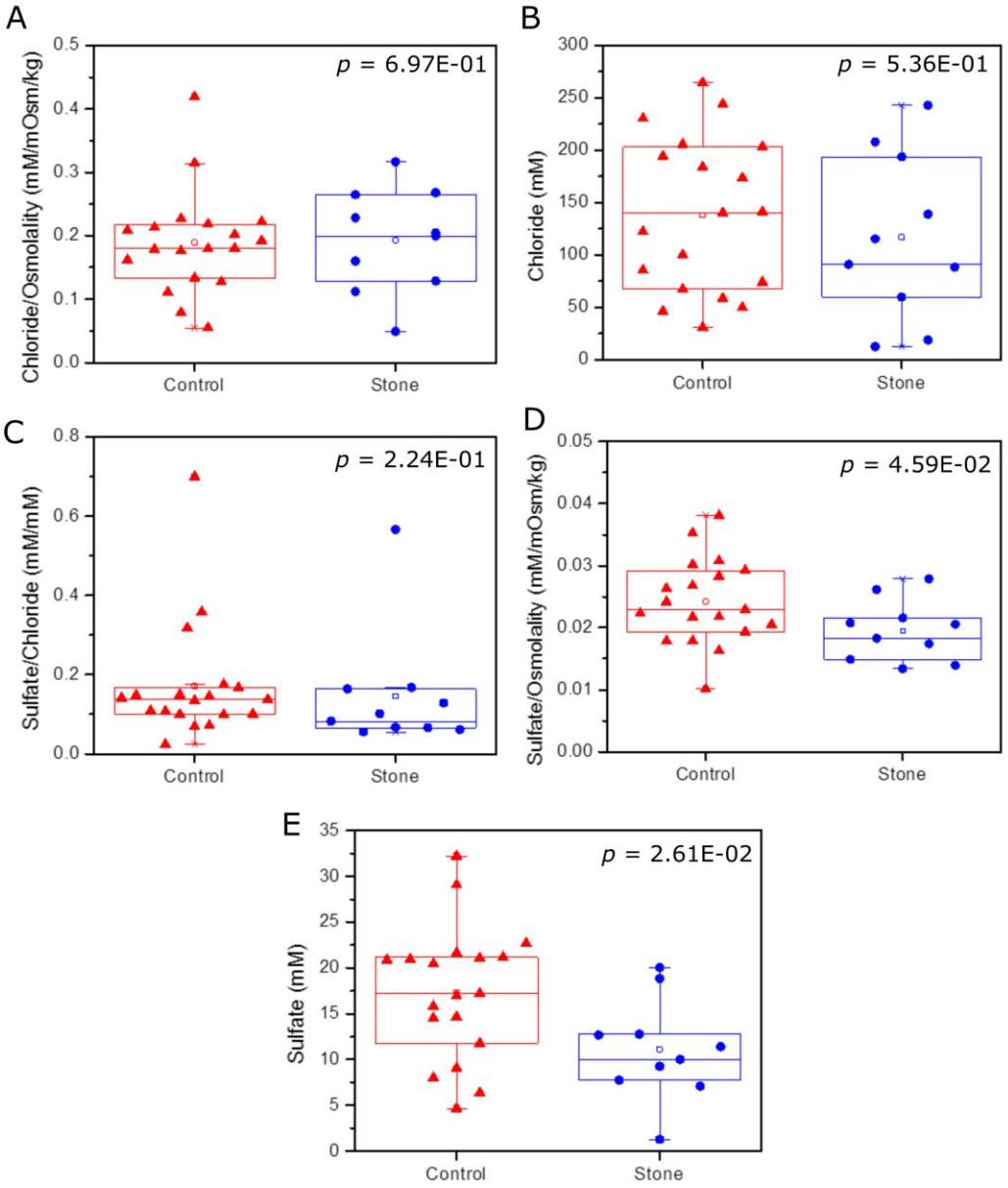

Figure S2.7. Boxplots comparing the performance of urinary chloride and/or sulfate in differentiation of kidney-stone formers from non-kidney stone controls. There was no significant difference between the two sub-groups ($p > 0.05$) when using (**A**) osmolality-normalized (or creatinine) chloride levels, (**B**) absolute chloride concentrations and (**C**) sulfate/chloride ratio levels in randomized single-spot urine samples due to high biological variance. Median urinary chloride levels and their interquartile ranges are (103 ± 95 mM, $n = 10$) and (131 ± 131 mM, $n = 19$) for kidney stone formers and their controls, respectively. In contrast, there was a statistical difference between the two sub-groups when using (**D**) osmolality-corrected sulfate levels ($p = 0.0460$), and (**E**) excreted sulfate concentrations that are lower ($p = 0.0261$) among kidney stone formers without correction for hydration status. In the latter case, median and interquartile range for urinary sulfate in non-kidney stone controls and kidney stone sub-groups correspond to 17 .2 ± 8.0 mM and 10.7 ± 4.6 mM, respectively.

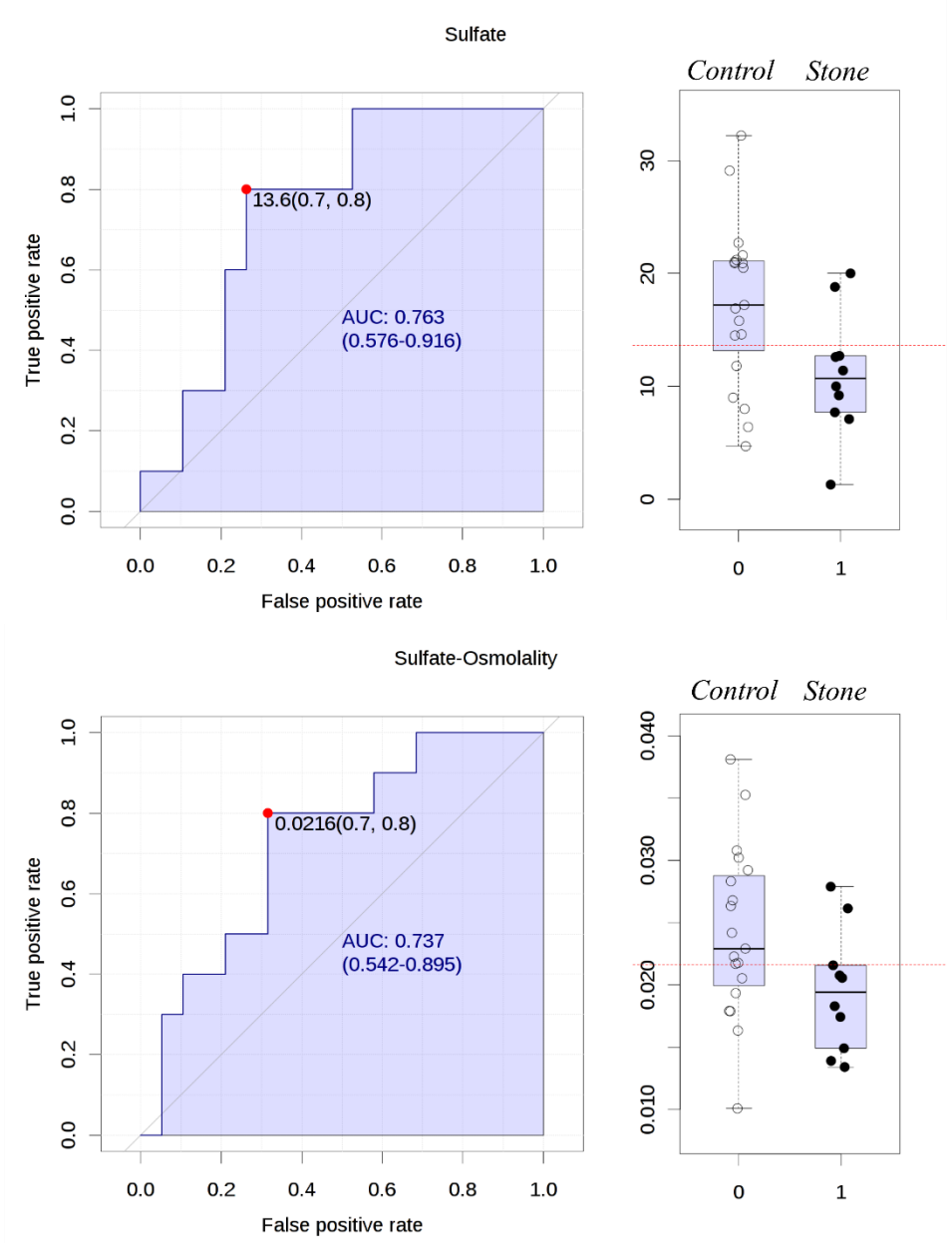

Figure S2.8. Comparison of receiver-operating characteristic (ROC) curves for differentiation of kidney stone formers (*n* = 10) from non-kidney stone controls (*n* = 19) based on (**A**) sulfate (AUC = 0.763) and (**B**) osmolality-corrected sulfate (AUC = 0.732) when using randomized single-spot urine samples collected from pediatric patients. The optimum cut-off concentration for distinguishing kidney stone formers was below 13.6 mM sulfate. In contrast, chloride has a weaker performance for distinguishing kidney stone formers (AUC = 0.571). The diagnostic performance of the urinary sulfate test for classifying kidney stone formers from controls at the nephrology clinic has a sensitivity of 80% and specificity of 74%. ROC curves were generated using ROC Curve Explorer & Tester (ROCCET) (Xia, J.; Broadhurst, D.I.; Wilson, M.; Wishart, D. S. *Metabolomics* **2013**, 9, 280-299).

Chapter III

A Robust Method for Iodine Status Determination in Epidemiological Studies by Capillary Electrophoresis

Authors of this work are Adriana Nori de Macedo, Koon Teo, Andrew Mente, Matthew McQueen, Johannes Zeidler, Paul Poirier, Scott A. Lear, Andy Wielgosz, and Philip Britz-McKibbin.

Anal. Chem. **86**, 10010-10015, 2014.

I conducted the experiments for optimization and validation of the CE-UV method, performed the data analysis, and wrote an initial manuscript draft for publication. Other co-authors provided urine samples from the PURE study and gave feedback on the manuscript draft.

Chapter III: A Robust Method for Iodine Status Determination in Epidemiological Studies by Capillary Electrophoresis

3.1 Abstract

Iodine deficiency is the most common preventable cause of intellectual disabilities in children. Global health initiatives to ensure optimum nutrition thus require continuous monitoring of population-wide iodine intake as determined by urinary excretion of iodide. Current methods to analyze urinary iodide are limited by complicated sample pretreatment, costly infrastructure, and/or poor selectivity, posing restrictions to large-scale epidemiological studies. We describe a simple yet selective method to analyze iodide in volume-restricted human urine specimens stored in biorepositories by capillary electrophoresis (CE) with UV detection. Excellent selectivity is achieved when using an acidic background electrolyte in conjunction with dynamic complexation via α-cyclodextrin in an unmodified fused-silica capillary under reversed polarity. Sample self-stacking is developed as an online sample preconcentration method to boost sensitivity with sub-micromolar detection limits for iodide ($S/N \approx 3$, 0.06 μM) directly in urine. This assay also allows for simultaneous analysis of environmental iodide uptake inhibitors, including thiocyanate and nitrate. Rigorous method validation confirmed good linearity ($R^2 = 0.9998$), dynamic range (0.20 to 4.0 μM), accuracy (average recovery of 93% at three concentration levels) and precision for reliable iodide determination in pooled urine specimens over 29 days of analysis (RSD = 11%, $n = 87$). Future work will evaluate the comparability of CE-based results with other methods currently used for urinary iodine determination to ensure consistent estimation of iodine nutrition in population-based studies.

3.2 Introduction

Iodine is an essential micronutrient needed for the biosynthesis of thyroid hormones, which are critical in the regulation of cellular metabolism, as well as in normal growth and mental development.[1,2] In order to provide a consistent source of iodine to the population and prevent iodine deficiency disorders (IDDs), many countries have adopted table salt iodization as a public health policy. Although significant improvement has been achieved in the reduction of endemic goiter and cretinism, other IDDs remain problematic with almost 2 billion people worldwide at risk for iodine insufficiency[3] that is associated with impaired cognitive development in children, as well as weight gain, depression, thyroid disorders and cardiovascular diseases later in life.[4–7] Several developed countries, in which iodine deficiency was eradicated some decades ago, are now facing mild to moderate iodine deficiency due to reduced intake of iodine-rich foods, increased consumption of noniodized processed foods and/or exposure to iodide uptake inhibitors in the environment.[8–11] For instance, about one third of pregnant women in the United States are marginally iodine deficient.[5] Therefore, continuous monitoring of iodine status is an essential part of universal salt iodization programs[10,12,13] with dietary iodide intake recommended to be 150 μg/day for adults and 250 μg/day for pregnant women.[3] The best single measurement to evaluate median iodine intake in the population is via excreted urinary iodide, which represents more than 90% of the iodine recently ingested.[2,3,14,15] For this reason, iodide concentrations from random spot urine samples are often used in large-scale epidemiological studies for iodine status assessment. However, simple, selective yet cost-effective assays are needed to analyze sub-micromolar levels of urinary iodide for population health.[16]

A kinetic spectrophotometric assay based on the classic Sandell-Kolthoff reaction is the most widely used method for urinary iodide determination, where iodide serves as a catalyst for the reduction of the yellow Ce(IV) to colorless Ce(III) in the presence of As(III).[16,17] Although the assay is well established, a

number of different protocols exist that are time-consuming, involve handling of toxic reagents, and require specially designed sealing cassettes for acid digestion in microplates to remove interferences in urine. Inductively coupled plasma-mass spectrometry (ICP-MS) is also used for urinary iodide analysis. A simple dilution step with addition of an isotopic internal standard is used to minimize matrix effects while achieving low detection limits.[17,18] However, the method is not specific for iodide, measuring instead total iodine in the sample, thus, it is prone to bias due to iodine-containing compounds not completely bioavailable for thyroid uptake, such as iodinated drugs (*e.g.,* amiodarone), radiologic contrast agents (*e.g.,* iopamidol), and food additives (*e.g.,* erythrosine). Also, large sample volumes (> 200 µL) are often required for sample preparation when using pneumatic nebulizers with ICP-MS that limit the use of stored urine specimens in biorepositories with finite volumes. Ion-exchange chromatography coupled to ICP-MS has been introduced for improved speciation of iodine, including iodide, iodate and iodine-containing analogues of tyrosine from edible seaweed.[19] However, ICP-MS and other MS-based methods[17,18] demand more costly infrastructure and operating costs that are not suitable for developing countries. Alternatively, capillary electrophoresis (CE) with UV detection has been reported for the analysis of iodide in urine[20,21] and other complex sample matrices.[21–25] Wide-bore capillaries[21] and/or transient isotachophoretic (tITP) preconcentration[20,22–24] are needed to achieve submicromolar detection limits for assessment of iodine nutritional insufficiency (< 0.79 µM or < 100 µg/L) by the World Health Organization.[3] However, the lack of rigorous method validation and long-term robustness studies has prevented the translation of CE-based assays to large-scale epidemiological or clinical studies.[26] In this report, we introduce a new CE assay to analyze submicromolar levels of urinary iodide, including simultaneous determination of nitrate and thiocyanate as relevant iodide uptake inhibitors in the environment. Adequate sensitivity and selectivity for iodide quantification were attained when combining online preconcentration sample self-

stacking[27] and dynamic complexation of iodine with α-cyclodextrin (α-CD), which provide a robust and cost-effect method for urinary iodine determination in epidemiological studies.

3.3 Experimental Section

3.3.1 Chemicals and reagents

Potassium iodide, sodium nitrate, lithium hydroxide, α-cyclodextrin, sodium sulfate decahydrate, ammonium chloride, sodium chloride, calcium chloride dehydrate, sodium phosphate monobasic monohydrate, potassium chloride, 1,5-naphthalenedisulfonic acid disodium salt hydrate (NDS), sodium hydroxide, and hydrobromic acid were purchased from Sigma-Aldrich (St. Louis, MO, USA). Phosphoric acid (85%) was obtained from Fisher Scientific Canada, and magnesium sulfate anhydrous was purchased from Anachemia (Montreal, QC, Canada). Stock solutions of iodide were prepared by dissolving potassium iodide in deionized water (Barnstead EASYpure II LF system, Dubuque, IA, USA) at the concentration of 50 mM. Stock solutions of bromide (100 mM) were prepared from hydrobromic acid, while chloride (1 M) and nitrate (100 mM) solutions were prepared from their sodium salts. A simulated urine solution was prepared for external calibration, containing 30 mM of potassium chloride, 60 mM of sodium chloride, 2 mM of magnesium sulfate, 13 mM of sodium sulfate, 5 mM of sodium phosphate, 4 mM of calcium chloride, and 15 mM of ammonium chloride, with pH adjusted to 6.0 using 0.1 M sodium hydroxide. This solution mimics the main electrolyte composition of urine, resulting in peak shapes and migration times for iodide and NDS that are comparable to authentic human urine samples.

3.3.2 Capillary electrophoresis with UV detection

All analyses were performed in a P/ACE MDQ system with photodiode array detector from Beckman-Counter (Fullerton, CA, USA), using uncoated fused-silica capillaries (Polymicro Technologies, Phoenix, AZ, USA) with 75 μm internal diameter, 60 cm of total length and 50 cm of length to the detector. New capillaries were conditioned with methanol for 5 min, followed by deionized water for 5 min and background electrolyte (BGE) for 20 min (20 psi). The BGE was composed of 180 mM lithium hydroxide, 180 mM phosphoric acid and 36 mM α-cyclodextrin (α-CD), pH 3.0, adjusted with 1 M phosphoric acid. In order to ensure a proper and quick solubilisation, the buffer solution was sonicated for 30 s after the addition of phosphoric acid, and for 5 min after the addition of α-CD. All the separations were performed at 25ºC using a hydrodynamic injection for 80 s (0.5 psi) under optimum conditions, which is equivalent to about a third of the total capillary length filled with sample. Electrokinetic focusing of trace levels of iodide by sample self-stacking[27] was critical to achieve adequate sensitivity and linearity for urinary iodide status determination. Reversed polarity was used to allow the selective detection of strong anions using an applied voltage of -18 kV (anode in the capillary outlet) with UV detection at 226 nm (iodide maximum absorbance) and 288 nm (more selective wavelength for the internal standard, NDS). The capillary was rinsed with BGE for 15 min (20 psi) each morning before analysis, and for 3 min (20 psi) prior to each separation. For overnight storage, the capillary was rinsed with de-ionized water for 10 min and kept in vials containing de-ionized water.

3.3.3 Determination of binding constant of strong anions with α-cyclodextrin

Nine BGE solutions containing 180 mM lithium hydroxide, 180 mM phosphoric acid, pH 3.0 adjusted with 1 M phosphoric acid were prepared with different concentrations of α-CD (0-70 mM). A standard solution composed of 10 μM

iodide, 100 µM thiocyanate, 100 µM bromide, 500 µM nitrate and 20 µM NDS was prepared in de-ionized water and analyzed in triplicate using a normal 5 s injection (0.5 psi) under reversed polarity (-18 kV). Since higher α-CD concentrations increase the BGE viscosity, this results in non-specific changes in apparent analyte mobility unrelated to binding. In order to correct for this effect, relative viscosity (ν) measurements were performed for each BGE, by calculating the ratio of the current for the BGE without α-CD (I_0) and the current for each other α-CD concentration (I_i). Viscosity-corrected electrophoretic mobilities ($\nu\mu_i = \mu_i \times I_0/I_i$) of iodide, thiocyanate, nitrate, bromide and NDS were plotted as a function of α-CD concentration for binding isotherms. A non-linear regression was performed using Igor Pro 5.0 (Wavemetrics Inc., Lake Oswego, OR) to determine the apparent binding constant (K_b) and the mobility of the iodide:α-CD complex ($\mu_{ep,AC}$) assuming a 1:1 dynamic complexation model according to equation (1), where $\nu\mu_{ep,A}$ is the viscosity-corrected apparent electrophoretic mobility of analyte and C is the α-CD concentration.

$$\nu\mu_{ep}^{A} = \frac{1}{1+K_b\times C}\mu_{ep,A} + \frac{K_b\times C}{1+K_b\times C}\times\mu_{ep,\,AC} \quad (1)$$

3.3.4 Sample storage and workup of human urine and other biological fluids

For method development and validation, single-spot urine samples were donated by healthy volunteers, whereas pooled 24 h samples were prepared by combining equal volumes of urine samples from thirty (n = 30) or 800 (n = 800) sex-matched Canadian adults with median age of 61 years from four regional centres across Canada, which were collected as part of the Prospective Urban and Rural Epidemiological (PURE) study.[28] A standard reference material for iodide, thiocyanate and nitrate in frozen human urine (SRM 3668) was purchased from NIST (Atlanta, GA, USA) and used for external method validation when comparing CE-derived results with independently measured urinary concentrations using ICP-MS for iodide and ion-exchange chromatography-ICP-

MS for thiocyanate and nitrate. Samples were stored in a -80ºC freezer in 1.5 mL centrifuge tubes, unless otherwise stated. Frozen samples were allowed to thaw at room temperature for approximately 1 h before preparation. All sample tubes were homogenized by gently inverting several times before volume measurement. A 50 µL aliquot of urine was then transferred to a 0.5 mL centrifuge tube, where 4 µL of 1 mM NDS (final concentration of 20 µM) and 46 µL of de-ionized water were added, resulting in a 2-fold dilution of original urine sample. Urine volumes as low as 10 µL can also be routinely analyzed. The mixture was vortexed for 30 s and centrifuged at 14,000 g for 5 min to sediment any particulates in diluted urine samples. A 40 µL aliquot of the supernatant was then analyzed by CE with UV detection at 226 nm. Overall, the method was able to tolerate urine matrices that vary between-subjects due to large differences in hydration status and diet, which may impact sample self-stacking performance due to differences in conductivity that alter electric field strength when using long sample injection plugs. In most cases, the dilution was minimized to 1.5-fold in order to allow the quantification of iodide at lower concentrations. Concentrated urine specimens with high ionic strength, however, needed further dilution in de-ionized water (2-fold) in order to maintain resolution of iodide from other interferences due to changes in electromigration behavior. Samples containing extremely high levels of iodide (> 6 µM) also needed further dilution (4-fold or more) when concentration levels exceeded the maximum linear range for calibration using the simulated urine matrix in deionized water, which helps to maintain minimum chloride levels for sample self-stacking with a stable current during separation (120 µA). The CE-UV assay was also applied to human sweat, which is a secondary route of iodine excretion. Sweat samples (n = 3) were collected from patients at the Cystic Fibrosis Clinic at McMaster University, using pilocarpine iontophoresis to stimulate sweat production, and a coiled microbore tube to collect the samples (Webster Model 3700 Macroduct Sweat Capillary Collection System, Wescor Inc., Logan, UT). Remaining sweat samples after routine analysis at the

McMaster Children's Hospital were kept frozen at -20ºC before iodide analysis. A 10 µL aliquot of sweat was 2-fold diluted in simulated urine, containing NDS to produce a final concentration of 20 µM. After homogenizing by vortex for 30 s, the samples were analyzed directly by CE with UV detection.

3.3.5 Method calibration and assay validation

Calibration standards at seven different concentrations of iodide (0.20-4.0 µM), thiocyanate (1.0-16.0 µM), and nitrate (50-500 µM) were prepared in triplicate in a 1:1 v mixture of simulated urine matrix and de-ionized water, using 20 µM NDS as an internal standard. In all cases, quantification of iodide, nitrate and thiocyanate was performed by integration of their peak are relative to an internal standard (NDS, 20 µM). In order to ensure reliable quantification of trace levels of urinary iodide, manual inspection of automated peak integration in each electropherogram was performed. External calibration curves were modeled using linear least squares regression, where linearity was evaluated by the coefficient of determination (R^2) and residuals plot, and the percentage relative error (Σ%RE) throughout the calibration range. The limit of detection ($S/N \approx 3$) and limit of quantification ($S/N \approx 10$) were determined from the signal of a serially diluted urine sample relative to the background noise measured near the iodide migration time. Accuracy was evaluated through spike-recovery experiments performed in triplicate using a pooled 24 h urine sample derived from 800 subjects from the PURE study at three concentration levels with iodide (0.50, 1.00, and 2.00 µM) and thiocyanate (4.00, 8.00, and 12.00 µM). Additional accuracy tests were performed using a standard reference material (SRM 3668) from the National Institute of Standards and Technology (NIST), consisting in two concentration levels for iodide, thiocyanate, and nitrate. The results obtained for the frozen NIST urine standards, analyzed in triplicate over three days ($n = 9$), were compared with the reference anion concentrations, and reported in terms of

percent bias. Intraday precision (repeatability) was evaluated for 10 replicate injections of a pooled 24 h urine sample analyzed within a single day based on the relative standard deviation (RSD) for relative peak areas (RPA) and relative migration times (RMT), where anion responses or migration times were normalized to the internal standard, NDS. For interday precision, NIST standard reference material (SRM 3668), with two concentration levels of iodide, thiocyanate, and nitrate, was analyzed in triplicate over three days, evaluating the RSD for RPA and RMT. Iodide stability was tested using a freshly collected spot urine sample, which was divided into individual aliquots for room temperature and freeze-thaw stability tests, as well as an immediate analysis, used as a control. Samples kept at room temperature (≈ 25ºC) were analyzed at each 40 min for up to 7 h. For freeze-thaw stability, samples were stored in a -80ºC freezer and were exposed to up to four freeze-thaw cycles, before being analyzed in triplicate. Stability was evaluated as the concentration of iodide in each test relative to the concentration measured in the freshly analyzed urine aliquot. Selectivity was tested in a pooled 24 h urine sample by using a BGE without α-CD and by selective precipitation of iodide using 50 μM silver nitrate. Other UV-active strong anions in urine were also spiked into the sample to confirm their resolution from iodide, including oxalate, iodate, thiosulfate, nitrate, nitrite, and bromide. Data processing and linear regressions were performed using Igor Pro 5.0 (Wavemetrics Inc., Lake Oswego, OR).

3.3.6 Robustness and intermediate precision assessment of CE assay

Robustness and intermediate precision were evaluated over five weeks, using a new capillary and new BGE batch each week, with analysis performed by a single analyst. Electrodes were cleaned every morning before starting the analysis, using a cleaning paper damped with de-ionized water, in order to prevent urine and salt deposits accumulating that can risk current discharge or sample contamination. A blank solution, composed of simulated urine and NDS in de-ionized water, was

first analyzed by CE-UV to check the absence of sample carry-over each morning. Then a calibrant solution with a known concentration of iodide was injected to check the detector response daily, whereas an external calibration curve was generated on a weekly basis by analyzing six different iodide standard solutions each week. This allowed for evaluation of method robustness when comparing the sensitivity and linearity of the method over a five-week period. A quality control (QC, pooled 24 h urine sample prepared from thirty subjects, n = 30) reference sample was prepared on the first day of analysis and divided into individual aliquots, which were stored in a -80ºC freezer. One aliquot of QC sample was thawed daily, diluted, and injected intermittently after a batch of 10 individual urine samples (≈ 3 h), resulting in three QC runs per days (n = 3 × 29 days), for assessment of intermediate precision for a total of 87 runs over 5 weeks of analysis using the same CE instrument.

3.4 Results and Discussion

On-line sample preconcentration by sample self-stacking was performed using chloride, naturally present in urine at high concentrations (≈ 100 mM) as the leading electrolyte (LE), whereas the background electrolyte (BGE) was composed of a slow-mobility anion (dihydrogenphosphate) that acts as buffer and terminating electrolyte (TE). **Figure 3.1** shows a schematic of the separation configuration used in CE, which offers a simpler and more effective approach for routine analysis of urinary iodide than previous tITP formats. For instance, our strategy avoids the use of various TEs injected as a segment after the sample and the addition of high concentrations of chloride to the BGE for matrix matching, which limits electric field strength resulting in longer analysis times.[20,22–24] However, sample self-stacking requires the analyte to migrate with an intermediate electrophoretic mobility (μ_A), relative to the LE (μ_{LE}) and TE (μ_{TE}). Since free iodide has a similar mobility to chloride in aqueous solution, dynamic inclusion complexation using α-CD was used for resolving trace levels of iodide

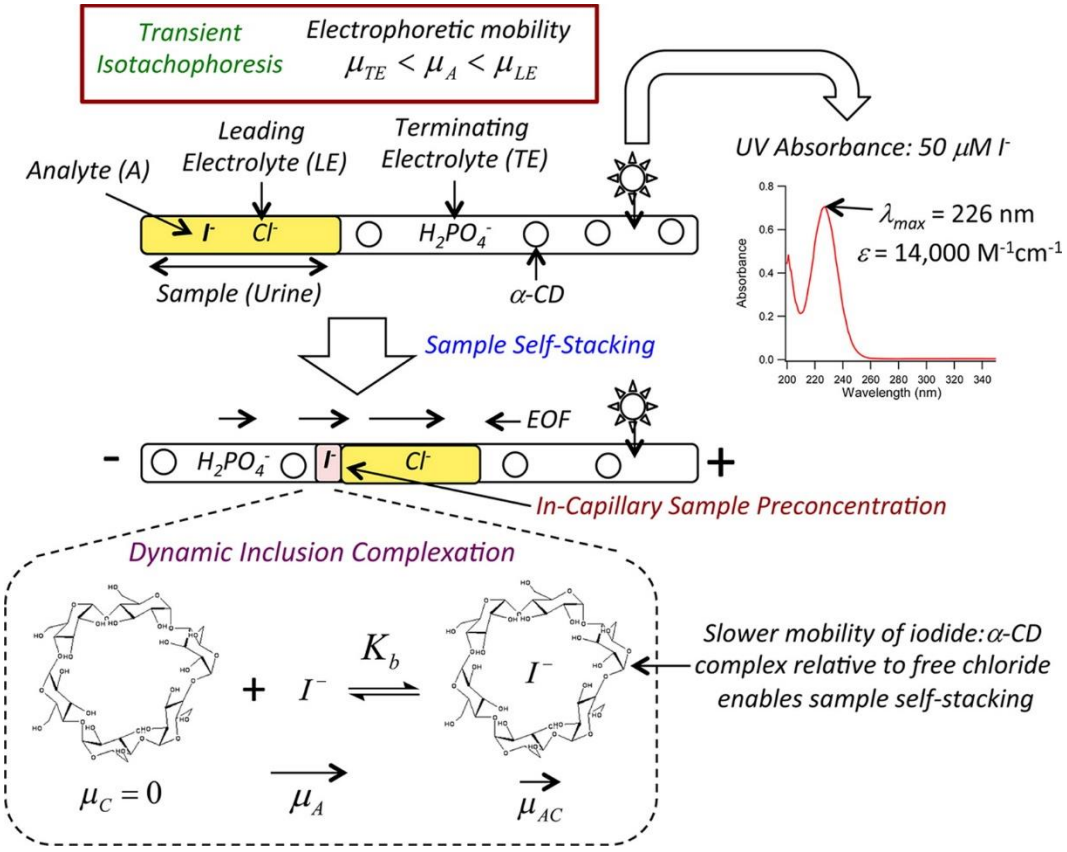

Figure 3.1. Injection configuration and buffer conditions used for iodide status determination by CE with UV detection via sample self-stacking. Chloride in urine samples serves as a LE, while a BGE containing dihydrogenphosphate (pH 3) serves as TE. Dynamic complexation of iodide with α-CD during electromigration is critical for method selectivity and sample self-stacking. The electrokinetic focusing mechanism allows for on-line sample preconcentration of iodide directly in human urine with sub-micromolar detection limits.

in urine while also providing the necessary conditions for sample self-stacking, since the mobility of the iodide/α-CD complex is slower than chloride, but still faster than dihydrogenphosphate. For instance, α-CD interacts differentially with inorganic anions,[29,30] including iodide and thiocyanate, whose binding constants (K_b) derived from viscosity-corrected mobility binding isotherms were measured as 15 ± 2 M^{-1} and 24 ± 2 M^{-1}, respectively. In contrast, chloride, bromide, and nitrate were found to have negligible binding to α-CD (**Figure S3.1**). Cationic surfactants have been largely used as additives to modulate iodide mobility in

CE,[20,22,24] however they also have a major impact on the separation performance as strong electroosmotic flow (EOF) modifiers. In our case, an acidic buffer condition (pH 3) is used to suppress the EOF while ensuring dihydrogenphosphate exists as the predominate species in solution. A critical aspect to separation optimization was the use of a high ionic strength BGE/TE (180 mM), in order to ensure good sample self-stacking performance for trace levels of iodide in the presence of up to a 10^5-fold excess of chloride in human urine. Also, lithium was selected as the counter-ion in order to reduce solution conductivity and Joule heating effects. Overall, 36 mM α-CD was used in the BGE in order to achieve on-line sample preconcentration of urinary iodide and its resolution from other abundant urinary interferences. Under these conditions, there was a monotonous increase in iodide signal with longer hydrodynamic injections up to 80 s (0.5 psi) while maintaining resolution that is equivalent to a urine sample filling approximately 34% of the total capillary length (**Figure S3.2**).

Figure 3.2A shows a representative electropherogram for a pooled 24 h urine sample (n = 800) diluted 2-fold in de-ionized water after a centrifugation to sediment particulates. NDS was included as an internal standard to improve migration time precision (*i.e.*, RMT) and quantitative performance (*i.e.*, RPA) due to run-to-run variations in EOF and sample injection volume, respectively. The average concentrations for iodide, thiocyanate and nitrate in a pooled urine sample collected from an adult population across Canada were measured to be 1.47 ± 0.05, 19.5 ± 1.2, and 968 ± 29 μM, respectively. Iodide levels were within the range of adequate iodine intake (0.78 – 1.47 μM),[3] which is consistent with recent literature in the Canadian Health Measures Survey reporting a geometric mean of 1.01 μM.[31] Also, the US National Health and Nutrition Examination Survey (NHANES) reports comparable urinary concentration levels in the adult population with geometric means of 1.29 μM iodide, 26.2 μM thiocyanate, and 814 μM nitrate.[32]

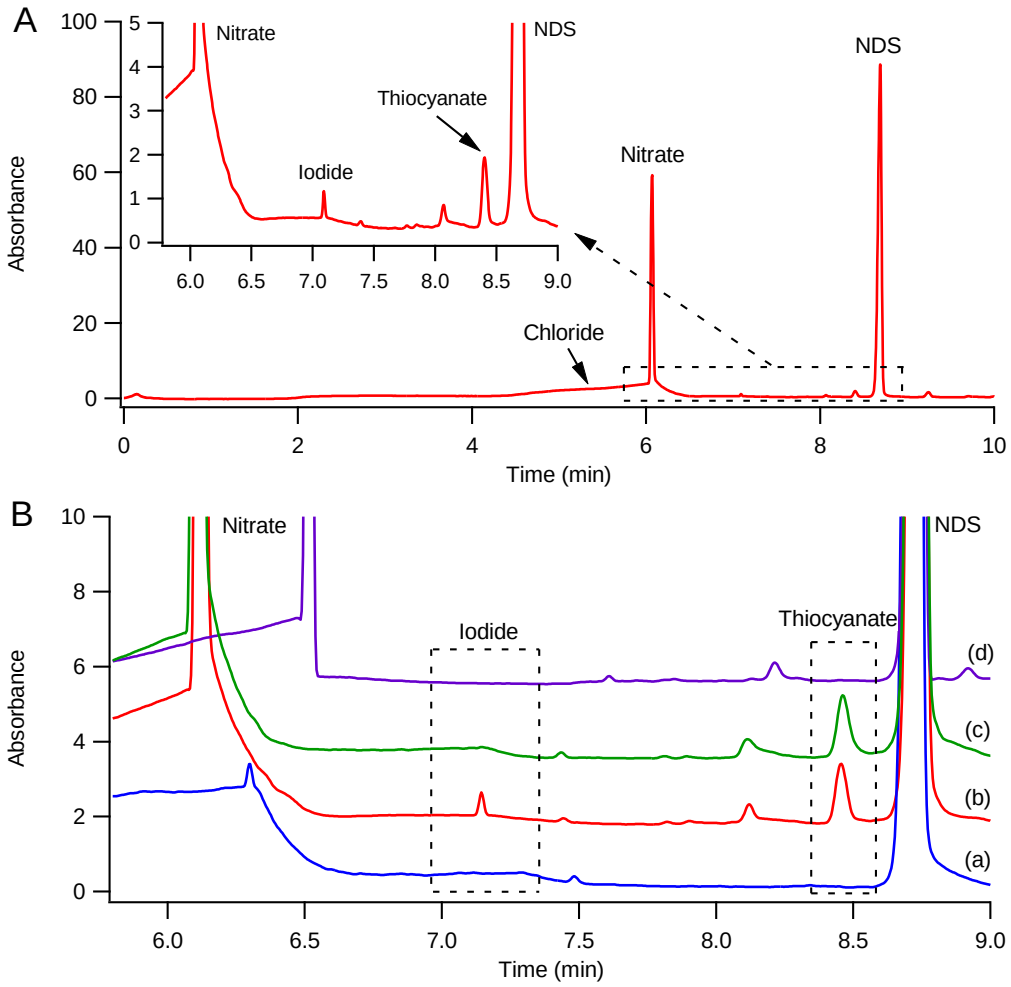

Figure 3.2. (**A**) Electropherogram of a pooled 24 h urine sample (*n* = 800) diluted 2-fold in de-ionized water, showing the anions detected at 226 nm, including nitrate (968 µM), NDS (20 µM, used as internal standard), iodide (1.47 µM), and thiocyanate (19.5 µM). Even though chloride does not absorb at 226 nm, its large excess causes a perturbation in the baseline before nitrate. (**B**) Electropherogram of a blank sample (a), composed of simulated urine with NDS and (b) a pooled 24h urine sample (*n* = 800). Selectivity was tested (c) by preparing the pooled urine sample with silver chloride to precipitate iodide and (d) by using a BGE without α-CD resulting in the comigration of iodide as a broad zone with chloride without sample self-stacking, whereas thiocyanate thiocyanate comigrates with nitrate.

Other UV-absorbing strong anions (*e.g.*, iodate, thiocyanate, thiosulfate, oxalate, nitrite, and citrate) spiked into urine did not interfere with iodide. Also, iodide was found to be stable in freshly collected random spot urine samples for at least 7 h at room temperature, as well as after four consecutive freeze/thaw cycles

(**Table S3.1**). Selectivity was further evaluated by analyzing a urine specimen using a BGE without α-CD (condition in which iodide co-migrates with chloride and the injection band remains broad and unfocused) and using silver ion to precipitate iodide (as AgI) prior to CE analysis (**Figure 3.2B**). In both cases, there was no signal at the RMT corresponding to iodide in contrast to the same sample spiked with iodide. The calibration curve [$y = (0.0169 \pm 0.0002)x + (0.0011 \pm 0.0002)$, iodide concentration in μM] demonstrated excellent linearity ($R^2 = 0.9998$) over a 20-fold concentration range (0.20 to 4.0 μM) as required for determination of urinary iodide status. Calibrant solutions were prepared in a simulated urine matrix in order to derive consistent iodide electromigration and sample self-stacking performance relative to authentic urine samples. Calibration curves and residual plots for thiocyanate and nitrate are also depicted in **Figure S3.3**. Intraday and interday precision measured for iodide had maximum RSD of 7.4% for relative peak areas, and 0.71% for RMT (**Table S3.2**). Method accuracy, evaluated on the basis of spike-recovery experiments were performed in triplicate at three different concentration levels, with an average recovery of 93% within the range of 80-110% (**Table S3.3**). Accuracy was also tested using a NIST reference urine samples (SRM 3668) with results derived from a validated ICP-MS method[33] with an acceptable bias of +15% at a higher iodide level (2.20 μM), but a slightly greater positive bias (+35%) was measured for a urine sample at a lower iodide level (1.12 μM). Similarly, average bias for urinary thiocyanate and nitrate at two levels was also found to be acceptable with +15% and -12% when comparing CE results with data from ion-exchange chromatography-ICP-MS. Decision charts to evaluate method acceptability for iodine deficiency tests rated "world-class" laboratories having a bias under 40% with imprecision at 10%, which are often not satisfied when using colorimetric kinetic methods.[34] However, consistent measurement of urinary iodide is important for adequate assessment of population iodine nutrition according to the categories recommended by the World Health Organization.[3] Therefore, future work will involve our participation

in the Ensuring the Quality of Iodine Procedures (EQUIP) program from the Centers for Disease Control and Prevention (CDC),[35] as well as an independent inter-laboratory study to evaluate the comparability of results obtained by CE and ICP-MS.

Method robustness was further evaluated by analyzing a pooled 24 h urine sample (n = 30) over 29 days. In this case, three replicate runs were analyzed intermittently each day between a block of ten individual urine samples when using new capillaries and preparing BGE stock solutions each week along with daily maintenance cleaning of the CE instrument. **Figure 3.3A** depicts representative electropherograms throughout the study period. An overall average RSD of 11% (n = 87) was derived for quantification of urinary iodide concentration, which is only marginally higher than the interday precision for the NIST standards over 3 days (RSD = 7.4%, n = 9), demonstrating acceptable intermediate precision (**Figure 3.3B**). Excellent long-term RMT precision was also realized for iodide (RSD = 0.74%) despite changes in fused-silica capillaries and buffer stock solutions over a five-week period. Furthermore, a series of five calibration curves derived from six calibrant solutions measured each day every week show excellent agreement in terms of method sensitivity (< 4% bias in slope) and long-term stability on the same instrument (**Figure 3.3C**). The validated method was applicable to urine samples with different iodide concentrations, which are representative of the main categories of iodine insufficiency according to the World Health Organization,[3] as shown in **Figure S3.4**. Due to the high ionic strength and buffer capacity of the BGE, sample self-stacking of urine samples was effective for the majority (> 92%) of urine specimens examined in our work after a 1.5-fold dilution in de-ionized water, including 800 different 24 h urine specimens from the PURE study.[28] This dilution level was found to be a trade-off between sensitivity and resolution in order to reliably quantify cases of moderate iodide deficiency near the *LOQ* of the CE method, as shown in **Figure S3.5**. In some cases, analysis (< 8%) with a 2-

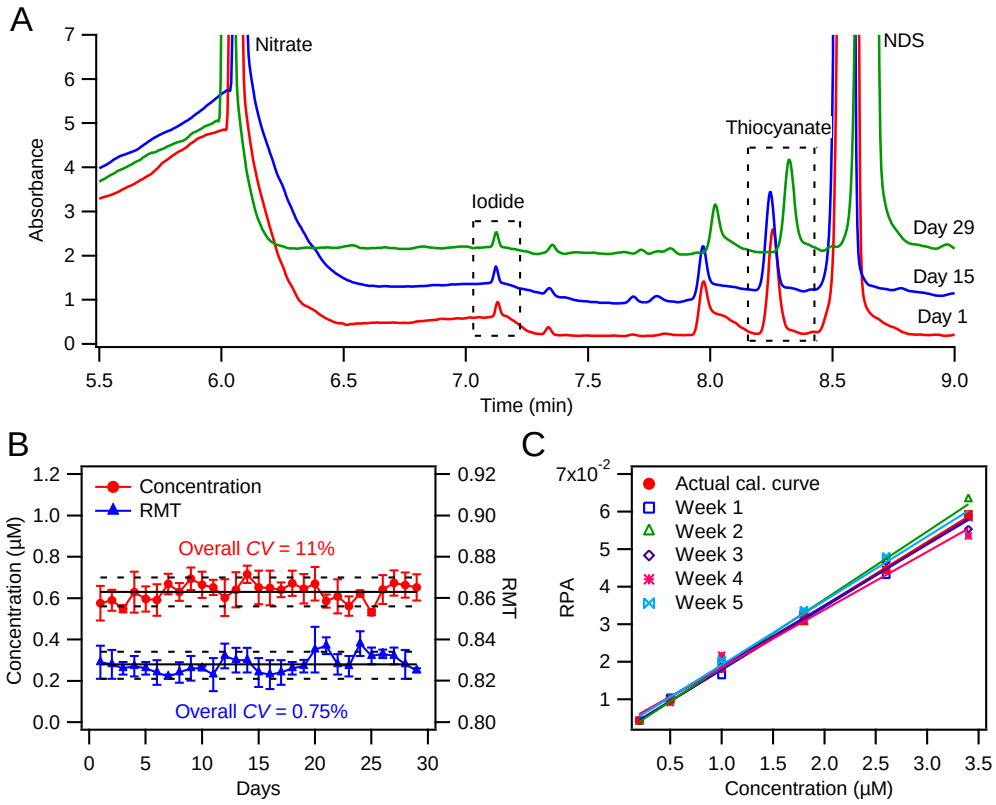

Figure 3.3. (**A**) Representative electropherograms of pooled 24 h urine samples (n = 30) analyzed over a 29 day robustness study. (**B**) Variability observed for these samples analyzed in triplicate each day using five different capillaries and five batches of BGE over 29 days (total of 87 runs), where error bars represent standard deviation (±SD) for the daily triplicate. The grand means for iodide concentration (0.63 µM) and RMT (0.827) are depicted by solid black lines, whereas dashed black lines represent the overall ±SD. (**C**) Calibration curves obtained by analyzing one calibrant solution per day each week during the study resulting in five independent curves with remarkable consistency to the original calibration performed prior to start of the study.

fold dilution in de-ionized water was required for certain urine samples with excessive iodide levels that exceeded the upper linear range of the method or concentrated urine samples with high conductivity that altered iodide migration resulting in co-migration with urine interference. Overall, the CE method was found to largely tolerate the vast majority of urine matrices collected within a large-scale epidemiological study that vary widely in hydration status and diet. The other strong anions analyzed in the assay, thiocyanate and nitrate, also were found to have acceptable intermediate precision (RSD < 7% for urinary

concentration; RSD < 1% for RMTs) as shown in **Figure S3.6**. Both nitrate and thiocyanate are known to inhibit iodide uptake by the thyroid, and thus have been studied in conjunction with iodide in urine and serum.[32,36] Nitrate exposure is typically derived from contaminated drinking water, whereas thiocyanate is a metabolite of cyanide that is derived from smoke-exposure and/or the consumption of certain foods, such as cassava. An iodide assay that provides additional insight into iodide uptake inhibitors, without increasing cost or time demands provides "added-value" to epidemiological studies.[11] Although iodine status was the primary focus of this work, this method is also applicable to iodide, nitrate and/or thiocyanate analysis in human sweat specimens (**Figure S3.7**). For instance, sweat, as a secondary route of iodide elimination in the body, may cause iodine deficiency in athletes undergoing vigorous exercise under hot weather conditions.[37] However, it is not feasible to analyze perchlorate, a potent inhibitor of iodide uptake, by our method as it is a UV-transparent strong anion, thus requires CE with indirect UV detection.[26]

3.5 Conclusions

In summary, this report introduces a robust CE assay for iodide status determination suitable for large-scale epidemiological studies as required for global health initiatives. Excellent selectivity and adequate sensitivity are achieved while using a simple on-line sample preconcentration method based on sample self-stacking that requires only a modest dilution of urine. This method takes advantage of the high saline content in urine specimens, a high ionic strength/acidic lithium phosphate buffer system as BGE, and α-CD as an additive to tune the mobility of iodide (and thiocyanate) using an unmodified fused-silica capillary under reversed polarity. Rigorous internal method validation demonstrates acceptable accuracy, intermediate precision and linear dynamic range to classify urinary iodide status among diverse urine specimens with excellent long-term stability over five weeks of continuous analysis. Although

ICP-MS can reach lower limits of quantification (< 0.08 μM), the sensitivity of the CE assay with sample self-stacking is comparable to the kinetic spectrophotometric assays (*LOQ* = 0.20-0.39 μM), with similar interday precision as both methodologies (RSD ≈ 10%).[17,33,38] Major benefits of this method include greater selectivity for resolution of iodide from other iodine-related interferences that also permit simultaneous analysis of nitrate and thiocyanate using volume-restricted urine specimens from biorepositories (≈ 10 μL) without complicated sample handling. The method can also tolerate large differences in urine conductivity caused by between-subject variation in hydration status that is readily corrected by appropriate dilution or matrix matching if required. Apart from infrastructure costs for the CE instrumentation and lifespan of deuterium lamp, operational cost for large-scale analyses are minimal (< $1/sample) due to the use of a small amount of aqueous buffer and largely inexpensive reagents with a sample throughput of about 80 samples/day, including sample workup. CE offers a robust yet cost-effective approach for ongoing surveillance of iodine iodine insufficiency by public health agencies to ensure optimum iodine nutrition in the population. Further work will involve extended method validation including an inter-laboratory method comparison to assess the consistency of CE-derived urinary iodine concentration relative to the reference method, ICP-MS.

3.6 Acknowledgements

P.B.M. wishes to acknowledge funding support from Natural Sciences and Engineering Research Council of Canada. A.N.M. acknowledges generous support from the Province of Ontario in the form of an Ontario Trillium Scholarship. The authors also acknowledge the Public Health Agency of Canada (PHAC) for supporting this work. Further thanks are also directed to Jeff Chapman and John Hudson at Beckman-Coulter Inc.

3.7 References

(1) FAO; WHO. In *Human vitamin and mineral requirements*; FAO: Rome, 2001; pp 181–194.

(2) Cavalieri, R. R. *Thyroid* **1997**, *7*, 177–181.

(3) World Health Organization. *Assessment of iodine deficiency disorders and monitoring their elimination: a guide for programme managers*, 3rd ed.; WHO: Geneva, 2007.

(4) Gnat, D.; Dunn, A. D.; Chaker, S.; Delange, F.; Vertongen, F.; Dunn, J. T. *Clin. Chem.* **2003**, *49*, 186–188.

(5) Perrine, C. G.; Herrick, K.; Serdula, M. K.; Sullivan, K. M. *J. Nutr.* **2010**, *140*, 1489–1494.

(6) Andersson, M.; Karumbunathan, V.; Zimmermann, M. B. *J. Nutr.* **2012**, *142*, 744–750.

(7) Benoist, B.; McLean, E.; Andersson, M.; Rogers, L. *Food Nutr. Bull.* **2008**, *29*, 195–202.

(8) Dunn, J. T. *J. Clin. Endocrinol. Metab.* **1998**, *83*, 3398–3400.

(9) Trumpff, C.; De Schepper, J.; Tafforeau, J.; Van Oyen, H.; Vanderfaeillie, J.; Vandevijvere, S. *J. Trace Elem. Med. Biol.* **2013**, *27*, 174–183.

(10) Zimmermann, M. B. *Proc. Nutr. Soc.* **2010**, *69*, 133–143.

(11) Ozpinar, A.; Kelestimur, F.; Songur, Y.; Can, O.; Valentin, L.; Caldwell, K.; Arikan, E.; Unsal, I.; Serteser, M.; Inal, T.; Erdemgil, Y.; Coskun, A.; Bakirci, N.; Sezgin, O.; Blount, B. *PLoS One* **2014**, *9*, e88206.

(12) Zimmermann, M. B. *J. Trace Elem. Med. Biol.* **2008**, *22*, 81–92.

(13) Andersson, M.; de Benoist, B.; Rogers, L. *Best Pract. Res. Clin. Endocrinol. Metab.* **2010**, *24*, 1–11.

(14) Dunn, J. T. *J. Clin. Endocrinol. Metab.* **1996**, *81*, 1332–1335.

(15) Brauer, V. F. H.; Paschke, R. In *Comprehensive handbook of iodine:nutritional, biochemical, pathological, and therapeutic aspects*; Preedy, V. R., Burrow, G. N., Watson, R. R., Eds.; Elsevier: Amsterdam, Boston, 2009; pp 411–420.

(16) Soldin, O. P. *Clin. Biochem.* **2002**, *35*, 575–579.

(17) Shelor, C. P.; Dasgupta, P. K. *Anal. Chim. Acta* **2011**, *702*, 16–36.

(18) Moreda-Piñeiro, A.; Romarís-Hortas, V.; Bermejo-Barrera, P. *J. Anal. At. Spectrom.* **2011**, *26*, 2107–2152.

(19) Romarís-Hortas, V.; Bermejo-Barrera, P.; Moreda-Piñeiro, A. *J. Chromatogr. A* **2012**, *1236*, 164–176.

(20) Hirokawa, T.; Yoshioka, M.; Okamoto, H.; Timerbaev, A. R.; Blaschke, G. *J. Chromatogr. B* **2004**, *811*, 165–170.

(21) Pantůcková, P.; Krivánková, L. *Electrophoresis* **2004**, *25*, 1102–1110.

(22) Huang, Z.; Ito, K.; Timerbaev, A. R.; Hirokawa, T. *Anal. Bioanal. Chem.* **2004**, *378*, 1836–1841.

(23) Xu, Z.; Doi, T.; Timerbaev, A. R.; Hirokawa, T. *Talanta* **2008**, *77*, 278–281.

(24) Hirokawa, T.; Ichihara, T.; Ito, K.; Timerbaev, A. R. *Electrophoresis* **2003**, *24*, 2328–2334.

(25) Timerbaev, A. R.; Fukushi, K.; Miyado, T.; Ishio, N.; Saito, K.; Motomizu, S. *J. Chromatogr. A* **2000**, *888*, 309–319.

(26) Macedo, A. N.; Jiwa, M. I. Y.; Macri, J.; Belostotsky, V.; Hill, S.; Britz-McKibbin, P. *Anal. Chem.* **2013**, *85*, 11112–11120.

(27) Gebauer, P.; Krivánková, L.; Pantůcková, P.; Bocek, P.; Thormann, W. *Electrophoresis* **2000**, *21*, 2797–2808.

(28) Teo, K.; Chow, C. K.; Vaz, M.; Rangarajan, S.; Yusuf, S. *Am. Heart J.* **2009**, *158*, 1–7.

(29) Masár, M.; Bodor, R.; Kaniansky, D. *J. Chromatogr. A* **1999**, *834*, 179–188.

(30) Gelb, R. I.; Schwartz, L. M.; Radeos, M.; Laufer, D. A. *J. Phys. Chem.* **1983**, *87*, 3349–3354.

(31) Statistics Canada. *Canadian Health Measures Survey: cycle 2 data tables - 2009 to 2011*; Statistics Canada: Ottawa, 2012.

(32) Bruce, G. M.; Corey, L. M.; Mandel, J. H.; Pleus, R. C. *J. Occup. Environ. Med.* **2013**, *55*, 52–58.

(33) Caldwell, K.; Maxwell, C. B.; Makhmudov, A.; Pino, S.; Braverman, L. E.; Jones, R. L.; Hollowell, J. G. *Clin. Chem.* **2003**, *49*, 1019–1021.

(34) Hussain, H.; Khalid, N. M.; Selamat, R.; Nazaimoon, W. M. W. *Ann. Lab. Med.* **2013**, *33*, 319–325.

(35) Makhmudov, A. A.; Caldwell, K. L. *IDD Newsl.* **2011**, 4–6.

(36) Mervish, N.; Blount, B.; Valentin-Blasini, L.; Brenner, B.; Galvez, M. P.; Wolff, M. S.; Teitelbaum, S. L. *J. Expo. Sci. Environ. Epidemiol.* **2011**, *22*, 212–218.

(37) Smyth, P. P. A.; Duntas, L. H. *Horm. Metab. Res.* **2005**, *353*, 1–4.

(38) Ohashi, T.; Yamaki, M.; Pandav, C. S.; Karmarkar, M. G.; Irie, M. *Clin. Chem.* **2000**, *46*, 529–536.

3.8 Supporting Information Section

Table S3.1. Stability tests for iodide and thiocyanate in urine, after storage at room temperature (≈ 25ºC) or multiple freeze-thaw cycles, represented as the recovery (%) relative to the results obtained for the freshly collected sample.

Freeze-thaw stability			Room temperature stability		
Cycles	**Iodide**	**Thiocyanate**	**Hours**	**Iodide**	**Thiocyanate**
1	98 ± 1	93 ± 6	1	98	103
2	97 ± 3	95 ± 14	2	98	92
3	101 ± 6	95 ± 2	4	101	109
4	99 ± 7	102 ± 2	7	104	95

Table S3.2. Interday and intraday precision for relative peak areas (RPA) and relative migration times (RMT) of iodide, thiocyanate, and nitrate by CE with UV detection, using pooled 24 h urine for intraday precision and NIST standard reference materials (SRM 3668) for interday precision.

Anions	Intraday precision (*n* = 10)			Interday precision (*n* = 3 x 3)		
	Conc. (µM)	RSD (%)		Conc. (µM)	RSD (%)	
		RPA	RMT		RPA	RMT
Iodide	1.47	3.4	0.71	1.12 2.20	7.4 5.3	0.074 0.21
Thiocyanate	19.5	6.0	0.074	20.0 119.1	7.2 5.6	0.050 0.055
Nitrate	977.6	3.0	0.87	624 1456	2.6 5.1	0.12 0.27

Table S3.3. Accuracy based on spike-recovery at three concentration levels analyzed in triplicate, and NIST reference urine samples (SRM 3668) at two concentration levels, analyzed in triplicate over three days.

Anion	Spike-recovery (*n* = 3)		NIST ref. material (*n* = 9)	
	Conc. spiked (µM)	Recovery ± SD (%)	Ref. conc. (µM)	Bias (%)
Iodide	0.50	88 ± 9	1.12	35
	1.00	99 ± 5	2.20	15
	2.00	93 ± 4	-	-
Thiocyanate	4.00	100 ± 10	20.0	23
	8.00	113 ± 16	119.1	6
	12.00	118 ± 10	-	-
Nitrate	-	-	624	-8
	-	-	1456	-14

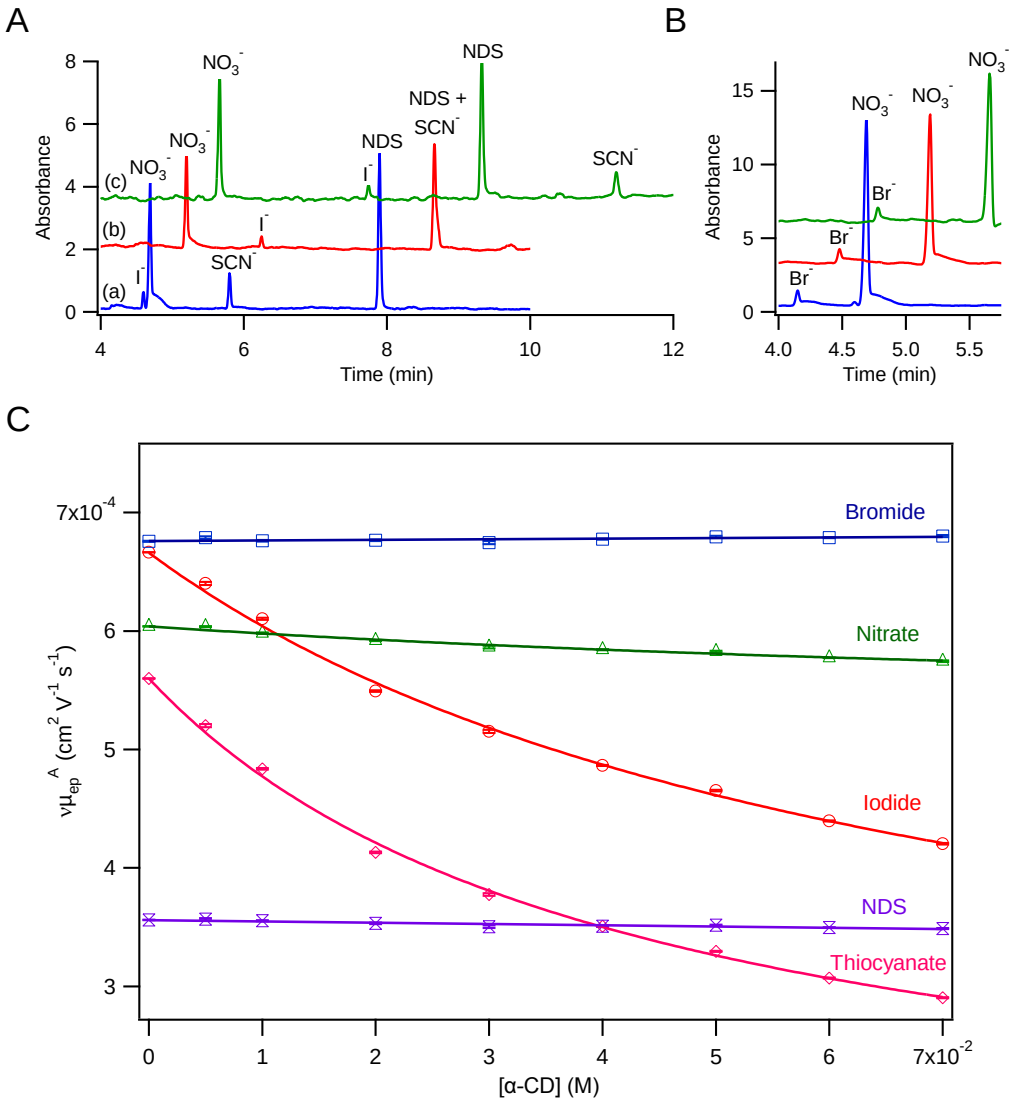

Figure S3.1. An electropherogram overlay showing the impact of α-CD concentration in the BGE, including (a) 10 mM, (b) 40 mM, and (c) 70 mM α-CD, for the separation of a standard solution containing bromide (100 µM), nitrate (500 µM), iodide (10 µM), thiocyanate (100 µM), and NDS (20 µM) at (**A**) 226 nm and (**B**) 214 nm. Bromide has weak absorbance at 226 nm (maximum absorbance optimum for iodide), but is detectable at 214 nm. The standard solution was prepared in water and hydrodynamicaly injected for 5 s (at 0.5 psi). (**C**) Binding isotherm showing the viscosity-corrected electrophoretic mobilities ($\nu\mu_{ep}^{A}$) of the anions as a function of α-CD concentration in the BGE. Bromide, NDS and nitrate have negligible interactions with α-CD, whereas iodide and thiocyanate have apparent binding constants of K_b = 15 ± 2 M^{-1} and K_b = 24 ± 2 M^{-1}, respectively. These binding constants are comparable with data reported by Gelb et al. (*J. Phys. Chem.* **1983**, *87*, 3349–3354).

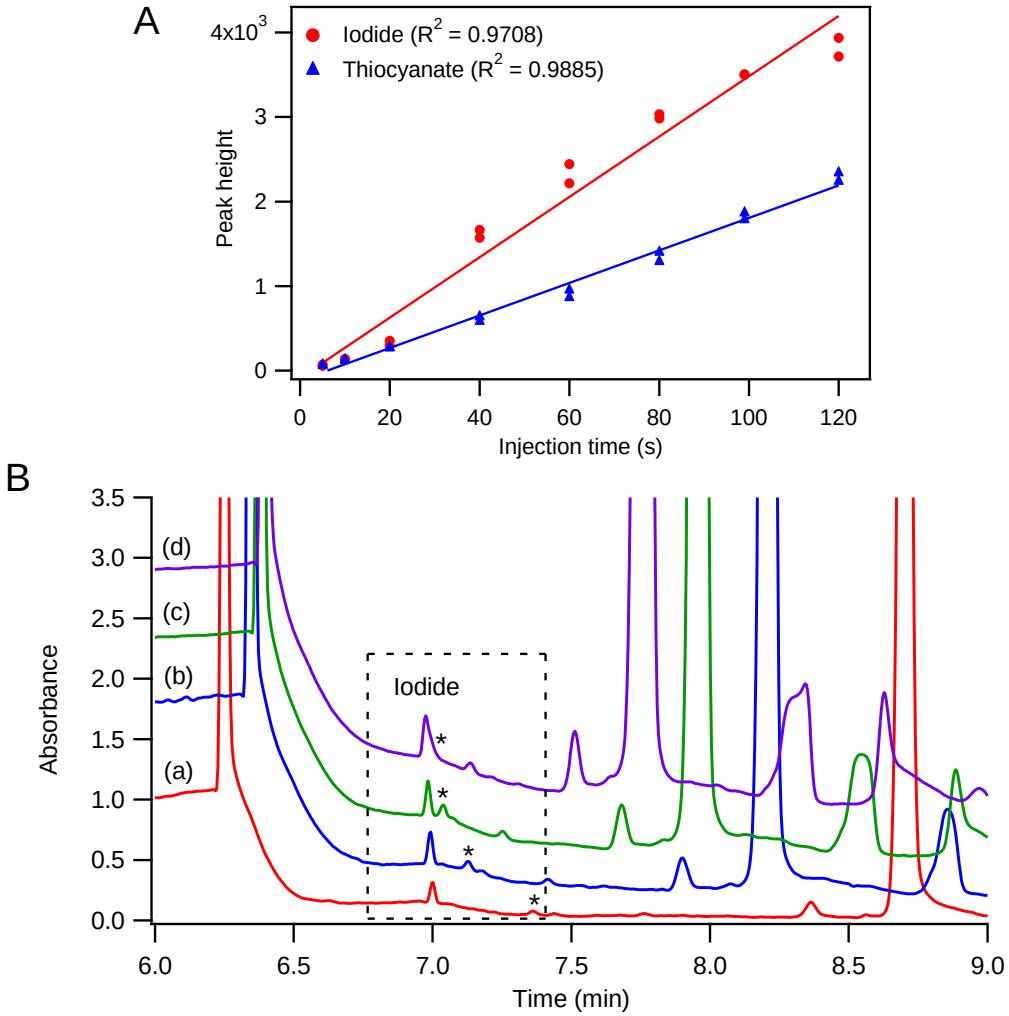

Figure S3.2. (**A**) Monotonous increase in peak height measured for a standard solution containing 10 µM iodide and 20 µM thiocyanate as a function of hydrodynamic injection length (from 5 to 120 s at 0.5 psi) when using sample self-stacking in CE with UV detection. All samples were prepared in a simulated urine matrix solution diluted 1:1 in de-ionized water. Although there is a continuous increase in absorbance response (226 nm) for iodide without significant band broadening in standard solutions, (**B**) resolution is compromised when using injections longer than 80 s for human urine specimens, as shown in the electropherogram overlay of a 2-fold diluted random spot urine sample containing 2.34 µM iodide. The resolution between iodide and an unknown interfering signal from human urine (indicated by asterisk) is adequate for (a) 40 s and (b) 80 s injections, but becomes problematic when the injection time increases to (c) 100 s with co-migratation at d) 120 s injection. Loss of resolution with longer sample injection times is a result of filling a major portion of the capillary with urine, which results in a shorter effective capillary length for separation (120 s injection, for example, corresponds to ≈ 50% of the total capillary length, 60 cm). For this reason, an optimum sample loading of 80 s (≈ 34% of the capillary length) was used in our work as it represents a compromise between sensitivity gain while resolution needed for reliable urinary iodide analysis.

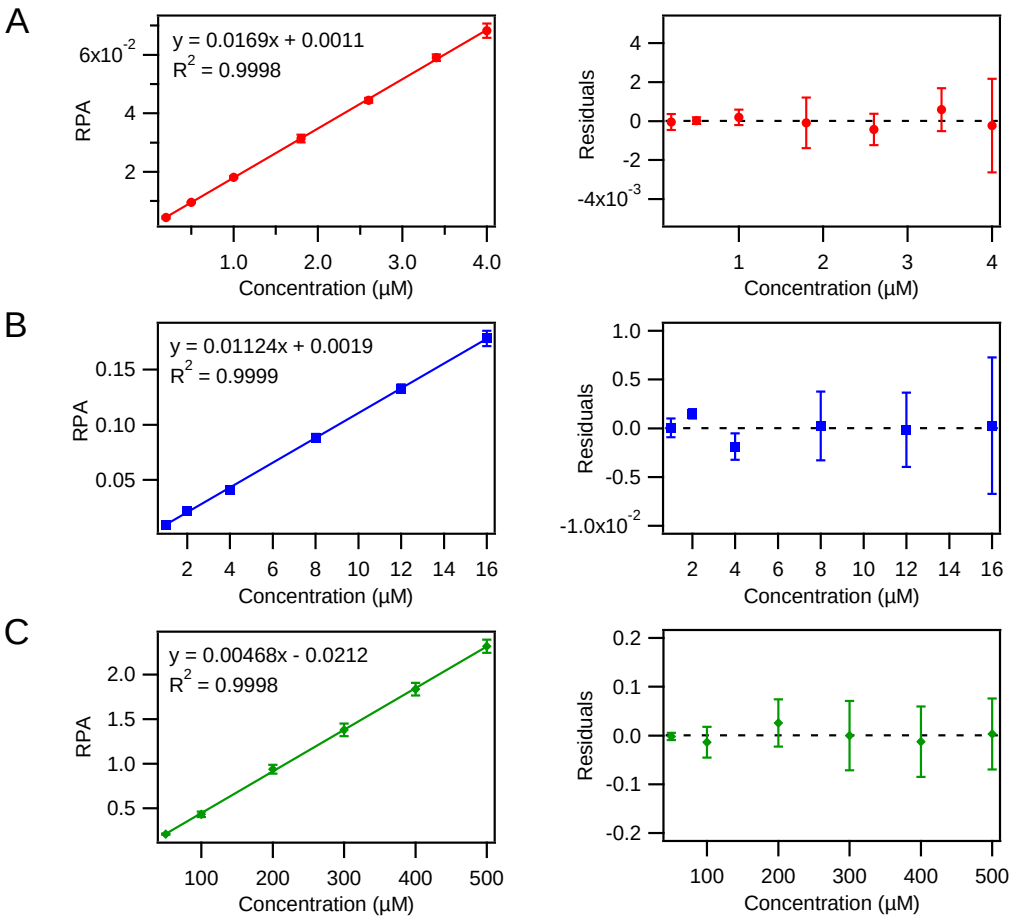

Figure S3.3. External calibration curves and residual plots for (**A**) iodide (0.20 – 4.00 µM), (**B**) thiocyanate (1.00 – 16.00 µM), and (**C**) nitrate (50 – 500 µM) highlighting the linear increase in measured responses (*i.e.*, relative peak area, RPA) as a function of analyte concentration. Solutions were prepared in triplicate, in a 1:1 v mixture of simulated urine matrix and de-ionized water, containing 20 µM NDS as internal standard. Determination coefficients (R^2) were > 0.999, what shows excellent linearity for all the three anions. Although the residual plots presented values scattered both above and below the zero line throughout all the calibration range, there was a trend for larger variance at higher concentration levels. For this reason, weighted linear least squares regression was evaluated as an option to counteract the possible excessive influence of larger concentrations. However, unweighted linear least squares regression was preferred, as it produced similar slopes and y-intercepts in comparison with weighted least squares, with equal (for iodide and nitrate) or even better (for thiocyanate) sum of percentage relative error (Σ%RE), as compared to weighted linear least squares. In all cases, %RE was below 14% for the LOQ and other concentration levels, which is a good indicator of the model goodness of fit (Almeida et al. *J. Chromatogr. B* **2002**, *774*, 215–222).

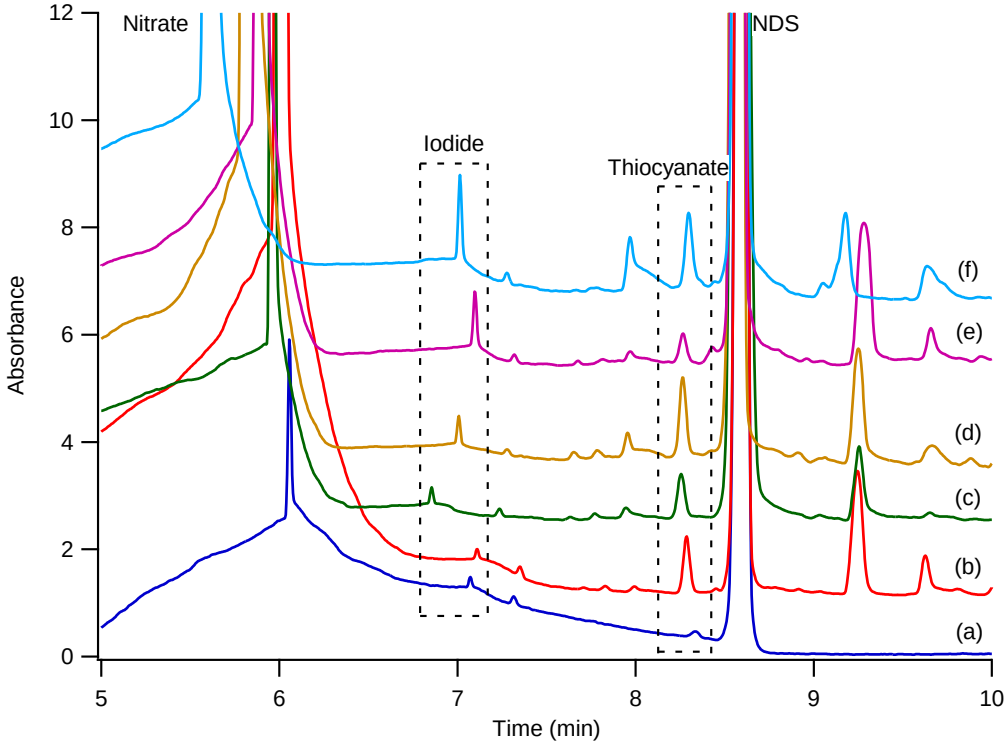

Figure S3.4. Electropherogram showing the application of the CE assay to (a) a standard solution containing iodide at the *LOQ* level (0.20 µM), as well as representative 24 h urine samples with different concentrations of iodide: (b) 0.30 µM, (c) 0.49 µM, (d) 0.92 µM, (e) 2.30 µM, and (f) 3.35 µM. These levels span the major categories of iodide nutritional status according to the World Health Organization (WHO, *Assessment of iodine deficiency disorders and monitoring their elimination: a guide for programme managers*; Geneva, 2007), including moderate deficiency (0.16 – 0.38 µM), mild deficiency (0.39 – 0.78 µM), adequate intake (0.79 – 1.57 µM), more than adequate (1.58 – 2.36 µM) and excessive intake (≥ 2.37 µM). Urine samples were diluted 1.5-fold in de-ionized water with 20 µM NDS as internal standard. Apparent migration times for iodide were found to vary considerably (RSD = 1.8% for five 24 h urine samples), due to variations in the ionic strength/conductivity of urine samples as a result of between-subject differences in hydration status/diet, however this does not impact iodide peak identification nor quantification. The use of relative migration times (RMTs) helps to improve the precision of the migration behaviour (RSD = 1.4% for iodide RMT in five 24 h urine samples), even though in this case the improvement is only moderate, as a result of the difference between the migration times of iodide and NDS (> 1.4 min).

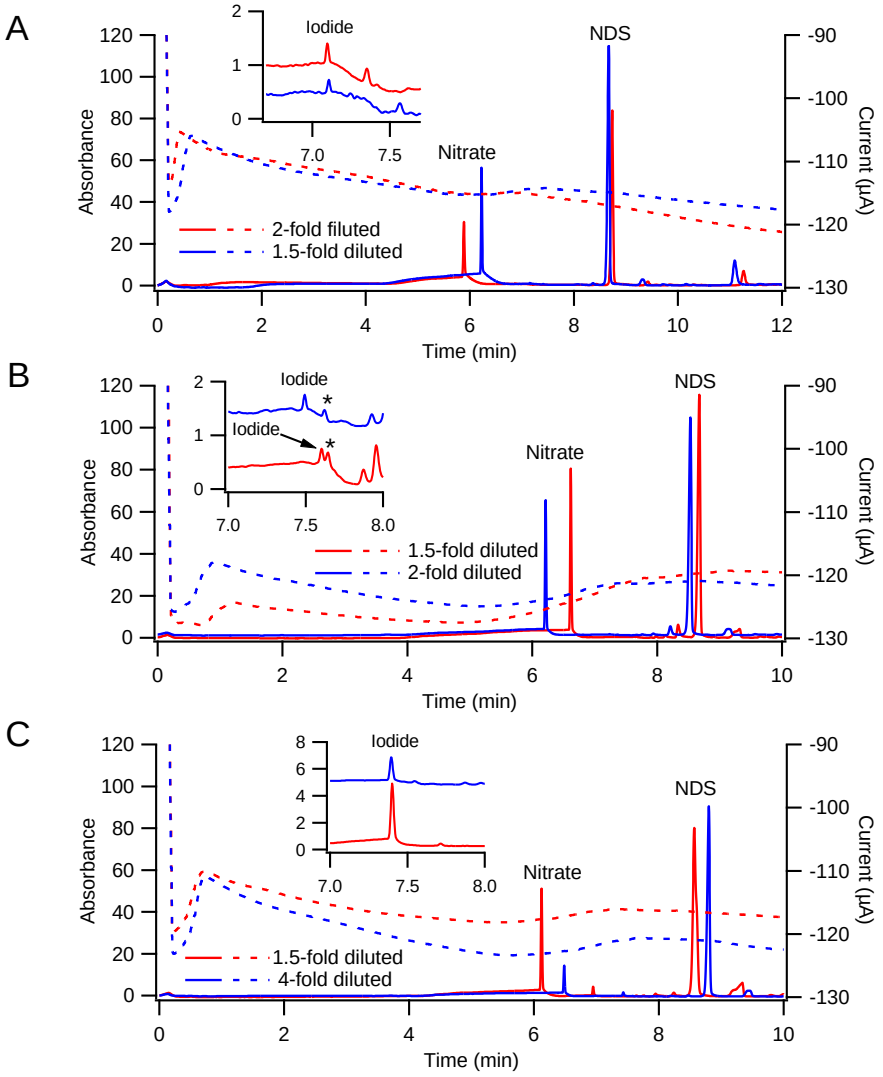

Figure S3.5. Electropherograms showing adjustments in sample dilution for specific urine samples (left y-axis, continuous trace) and the variability in the resultant current (right y-axis, dashed trace under reversed polarity). Between-subject variations in 24 h urine samples reflect differences in hydration status/diet that alters urine conductivity and can impact CE separation when using sample self-stacking. Overall, the separation current was found not to be constant over the entire run due to the large sample injection of minimally diluted human urine for online sample preconcentration. For instance, (**A**) some individual 24 h urine samples in which iodide was slightly below the *LOQ* when the samples were 2-fold diluted, could be quantified by minimizing dilution to 1.5-fold. While 1.5-fold dilution works well for the majority of urine samples examined in our study (> 92% of 800 24 h urine samples), (**B**) it can affect the resolution between iodide and an interference present in the urine matrix (indicated with asterisk) for some samples with very high conductivity (current > 125 µA). In these cases, the problem is solved by simply increasing the sample dilution to 2-fold in de-ionized water. (**C**) Also, samples that had a very high excess of iodide, required additional dilution to fall within the linear range of the method (0.20-4.00 µM), as shown in a urine sample with 10.12 µM iodide, which requires further dilution of 4-fold in 1:1 simulated urine in de-ionized water.

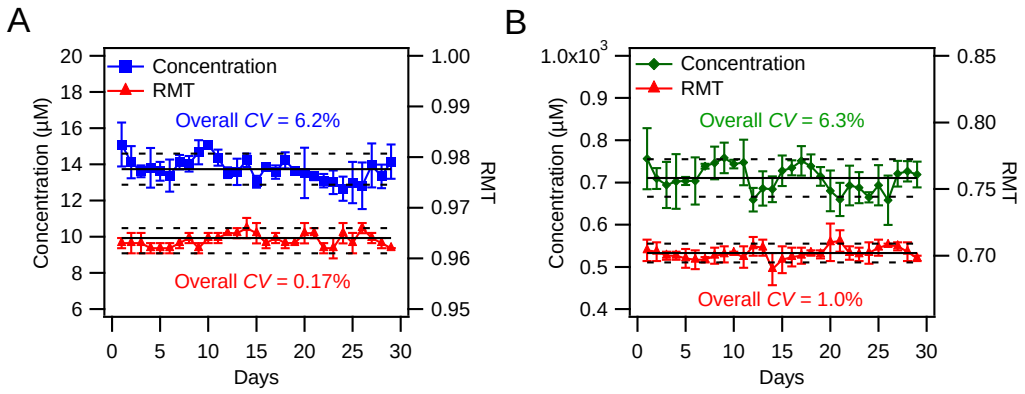

Figure S3.6. Long-term variability in (**A**) thiocyanate and (**B**) nitrate measurements derived from a 24 h pooled urine sample (n = 30) analyzed in triplicate over 29 days (total of 87 runs) using five different capillaries and five batches of BGE throughout the study (on days 1, 8, 14, 20 and 26). Overall RSD for measured urinary concentrations were 6.2% and 6.3% for thiocyanate and nitrate, respectively. Also, relative migration times (RMTs) had excellent intermediate precision with overall RSD of 0.17% for thiocyanate and 1.0% for nitrate. The better precision measured for the RMT of urinary thiocyanate is due to its close migration time with internal standard. Compared to their interday precision (Table 3.S2), thiocyanate and nitrate had similar RSDs for concentrations, but higher (yet still acceptable) RSDs for RMTs over a longer time period. Error bars represent the standard deviation (SD) for the daily replicates, while the solid black lines indicate the overall mean concentrations and RMT of thiocyanate (13.7 µM and RMT = 0.963) and nitrate (710 µM and RMT = 0.702). Dashed black lines show the interval of the overall mean ± SD for concentrations (12.9-14.6 and 666-755 µM for thiocyanate and nitrate, respectively), as well as RMT (0.962-0.965 for thiocyanate and 0.695-0.709 for nitrate). Overall, the CE assay provides excellent long-term stability with adequate robustness for reliable measurements of iodide, as well as two relevant iodide-uptake inhibitors in the environment, namely nitrate and thiocyanate.

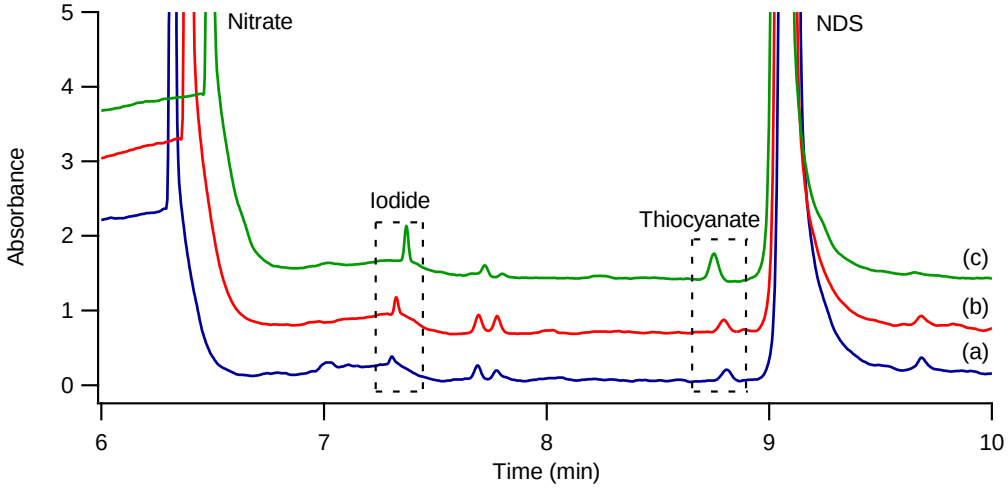

Figure S3.7. Electropherograms of three individual sweat samples collected by pilocarpine iontophoresis, containing (a) 0.32 µM iodide and 2.34 µM thiocyanate, (b) 0.71 µM iodide and 2.33 µM thiocyanate, and (c) 1.59 µM iodide and 4.83 µM thiocyanate. In this case, nitrate was not quantified due to the application of pilocarpine nitrate as a sweat stimulant before sample collection, so that nitrate present in the sample is not just from endogenous source. Although most iodide is excreted through the urine, sweat is another route of iodide excretion in the human body, which may be of interest especially in studies involving iodide loss in athletes undergoing intense exercise (Smyth, P. P. A.; Duntas, L. H. *Horm. Metab. Res.* **2005**, *353*, 1–4.).

Chapter IV

Validation of a Capillary Electrophoresis Assay for Monitoring Iodine Nutrition in Populations for Prevention of Iodine Deficiency: An Inter-Laboratory Method Comparison

Authors of this work are Adriana Nori de Macedo, Joseph Macri, Patricia Hudecki, Michelle Saoi, Matthew McQueen, and Philip Britz-McKibbin.

I conducted the urinary iodine analysis using the original and optimized CE-UV methods, performed the experiments to evaluate sources of bias and did most of the data analysis, as well as wrote an initial manuscript draft for publication. Other co-authors performed the ICP-MS analysis and provided feedback on the manuscript draft (accepted for publication in the Journal of Applied Laboratory Medicine).

Chapter IV: Validation of a Capillary Electrophoresis Assay for Monitoring Iodine Nutrition in Populations for Prevention of Iodine Deficiency: An Inter-Laboratory Method Comparison

4.1 Abstract

A capillary electrophoresis (CE) assay was recently introduced as a new method for monitoring iodine nutrition in large-scale epidemiological studies. However, further tests revealed unanticipated matrix-dependent interferences when analyzing sub-micromolar levels of iodide in human urine, as the predominate, bioavailable form of dietary iodine. Herein, we describe a rigorous validation study that was used to identify sources of bias and establish modifications to the original CE method to improve method accuracy. An inter-laboratory method comparison using CE with UV detection and inductively coupled plasma-mass spectrometry (ICP-MS) was performed to quantify urinary iodine concentrations (n = 71) independently at McMaster University and Hamilton General Hospital, as well as the Centers for Diseases Control (CDC) as part of their global quality assurance program. A positive bias in the original CE method was indicated and buffer conditions were subsequently optimized to overcome matrix interferences for reliable iodine determination. Positive bias in CE was attributed to variable concentrations of sulfate, a major urinary anion interference with similar mobility to iodide under the conditions originally reported. By increasing the concentration of α-cyclodextrin in the background electrolyte, the CE method was able to tolerate urinary sulfate over its normal physiological range without loss in signal response for iodide. The optimized CE assay generated results that were consistent with ICP-MS using two different internal standards (^{187}Re and ^{130}Te) with a median bias under 10%. CE offers a simple, selective, and cost-effective platform for surveillance of iodine status of a population requiring only small volumes (< 10 µL) of bio-banked urine specimens, which is comparable to

previously validated screening methods currently used in global health initiatives for prevention of iodine deficiency disorders.

4.2 Introduction

Iodine deficiency remains a global public health problem that is related to a spectrum of disorders, including goiter, hypothyroidism, depression, obesity and increased risk for cardiovascular diseases and cancer in adults, as well as impaired physical and cognitive development in children.[1–7] Despite well-established international salt iodization programs, dietary iodine intake patterns have changed over time in many regions due to lifestyle modifications that have contributed to increased ingestion of processed foods largely derived from non-iodized salt.[8,9] Arbitrarily increasing dietary iodine is not a viable solution in population health, since both chronic iodine deficiency and excess intake are associated with adverse health effects.[10] Therefore, continuous monitoring is essential to evaluate the efficacy of global iodization programs.[7,11] In this case, the median urinary iodine concentration is widely used to evaluate iodine nutrition of a population since more than 90% of iodine recently ingested is excreted in the urine as iodide.[12] The availability of simple yet affordable methods for reliable determination of iodine status is essential to advance preventative health initiatives for population health, such as iodine supplementation of at least 150 µg daily for pregnant and breastfeeding women now recommended by the American Academy of Pediatrics.[13]

The most common approach to analyze urinary iodine is kinetic spectrophotometry based on the Sandell-Kolthoff (S-K) reaction.[14] Despite its low operational cost, the S-K method and its variants have a number of limitations, including the need for heat digestion and oxidation of urine prior to the analysis, use of toxic reagents (*e.g.*, arsenic, perchloric acid), redox interferences in urine and changes in experimental conditions that affect reaction kinetics.[15–18] As a

result, inductively coupled plasma-mass spectrometry (ICP-MS) is considered the reference method for urinary iodine determination, which provides excellent precision and sensitivity without complicated sample workup.[19] However, ICP-MS lacks specificity as it measures total iodine in urine, including iodinated contrast agents, drugs, and food additives,[20] whereas the instrumentation is expensive with high operational costs due to argon consumption.[15] Alternatively, capillary electrophoresis (CE) with UV detection offers a simple microseparation platform for direct analysis of sub-micromolar levels of iodide in complex biological samples with adequate sensitivity when using on-line sample preconcentration.[21–23] However, rigorous method validation studies are lacking for reliable urinary iodine determination by CE, despite the successful translation of CE-based assays for routine molecular diagnostics in clinical laboratories.[24]

A robust CE method was recently introduced for nutritional iodine status assessment with acceptable intermediate precision (CV = 12%, n = 87) over several weeks of operation as required for large-scale epidemiological studies.[25] The assay was optimized to provide adequate sensitivity and selectivity for quantification of iodide in human urine samples after a simple dilution step in de-ionized water. Dynamic complexation of iodide with α-cyclodextrin (α-CD) in the background electrolyte (BGE) was critical for resolving sub-micromolar levels of urinary iodide from up to a 10^6-fold excess of chloride, which also provided optimum conditions for on-line sample preconcentration via sample self-stacking.[25] Internal method validation demonstrated good linearity (R^2 = 0.9998), sensitivity (LOQ = 0.20 µmol/L), and inter-day precision (CV < 8%). However, a positive bias of up to 35% was reported in a limited set of reference urine samples from the National Institute of Standards and Technology (NIST) that were measured by ICP-MS. This prompted us to conduct a more extensive inter-laboratory validation study to investigate the potential source(s) of bias in the original CE-UV assay relative to ICP-MS. Unexpectedly, the major UV-transparent strong anion in human urine, sulfate[26] was found to act as a matrix

interference by impairing sample self-stacking of iodide, resulting in a loss of signal intensity exceeding 50% at high sulfate concentrations. By increasing the concentration of α-CD in the BGE, the effective mobility of iodide was shifted to avoid urinary sulfate interferences resulting in consistent results to ICP-MS, which were performed independently at Hamilton General Hospital, as well as the Centers for Disease Control and Prevention (CDC) as part of their Ensuring the Quality of Urinary Iodine Procedures (EQUIP) program.[27] Additionally, the performance of two commonly used internal standards for urinary iodine analysis by ICP-MS, namely ^{187}Re and ^{130}Te, was also evaluated in terms of overall method precision and accuracy due to the lack of a suitable stable natural isotope for iodine.

4.3 Experimental Section

4.3.1 Urine samples and study design

The first method comparison comprised representative 24 h human urine samples (n = 50) obtained from the Prospective Urban and Rural Epidemiological (PURE) study,[28] where CE-UV and ICP-MS analyses were conducted in a double-blinded manner at McMaster University and Hamilton General Hospital, respectively. All urine samples were labeled by a third person prior to analysis, with results processed by a fourth individual in order to keep analysts blinded during sample preparation and data processing. Spiked samples were prepared from three independent pooled samples, each containing 20 randomly selected 24 h urine samples from the PURE study, excluding participants who were taking *L*-thyroxine (T4) and/or had iodine levels > 0.79 µmol/L. These pooled urine samples were spiked with iodide calibrants at four levels that span physiologically relevant iodine concentrations (0.79, 1.58, 2.36 and 3.15 µmol/L) in order to compare the recovery for iodine when using CE-UV and ICP-MS. Similarly, serially diluted samples in de-ionized water were prepared to evaluate potential

matrix effects in urine from three independent pooled samples, each containing 10 randomly selected 24 h urine samples from the PURE study, excluding participants who were taking T4 and/or had iodine < 1.93 or > 3.94 μmol/L in order to allow for multiple dilutions over an adequate dynamic range. In this case, the three pooled urine samples were diluted 1, 1.5, 2, 4 and 8-fold in de-ionized water. Five samples with high iodide (> 3.94 μmol/L) were also selected randomly among the PURE study participants who were not taking T4 to investigate potential bias in cases of excess iodine nutrition. Additionally, ten urine samples from participants taking T4 were randomly selected from the PURE study, to evaluate potential bias from urinary iodine-containing compounds. Five samples from the CDC's EQUIP program were included in the study as well. A pooled QC was prepared by combining equal volumes from all urine samples in this study, which was analyzed intermittently (n = 9) after every 10 urine samples to evaluate method precision, whereas a blank sample (internal standard NDS prepared in 2-fold diluted simulated urine matrix and de-ionized water) was daily analyzed to test for potential sample carry-over. In addition, vendor-supplied samples for QC at levels I (mean, 95% CI = 0.944, 0.708 to 1.18 μmol/L) and II (mean, 95% CI = 3.92, 2.94 to 4.90 μmol/L) were obtained from RECIPE (ClinChek lyophilized urine controls, reference values determined by ICP-MS) and analyzed intermittently (n = 9) to evaluate method accuracy. A summary of the 50 urine samples in this inter-laboratory validation study is described in **Table S4.1**. The second method comparison was performed on human urine samples (n = 21) collected over a 2 year period following participation in the CDC's EQUIP program[29] over six rounds from May 2014 to October 2015, which is a round-robin study involving up to 120 different laboratories around the world. In this case, EQUIP samples were analyzed by CE-UV at McMaster University, whereas results for the CDC target values derived from an ICP-MS reference method, and mean results were generated from all laboratories (n = 88-102) participating in the EQUIP after exclusion of outliers. In the latter case, urinary iodine measurements

were performed by eight different analytical methods, primarily ICP-MS and various formats of the S-K method. Experimental details for urinary iodine determination using the optimized CE-UV assay and ICP-MS method validated according to the recommendations outlined in CLSI guideline EP19 are described in the Supplemental Experimental, including chemicals/reagents, preventative maintenance procedures, as well as tests performed to identify the source of bias in the original CE-UV assay.[25]

4.3.2 Statistical analysis

Data analysis was performed using Excel (Microsoft Office) to calculate relative peak areas and determine recoveries and dilution ratios. The Statistical Package for the Social Science (SPSS) was used to perform normality tests (Shapiro-Wilk), Spearman correlation analysis, and statistical comparisons by 2-tailed student's t-test. MedCalc (MedCalc Software) was used for Passing-Bablok regression analysis, and difference or % difference Bland-Altman plots when comparing CE-UV and ICP-MS methods. Igor Pro (Wavemetrics) was used to plot electropherograms and other graphs.

4.4 Results

4.4.1 Sources of bias and modifications in the CE-UV assay

A significant positive bias of 40-50% was confirmed for the original CE-UV assay[25] in comparison with ICP-MS results. Further details from the method comparison between the original CE-UV method and ICP-MS are described in the Supplemental Results and **Figures S4.1-S4.3**. Briefly, calibrant solutions were prepared in 2-fold diluted simulated urine matrix, containing several major urinary electrolytes to mimic the ionic strength of human urine. To investigate the underlying cause(s) of the bias, iodide standard solutions were prepared in 2- and

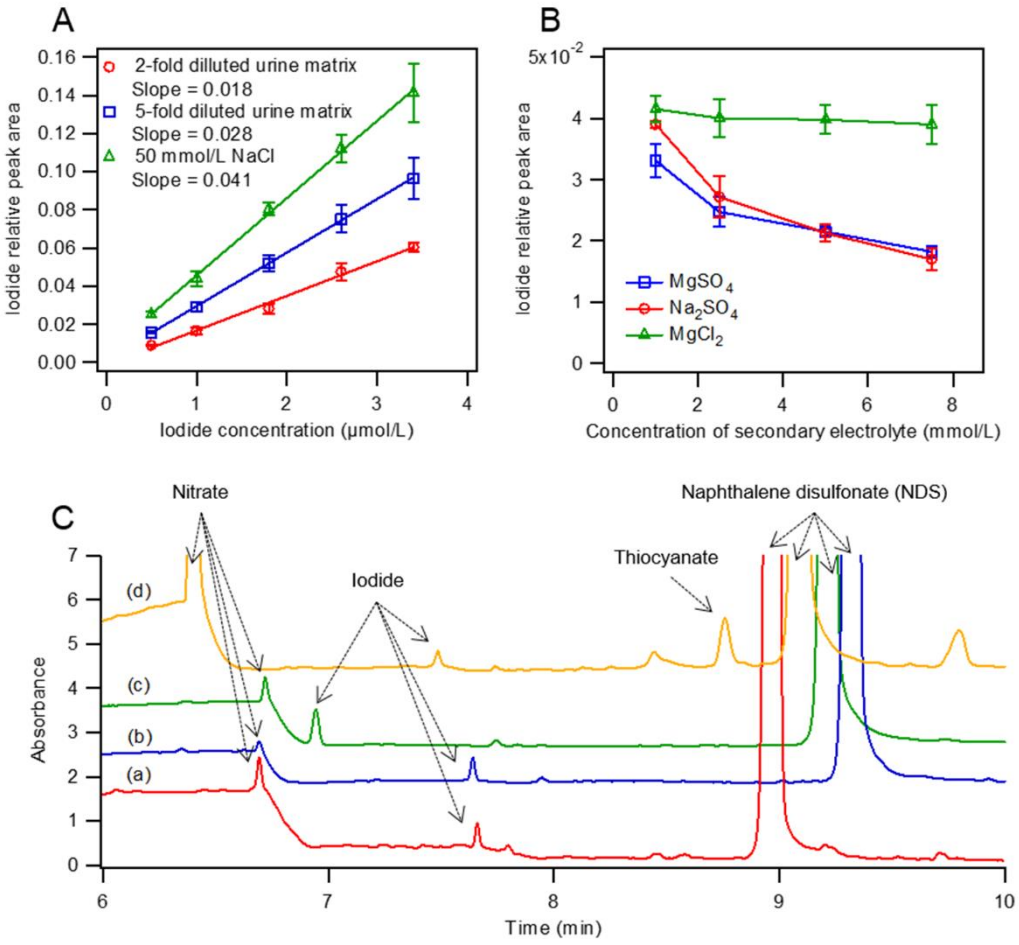

Figure 4.1. Identification of source(s) of bias in the original CE-UV assay. (**A**) Calibration curve for iodide in simulated urine matrix and sodium chloride. (**B**) Iodide response with addition of secondary electrolytes to iodide solutions in sodium chloride. (**C**) Electropherograms for iodide in (a) simulated urine matrix, (b) sodium chloride and sodium sulfate, (c) sodium chloride, and (d) pooled urine sample.

5-fold diluted urine matrix, as well as in 50 mmol/L sodium chloride (**Figure 4.1A**). The slopes of the calibration curves changed by > 2-fold when comparing calibrants in sodium chloride and in 2-fold diluted urine matrix, suggesting that the source of bias was related to some other ion(s) in the simulated urine matrix. After testing binary mixtures of sodium chloride and other electrolytes, sulfate was found to be the co-ion causing a concentration-dependent decrease in apparent iodide signal response and lower sensitivity (**Figure 4.1B**). Nonetheless,

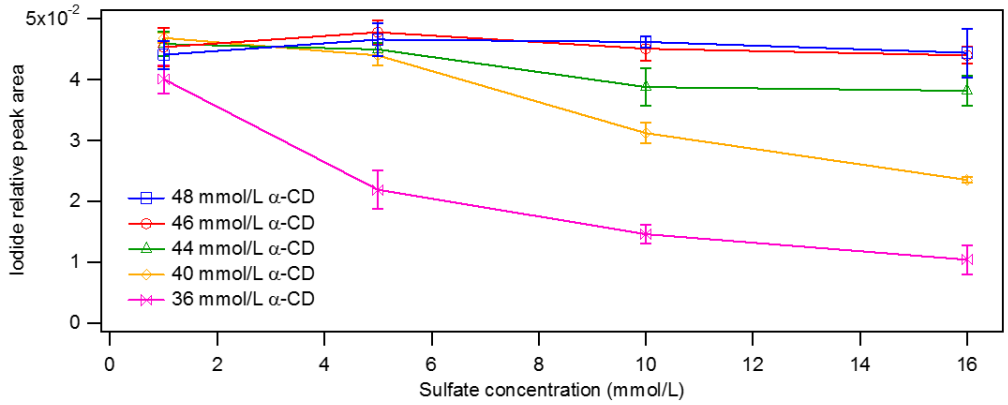

Figure 4.2. Effect of α-CD concentration in the BGE on the response of iodide solutions prepared in 50 mmol/L sodium chloride containing different concentrations of sodium sulfate.

sulfate was also identified as an important co-ion impacting iodide migration time and peak shape during sample self-stacking to generate electropherograms analogous to authentic urine samples (**Figure 4.1C**). Additional tests confirming the key role of sulfate as a matrix interference that altered the measured response (*i.e.*, integrated peak area) of iodide are described in the Supplemental Results and **Figure S4.4**, such as precipitating urinary sulfate as its barium salt prior to CE analysis to restore the iodide response. Sulfate has an effective mobility similar to iodide under the conditions used in the original CE-UV assay when using 36 mmol/L α-CD in the BGE, which resulted in a lower apparent iodide signal than corresponding sulfate-free urine samples or matrix-matching calibrant solutions. The sulfate interference was resolved by increasing the α-CD concentration in the BGE, which selectively slows the mobility of iodide relative to sulfate due to the former ion's higher binding affinity. As shown in **Figure 4.2**, when α-CD concentration is ≥ 46 mmol/L, the measured iodide response remains unaffected by changes in sulfate levels as high as 16 mmol/L that is equivalent to 32 mmol/L in a non-diluted urine sample. Another potential source of bias for the CE-UV assay is the presence of oxidizing agents, such as nitrite or sulfite, as well as sulfamic acid (Supplemental Results), which is used as a preservative in NIST derived urine samples for the concomitant analysis of mercury by ICP-MS.[30] As a

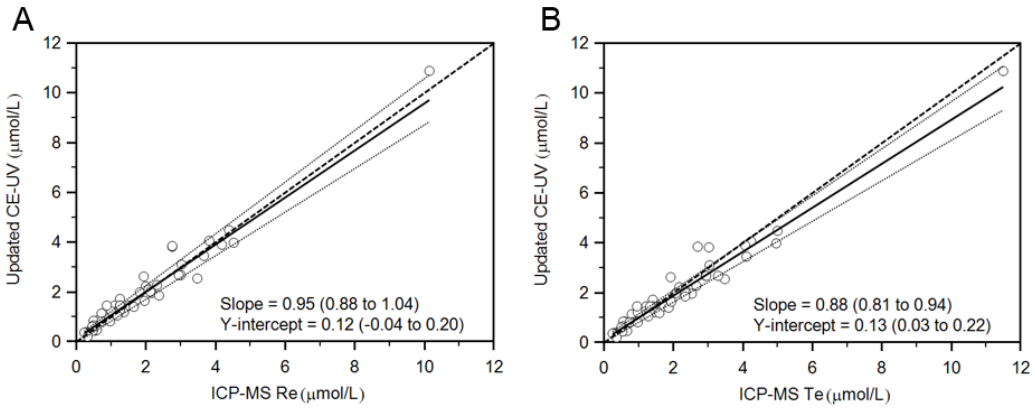

Figure 4.3. Passing-Bablok regression comparing the optimized CE-UV assay with ICP-MS using the internal standards ^{187}Re (**A**) and ^{130}Te (**B**). Plots show slopes and y-intercepts followed by their 95% CI. Regression, 95% CI and equality line are represented by solid, dotted and dashed lines, respectively.

result, this work highlights the need for careful selection of compatible preservatives in urine specimens to avoid potential interferences when measuring iodide by CE as the predominate iodine species from diet and most stable form of iodine found in urine that has been previously shown to tolerate repeat freeze-thaw cycles and delays to storage when left at room temperature.[25]

4.4.2 Method comparison between ICP-MS and optimized CE-UV assay

Iodide concentrations in 24 h urine samples ranged from approximately 0.20 to 11.50 µmol/L and were not normally distributed (Shapiro-Wilk, $p < 0.001$, $n = 50$). The optimized CE-UV assay using 46 mmol/L α-CD in the BGE provided results consistent with ICP-MS, with a median bias of 2.1 and -4.8% when using the internal standards ^{187}Re and ^{130}Te, respectively. In this case, a strong correlation between the methods was observed with Spearman correlation coefficients of 0.959 and 0.963 ($p < 0.001$) for ^{187}Re and ^{130}Te, respectively. No evidence of systematic bias was observed between the optimized CE-UV assay and ICP-MS using ^{187}Re as internal standard as indicated by the Passing-Bablok

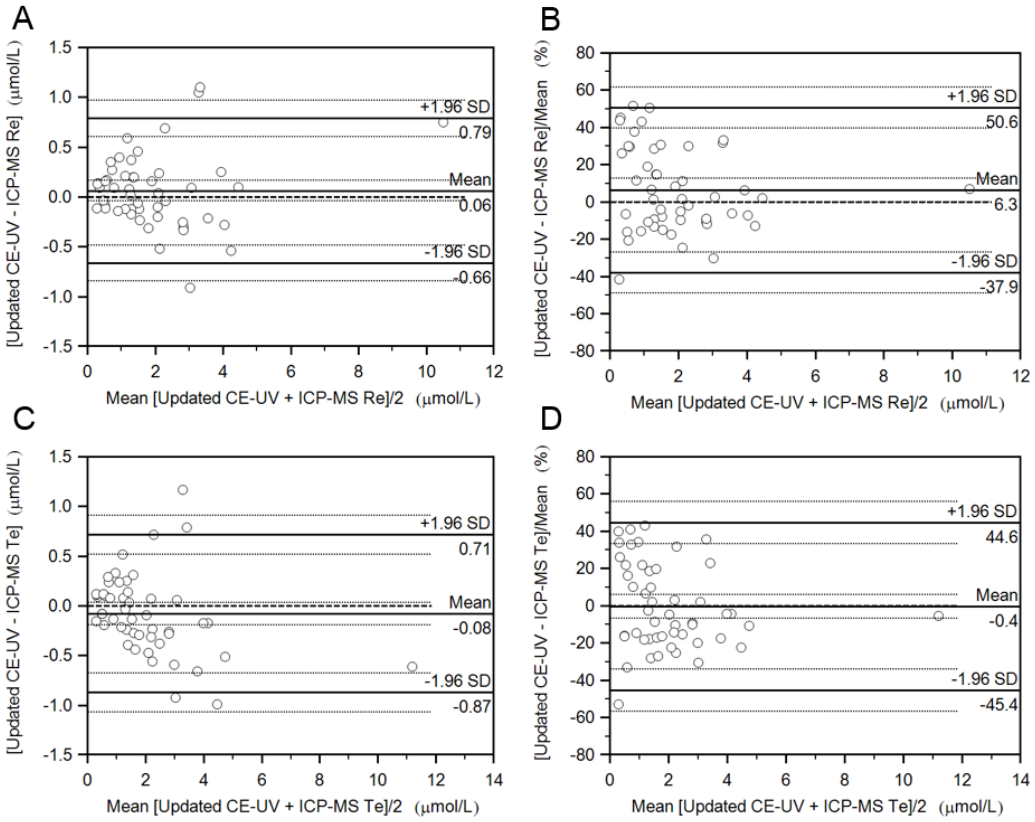

Figure 4.4. Bland-Altman plots of differences (**A**, **C**) and % differences (**B**, **D**) between the updated CE-UV assay and ICP-MS using the internal standards ^{187}Re and ^{130}Te, respectively. The mean difference/% difference and limits of agreement (± 1.96 SD) are represented as solid lines, while their 95% CI and the zero are indicated by dotted and dashed lines, respectively.

regression as reflected by a slope and y-intercept not significantly different from 1 and zero, respectively (**Figure 4.3A**), whereas a small negative bias was detected when using ^{130}Te as internal standard (**Figure 4.3B**). Overall, the CE-UV assay had good agreement with ICP-MS, with 95% of the differences within -0.66 to 0.79 µmol/L for ^{187}Re (**Figure 4.4A**) and -0.87 to 0.71 µmol/L for ^{130}Te (**Figure 4.4C**). Similarly, the mean percentage differences between the methods were 6.3 and -0.4% for ^{187}Re and ^{130}Te when using % difference Bland-Altman plots, respectively (**Figure 4.4B, 4.4D**). Excellent accuracy was also indicated by recoveries in the CE-UV method ranging from 99.5 to 102.7% (**Table 4.1**) and a

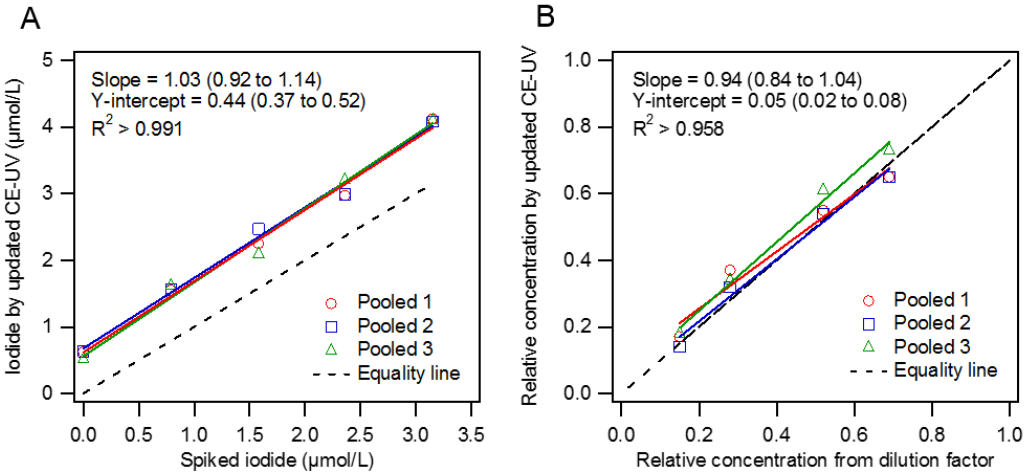

Figure 4.5. Spike-recovery (**A**) and serial dilution (**B**) for three independent pooled urine samples analyzed by the optimized CE-UV assay. Solid lines represent the least-squares linear regression and slopes and y-intercepts are shown in the graphs, followed by their 95% CI.

mean slope for the spike-recovery studies not significantly different from unity (**Figure 4.5A**). Also, data points in the serial dilution were very close to the ideal line, as shown in **Figure 4.5B** (mean y-intercept, 95% CI = 0.05, 0.02 to 0.08). Among the samples with very high iodine, only two remained for comparison, after exclusion of an outlier and the re-classification of other two samples as having normal iodine levels when using ICP-MS and the updated CE-UV method, which resulted in bias under 10%. Samples from subjects taking T4 did not reveal clear systematic difference between the optimized CE-UV method and ICP-MS, with average bias of -2.3 and -7.2% for ^{187}Re and ^{130}Te, respectively. Similarly, the median bias for the EQUIP samples was reduced to 10.4 and 15.6% compared to the CDC target using ICP-MS and the mean from all laboratories (ICP-MS and S-K methods), respectively (**Figure S4.5**). The precision of the validated CE-UV assay remained under 12% when using a single non-isotope internal standard based on intermittent analysis of pooled QC and vendor-derived reference QC samples (**Table S4.2**). Additionally, the calibration curve [y = (0.0454 ± 0.0006) x, for iodide concentrations in µmol/L] showed good linearity (R^2 = 0.9989) over

Table 4.1. Mean recoveries for three independent pooled 24 h urine samples (n = 20) spiked with 0.79 to 3.15 µmol/L iodide and analyzed by CE-UV and ICP-MS.

Iodide spiked (µmol/L)	Mean recovery ± SD (%)			
	Original CE-UV	Updated CE-UV	ICP-MS Re	ICP-MS Te
0.79	136.9 ± 36.0	100.0 ± 4.8	100.6 ± 2.8	110.8 ± 11.1
1.58	136.2 ± 15.0	99.5 ± 5.9	100.5 ± 3.4	115.0 ± 2.1
2.36	139.1 ± 8.6	102.5 ± 6.7	103.0 ± 1.2	104.5 ± 10.4
3.15	135.7 ± 9.8	102.7 ± 9.5	101.5 ± 0.9[a]	113.3 ± 0.3[a]

[a]*An outlier was excluded from this calculation for ICP-MS.*

the concentration range of 0.15 to 4.00 µmol/L (**Figure S4.6**) as required for assessment of the iodine nutritional status on a population level.

4.4.3 Comparison of internal standards in ICP-MS method

In the method comparison, ^{187}Re and ^{130}Te were both used as internal standards for ICP-MS since other isotopes of iodine are radioactive. Based on intermittently analyzed QC samples used to evaluate system stability and sample carry-over during analysis, ^{187}Re was significantly ($p < 0.05$, student's t test) more precise and accurate (mean CV = 1.78%, bias < 6%) than ^{130}Te (mean CV = 5.63%, bias < 12%) (**Table S4.2**). Similarly, better accuracy in ICP-MS was achieved in spike-recovery studies (**Table 4.1**) when using ^{187}Re as an internal standard with average recoveries ranging from 100.5 to 103.0%, whereas ^{130}Te had a higher bias ranging from 104.5 to 115.0%. As expected, a comparison between the two internal standards showed a very strong correlation with a Spearman's correlation coefficient of 0.996 ($p < 0.001$), but results obtained with ^{130}Te were on average 6.8% higher than with ^{187}Re. This is a small, but significant difference given the high precision of the ICP-MS method (**Figure S4.7**).

4.5 Discussion

The CE-UV assay reported here offers a simple, selective and cost-effective method for urinary iodine determination in population studies as compared to the classical S-K kinetic spectrophotometric assay and ICP-MS. The original CE-UV method[25] was determined to be susceptible to bias due to the dependence of measured iodine responses on sulfate present in matrix matching solutions used for calibrants and found endogenously in authentic human urine samples. Sulfate is a highly abundant yet variable inorganic electrolyte in human urine reflecting dietary protein intake with concentration levels varying from 0.5 to 32 mmol/L.[26,31] Sulfate is a stable and UV-transparent strong anion, thus it does not present a direct spectral interference to iodide whose absorbance is optimally monitored at 226 nm. However, since sulfate has an apparent mobility similar to iodide under the original CE method conditions, it can contribute to interferences during sample self-stacking that is used as an on-line sample preconcentration technique to enhance concentration sensitivity in CE.[32,33] This effect was previously reported in a CE-UV assay for iodide analysis in complex biological samples,[22] where sulfate was found to impact the apparent signal and migration time for iodide during sample self-stacking. In our case, this interference was resolved by increasing the concentration of α-CD in the BGE to slow down the effective mobility of iodide relative to sulfate, due to larger fraction of iodide:α-CD complex, which generated equivalent separation performance in both authentic urine samples and calibrant solutions containing sulfate. Importantly, the CE-UV assay is able to tolerate high concentration levels of urinary sulfate while requiring up to a 50-fold lower sample volume (10 µL) of urine than conventional ICP-MS and kinetic spectrophotometric assays.

The inter-laboratory method comparison conducted independently at McMaster University and Hamilton General Hospital together with participation in six rounds of the CDC's EQUIP initiative over two years provides strong evidence that results obtained by the CE-UV assay are in good agreement with

previously validated methods widely used for urinary iodine determination in large-scale epidemiological studies, including the CDC reference method, ICP-MS. In fact, measured differences between the methods (mean, 95% CI = 0.06, -0.66 to 0.79 µmol/L for optimized CE-UV vs. ICP-MS using ^{187}Re) are comparable with differences previously reported for a comparison between ICP-MS and the S-K assay (mean, 95% CI = 0.03, -0.55 to 0.49 µmol/L).[34] Concentration-dependent differences between the methods reported for ICP-MS vs. S-K assay[34] are also consistent with our results reported here when comparing ICP-MS vs. CE-UV. Furthermore, a much better agreement was also obtained for EQUIP urine samples used in an international round-robin study, including both the CDC target (ICP-MS) and the mean of all laboratories (S-K assay and ICP-MS). Although ICP-MS has better precision and lower limit of quantification, the CE-UV method offers acceptable precision ($CV \leq 12\%$) and adequate sensitivity to measure urinary iodine levels associated with moderate deficiency (0.16-0.38 µmol/L) according to the World Health Organization (WHO) categories.[12] Both techniques require a simple dilution step for urine prior to analysis unlike the S-K method. As an analytical technique for separation of ions based on their electric charge and hydrated radius, the CE-UV assay offers highly selective determination of iodide (I^-), the chemical form of iodine that is bioavailable for the thyroid gland after gastrointestinal absorption from food and water sources. On another hand, ICP-MS quantifies total iodine by atomization of iodine-containing compounds in the plasma, which includes iodinated drugs, radiologic contrasts, and food additives that are not amenable for thyroid uptake. Also, our previous study demonstrated that CE offers excellent robustness[25] when analyzing iodine in pooled 24 h urine samples (n = 87) over five weeks of continuous operation while applying standard operating protocols and daily preventative maintenance on the instrument (Supplemental Methods). Although direct comparison of measured results using different methods should always be interpreted with caution, this validation study provides compelling evidence that

CE-UV reliably measures urinary iodine nutritional status that is in close agreement with the reference method, ICP-MS.

A small but significant difference was observed for ICP-MS results normalized to ^{187}Re and ^{130}Te. The choice of internal standard in ICP-MS is essential to correct for urine matrix effects, which affect quantification due to variable sample components that influence ionization efficiency and ion transmission over time. Isotope dilution analysis provides the most accurate and precise results in ICP-MS, as an isotope internal standard has very similar *m/z* and identical first ionization potential energies. Iodine, however, is a monoisotopic element with a single radioisotope that is substantially stable (^{129}I, $t_{1/2}$ = 15.7 million years). Although ^{129}I has been reported as the optimum internal standard for urinary iodine analysis,[35,36] other non-isotopic internal standards are generally used due to concerns related to potential radiological hazards and special safety measures required for handling ^{129}I. Our study has demonstrated that ^{187}Re provides more precise and accurate results than ^{130}Te, which was unexpected considering that ^{130}Te has a *m/z* and first ionization potential (9.01 eV) that better matches iodine (*m/z* 127, 10.45 eV) relative to ^{187}Re (7.83 eV) based on data from the NIST atomic spectra database. Therefore, other factors aside from the mass gain region and the ionization potential play an important role in correcting for ion suppression effects in ICP-MS that requires further investigation. Indeed, the internal standard used in the ICP-MS reference method at the CDC was recently changed in 2014 from ^{130}Te to ^{187}Re due to better performance that also allows for simultaneous analysis of iodine and mercury.[37,38] In this work, better agreement was also found for measured urinary iodine concentrations between CE-UV assay and ICP-MS using ^{187}Re.

In summary, a validated CE-UV assay presented here offers laboratories a simple method for urinary iodine determination with adequate sensitivity, selectivity, and precision with minimal sample handling. Importantly, this method has excellent accuracy for urinary iodine measurements that is consistent with

both ICP-MS and S-K methods. CE-UV also provides a cost-effective platform for reliable estimation of iodine intake in certain regions where ICP-MS is not feasible due to high infrastructure and long-term operating costs. Additionally, CE offers better selectivity for iodide (*i.e.*, the active iodine species for thyroid uptake) than ICP-MS, while allowing analysis of volume-restricted bio-banked urine specimens. Urinary thiocyanate and nitrate levels can also be measured by the same CE assay,[25] which are relevant environmental iodine-uptake inhibitors contributing to thyroid-related health effects in populations with adequate dietary iodine.[39] Interferences caused by urinary sulfate was resolved by increasing the concentration of α-CD in the BGE. Samples containing high levels of oxidizing agents could still contribute to incidental bias with signal loss of iodide in CE via *in-situ* reduction to molecular iodine that is electrically neutral. Nevertheless, nitrite and sulfite are reactive anions normally absent in urine, present at low levels in cases of bacterial infection/unpreserved stored urine samples[40] or sulfite oxidase deficiency,[26] whereas sulfamic acid is a preservative that can be avoided for samples intended for iodine quantification. Future work will evaluate the iodine nutritional status of the Canadian population that is at higher risk for iodine deficiency due to recent changes in habitual diet and lifestyle.

4.6 Acknowledgements

P.B.M. acknowledges funding from the Natural Sciences and Engineering Research Council of Canada. A.N.M. acknowledges support from the Province of Ontario in the form of an Ontario Trillium Scholarship. The authors also acknowledge support from the Public Health Agency of Canada. Further thanks go to Jeff Chapman and John Hudson at SCIEX, and Amir Makhmudov from the CDC's EQUIP program.

4.7 References

(1) Andersson, M.; Karumbunathan, V.; Zimmermann, M. B. *J. Nutr.* **2012**, *142*, 744–750.

(2) Bath, S. C.; Steer, C. D.; Golding, J.; Emmett, P.; Rayman, M. P. *Lancet* **2013**, *382*, 331–337.

(3) Nyirenda, M. J.; Clark, D. N.; Finlayson, A. R.; Read, J.; Elders, A.; Bain, M.; Fox, K. A. A.; Toft, A. D. *Thyroid* **2005**, *15*, 718–724.

(4) Patrick, L. *Altern. Med. Rev.* **2008**, *13*, 116–127.

(5) Trumpff, C.; De Schepper, J.; Tafforeau, J.; Van Oyen, H.; Vanderfaeillie, J.; Vandevijvere, S. *J. Trace Elem. Med. Biol.* **2013**, *27*, 174–183.

(6) Zimmermann, M. B. *Proc. Nutr. Soc.* **2010**, *69*, 133–143.

(7) Li, M.; Eastman, C. *Nat. Rev. Endocrinol.* **2012**, *8*, 434–440.

(8) Dunn, J. T. *J. Nutr.* **2003**, *133*, 3008S–10S.

(9) Als, C.; Lauber, K.; Brander, L.; Lüscher, D.; Rösler, H. *Experientia* **1995**, *51*, 623–633.

(10) Laurberg, P.; Pedersen, I. B.; Knudsen, N.; Ovesen, L.; Andersen, S. *Thyroid* **2001**, *11*, 457–469.

(11) Andersson, M.; de Benoist, B.; Rogers, L. *Best Pract. Res. Clin. Endocrinol. Metab.* **2010**, *24*, 1–11.

(12) WHO. *Assessment of iodine deficiency disorders and monitoring their elimination: A guide for programme managers*, 3rd ed.; WHO: Geneva, 2007.

(13) Leung, A. M.; Pearce, E. N.; Braverman, L. E.; Stagnaro-Green, A. *Pediatrics* **2014**, *134*, e1282.

(14) Soldin, O. P. *Clin. Biochem.* **2002**, *35*, 575–579.

(15) Shelor, C. P.; Dasgupta, P. K. *Anal. Chim. Acta* **2011**, *702*, 16–36.

(16) Moreda-Piñeiro, A.; Romarís-Hortas, V.; Bermejo-Barrera, P. *J. Anal. At. Spectrom.* **2011**, *26*, 2107–2152.

(17) May, W.; Wu, D.; Eastman, C.; Bourdoux, P.; Maberly, G. *Clin. Chem.* **1990**, *36*, 865–869.

(18) Dung, N. T.; Wellby, M. L. *Clin. Chem.* **1997**, *43*, 1084–1085.

(19) Macours, P.; Aubry, J. C.; Hauquier, B.; Boeynaems, J. M.; Goldman, S.; Moreno-Reyes, R. *J. Trace Elem. Med. Biol.* **2008**, *22*, 162–165.

(20) European Commission. *Opinion of the Scientific Committee on Food on the tolerable upper intake level of iodine (26 September 2002)*; SCF/CS/NUT/UPPLEV/26: Brussels, 2002.

(21) Hirokawa, T.; Yoshioka, M.; Okamoto, H.; Timerbaev, A. R.; Blaschke, G. *J. Chromatogr. B* **2004**, *811*, 165–170.

(22) Pantůcková, P.; Krivánková, L. *Electrophoresis* **2004**, *25*, 1102–1110.

(23) Pantůčková, P.; Urbánek, M.; Křivánková, L. *Electrophoresis* **2007**, *28*, 3777–3785.

(24) Petersen, J. R.; Okorodudu, A. O.; Mohammad, A.; Payne, D. A. *Clin. Chim. Acta* **2003**, *330*, 1–30.

(25) Macedo, A. N.; Teo, K.; Mente, A.; McQueen, M. J.; Zeidler, J.; Poirier, P.; Lear, S. A.; Wielgosz, A.; Britz-McKibbin, P. *Anal. Chem.* **2014**, *86*, 10010–10015.

(26) Macedo, A. N.; Jiwa, M. I. Y.; Macri, J.; Belostotsky, V.; Hill, S.; Britz-McKibbin, P. *Anal. Chem.* **2013**, *85*, 11112–11120.

(27) Caldwell, K. L.; Makhmudov, A.; Jones, R. L.; Hollowell, J. G. *Accredit. Qual. Assur.* **2005**, *10*, 356–361.

(28) Teo, K.; Chow, C. K.; Vaz, M.; Rangarajan, S.; Yusuf, S. *Am. Heart J.* **2009**, *158*, 1–7.

(29) Makhmudov, A. A.; Caldwell, K. L. *IDD Newsl.* **2011**, 4–6.

(30) Taylor, A.; Jones, R. L.; Leblanc, A.; Mazarrasa, O.; Lee, M. Y.; Parsons, P. J.; Patriarca, M.; Weber, J. P.; Weykamp, C. *Accredit. Qual. Assur.* **2009**, *14*, 461–466.

(31) van den Born, J. C.; Frenay, A.-R. S.; Bakker, S. J. L.; Pasch, A.; Hillebrands, J.-L.; Lambers Heerspink, H. J.; van Goor, H. *Nitric Oxide* **2016**, *55–56*, 18–24.

(32) Boden, J.; Bachmann, K. *J. Chromatogr. A* **1996**, *734*, 319–330.

(33) Gebauer, P.; Krivánková, L.; Pantůcková, P.; Bocek, P.; Thormann, W. *Electrophoresis* **2000**, *21*, 2797–2808.

(34) Caldwell, K.; Maxwell, C. B.; Makhmudov, A.; Pino, S.; Braverman, L. E.; Jones, R. L.; Hollowell, J. G. *Clin. Chem.* **2003**, *49*, 1019–1021.

(35) Dyke, J. V; Dasgupta, P. K.; Kirk, A. B. *Talanta* **2009**, *79*, 235–242.

(36) Haldimann, M.; Zimmerli, B.; Als, C.; Gerber, H. *Clin Chem* **1998**, *44*, 817–824.

(37) CDC. *Urine iodine and mercury by inductively coupled plasma dynamic reaction cell mass spectrometry (ICP-DRC-MS) (Method 3002.1)*; Laboratory Procedure Manual: Atlanta (GA), 2005.

(38) CDC. *Iodine and mercury in urine by ICP-DRC-MS (Method No. 3002.7-02)*; Laboratory Procedure Manual: Atlanta (GA), 2014.

(39) De Groef, B.; Decallonne, B. R.; Van der Geyten, S.; Darras, V. M.; Bouillon, R. *Eur. J. Endocrinol.* **2006**, *155*, 17–25.

(40) Moshage, H.; Stegeman, C. A.; Jansen, P. L. M. *Clin. Chem.* **1998**, *44*, 1780–1781.

4.8 Supplemental Experimental

4.8.1 Chemicals and reagents

Potassium iodide, sodium nitrate, lithium hydroxide, α-CD, sodium phosphate monobasic monohydrate, magnesium chloride, barium chloride dihydrate, sodium nitrite and 1,5-naphthalenedisulfonic acid disodium salt hydrate (NDS) were purchased from Sigma-Aldrich. Sodium sulfate, sodium chloride, EDTA and sodium sulfite were purchased from Alfa Aesar. In all cases, the purity of electrolytes used in this work exceeded 99.0%, including potassium iodide. Phosphoric acid was obtained from Fisher Scientific Canada and magnesium sulfate anhydrous was obtained from Anachemia. In the original CE-UV assay, a simulated urine matrix was used to matrix-match external calibrant solutions, which mimics the main electrolyte composition of human urine, resulting in peak shapes and migration times in CE that are comparable to the analysis of authentic human urine [Macedo, A. N.; Teo, K.; Mente, A.; McQueen, M. J.; Zeidler, J.; Poirier, P.; Lear, S. A.; Wielgosz, A.; Britz-McKibbin, P. *Anal. Chem.* **2014**, 86, 10010–10015]. A simplified simulated urine matrix containing only 100 mmol/L sodium chloride and 10 mmol/L sodium sulfate was used in the optimized CE-UV method, as this composition was found to be enough to mimic urine in terms of iodide peak shape and migration times. For the ICP-MS analysis, iodide, ^{187}Re and ^{130}Te TraceCert standards of 1000 mg/L were purchased from Fluka

Analytical. Trace metal grade ammonium hydroxide and isopropanol were obtained from Fisher Scientific. Triton X-100 and trace metal grade EDTA were purchased from Sigma-Aldrich. Tuning solution containing ^{7}Li, ^{59}Co, ^{89}Y, ^{140}Ce and ^{205}Tl (10 μg/mL) were obtained from Agilent Technologies. ClinChek lyophilized urine controls purchased from RECIPE were used as QCs at level I (mean, 95% CI = 0.944, 0.708 to 1.18 μmol/L) and level II (mean, 95% CI = 3.92, 2.94 to 4.90 μmol/L).

4.8.2 Urinary iodine determination by CE-UV

The original CE-UV assay for urinary iodine determination has been previously described [Macedo, A. N.; Teo, K.; Mente, A.; McQueen, M. J.; Zeidler, J.; Poirier, P.; Lear, S. A.; Wielgosz, A.; Britz-McKibbin, P. *Anal. Chem.* **2014**, 86, 10010–10015]. Briefly, the major UV-transparent anion in urine, sulfate, that was also included in a simulated urine matrix used for preparing all calibrant solutions, was found to cause a concentration-dependent reduction of the signal intensity measured for iodide. This effect was prevented by increasing the α-CD concentration in the BGE from 36 to 46 mmol/L in order to reduce the apparent mobility of iodide relative to sulfate (which does not bind to α-CD) by increasing the fraction of complex formed during electromigration from 35 to 41% based on its apparent binding constant (K_b = 15 M^{-1}) [Macedo, A. N.; Teo, K.; Mente, A.; McQueen, M. J.; Zeidler, J.; Poirier, P.; Lear, S. A.; Wielgosz, A.; Britz-McKibbin, P. *Anal. Chem.* **2014**, 86, 10010–10015]. As a result, this BGE modification prevented co-migration of sulfate that impaired sample self-stacking of iodide. All urinary iodine analyses were performed using a P/ACE MDQ capillary electrophoresis system with a photodiode array detector (Beckman-Coulter) using uncoated fused-silica capillaries (Polymicro Technologies) with 75 μm inner diameter, 60 cm of total length and 50 cm of length to the detector. The BGE was composed of 180 mmol/L lithium phosphate, 46 mmol/L α-CD

(updated CE-UV assay), pH 3.0, adjusted with 1 mol/L phosphoric acid. Samples were hydrodynamically injected for 80 s at 0.5 psi and separations were performed at 25°C using a constant applied voltage of 18 kV under reversed polarity. Iodide was detected at 226 nm for maximum sensitivity, while the internal standard naphthalene disulfonate (NDS) was detected at 288 nm for improved specificity. Urine samples (50 µL) were diluted 2-fold in simulated urine matrix (100 mmol/L sodium chloride and 10 mmol/L sodium sulfate) containing NDS (20 µmol/L final concentration), vortexed for 30 s and centrifuged at 14,000 *g* for 5 min. A 30 µL aliquot of the supernatant was used for CE-UV analysis. Calibrant solutions were prepared using potassium iodide (0.15 to 4.00 µmol/L) in 2-fold diluted simulated urine matrix. The accuracy of the CE-UV assay was evaluated by analyzing human urine samples from PURE (n = 50) at McMaster University, as well as EQUIP urine samples from the CDC (n = 21), in addition to vendor-supplied QC reference samples. Overall, a minimum urine volume of 10 µL is adequate for routine iodine determination by CE.

4.8.3 Urine iodine analysis by ICP-MS

Urinary iodine measurements from PURE (n = 50) were conducted using an Agilent Technologies 8800 triple-quadrupole ICP-MS instrument (ICP-QQQ) in the Clinical Chemistry and Immunology Department of the Hamilton Regional Laboratory Medicine Program at Hamilton General Hospital. The urinary iodine assay is an in-house developed method validated according to the recommendations outlined in CLSI guideline EP19 and is used for routine diagnostic analysis of patient samples. Briefly, calibration standards and urine samples (500 µL) were prepared by a 20-fold dilution in 0.5% w/w ammonium hydroxide containing 2% w/w isopropanol, 0.025% w/w EDTA, 0.025% w/w Triton X-100 as well as ^{187}Re and ^{130}Te both with a concentration of 420 µg/L. A total of seven calibration standards (0 to 1.970 µmol/L) were prepared for iodine

quantitation. Analysis was conducted using oxygen as reaction gas and an integration time of 0.5 sec.

4.8.4 Investigation of sources of bias in the original CE-UV assay

The effect of major urinary electrolytes on the iodide response by the original CE-UV assay was initially studied by changing the concentration and/or composition of the simulated urine matrix. Calibration curves were prepared in triplicate in 2- and 5-fold diluted simulated urine matrix, as well as in 50 mmol/L sodium chloride alone. After observing a proportional decrease in the iodide response as the level of simulated urine matrix increased, binary combinations of sodium chloride and each one the other simulated urine matrix components (*i.e.*, potassium chloride, magnesium sulfate, sodium sulfate, sodium phosphate, calcium chloride, and sodium hydroxide) were used to prepare 1.00 μmol/L iodide solutions in triplicate, in order to identify which components were affecting iodide response. Only salts containing sulfate decreased the iodide signal independent of cation type, which prompted us to test iodide solutions (1.00 μmol/L, triplicate) prepared in a binary mixture of 50 mmol/L sodium chloride and 1.0, 2.5, 5.0 and 7.5 mmol/L of a secondary electrolyte, including magnesium chloride (control), and sodium sulfate or magnesium sulfate.

The effect of sulfate in authentic human urine was studied by sulfate standard addition, as well as barium pretreatment to precipitate and deplete endogenous sulfate. A pooled 24 h urine sample (n = 800) from participants of the PURE study was analyzed using the original CE-UV method after a 1.5-fold dilution in de-ionized water containing the internal standard NDS (20 μmol/L final concentration). The same sample was prepared in a solution containing increasing concentrations of sodium sulfate (1.0, 5.0 and 10.0 mmol/L). The urine sample was also pretreated with 4.0, 8.0 and 12.0 mmol/L barium chloride to precipitate the sulfate originally present in the urine sample. The barium sulfate

precipitate was removed after sedimentation by centrifugation at 14,000 g for 5 min, before collection of the supernatant for CE-UV analysis. For additional confirmation, endogenous sulfate levels were determined using another CE-UV assay previously reported for sulfate analysis in complex matrices, including urine [Macedo, A. N.; Jiwa, M. I. Y.; Macri, J.; Belostotsky, V.; Hill, S.; Britz-McKibbin, P. *Anal. Chem.* **2013**, 85, 11112–11120.].

Although sulfate is not detected in direct UV absorbance, it is one of the main urinary ions, which migrates close to iodide under the electrophoretic conditions used in this method. The combination of its mobility match and large excess concentration presumably prevents a complete peak focusing of iodide by sample self-stacking. As iodide electrophoretic mobility can be modified according to the concentrations of the additive α-CD in the BGE, the effect of 36, 40, 44, 46 and 48 mmol/L of α-CD was studied in the analysis of iodide standard solutions (1.00 μmol/L, triplicate) containing 50 mmol/L sodium chloride and increasing concentrations of sulfate (1.0, 5.0, 10.0 and 16.0 mmol/L), in order to evaluate their influence on the iodide response. The simulated urine matrix was also simplified to contain only 100 mmol/L sodium chloride and 10 mmol/L sodium sulfate, which were determined as the important co-ion species in calibrant solutions that influence sample self-stacking efficiency and apparent migration times measured for iodide similar to authentic urine samples. As a result, all calibrant solutions (and urine samples) for the optimized CE method were prepared in the 2-fold diluted simulated urine matrix (only 100 mmol/L sodium chloride and 10 mmol/L sodium sulfate) with iodide concentrations ranging from 0.15 to 4.00 μmol/L containing the internal standard NDS (20 μmol/L final concentration).

Other potential interferences, including trace metals that could precipitate iodide (*e.g.*, mercury, copper, lead, silver), as well as oxidizing agents that could cause loss of iodide by oxidation to molecular iodine (*e.g.*, nitrite, sulfite), were hypothesized as another possible source of bias if present as impurities in reagents

used for calibrant solutions. The effect of trace metals was investigated by treating iodide solutions (1.00 μmol/L, triplicate) with 1 mmol/L EDTA prior to the analysis in order to chelate the metals. The solutions were prepared in 50 mmol/L sodium chloride containing 1.0 or 2.5 mmol/L sodium sulfate to evaluate if there was any association with the levels of sulfate salt. The oxidizing agents sulfite and nitrite were studied in iodide solutions (1.00 μmol/L, triplicate) prepared in 50 mmol/L sodium chloride containing increasing concentrations of sodium sulfite (1.0, 2.5, 5.0 and 7.5 mmol/L) or sodium nitrite (0.1, 0.25, 0.5 and 1.0 mmol/L). These studies demonstrate that high levels of sulfate (> 1 mM) in urine was the major source of positive bias measured in the original CE-UV assay that was resolved by performing separations containing 46 mmol/L α-CD in the BGE.

4.8.5 Preventative maintenance protocol for CE-UV method

When performing the inter-laboratory method comparison study, electrodes were cleaned every day before starting the analysis with a clean paper damped with de-ionized water, in order to prevent salt and urine deposits that could cause contaminations or current discharge if accumulated over time. After flushing the capillary with BGE for 15 min (20 psi), current stability was checked by applying voltage for 1 min. A voltage of 18 kV applied to the capillary (75 μm inner diameter, 60 cm total length) filled with BGE is expected to generate a stable current of 119-121 μA at 25°C. Significant deviations from this current range indicated a problem with the system that should be addressed before starting urine analysis (*e.g.*, BGE composition is not correct, fused-silica capillary is broken or not in the right dimensions etc.). The first analysis of the day was a blank solution composed of 2-fold diluted simulated urine matrix and NDS in de-ionized water, which is used to check the absence of sample carry-over. Following the blank, an iodide calibrant solution was analyzed to confirm that the instrument response was in accordance with the calibration curve. Three QC samples (in-house

prepared pooled sample and vendor-supplied QCs levels I and II) were prepared in advance, aliquoted and stored in a -80°C freezer. Aliquots of the QCs were thawed before analysis and analyzed intermittently between a randomized batch of 10 urine samples, in order to monitor system stability over time. For overnight storage, the capillary was flushed with de-ionized water for 10 min (20 psi) and placed in vials containing de-ionized water.

4.9 Supplemental Results

4.9.1 Method comparison to study bias in the original CE-UV assay

A significant positive bias of 44.1 and 35.5% was confirmed for the original CE-UV assay in comparison with ICP-MS for the internal standards ^{187}Re and ^{130}Te, respectively. The correlation between the methods was relatively strong, with Spearman correlation coefficients of 0.811 and 0.817 ($p < 0.001$) for ICP-MS with ^{187}Re and ^{130}Te, respectively. However, the trend to higher iodine concentrations in the original CE-UV assay was clearly observed in the Passing-Bablok regression plot (**Figure S4.1A, S4.1B**), which confirms the presence of systematic bias, as indicated by y-intercepts significantly higher than zero. Differences between the methods tended to increase with concentration (**Figure S4.1C, S4.1E**) and were not normally distributed. Therefore, a better indication of agreement between the methods over the iodine concentration range is given by the percentage difference Bland-Altman plots (**Figure S4.1D, S4.1F**), which are normally distributed and support the conclusion that iodine concentrations measured by the original CE-UV assay using 36 mmol/L α-CD in the BGE are on average 40-50% higher than in ICP-MS. Results from the EQUIP samples (n = 21, after removing 3 extreme outliers confirmed by the Tukey boxplot method) also reinforced the presence of a 40% positive bias (**Figure S4.2**). Additionally, recoveries of 135-140% were obtained for the original CE-UV assay in spike-recovery experiments (**Table 4.1**), revealing bias that remains constant

independently of the iodide level spiked into urine samples, as illustrated by the good linearity in **Figure S4.3A** (R^2 > 0.994). Also, relative concentrations measured for the serially diluted samples were plotted against relative concentrations calculated from the dilution factors (**Figure S4.3B**). In this case, all data points were significantly above the equality line (mean y-intercept, 95% CI = 0.20, 0.12 to 0.28). Therefore, positive bias was also confirmed by spike-recovery and serial dilution experiments, which are independent of any errors associated to the reference method.

4.9.2 Sources of bias in the original CE-UV assay

Clear evidence that bias was associated to a component of the simulated urine matrix was obtained from calibration curves prepared in more diluted urine matrix or in a sodium chloride solution devoid of other electrolytes (**Figure 4.1A**), which shows a decrease in iodide response that is proportional to the level of simulated urine matrix in solution, whereas increasing concentrations of sodium chloride alone did not impact the iodide signal measured. When evaluating iodide response in binary mixtures of sodium chloride and other components of the simulated urine matrix, mixtures containing sulfate salts had a concentration-dependent impact on lowering the iodide signal, confirming the important role of urinary sulfate related to the source of bias in the original CE-UV method (**Figure 4.1B**). Sulfate was also found to be an essential co-ion influencing iodide peak shapes and migration times in CE with sample self-stacking that are comparable to electropherograms derived from authentic human urine samples (**Figure 4.1C**). Due to an effective mobility similar to iodide under the conditions in the original CE-UV assay that used 36 mmol/L α-CD, sulfate can negatively impact iodide peak focusing during the separation. This problem can be avoided by increasing the α-CD concentration in the BGE, which selectively reduces the iodide mobility, eliminating the sulfate interference (**Figure 4.2**). In analysis performed

with BGE containing at least 46 mmol/L α-CD, iodide response was not impacted by changes in sulfate levels over its normal physiological range (up to 32 mmol/L) highlighting the CE assay's ability to tolerate a wide range in sulfate concentrations without bias.

The possibility that the bias was related to interferences other than sulfate was eliminated by tests involving intentional addition and/or depletion of potential interferences, such as metal impurities and oxidizing agents. Additionally, the role of sulfate itself was further confirmed by restoration of the signal intensity for iodide in CE after sample pretreatment of urine with barium for selective sulfate precipitation prior to analysis. In experiments using authentic human urine, sulfate levels found in the samples (11.4 ± 0.2 mmol/L in the original urine, equivalent to 7.6 mmol/L in 1.5-fold diluted sample) closely matched the barium concentration needed to restore the iodide response (*i.e.*, 8.0 mmol/L), as shown in **Figure S4.4A**. The presence of EDTA had no significant effect on the iodide signal (p = 0.152 and 0.191 for 1.0 and 2.5 mmol/L sulfate, respectively), which indicates that the chemicals used in the assay are not a significant source of transition metals (*e.g.*, Ag, Pb, Cu, Hg) that could precipitate iodide (**Figure S4.4B**). A concentration dependent decrease in iodide signal was observed for the oxidizing agents sulfite and nitrite (**Figure S4.4C, S4.4D**). However, the concentrations (mmol/L) needed to considerably affect iodine quantification are considerably higher than the trace levels that could be present as impurities in the chemicals. These anions are also usually not detectable in human urine samples, except in the case of extremely rare genetic disorders, such as sulfite oxidase deficiency [Tan, W.-H.; Eichler, F. S.; Hoda, S.; Lee, M. S.; Baris, H.; Hanley, C. A.; Grant, P. E. Krishnamoorthy, K. S.; Shih, V. *Pediatrics* **2005**, 116, 757–66] or abnormally elevated nitrite due to urinary tract infection [Visser, J. J.; van Kamp, G. J.; Donker, A. J. *Clin. Chem.* **1991,** 37, 1303]. As a UV-absorbing anion, nitrite can be detected by our CE-UV method for iodide analysis, which allows the identification of potentially problematic samples. As a

result, it is very unlikely that they would substantially affect the iodide signal if present as impurities in the simulated urine matrix or matrix interference in authentic urine samples. In any case, it is important to note that any strong oxidizing agent can potentially affect iodide quantification if present in large enough concentrations. For instance, sulfamic acid, added to NIST reference urine samples as a preservative for the simultaneous analysis of mercury, is an oxidizing agent present at high levels (20 mmol/L) that affects iodide quantification by CE-UV. Analysis of NIST urine samples using a CE method with indirect UV detection [Macedo, A. N.; Jiwa, M. I. Y.; Macri, J.; Belostotsky, V.; Hill, S.; Britz-McKibbin, P. *Anal. Chem.* **2013**, 85, 11112–11120.] indicated the presence of an abundant strong anion tentatively assigned as sulfamic acid, based on migration time prediction using PeakMaster [Hruška, V.; Riesová, M.; Gaš, B. *Electrophoresis* **2012**;33:923–30]. Sulfamic acid migrates slightly after sulfate, potentially affecting iodide response due to interference with self-stacking preconcentration. In this case, the impact on iodide quantification can be attributed to the redox activity of sulfamic acid, as well as to potential interference with iodide focusing during separation, which can be prevented by avoiding the used of sulfamic acid in samples intended for iodide analysis.

Table S4.1. Summary of the composition of 50 human urine samples comprising the inter-laboratory method comparison study using CE-UV and ICP-MS.

No.	Sample description	Iodine concentration (µmol/L)			
		ICP-MS ^{187}Re	ICP-MS ^{130}Te	Original CE-UV	Optimized CE-UV
1	CDC UI 100623 round 39	3.47	3.48	4.84	2.56
2	CDC UI 100692 round 40	0.73	0.80	2.07	1.13
3	CDC UI 100668 round 41	1.99	2.16	4.13	2.23
4	CDC UI 100657 round 41	3.01	3.04	4.02	3.10
5	CDC UI 100608 round 40	1.10	1.22	2.88	1.47
6	Serial dilution pooled 1 level 1	2.32	2.66	3.09	2.28
7	Serial dilution pooled 1 level 2	1.59	1.60	2.81	1.47
8	Serial dilution pooled 1 level 3	1.18	1.18	2.44	1.26
9	Serial dilution pooled 1 level 4	0.58	0.61	1.85	0.85
10	Serial dilution pooled 1 level 5	0.30	0.30	0.94	0.39
11	Serial dilution pooled 2 level 1	1.94	1.91	5.21	2.63
12	Serial dilution pooled 2 level 2	1.26	1.41	3.77	1.72
13	Serial dilution pooled 2 level 3[a]	32.97	58.08	3.54	1.42
14	Serial dilution pooled 2 level 4	0.50	0.56	2.32	0.85
15	Serial dilution pooled 2 level 5	0.24	0.27	1.12	0.38
16	Serial dilution pooled 3 level 1	1.82	2.07	3.20	1.98
17	Serial dilution pooled 3 level 2	1.25	1.42	2.65	1.45
18	Serial dilution pooled 3 level 3	1.00	0.97	2.23	1.21
19	Serial dilution pooled 3 level 4	0.49	0.56	1.58	0.66
20	Serial dilution pooled 3 level 5	0.23	0.24	1.11	0.36
21	Spike-recovery pooled 1 level 1	0.54	0.54	0.62	0.46
22	Spike-recovery pooled 1 level 2	1.35	1.47	1.80	1.23
23	Spike-recovery pooled 1 level 3	2.07	2.34	2.59	2.11
24	Spike-recovery pooled 1 level 4	2.97	2.93	3.92	2.67
25	Spike-recovery pooled 1 level 5[a]	22.85	42.38	4.59	3.59
26	Spike-recovery pooled 2 level 1	0.59	0.67	0.69	0.48
27	Spike-recovery pooled 2 level 2	1.37	1.59	1.98	1.20
28	Spike-recovery pooled 2 level 3	2.16	2.52	3.10	1.96
29	Spike-recovery pooled 2 level 4	3.00	2.95	4.17	2.99
30	Spike-recovery pooled 2 level 5	3.81	4.23	4.95	4.06
31	Spike-recovery pooled 3 level 1	0.48	0.53	1.05	0.45
32	Spike-recovery pooled 3 level 2	1.26	1.31	1.81	1.28
33	Spike-recovery pooled 3 level 3	2.12	2.33	3.11	2.02
34	Spike-recovery pooled 3 level 4	2.94	3.28	4.13	2.69
35	Spike-recovery pooled 3 level 5	3.66	4.11	5.64	3.45
36	High iodine 1[a]	0.27	0.32	5.50	2.75
37	High iodine 2	2.76	3.02	3.70	3.81
38	High iodine 3	10.13	11.49	9.45	10.88
39	High iodine 4	4.39	5.00	3.69	4.49
40	High iodine 5	0.87	0.94	4.70	1.46
41	T4 1	1.52	1.73	2.03	1.46
42	T4 2	1.65	1.86	2.15	1.42
43	T4 3	2.38	2.33	2.49	1.86
44	T4 4	4.51	4.96	3.09	3.97
45	T4 5	1.95	1.93	2.15	1.64
46	T4 6	0.45	0.49	1.37	0.61
47	T4 7	1.18	1.27	1.18	1.06
48	T4 8	2.76	2.69	5.41	3.86
49	T4 9	0.73	0.74	0.93	0.82
50	T4 10	0.32	0.36	0.41	0.21
51	Pooled QC (9 aliquots)	1.26	1.32	1.97	1.46
52	QC level I (9 aliquots)	0.97	0.96	1.92	0.83
53	QC level II (9 aliquots)	4.17	4.06	3.90	3.89

[a] *Samples excluded from method comparison as extreme outliers (Tukey boxplot method)*

Table S4.2. Summary results for QC samples intermittently assessed (*n* = 9) during the analysis of 50 urine samples included in the method comparison by CE-UV and ICP-MS.

Method	QC	Mean iodine ± SD (µmol/L)	CV (%)	Mean CV (%)	Bias (%)[a]
Original CE-UV	Level I	1.96 ± 0.08	4.12	8.80	107.3
	Level II	3.77 ± 0.37	9.91		-3.9
	Pooled	1.73 ± 0.21	12.36		NA
Updated CE-UV	Level I	0.83 ± 0.09	11.11	9.88	-11.7
	Level II	3.89 ± 0.25	6.41		-0.8
	Pooled	1.46 ± 0.18	12.14		NA
ICP-MS Re	Level I	0.97 ± 0.02	1.55	1.78	3.2
	Level II	4.13 ± 0.09	2.08		5.2
	Pooled	1.25 ± 0.02	1.72		NA
ICP-MS Te	Level I	1.04 ± 0.06	6.24	5.63	9.7
	Level II	4.37 ± 0.26	5.83		11.6
	Pooled	1.36 ± 0.07	4.83		NA

[a]*Bias determined based on reference iodine concentration from manufacturer (QC level I = 0.94 µmol/L and QC level II = 3.92 µmol/L. Reference concentrations not available for the pooled QC.*

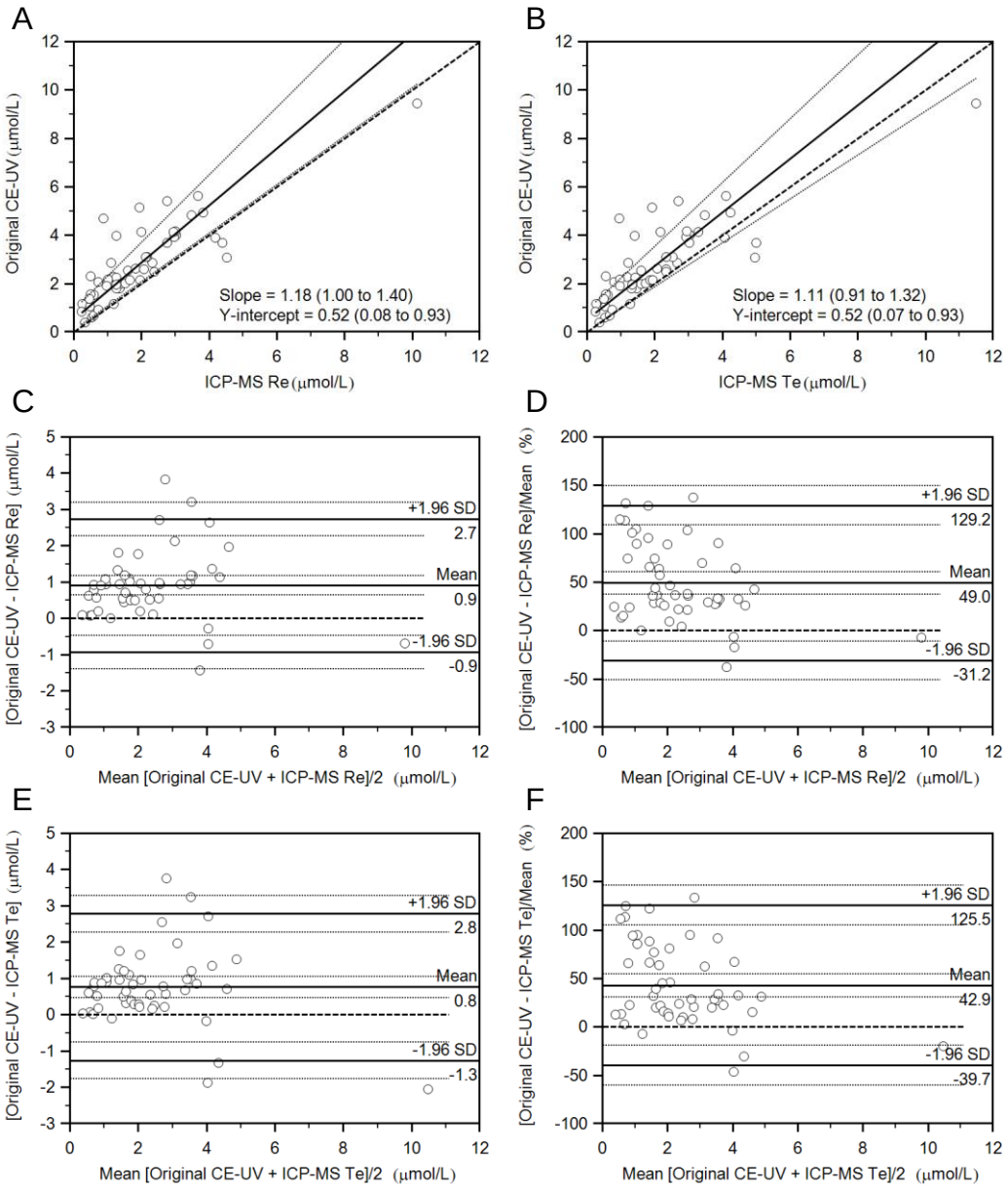

Figure S4.1. Passing-Bablok regression comparing the original CE-UV assay with ICP-MS using the internal standards ^{187}Re (**A**) and ^{130}Te (**B**). Bland-Altman plots of differences (**C**, **E**) and % differences (**D**, **F**) between the original CE-UV assay and ICP-MS using the internal standards ^{187}Re and ^{130}Te, respectively. Passing-Bablok plots show slopes and y-intercepts followed by their 95% CI. Regression, 95% CI and equality line are represented by solid, dotted and dashed lines, respectively. In the Bland-Altman plots, the mean difference/percentage difference and limits of agreement (± 1.96 SD) are represented as solid lines, while their 95% CI and the zero are indicated by dotted and dashed lines, respectively.

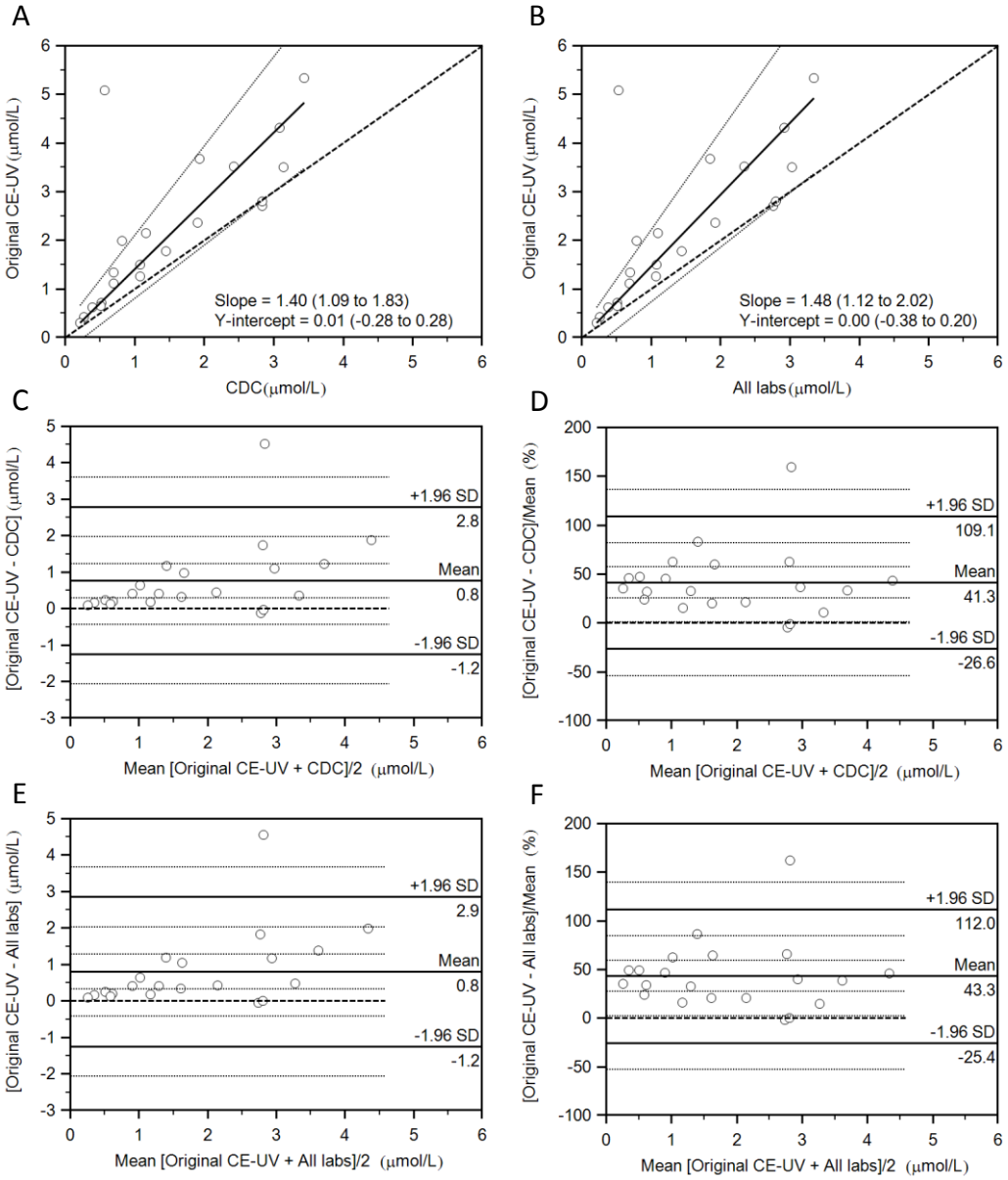

Figure S4.2. Passing-Bablok regression of iodine concentrations in the EQUIP urine samples (n = 21), comparing the original CE-UV assay with the CDC target (**A**) and the mean of all laboratories (**B**). Bland-Altman plots of the differences (**C**, **E**) and % differences (**D**, **F**) for the CDC target and the mean of all laboratories, respectively. See Figure S4.1 for a description of the line notation used in the graphs.

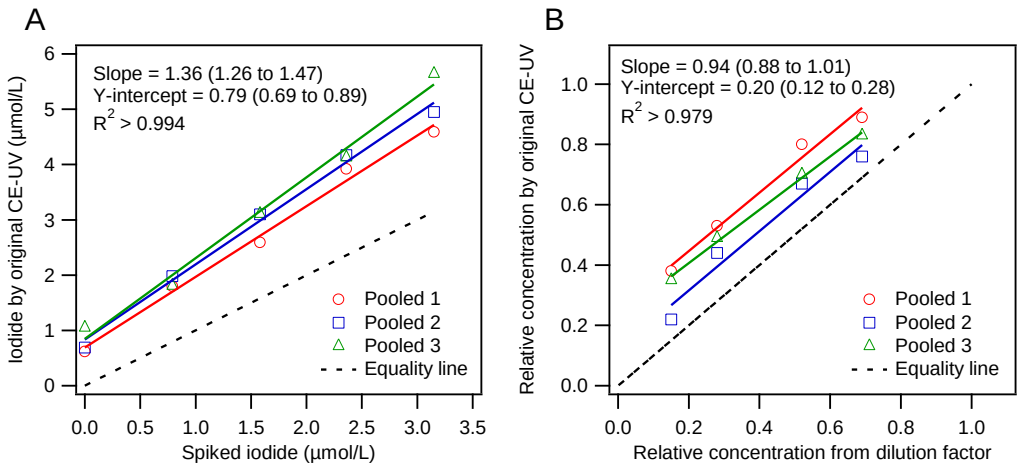

Figure S4.3. Spike-recovery (**A**) and serial dilution (**B**) for three independent pooled urine samples analyzed by the original CE-UV assay. Solid lines represent the least-squares linear regression, while slopes and y-intercepts are shown in the graphs, followed by their 95% CI.

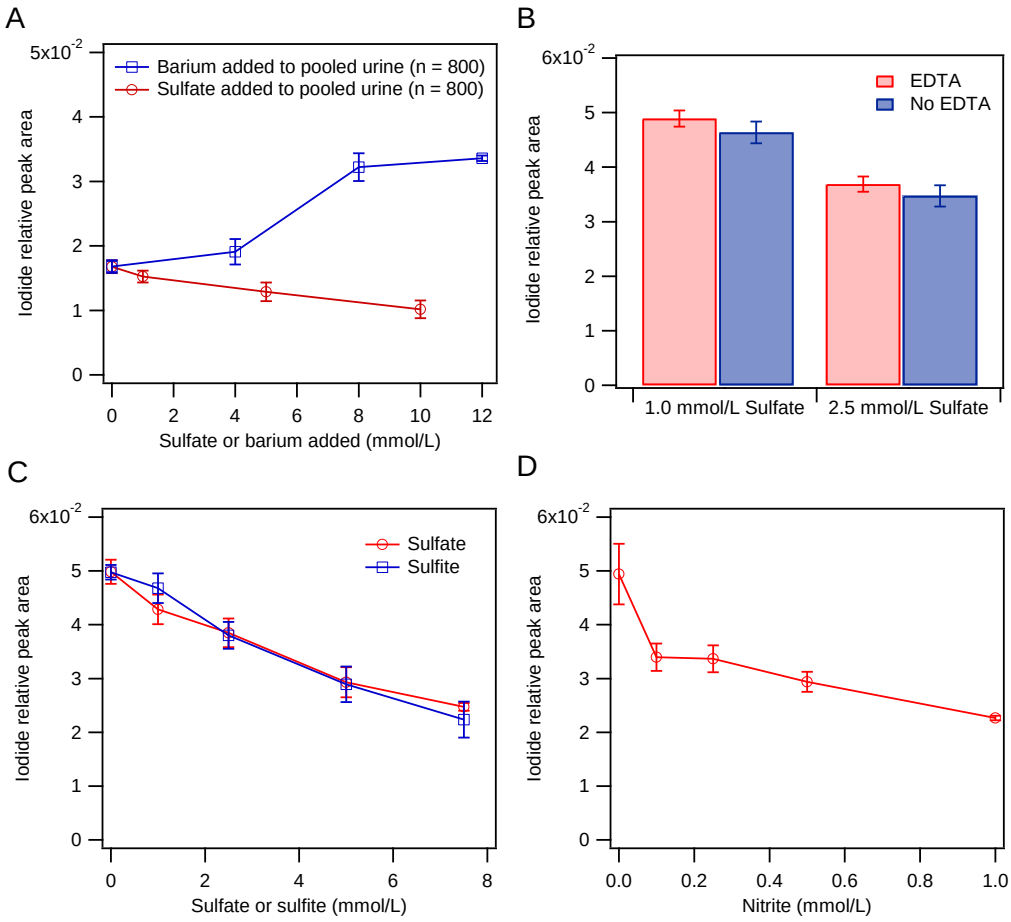

Figure S4.4. (**A**) Effect of sulfate addition or barium treatment on the iodide signal obtained for a 1.5-fold diluted pooled urine sample (n = 800) after analysis by the original CE-UV method. The levels of sulfate present in the urine (equivalent to 7.6 mmol/L in the 1.5-fold diluted sample) are comparable to the amount of barium needed to restore the iodide response (*i.e.*, 8.0 mmol/L). (**B**) Iodide standard prepared in solutions containing 1.0 and 2.5 mmol/L sulfate and treated with 1 mmol/L EDTA before analysis by the original CE-UV assay to evaluate the potential interference of trace metals. There was no significant effect of EDTA treatment on the iodide response (p = 0.152 and 0.191 for 1.0 and 2.5 mmol/L sulfate, respectively). A decrease in the iodide measured response was observed in solutions containing the oxidizing agents sulfite (**C**) and nitrite (**D**).

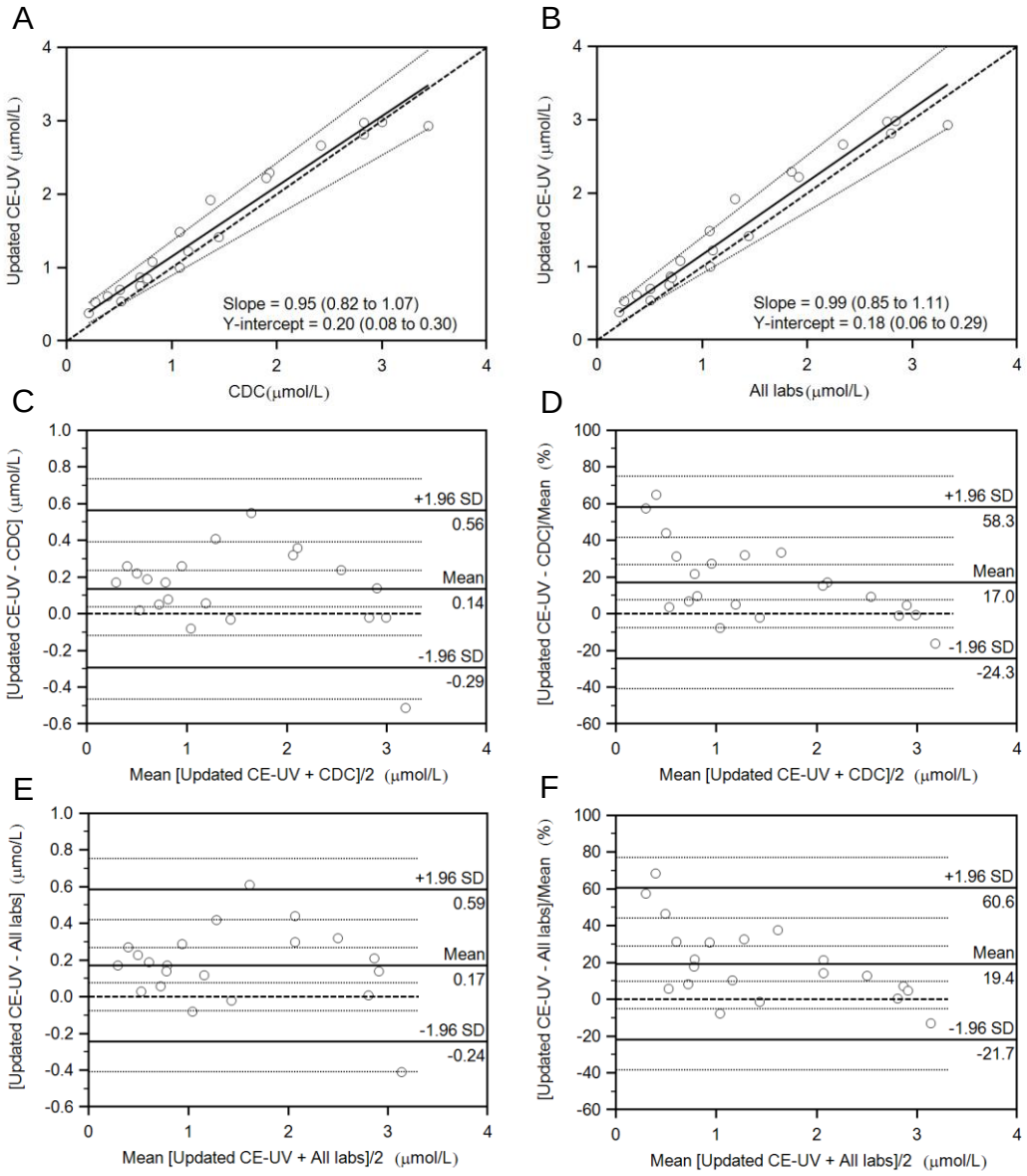

Figure S4.5. Passing-Bablok regression of iodine concentrations in the EQUIP urine samples (n = 21), comparing the optimized CE-UV assay with the CDC target (**A**) and the mean of all laboratories (**B**). Bland-Altman plots of the differences (**C**, **E**) and % differences (**D**, **F**) for the CDC target and the mean of all laboratories, respectively. See Figure S4.1 for a description of the line notation used. In this case, the measurement of the median differences and percentage differences (0.17 µmol/L, 9.9% and 0.17 µmol/L, 14.5% for the CDC and mean of all labs, respectively) are more representative of the overall agreement, as the data is not normally distributed (Shapiro-Wilk, $p < 0.05$).

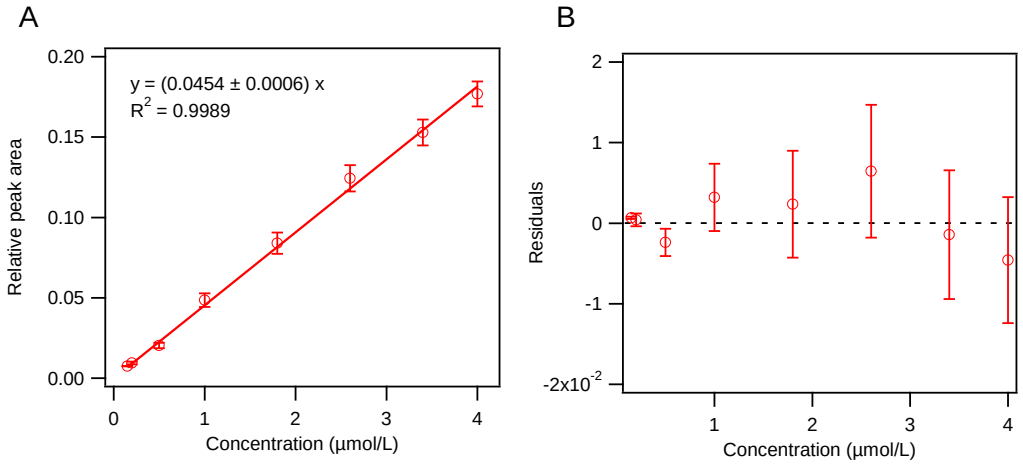

Figure S4.6. Calibration curve (**A**) and residuals plot (**B**) for iodide standard solutions (0.15 to 4.00 µmol/L) prepared in a 2-fold diluted simplified urine matrix (100 mmol/L sodium chloride and 10 mmol/L sodium sulfate) and analyzed by the optimized CE-UV assay. Linear least squares regression was used to obtain the regression line. Error represents ± 1SD for solutions prepared and analyzed in triplicate over three consecutive days.

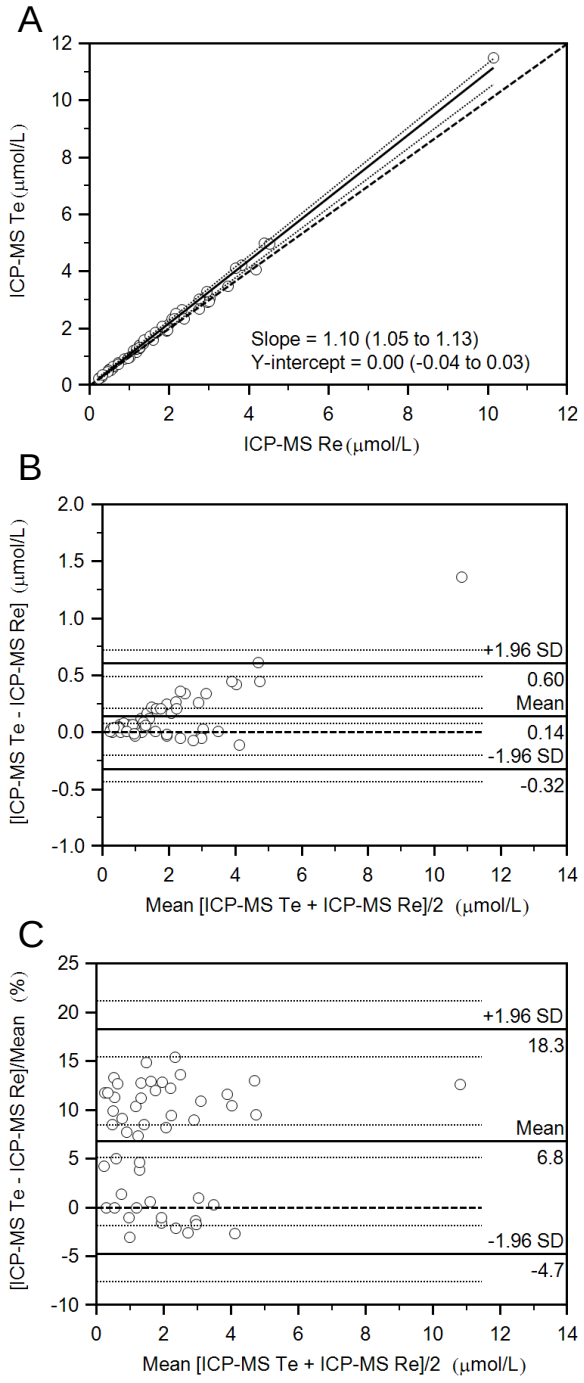

Figure S4.7. Passing-Bablok regression comparing results from ICP-MS using the internal standards ^{187}Re and ^{130}Te (**A**). Bland-Altman plots of the differences (**B**) and % differences (**C**). See Figure S4.1 for a description of the line notation used in the graphs.

Chapter V

Characterization of the Sweat Metabolome in Screen-Positive Cystic Fibrosis Infants: Looking Beyond the Chloride Transport Defect

Authors of this work are Adriana Nori de Macedo, Tiffany Chan, Stellena Mathiaparanam, Biban Gill, Nadine Wellington, Lauren Brick, Katherine Keenan, Tanja Gonska, Linda Pedder, Stephen Hill, and Philip Britz-McKibbin.

I conducted the untargeted metabolomics experiments using MSI-CE-MS, performed MS/MS experiments for unknown identification, did most of the data processing and statistical analysis, and wrote an initial manuscript draft for publication. Other co-authors contributed with research ethics submission, specimen storage, de-identification and compilation of patient information, as well as feedback on the initial manuscripts draft (in preparation).

Chapter V: Characterization of the Sweat Metabolome in Screen-Positive Cystic Fibrosis Infants: Looking Beyond the Chloride Transport Defect

5.1 Abstract

The sweat chloride test remains the gold standard for confirmatory diagnosis of cystic fibrosis (CF) in support of newborn screening programs. However, this approach provides ambiguous results for intermediate/borderline chloride levels, and lacks discrimination for classifying the complex CF disease spectrum and treatment responsiveness to therapy. Our objective in this study was to characterize the sweat metabolome from CF screen-positive infants and identify other metabolites associated with CF that may complement sweat chloride testing. Residual specimens of pilocarpine-stimulated sweat were collected from screen-positive infants at two CF clinics in Ontario, including 50 unaffected CF (*i.e.*, false positives) and 18 confirmed CF cases. Untargeted metabolite profiling was performed using multisegment injection-capillary electrophoresis-mass spectrometry for the analysis of polar/ionic compounds in volume-restricted sweat specimens (< 5 μL). Unknown sweat metabolites were identified with authentic standards or characterized using high resolution, accurate tandem mass spectrometry in conjunction with spectral database matches and *in silico* fragmentation modeling. Amino acids, organic acids, amino acid derivatives, dipeptides, purine derivatives and several exogenous compounds were detected in sweat, including several differentiating metabolites associated with affected yet asymptomatic CF infants (< 3 months), such as asparagine and glutamine. Unexpectedly, the pilocarpine metabolite, pilocarpic acid, and a plasticizer metabolite, mono(2-ethylhexyl)phthalic acid were both found to be significantly lower in the sweat of CF affected infants, suggesting lower activity of the arylesterase/lactonase, human paraoxonase. Additionally, repeat sweat samples from a late-diagnosed female teenage CF patient with a G551D mutation

demonstrated that distinct metabolomic changes were associated with nutritional intervention and/or drug therapy with the CFTR potentiator, ivacaftor, that resulted in improved lung function, growth and sweat chloride transport. In summary, this work presents the first in-depth characterization of sweat metabolites in screen-positive CF infants, which may improve the diagnosis, prognosis and treatment responses to drug interventions in precision medicine.

5.2 Introduction

Cystic fibrosis (CF) is a life-shortening and multi-organ autosomal recessive disease mainly characterized by meconium ileus, pancreatic insufficiency and recurrent lung infections that contribute to growth failure and progressive respiratory dysfunction with a highly variable clinical phenotype.[1] Although there is currently no cure for CF, life expectancy and quality of life is considerably improved if the disease is diagnosed early in life (*i.e.*, within 2-3 months after birth), which allows prompt therapeutic interventions to initiate before the onset of the first debilitating symptoms.[2,3] Early detection of CF in asymptomatic neonates is now included into universal newborn screening (NBS) programs in many western countries given its high incidence rate in the Caucasian population.[4] Moreover, growing evidence demonstrates the cost-effectiveness and efficacy of improved nutritional status with early diagnosis on later growth, lung function and survival for individuals diagnosed through NBS as compared to symptomatically.[5,6] In most cases, NBS for CF adopts a two-tier screening algorithm that starts with an immunoreactive trypsinogen (IRT) test in dried blood spot samples followed by a DNA analysis for a panel of disease-causing mutations of the CF transmembrane conductance regulator (*CFTR*) gene that is dependent on demographics of the population.[3,7] However, the low specificity of IRT in newborns results in a high rate of false-positives, whereas genetic testing leads to unaffected carrier identification that comprises a majority (≈ 75%) of screen positive CF cases.[8] As a result, a sweat chloride test is required for

confirmatory diagnosis of CF from screen-positive infants, including cases of highly elevated IRT concentrations without an identifiable *CFTR* mutation.[9]

The sweat chloride test is simple, non-invasive and remains the gold standard for CF diagnosis since its introduction in the late 1950's,[10] with a value of ≥ 60 mM for CF screen-positive infants. However, ambiguous test results complicate clinical decision-making especially in borderline cases or when chloride levels are intermediate (30-59 mM), which is classified as CF-screen positive inconclusive diagnosis (CF-SPID).[11] The latter indeterminate result includes carriers, individuals with mild manifestations of the disease (*i.e.*, atypical or non-classic CF) and even patients who will later develop classic CF symptoms.[7,12] Additionally, the highly variable phenotypes and degrees of disease severity within CF-affected infants are not clearly explained by sweat chloride levels or *CFTR* genotype alone.[13,14] Therefore, new biomarkers are needed to complement the sweat chloride test and support better decision-making in the clinic by facilitating diagnosis, disease stratification and treatment monitoring of patients. As downstream biochemical products of gene expression that also reflect lifelong environmental exposures, metabolites are closely associated to clinical outcomes, which highlights their great potential as biomarkers for pre-symptomatic diagnosis of human diseases.[15,16] For instance, metabolites serve as primary biomarkers for screening a diverse array of in-born errors of metabolism in expanded NBS programs using high throughput and multiplexed tandem mass spectrometry (MS/MS) technology.[17] In the case of CF, the sweat gland provides invaluable information for disease diagnosis reflecting the underlying function of the CFTR protein in other less accessible organs, such as the lungs or pancreas.[18] However, the sweat metabolome remains largely uncharacterized[19] to date especially in infants. Targeted analysis has shown that sweat is composed primarily of water, electrolytes, urea and lactate, but also contains other metabolites, including amino acids and organic acids.[20] Only a few studies have reported non-targeted metabolite profiling of human sweat,[21–26] however these

studies were not focused on infants or designed to evaluate their potential as CF biomarkers in order to improve the diagnosis of borderline/intermediate sweat chloride cases or assess treatment responsivity to therapy.

Herein, we present the first metabolomic characterization of polar/ionic metabolites in the sweat from CF screen-positive infants (≤ 3 months old), including a number of unknown compounds reported for the first time. Residual pilocarpine-stimulated sweat samples collected from CF affected (chloride ≥ 60 mM, 2 *CFTR* mutations) and unaffected (chloride < 30 mM, 1 or none *CFTR* mutations) infants were analyzed using multisegment injection-capillary electrophoresis-mass spectrometry (MSI-CE-MS)[27] for increased sample throughput and data fidelity to reduce false discoveries that is also applicable to volume-restricted biospecimens. Unknown metabolites were identified by high resolution, accurate MS/MS and confirmed with authentic standards or tentatively assigned based on spectral database matches in conjunction with *in silico* fragmentation modeling.[28] Moreover, a comparison between batch-corrected metabolomic data of sweat samples from CF affected and non-affected infants collected from two CF clinics in Ontario identified a panel of differentiating metabolites of significance in addition to sweat chloride. Time-dependent metabolic changes were also analyzed in repeat sweat specimens collected from a teenage CF patient diagnosed symptomatically (born prior to advent of NBS for CF), who received nutritional intervention and subsequent drug therapy with the CFTR potentiator ivacaftor. This study demonstrates the potential that sweat metabolites beyond chloride are associated with impaired/loss of CFTR function in screen-positive CF infants that can also be partially restored via genotype-specific drug intervention, which elicit positive clinical outcomes even in late diagnosed underweight CF affected children resulting in improved nutritional status, growth and importantly lung function.

5.3 Experimental Section

5.3.1 Chemicals and reagents

Ultra-grade LC-MS solvents (water, methanol and acetonitrile) obtained from Caledon Laboratories Ltd. (Georgetown, ON, Canada) were used to prepare all buffer and sheath liquid solutions. All other chemicals were obtained from Sigma-Aldrich Inc. (St. Louis, MO, USA), except for malic acid, xanthine, uric acid, and citric acid, which were purchased from Alfa Aesar Inc. (Heysham, Lancashire, UK), and pilocarpic acid, which was obtained from Toronto Research Chemicals Inc. (Toronto, ON, Canada).

5.3.2 Study design and sweat collection for CF screen-positive infants

In this study, residual sweat samples with a minimum volume of about 5 μL were obtained from first-time/screen-positive CF infants following standardized pilocapine-stimulated sweat chloride testing, excluding samples with intermediate chloride levels (30-59 mM). All sweat specimens were de-identified and relabeled with a research ID number at McMaster Children's Hospital and The Hospital for Sick Children (Sick Kids) in order to protect patient privacy, as approved by the Hamilton Integrated Research Ethics Board and The Hospital for Sick Children's Research Ethics Board. Patient medical records from Newborn Screening Ontario (NSO) and CF clinics were linked directly to the research ID, maintaining confidentiality of personal health information. Sweat collection was performed using a Webster Model 3700 Macroduct Sweat Capillary Collection System (Wescor Inc., Logan, UT, USA). Electrodes and agar gel discs containing 0.5% w/w pilocarpine nitrate were placed in the infant's forearm for sweat stimulation after carefully cleaning the region with ethanol and distilled water. A low current (1.5 mA) was applied for 5 min to deliver pilocarpine to the sweat gland by iontophoresis. Sweat was then collected for 25 min using a coiled microbore tube containing a blue dye to facilitate visualization of the sample volume. Samples

were transferred to a 0.5 mL centrifuge tube and stored in a fridge (+4^{o}C) after taking an aliquot for chloride analysis by chloridometer (Wescor Sweat-Check Model 3120). Residual sweat samples were subsequently stored frozen at -80^{o}C prior to thawing when performing metabolomic studies in two batches of randomized samples. Overall, sixty-eight sweat specimens from screen-positive infants (≤ 3 months old) using a two-tiered algorithm based on elevated IRT/genetic mutation panel at NSO were analyzed in this study, including 50 CF non-affected infants (31 from McMaster, 19 from Sick Kids) and 18 CF affected (13 from McMaster, 5 from Sick Kids).

5.3.3 Instrumentation and sweat analysis by MSI-CE-MS

Non-targeted metabolite profiling was performed using an Agilent 7100 CE instrument and an Agilent 6550 quadrupole time-of-flight (QTOF) mass spectrometer equipped with a dual jet stream electrospray ion source (dual AJS ESI) with ion funnel technology (Agilent Technologies, Mississauga, ON, USA). Sweat samples were analyzed by MSI-CE-MS in positive (ESI+) and negative (ESI-) ion modes to cover cationic and anionic metabolites after thawing specimens slowly to room temperature on ice.[27,29] A complete description of the experimental conditions for MSI-CE-MS is provided in the Supporting Section. All samples were prepared by a simple dilution step using a minimum volume of about 5 µL of sweat in ultra-grade LC-MS water containing 10 µM of the internal standards, 3-chloro-*L*-tyrosine (Cl-Tyr) and sodium 2-naphthalenesulfonate (NMS), followed by mixing using a vortex for 30 s. A pooled quality control (QC) sample was prepared from a sub-set of sweat samples (n = 10) that had adequate volume as described in the Supporting Information Section.

Metabolomic studies were initially performed using a seven sample plug serial dilution trend filter in MSI-CE-MS[27] when using a QC sample for rigorous peak selection/data filtering of cationic and anionic metabolites derived from

infant sweat under positive and negative ion modes, respectively as shown in **Figure 5.1**. This process allows for unambiguous identification of authentic yet reproducible molecular features (*i.e.*, $[M+H]^+$ and $[M-H]^-$) in sweat from a large fraction of background ions or spurious signals based on their distinctive dilution signal pattern that has adequate precision (RSD < 40%, $n = 3$) with no measurable signal in the blank sample. Using this approach, a total of 52 spurious/background signals were removed from over 206 features originally obtained from Mass Hunter Molecular Feature Extractor (MFE). A list of authentic features defined by their characteristic mass-to-charge ratio and relative migration time (*m/z:*RMT) was then further filtered to remove redundant signals originating from the same compound which have the same RMT as the ionized molecule, including adducts, dimers, isotopes and in-source fragments. This data filtering procedure was often confirmed when running MSI-CE-MS with authentic standards and comparing their mass spectral data under the same conditions. MFE was also performed in representative individual sweat samples from four authentic CF and two unaffected CF infants in order to identify unique molecular features (*m/z*:RMT) that were not detected in the original pooled QC.

Individual sweat samples were then analyzed using in duplicate using temporal signal pattern recognition in MSI-CE-MS (DiBattista, unpublished data) for confident assignment of peaks to their sample of origin even when a compound is not detected in one or more samples in the serial injection sequence. As presented in **Figure S5.1**, three sweat samples were prepared in duplicate using different dilution factors, which results in a pattern of ion signals that allows for simple visual peak assignment. Furthermore, this configuration allows the introduction of a pooled QC sample within each run, which is critical for evaluating system variability and helps with batch correction due to system drift as a result of non-biological experimental variation (*i.e.,* MS instrumental conditions) during data acquisition.[30] Sweat samples were analyzed in randomly assigned order and injection positions by MSI-CE-MS with a QC randomly

inserted in positions 1, 3, 5 or 7. Sample dilution was optimized for each ionization mode in order to prevent saturation and signal suppression due to certain high abundant sweat components. In this case, sweat samples were 10- and 20-fold diluted for cation analysis and 4 and 8-fold diluted for anion analysis. Sweat samples were analyzed in two separate batches of runs performed about 10 months apart due to delays required for acquisition of sweat specimens from screen-positive CF infants from two pediatric hospitals. Further details about the conditions used in MS/MS experiments for unknown metabolite identification, as well as the procedure for the pilocarpine gel extraction and preparation of blanks for the sweat collection device are described in the Supporting Information Section.

5.3.4 Data processing and statistical analysis

Raw data was extracted using Mass Hunter Workstation Software (Qualitative Analysis, version B.06.00, Agilent Technologies, 2012). Untargeted analysis was performed using Mass Hunter Molecular Feature Extractor and Molecular Formula Generator tools followed by a personal compound database search. Features were extracted in centroid using 10 ppm mass window and labelled according to their *m/z*, RMT and ionization mode (p = ESI+, n = ESI-). Peaks were integrated after smoothing (quadratic/cubic Savitzky-Golay, 15 points) and peak areas and migration times were transferred to Excel (Microsoft Office) for calculation of relative peaks areas (RPA), relative migration times (RMT), relative standard deviations (RSD) and fold-changes, as well as conversion into a data matrix format. Only molecular features detected in at least 75% of the samples were included in the data matrix for subsequent data transformation and statistical analysis. Due to between-subject variations in sweat rate/volume among infants, a probabilistic quotient normalization (PQN) method was evaluated for normalizing sweat metabolomic data to correct for dilution/hydration status.[31] Additionally, batch effect correction using QCs was performed on randomized

samples via an Empirical Bayes method (ComBat-adjusted matrix) on MetaboAnalyst 3.0,[32] whereas normality tests and univariate statistical analysis were conducted using the Statistical Package for the Social Science (SPSS, version 18) and MedCalc (MedCalc Inc.) was used to obtain receiver operating characteristic (ROC) curves and boxplots.

5.3.5 Sweat analysis in CF patient undergoing ivacaftor therapy

Repeat sweat specimens were collected from a 12 year old female CF patient diagnosed symptomatically at McMaster Children's Hospital as she was born prior to advent of universal screening for CF in Ontario. As part of her clinical laboratory tests, sweat samples were collected at three time points: (1) at diagnosis; (2) after seven months following therapeutic intervention comprising pancreatic enzyme replacement, high fat, vitamin supplementation and physiotherapy; and then (3) three months after introduction of drug therapy together with on-going nutritional supplementation. As the patient was a compound heterozygote with a gating mutation (G551D/DF508), she was eligible for treatment with the CFTR-potentiator drug ivacaftor. Clinical assessment demonstrated good response to treatment, as indicated by improved growth (*i.e.*, height and weight gain) and lung function in terms of increased forced expiratory volume in 1 second (FEV_1) and forced expiratory vital capacity (*FVC*), which was accompanied by a significant decrease in sweat chloride levels from 100 to 38 mM. Residual pilocarpine-stimulated sweat specimens following chloridometer measurements were then used for untargeted metabolite profiling by MSI-CE-MS in order to investigate dynamic changes in metabolism associated with nutritional intervention and/or ivacaftor therapy. Sample workup, metabolite analysis and data processing of the sweat metabolome for this late-diagnosed CF patient used the same procedures as described for infant samples.

5.4 Results

5.4.1 Characterization of polar/ionic metabolites in sweat from infants

Comprehensive characterization of the sweat metabolome from screen-positive CF infants was performed by MSI-CE-MS when using a dilution trend filter (**Figure 5.1**) on a pooled sweat QC and representative individual sweat samples from CF affected and unaffected infants, which resulted in a total of 64 authentic compounds (35 cations and 29 anions) denoted by their characteristic *m/z*:RMT after rejection of spurious, background, irreproducible and/or redundant signals. As shown in **Table 5.1**, the majority of the 64 polar/ionic metabolites detected in screen-positive CF sweat comprise amino acids, amino acid derivatives, dipeptides, organic acids, fatty acids and several exogenous compounds, including paraben-based preservatives (*e.g.*, methylparaben and propylparaben) from the gel pad used in iontophoresis and the synthetic blue dye (*i.e.*, FD&C blue dye no. 1) used for visualization during pilocarpine-stimulated sweat collection. All molecular features in sweat were characterized based on their unique *m/z*:RMT, including accurate mass and isotopic distribution to determine a most likely molecular formula with low mass error (< 3 ppm). Confidence levels for metabolite identification are presented in **Table 5.1** according to recommendation of the Metabolomics Standards Initiative.[33] Unambiguous metabolite achieved based on co-migration and high resolution, accurate MS/MS spectral comparison after spiking sweat samples using authentic chemical standards, which was the case for about 73% of total molecular features in the sweat of screen-positive infants. For instance, two unknown compounds were subsequently identified as pilocarpic acid (PA) and mono(2-ethylhexyl)phthalic acid (MEHP) as they were confidently assigned (level 1) with standards that displayed consistent *m/z* and RMTs, in addition to MS/MS fragmentation spectra with matching scores over 90% (**Figure S5.2**). Otherwise, when commercial standards were not available,

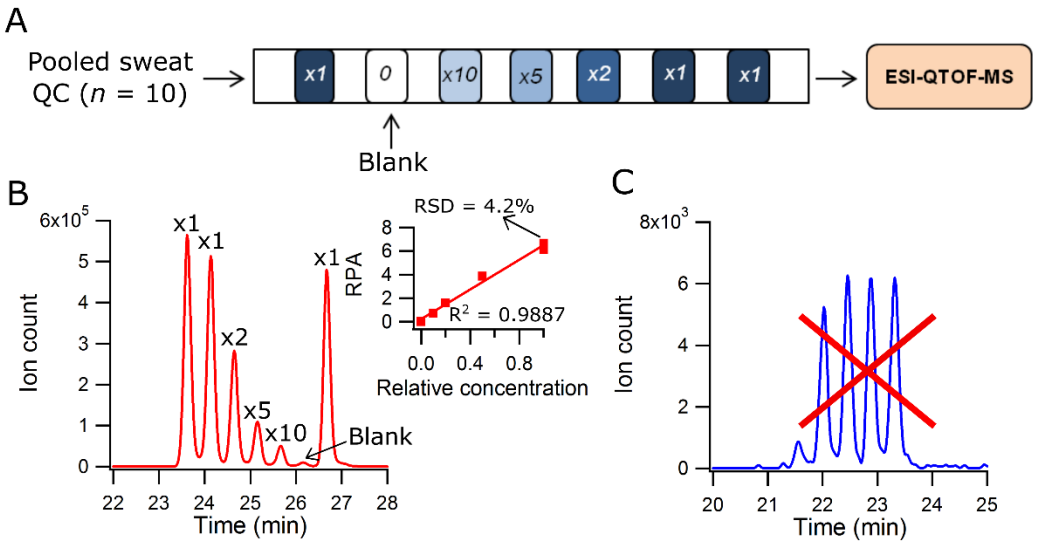

Figure 5.1. (A) Injection configuration for the dilution trend filter using a pooled sweat QC (*n* = 10) serially diluted by factors of 1, 2, 5, and 10, including a triplicate for the least diluted sample and a blank. **(B)** Example extracted ion electropherogram (EIE) of an authentic feature (citrulline, *m/z* 176.1030, ESI+), which follows the dilution trend (R^2 = 0.9887), has a relatively low RSD for the triplicate injection (4.2%), and shows no signal in the blank. **(C)** Example of a spurious signal (*m/z* 178.1588, ESI+), which does not follow the dilution trend and can be confidently excluded from the mass list.

unknown metabolites were tentatively identified (*e.g.*, glycylglycine, level 2) based on comparative matches with public MS and MS/MS spectral databases (HMDB, Metlin) and Agilent Mass Hunter Molecular Structure Correlator using ChemSpider and Agilent Metlin Compound Database search with collision-induced fragmentation of the precursor ion performed at different collisional energies (10, 20, 40 V). In cases when no MS/MS matches were found in a spectral library or literature search, *in silico* MS/MS fragmentation prediction using CFM-ID was performed for putative candidates in combination with manual assignment of common mass losses that are characteristic of metabolite classes with consistent electromigration behavior and functional groups derived from annotation of MS/MS spectra (*e.g.*, *m/z* 168.0770, RMT 0.733, ESI+, level 3, assigned as an amino acid derivative). Additionally, a total of eight compounds remain unknown with no defined chemical structure/metabolite class, which were

Table 5.1. Summary of 64 metabolites detected in sweat from screen-positive CF infants, including *m/z*, RMT, ionization mode (p = ESI+, n = ESI-), molecular formula, compound ID or tentative ID, confidence level for identification, and chemical classification.

***m/z*:RMT:mode**	**Formula[a]**	**Compound ID[b]**	**Confidence level[c]**	**Classification**
76.0393:0.757:p	$C_2H_5NO_2$	Glycine	1	Amino acid
90.0550:0.805:p	$C_3H_7NO_2$	Alanine	1	Amino acid
104.1075:0.645:p	$C_5H_{14}NO$	Choline	1	Quaternary ammonium salt
106.0499:0.874:p	$C_3H_7NO_3$	Serine	1	Amino acid
114.0662:0.687:p	$C_4H_7N_3O$	Creatinine	1	Heterocyclic compound
116.0706:0.920:p	$C_5H_9NO_2$	Proline	1	Amino acid
118.0863:0.868:p	$C_5H_{11}NO_2$	Valine	1	Amino acid
120.0655:0.909:p	$C_4H_9NO_3$	Threonine	1	Amino acid
132.0655:1.009:p	$C_5H_9NO_3$	3-Hydroxyproline	1	Amino acid derivative
132.0766:0.798:p	$C_4H_9N_3O_2$	Creatine	1	Amino acid
132.1019:0.879:p	$C_6H_{13}NO_2$	Isoleucine	1	Amino acid
132.1019:0.888:p	$C_6H_{13}NO_2$	Leucine	1	Amino acid
133.0608:0.773:p	$C_4H_8N_2O_3$	Glycylglycine	2	Dipeptide
133.0608:0.912:p	$C_4H_8N_2O_3$	Asparagine	1	Amino acid
133.0972:0.645:p	$C_5H_{12}N_2O_2$	Ornithine	1	Amino acid
134.0448:0.973:p	$C_4H_7NO_4$	Aspartic acid	1	Amino acid
139.0500:0.772:p	$C_6H_6N_2O_2$	Urocanic acid	1	Amino acid derivative
147.0764:0.930:p	$C_5H_{10}N_2O_3$	Glutamine	1	Amino acid
147.1128:0.648:p	$C_6H_{14}N_2O_2$	Lysine	1	Amino acid
148.0604:0.940:p	$C_5H_9NO_4$	Glutamic acid	1	Amino acid
150.0583:0.916:p	$C_5H_{11}NO_2S$	Methionine	1	Amino acid
150.1119:0.763:p	$C_6H_{15}NO_3$	Triethanolamine	2	Amine
156.0768:0.686:p	$C_6H_9N_3O_2$	Histidine	1	Amino acid
162.1125:0.782:p	$C_7H_{15}NO_3$	Carnitine	1	Amino acid derivative
163.0719:0.827:p	$C_5H_{10}N_2O_4$	Glycylserine	2	Dipeptide
166.0863:0.940:p	$C_9H_{11}NO_2$	Phenylalanine	1	Amino acid
168.0770:0.733:p	$C_7H_9N_3O_2$	*Amino acid derivative*	3	Amino acid derivative
175.1190:0.677:p	$C_6H_{14}N_4O_2$	Arginine	1	Amino acid
176.1030:0.952:p	$C_6H_{13}N_3O_3$	Citrulline	1	Amino acid
182.0812:0.967:p	$C_9H_{11}NO_3$	Tyrosine	1	Amino acid
194.1380:0.802:p	$C_8H_{19}NO_4$	*Unknown[d]*	4	Unknown
205.0972:0.944:p	$C_{11}H_{12}N_2O_2$	Tryptophan	1	Amino acid
209.1290:0.795:p	$C_{11}H_{16}N_2O_2$	Pilocarpine	1	Exogenous
213.0990:0.635:p	$C_8H_{12}N_4O_3$	Glycylhistidine	1	Dipeptide

235.1199:0.841:p	$C_{11}H_{14}N_4O_2$	*Unknown*	4	Unknown
89.0244:1.146:n	$C_3H_6O_3$	Lactic acid	1	Hydroxy carboxylic acid
96.9696:1.686:n	H_3PO_4	Phosphate[d]	1	Oxoanionic compound
128.0352:1.020:n	$C_5H_7NO_3$	Oxoproline	1	Amino acid derivative
133.0149:1.857:n	$C_4H_6O_5$	Malic acid	1	Hydroxy dicarboxylic acid
135.0299:0.994:n	$C_4H_8O_5$	Threonic acid	2	Sugar acid
143.1078:0.899:n	$C_8H_{16}O_2$	Caprylic acid[d]	1	Medium-chain fatty acid
151.0262:0.938:n	$C_5H_4N_4O_2$	Xanthine	1	Purine derivative
151.0402:0.755:n	$C_8H_8O_3$	Methylparaben	1	Exogenous
160.0615:0.904:n	$C_6H_{11}NO_4$	α-Aminoadipic acid[d]	1	Amino acid derivative
167.0211:0.962:n	$C_5H_4N_4O_3$	Uric acid	1	Purine derivative
171.1391:0.856:n	$C_{10}H_{20}O_2$	Capric acid	1	Medium-chain fatty acid
179.0714:0.725:n	$C_{10}H_{12}O_3$	Propylparaben	1	Exogenous
188.0929:0.860:n	$C_8H_{15}NO_4$	*Unknown*	4	Unknown
191.0197:2.064:n	$C_6H_8O_7$	Citric acid[d]	1	Tricarboxylic acid
195.0510:0.880:n	$C_6H_{12}O_7$	Gluconic acid[d]	1	Sugar acid
199.0725:0.868:n	$C_8H_{12}N_2O_4$	*Unknown*	4	Unknown
199.1704:0.824:n	$C_{12}H_{24}O_2$	Lauric acid	1	Medium-chain fatty acid
201.0769:0.819:n	$C_9H_{14}O_5$	*Unknown*[d]	4	Unknown
215.0673:0.866:n	$C_8H_{12}N_2O_5$	*Unknown*	4	Unknown
225.1245:0.777:n	$C_{11}H_{18}N_2O_3$	Pilocarpic acid	1	Exogenous
227.1041:0.834:n	$C_{10}H_{16}N_2O_4$	Prolyl-4-hydroxyproline	2	Dipeptide
243.0624:1.276:n	$C_9H_{12}N_2O_6$	*Unknown*[d]	4	Unknown
257.1146:0.813:n	$C_{11}H_{18}N_2O_5$	*Unknown*	4	Unknown
265.0940:0.817:n	$C_{11}H_{14}N_4O_4$	Oxoprolylhistidine[d]	2	Dipeptide
265.1478:0.837:n	$C_{12}H_{26}O_4S$	Lauryl sulfate	1	Exogenous
277.1445:0.794:n	$C_{16}H_{22}O_4$	MEHP	1	Exogenous
320.1900:0.779:n	$C_{15}H_{31}NO_4S$	*N*-Lauroyl-*N*-methyltaurine[d]	2	Exogenous
329.2333:0.739:n	$C_{18}H_{34}O_5$	TriHOME[d,e]	2	Hydroxy fatty acid
373.0720:0.874:n	$C_{37}H_{37}N_2O_9S_3$	FD&C blue dye no. 1	1	Exogenous

[a] *Most probable formula is presented in the case of unknowns or tentatively identified compounds*
[b] *Stereochemistry (D/L) not confirmed (presumably mainly L-amino acids)*
[c] *Confidence levels: (1) confidently identified compound; (2) putatively identified compound; (3) putatively annotated compound class; (4) unknown compound*
[d] *Compounds not included in the data matrix for being non-detectable in more than 25% of the samples*
[e] *Tentatively identified as one of the isomers of trihydroxyoctadecenoic acid*

annotated only in terms of the most probable molecular formula (*e.g.*, *m/z* 194.1380, RMT 0.802, ESI+, level 4).

5.4.2 Batch correction adjustment and PQN normalization

Individual sweat samples were distributed into two analytical batches due to the time required to collect a sufficient number of sweat samples notably from CF affected infants. When combining results for both batches, a step-wise change in the signals (RPAs) was observed for some compounds, due to batch effect caused by variability in instrumental performance over time despite implementation of standard operating protocols, including routine cleaning/maintenance, instrument tuning/calibration and running of daily calibrant mixtures. This constitutes a common problem for long-term performance in metabolomic studies when using electrospray ionization (ESI)-MS unlike more robust and stable NMR platforms.[30] In order to improve signal comparability across batches, an adjustment algorithm based on empirical Bayesian frameworks[34] was used to obtain batch-corrected RPAs using the pooled QC sweat samples that were analyzed in every serial injection run by MSI-CE-MS together with each three randomly assigned infant sweat samples. Batch correction improved the consistency of QC signals measured for some metabolites (28 out of 54), while others were somewhat negatively affected (**Figure S5.3A-B**) resulting in only a modest improvement in the median RSD and overall variance range for all metabolites from 25% (9-121%) to 24% (11-94%) when comparing RPAs and batch-corrected RPAs for all QCs (n = 24) by MSI-CE-MS performed under positive and negative ion modes. Nevertheless, overall signal comparability across batches was improved following batch correction as reflected by greater overlap between individual QC samples from batches 1 and 2 in the principal component analysis (PCA) scores plots for the RPAs before and after batch correction (**Figure S5.3C-D**). Therefore, this approach was adopted to reduce the contributions of non-biological experimental variation in the data set. Another aspect that contributes to unwanted variability is the hydration status and/or sweat rate that impact the effective concentration of sweat components.[19] In this case, PQN was explored as a way to correct for underlying sweat dilution variability, using the QCs within each MSI-CE-MS run

as reference samples to calculate the most probable relative dilution for individual sweat specimens. In general, the CF affected (n = 18) and non-affected (n = 50) groups had an overall median RSD of 60-80% independent of data transformation by batch correction or PQN normalization, which indicates large between-subject biological variability that is considerably higher than the experimental/technical variability observed in the QCs (median RSD of 20-24%), as shown in **Table S5.1**. Within group variability was highly metabolite-dependent, ranging from 42 to 258% for CF affected and 33 to 228% for CF non-affected infants, when considering batch-corrected RPAs.

5.4.3 Differential metabolite levels in CF affected and non-affected infants

This study involved a sex-balanced cohort of infants with normal birth weight and gestational age, who were screened-positive for CF following universal NBS in Ontario and referred for a sweat chloride test at two regional hospitals with CF clinics. A summary of the study cohort characteristics is presented in **Table 5.2** for confirmed CF cases with elevated sweat chloride (≥ 60 mM) and two *CFTR* mutations, and screen-positive yet unaffected CF infants with low sweat chloride (< 30 mM), including carriers with a single identified disease-causing *CFTR* mutation or a combination of no mutations identified, but with an IRT above the 99.9th percentile cut-off. Most continuous variables with the exception of birth weight, were considered non-normally distributed (Shapiro-Wilk test, $p < 0.05$), and described in terms of their median and interquartile ranges (IQR). A highly heterogeneous genotype is present in CF affected infants, including mainly homozygote or compound heterozygotes for DF508 and a fewer cases with other less common CF-causing mutations. Additionally, an indication of variable disease phenotypes in CF is reflected by different pancreatic status as measured by fecal elastase, including three cases of pancreatic sufficiency and two of borderline pancreatic disorder, although the majority of CF infants were pancreatic insufficient. In the case of CF unaffected infants, the majority were

Table 5.2. Summary of study cohort characteristics for screen-positive CF infants (≤ 3 months) identified by NSO. Also, IRT (p = 1.03 E-07) and chloride (p = 7.85 E-17) concentrations were the only continuous variables significantly different between the CF and non-CF infants (Mann-Whitney U test, $p < 0.05$).

Variable	Non-CF (*n* = 50)	CF (*n* = 18)
Sex		
Female - no.	25	9
Male - no.	25	9
Age (days) - range (median ± IQR)	11-60 (22 ± 7)	9-95 (18.5 ± 16)
Birth weight (g) - range (mean ± SD)	2232-5310 (3594 ± 540)	2650-4290 (3385 ± 430)
IRT (ng/mL) - range (median ± IQR)	48.3-350.0 (63.2 ± 33.1)	95.0-376.0 (137.8 ± 54.9)
Gestational age (weeks) - range (median ± IQR)	37.0-41.3 (40.0 ± 1.6)	37.3-41.3 (40.0 ± 3.0)
Chloride (mM) - range (median ± IQR)	6-28 (13 ± 7)	60-103 (92 ± 17)
CFTR genotype		
0 mutations	8	-
1 mutation - DF508/null	29	-
1 mutation - non-DF508/null	13	-
2 mutations - DF508/DF508	-	6
2 mutations - DF508/non-DF508	-	8
2 mutations - non-DF508/non-DF508	-	4
Collection site		
McMaster	31	13
Sick Kids	19	5
Pancreatic status (fecal elastase)		
Pancreatic sufficient	50	3
Moderate pancreatic disorder	-	2
Pancreatic insufficient	-	13

carrier of DF508 or other mutations, while only eight infants had no mutation identified from the NBS panel that comprises 39 disease-causing mutations and three variants in the population. Comparison of metabolite levels in sweat samples from CF affected and non-affected infants was performed using nonparametric

univariate statistical analysis due to a large fraction of sweat metabolites (≈ 80%) that deviate significantly from a normal distribution (Shapiro-Wilk test, $p < 0.05$). **Table 5.3** summarizes the most significant metabolites based on batch corrected RPAs, including *p*-values (Mann-Whitney U test), effect sizes (estimated from z-scores), fold-change and false discovery rate (*q*-values). Metabolites considered significant using Bonferroni correction ($p <$ 9.26 E-04) or false discovery rate (FDR, $q < 0.05$) in order to correct for multiple hypothesis testing. The top ranked metabolites obtained for batch corrected data were remarkably consistent with those for non-normalized RPAs (**Table S5.2**) and PQN normalized RPAs (**Table S5.3**), although the levels of significance changed to some extent with the type of data treatment used. For comparison, sweat chloride levels in the CF and non-CF groups were significantly different (p = 7.85 E-07, effect size = 0.76, fold-change = 7.1), performing extremely well in this case, as samples with intermediate chloride levels were not included in this pilot study. Overall, four major differentiating sweat-derived metabolites were found to be statistically significant even when using a conservative Bonferroni adjustment for multiple hypothesis testing, namely pilocarpic acid (PA), asparagine (Asn), mono(2-ethylhexyl)phthalic acid (MEHP) and glutamine (Gln) (**Figure 5.2**), which were confirmed to be independent of sex or hospital collection site (Mann-Whitney U test, $p > 0.05$).

Two unexpected results in this work were the detection of PA, a hydrolysis product from the sweat stimulating drug pilocarpine, and MEHP, a metabolite from the ubiquitous plasticizer bis(2-ethylhexyl) phthalate (DEHP) as among the most significant sweat metabolites differentiating CF status in screen-positive infants. In order to evaluate if these compounds were metabolized *in vivo* or originally present in the gel discs and collection tubes as hydrolysis artifacts, samples of pilocarpine gel disc extracts and blanks for the collection device were analyzed by MSI-CE-MS (**Figure S5.4**). The fraction of pilocarpine hydrolyzed to PA in the gel discs ranged from 0.1 to 1.2% (median = 0.3%) in two new and

Table 5.3. Top significant metabolites when comparing batch corrected RPAs for CF affected and unaffected infants. Correction for multiple hypothesis testing is done by FDR ($q < 0.05$) or Bonferroni adjustment ($p < 9.26$ E-04).

m/z:RMT:mode	Compound ID	*p*-value[b]	Effect size	Fold-change[c]	*q*-value
225.1245:0.777:n	Pilocarpic acid	1.12E-06**	0.55	0.37	6.06E-05*
133.0608:0.912:p	Asparagine	3.88E-05**	0.48	7.18	1.05E-03*
277.1445:0.794:n	MEHP	2.67E-04**	0.43	0.50	4.81E-03*
147.0764:0.930:p	Glutamine	5.44E-04**	0.41	2.16	7.34E-03*
168.0770:0.733:p	Amino acid derivative[a]	1.92E-03	0.37	0.54	2.07E-02*
151.0402:0.755:n	Methylparaben	6.14E-03	0.33	0.57	5.52E-02
188.0929:0.860:n	Unknown	7.19E-03	0.32	0.51	5.55E-02
134.0448:0.973:p	Aspartic acid	1.03E-02	0.31	1.66	6.95E-02
213.0990:0.635:p	Glycylhistidine	1.63E-02	0.29	2.05	9.61E-02
199.0725:0.868:n	Unknown	1.78E-02	0.29	2.04	9.61E-02
163.0719:0.827:p	Glycylserine[a]	3.09E-02	0.26	1.77	1.51E-01
215.0673:0.866:n	Unknown	3.42E-02	0.26	1.72	1.54E-01

[a] *Compound or chemical class tentatively identified*
[b] *Two-tailed exact p values from Mann-Whitney U test*
[c] *Fold-change calculated from median batch-corrected RPAs for CF/non-CF*
***Compounds significantly different after Bonferroni correction (p < 9.26E-04)*
**Compounds significantly different when using FDR (q < 0.05)*

four used gel discs examined, indicating that enzyme-mediated hydrolysis is likely responsible for a major fraction of PA detected in sweat specimens from CF unaffected infants (% PA range = 0.2-11.5%, median = 1.1%, p = 4.47 E-05), although the extent of hydrolysis was similar to the blank extracts for CF infants (% PA range = 0.1-4.5%, median = 0.3%, p = 6.62 E-01). Other compounds detected in the gel disc extracts included methylparaben and propylparaben, which are added by the manufacturer as preservatives. The blanks for the collection device also contained the synthetic blue dye used for sweat volume visualization (FD&C blue dye no. 1), as well as lauric acid and capric acid originated from the plastic tube. However, the concentration of MEHP in the blank (range = 1.35-1.71 µM, median = 1.60 µM in 55 µL) was significantly lower than the levels found in CF unaffected infants (range = 0.8-14.5 µM,

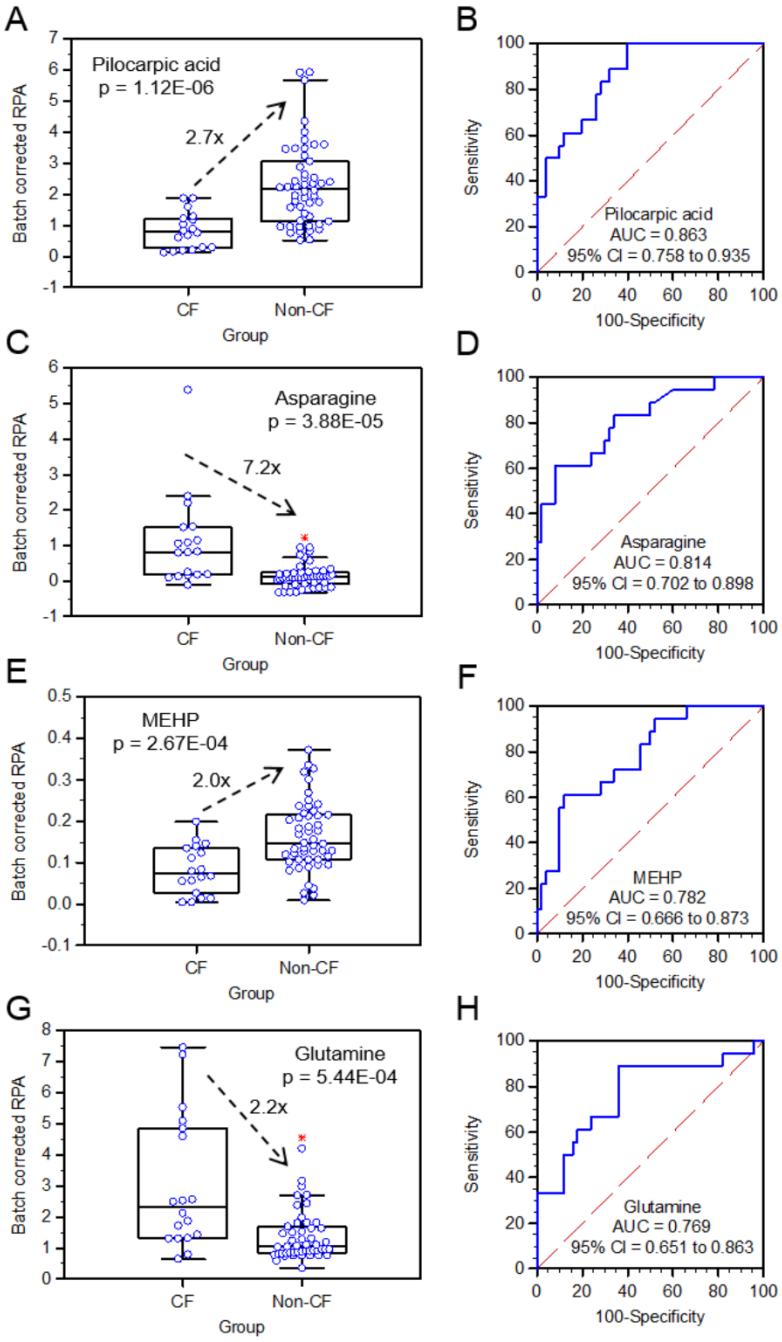

Figure 5.2. Boxplots with scatter plot overlay and ROC curves for differentiating metabolites in affected and non-affected screen-positive CF infants based on batch corrected ion responses based on relative peak areas (RPA) for PA (**A**, **B**), Asn (**C**, **D**), MEHP (**E**, **F**) and Gln (**G**, **H**). ROC curves indicate the area under the curve (AUC) and their 95% confidence interval (95% CI).

median = 4.9 µM, p = 4.91 E-05), although no difference was observed for CF infants (range 0.7-6.6 µM, median = 3.0 µM, p = 8.72 E-02) compared to the blank levels, with 88% of all sweat samples above the concentrations in the blank, which supports that a major contribution of MEHP is derived from infant sweat samples collected following pilocarpine iontophoresis stimulation in CF unaffected cases.

An additional comparison was performed for sweat samples included in the first batch (9 CF and 31 non-CF infants) and second batch (9 CF and 19 non-CF infants) separately. For the first data batch, PA, MEHP and Asn were also found to be significant when using FDR for multiple hypothesis testing correction. In the second batch, only PA and Gln were significantly different between affected and non-affected CF infants, although the same trends observed in the first batch were consistently present in terms of fold-changes for these four metabolites (**Table S5.4**). In this case, the lower significance level measured in the second batch is probably due to the smaller overall sample size. Nevertheless, the consistency of trends in metabolite rankings for highly variable sweat specimens derived from screen-positive CF infants who have quite diverse CFTR genotypes and pancreas function, which were collected from two different pediatric hospitals (McMaster and Sick Kids) and analyzed in different batches over time supports that these differentiating metabolites represent robust markers reflecting CF status that are likely related to CFTR dysfunction, rather than a spurious finding or product of other underlying differences between the CF and non-CF groups.

5.4.4 Differential sweat metabolites with ivacaftor therapy

Untargeted metabolite profiling was also performed on sweat samples repeated at three time points from an individual female CF patient symptomatically diagnosed at 12 years of age who subsequently was initiated with nutritional

Table 5.4. Clinical assessment of a female CF patient with G551D genotype diagnosed symptomatically following therapeutic intervention.

Parameter	**(1) Diagnosis**	**(2) Pre-ivacaftor[a]**	**(3) Ivacaftor[b]**
Dates	11/2015	05/2016	11/2016
Body weight (kg)	29.4	39.5	43.0
Height (m)	1.38	1.43	1.475
BMI (kg/m^2)	15.4	19.3	19.8
FEV_1 (L; %)	0.76; 35	0.71; 34	1.03; 46
FVC (L; %)	1.32; 62	1.36; 58	1.95; 77
Sweat chloride (mM)	100	109	38

[a]*Measurement taken approximately a month before sweat collection (06/2016)*
[b]*Ivacaftor oral dosage of 150 mg twice a day.*

supplementation followed by ivacaftor therapy. Poor lung function and impaired growth were recognized at the time of diagnosis and she was considerably underweight (**Table 5.4**). After seven months of nutritional intervention (*i.e.*, enzyme replacement therapy, high fat diet and fat-soluble vitamin supplementation), major improvement was observed in growth (body weight, height and *BMI*), whereas lung function (FEV_1 and *FVC*) and sweat chloride concentrations remained unchanged near baseline levels measured upon first diagnosis. Subsequent treatment with ivacaftor for three months in combination with on-going nutritional intervention resulted in a considerable enhancement in lung function, with additional improvement in growth and a remarkably lower sweat chloride test (from 109 to 38 mM), which is indicative of drug responsiveness and improved CFTR gating function in a late-diagnosed CF patient with a G551D mutation.

In sweat samples obtained from this older CF patient, 62 polar/ionic sweat metabolites were detected as summarized in **Table 5.3** with the exception of two low abundance anionic metabolites, namely caprylic acid and α-aminoadipic acid. Due to lack of biological replicates for each time point, analytical replicates (n = 4) were used for comparison between the samples using one-way ANOVA.

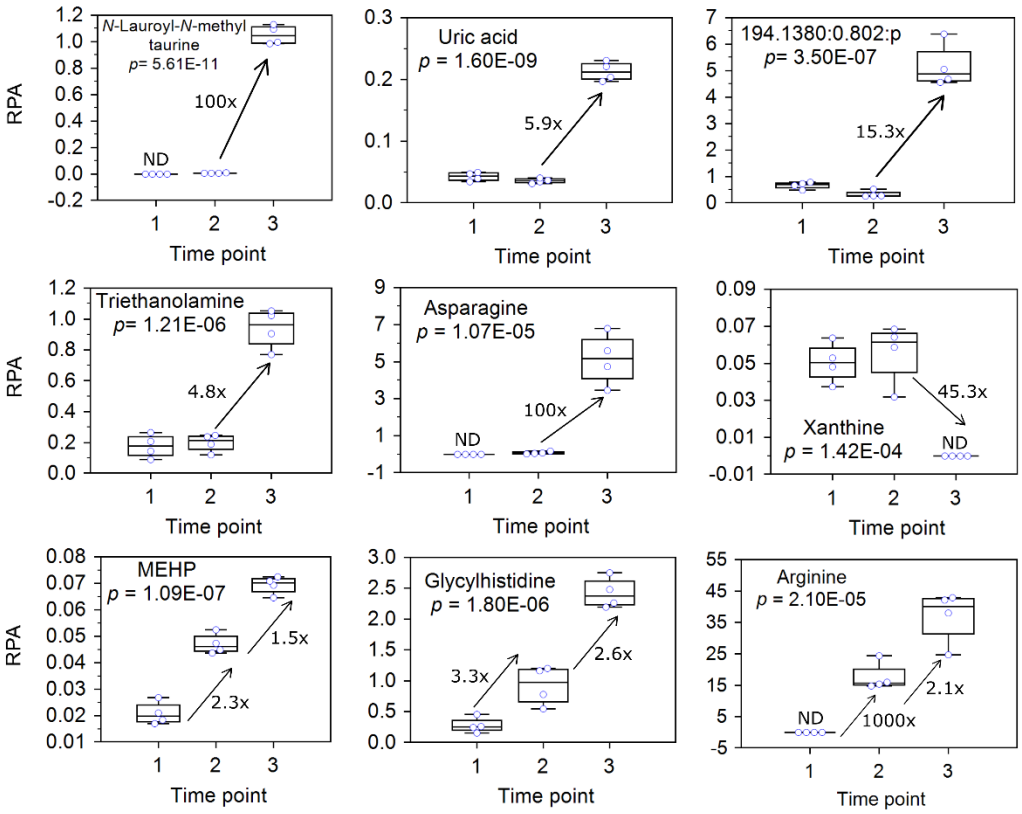

Figure 5.3. Boxplots with scatter plot overlays for differentiating sweat metabolites indicative of drug responsivity from a single CF patient with G551D genotype who had a late symptomatic diagnosis, where time points represent sweat samples collected at baseline (1), then following a 7 month nutritional supplementation regime (2) that is later combined with ivacaftor therapy over 3 months (3), including (**A**) the cosmetic component *N*-lauroyl-*N*-methyltaurine (tentatively identified, level 2), (**B**) uric acid, (**C**) unknown 194.1380:0.802:p, (**D**) triethanolamine (tentatively identified, level 2), (**E**) Asn, (**F**) xanthine, (**G**) MEHP, (**H**) Gly-His, and (**I**) Arg. ND indicates metabolites that were not detected at specific time points. The plots present two-tailed *p*-values obtained from one-way ANOVA and fold-changes based on the mean RPA in each time point. For comparison, chloride had fold-change of 2.9 when comparing points (2) and (3).

Although this approach is not adequate for comparison of non-independent samples, it was selected as a simple way for preliminary group comparison. A total of 27 metabolites were found to be significant for both RPAs and PQN normalized RPAs even when using Bonferroni correction (p < 8.06 E-04). Given the lack of authentic replicates within each time point, some of those metabolites are likely significant due to other underlying variables that affect sweat

composition (*e.g.*, hydration, sweat rate, diet, cosmetic products). In order to minimize false discoveries, a list of top ranked differentiating metabolites was derived for compounds that satisfy a Bonferroni correction, as well as exhibit at least a 2-fold change over time that are measurable in at least two of three repeat sweat specimens, yet are consistently significant when comparing responses in terms of RPAs and PQN normalized RPAs (**Table S5.5**). **Figure 5.3** depicts a series of the most discriminating metabolites reflecting nutritional and/or drug responsitivity. For instance, dramatic changes of up to 100-fold were observed for some metabolites only after ivacaftor treatment (*e.g.*, Asn, uric acid, xanthine, triethanolamine), whereas others were progressively increased with nutritional and subsequent drug intervention, including MEHP, arginine (Arg) and glycylhistidine (Gly-His). However, one of the top metabolites, tentatively identified as the synthetic surfactant, *N*-lauroyl-*N*-methyltaurine, which is likely derived from use of a skin care cosmetic product, was not detected at diagnosis yet had a massive 100-fold increase coincident with ivacaftor therapy, highlights that even the stringent significance criteria adopted here may fail to prevent association with external factors not considered in the study (*e.g.*, cosmetic usage, environmental exposures, diet intake), and thus require further validation in future studies.

5.5 Discussion

Herein, we present the first non-targeted characterization of the sweat metabolome in screen-positive CF infants, along with preliminary results that demonstrate that other differentiating metabolites associated with CFTR dysfunction exist in asymptomatic infants in addition to sweat chloride. Additionally, a panel of sweat metabolites can also potentially serve as markers of treatment responsiveness in older children undergoing treatment with the CFTR potentiator, ivacaftor that are linked to positive clinical outcomes, such as

improved lung function and/or growth. Similar to other metabolomics studies that were performed in sweat samples from adults,[21–26] most of the metabolites identified in sweat from infants were amino acids, organic acids (mono-, di- and tricarboxylic acids, sugar acids and medium-chain fatty acids), amino acids derivatives, dipeptides and purine derivatives, including also xenobiotic compounds derived from sweat collection, diet, cosmetics or environmental exposure. A majority of sweat metabolites rigorous filtered from background/spurious signals after applying a dilution trend filter were conclusively (level 1) or tentatively identified (level 2) as summarized in **Table 5.1** after confirmation with authentic standards and/or matches with mass spectral database libraries (MS/MS). In this case, only a few molecular features (*m/z*:RMT) with an elemental composition were associated with a probable metabolite class (level 3) or were considered as having no known/reported chemical structure (level 4). The latter case often occurred for novel yet low abundance sweat metabolites that generated poor quality MS/MS spectra with low signal-to-noise ratio for product ions. However, these compounds were still extracted in individual sweat samples and included in the comparisons between CF and non-CF infants provided they were detected consistently in a majority (> 75%) of sweat samples. Samples involved in this study were collected from a cohort of age- and sex-balanced infants under three months of age, with no significant differences in gestational age or birth weight. **Table 5.2** highlights that the major characteristics that are different between the two groups of screen-positive CF cases were genotype status, sweat chloride and blood IRT levels as measured by universal NBS from dried blood spot extracts collected shortly after birth. Indeed, there is considerable heterogeneity in CFTR mutation status and pancreatic function even among the CF cases from two pediatric hospital sites in Ontario. For instance, a sub-set of CF infants were considered pancreatic sufficient or had intermediate pancreatic function based on fecal elastase following a high sweat chloride test result (≥ 60 mM). Despite high biological

variability of pilocarpine-stimulated sweat specimens measured within groups (median RSD of 60-80% with individual metabolite variability ranging from 33 to 258% after batch correction) and occurrence of batch effects during data acquisition that were adjusted with use of QC samples, a group of differentiating metabolites were consistently identified in infants, which were largely consistent when comparing ion responses in terms of RPAs, batch-corrected RPAs or PQN normalization.

Surprisingly, two exogenous metabolites, PA and MEHP, were found to be differentially expressed in CF affected and non-affected infants. Indeed, these two exogenous compounds were detected in sweat samples while applying standardized cleaning procedures on forearms with repeated wipes of fresh gauze with de-ionized water and ethanol prior to pilocarpine ionotophoresis. PA is a by-product from the sweat stimulating and muscarinic cholinergic agent pilocarpine, which is formed in the presence of the enzyme human paraoxonase 1 (PON1).[35] Although a small residual fraction of pilocarpine was found to be hydrolysed to pilocarpic acid in new and used (after iontophoresis) pilocarpine gel discs, a far larger fraction of pilocarpic acid was detected only in sweat samples from CF unaffected infants supporting the hypothesis that enzyme-mediated hydrolysis of the lactone moiety of pilocarpine to generate the drug metabolite was likely occurring *in vivo* possibly in the sweat gland following drug delivery via iontophoresis. Similarly, MEHP is a hydrolyzed monoester derived from the plasticizer DEHP, which is used in the production of polyvinyl chloride (PVC) plastics, and is ubiquitously present in food packages, toys, household items, footwear and even medical devices.[36] MEHP has been found in human blood, urine and sweat,[37] as well as in amniotic fluid.[38] In fact, infants have been shown to have the highest total intake of DHEP relative to other age groups with highest exposure for mothers who consume high amounts of meats and dairy products in their diet.[39] Previous studies in older population (≥ 6 years old) have reported urinary MEHP levels of up to 2.6 µM,[40] including evidence that sweat may be a

preferred route of excretion in comparison with urine with a ratio of MEHP concentrations in sweat to urine of about 4.6.[37] In our study, only a small amount of MEHP originated from the plastic sweat collection tube when assessing the collection device blank. However, concentrations found in sweat from CF unaffected infants (0.8-14.5 µM) were significantly higher than in the blank for the majority of samples, which is likely attributed to *in vivo* metabolism of circulating DHEP and its excretion in pilocarpine stimulated sweat. In fact, the enzyme PON1 is a non-specific arylesterase/lactonase associated with xenobiotic detoxification and lipid metabolism[41] that may also be involved in the hydrolysis of DEHP to generate MEHP. Given the observations that both PA and MEHP are depleted in sweat specimens from CF affected infants and both may be metabolized via esterase action, we hypothesize that PON1 expression and/or activity may be impaired in CF. Indeed, recent studies have found that major PON isoforms (*i.e.*, PON1, PON2, PON3) present in serum and airway epithelial cells inhibit *Pseudomonas aeruginosa* infection by hydrolysing their quorum-sensing molecules (*N*-acylhomoserine lactones), which control virulense factors and biofilm formation.[42] Furthermore, Griffin *et al*.[43] reported lower expression of genes for PON2 in brochoalveolar lavage fluid (BALF) in CF patients with *Pseudomonas aeruginosa* infection, which suggests an association between PONs and early lung infection in CF, although their study could not determine whether it was a cause or an effect. In fact, PON was the first reported gene linkage associated with CF along with other polymorphic biochemical markers prior to the discovery of the *CFTR* gene in 1989.[44] Herein, we suggest that impaired PON activity may be present in asymptomatic CF infants early in life prior to the occurrence of lung infections, a hypothesis that will be tested in future studies.

Asn and Gln were other differentiating metabolites in sweat from CF affected compared to non-affected infants – the majority who were carriers with one disease-causing CFTR mutation. To the best of our knowledge, no previous report has described a direct association between these conditionally essential and

physiologically important amino acids and CF. Although lower levels of Gln have been found in circulating neutrophils in CF children compared to non-CF, no alterations were identified in plasma concentrations,[45] and therapeutic interventions involving Gln supplementation in CF patients have generated no clear effect on markers of pulmonary inflamation.[46] In the case of human sweat, metabolite concentrations are dependent on solute partitioning during sweat production, including metabolites that are dependent or independent of sweat rate, actively or passively transported from blood to sweat or even generated within the sweat gland as part of its own metabolism.[47] For example, a good correlation has been reported for glucose in blood and sweat in diabetic patients for sweat samples collected after properly cleaning to avoid glucose diffusion from the skin layer, whereas lactate is mostly produced within the sweat gland and does not necessarily reflect blood lactate, which is used to assess anaerobic conditions in athletes and critically ill patients.[47] Indeed, it is likely that both Gln and Asn in sweat are co-transported by cationic/neutral amino acid transport systems that have been shown to be sodium and chloride dependent in human tissue,[48] in order to maintain amino acid homeostasis given their myriad roles in regulating cell metabolism and function.[49] Thus, disease-causing *CFTR* mutations that disrupt sodium and chloride reuptake in the sweat gland likely also impair transport of the neutral amino acids, Gln and Asn. More insight into the metabolic roles of these metabolites related to altered excretion in CF requires future studies involving paired comparison of sweat and blood/dried blood spots for CF affected and unaffected infants. For example, an earlier study in healthy men has indicated selective amino acid excretion and/or duct reabsorption that is compound-dependent, including Gln levels consistently lower in sweat compared to plasma (mean plasma/sweat fold-change of about 33), and Asn concentrations that were highly variable yet generally higher in sweat (mean sweat/plasma fold-change of about 2.5).[50]

Some sweat metabolites characterized in screen-positive CF infants in this study were also associated to improvements in nutritional status and/or CFTR function as demonstrated in a case study involving a three-time point sweat collection from a teenage CF patient confirmed to have a G551D genotype who qualified for treatment with the CFTR potentiator ivacaftor following an initial period of nutritional supplementation and physiotherapy. This patient was diagnosed symptomatically later in life since neonatal screening for CF was first introduced in the province of Ontario in 2008. Although cases of meconium ileus at birth or family history of known CF may allow for early detection of CF in some cases,[51] delayed diagnosis for affected children is most likely to occur in regions without NBS for CF with a median age of diagnosis of 20.4 months and 9.2 months for children with respiratory symptoms, and combined respiratory and gastrointestinal symptoms, respectively.[52] Growing evidence demonstrates that neonatal screening for CF contributes to better growth and development into late childhood with less lung damage, reduced hospitalization and improved survival as compared to non-screened populations.[3,53,54] As shown in **Table 5.4**, the teenage CF patient was considerably underweight upon initial diagnosis, but was observed to undergo a dramatic improvement in weight and height with a *BMI* change from 15.4 to 19.3 kg/m^2 following 7 months of pancreatic enzyme and fat-soluble vitamin supplementation. However, there was no significant change in lung function, including sweat chloride, until ivacaftor therapy was introduced for 3 months with on-going nutritional intervention. Recent work has demonstrated that there is no correlation between sweat rate and measured chloride concentrations, whereas within-subject biological variations from repeat sweat sampling had a median variability of 8.3% with a reference change value of 36%.[55] Therefore, a change in sweat chloride of -71 mM (65%) observed in this study following ivacaftor treatment is considered a clinically significant response to targeted modulator therapy that increases the gating and conductance of CFTR channels.[56] Importantly, this reduction in sweat chloride was associated with

better lung function with a 12% and 19% improvement in *FEV_1* and *FVC*, respectively that is consistent with previously reported ivacaftor drug trials on CF children with G551D mutation.[57-59] For the first time, we demonstrate that other sweat metabolites show promise as potential biomarkers for treatment monitoring in CF as they exhibit a significant treatment response following ivacaftor therapy and/or nutritional intervention (**Figure 5.4**). Interestingly, one of the top significant metabolites was tentatively identified as *N*-lauroyl-*N*-methyltaurine, a compound present in cosmetic products, which was detected in only one subject from the infant cohort. This compound, likely originated from changes in cosmetic usage over time that coincided with CF treatment intervention and diffused into sweat despite the standardized cleaning procedure before sweat collection, highlights the need for caution when applying non-targeted metabolite profiling. Arg, non-detected in sweat at diagnosis, was significantly increased by nutritional intervention, and further increased after three months under ivacaftor therapy (2.1-fold). This observation is in agreement with previous studies indicating lower plasma arginine levels and increased arginase activity in CF airways,[60] which impairs nitric oxide formation affecting a number of pulmonary physiological processes.[61] In addition, a recent study reported that treatment with ivacaftor increased exhaled nitric oxide in CF patients,[62] which is consistent with an increase in arginine availability. Other metabolites altered with ivacaftor treatment were uric acid (increased) and xanthine (decreased), which constitute end-products of the purine degradation pathway and may be related to greater xanthine oxidase activity. A previous metabolomics study in airway epithelial cells from CF patients has also revealed significant changes in compounds involved in the purine degradation pathway, although uric acid was not measured and xanthine had borderline significance with a trend of lower levels in CF cells.[63]

Asn, also found to be significant in discriminating CF from unaffected screen-positive CF infants, showed an opposite trend in the teenage CF patient with dramatically higher levels (100-fold higher) measured in sweat only after

initiating ivacaftor treatment, which was far more significant than the decrease in sweat chloride as an indicator of drug responsivity. However, PA and Gln did not present clear trends with repeat sweat samples during therapy, with increased levels after nutritional intervention, which subsequently declined with ivacaftor therapy. On the other hand, MEHP increased progressively following both nutritional intervention and ivacaftor therapy, which agrees with the trend observed for infants with higher MEHP levels in sweat for unaffected CF in comparison with CF cases. Certain dipeptides were also found to show a progressive increase in repeat sweat samples following both nutritional supplementation and ivacaftor treatment, such as Gly-His. Growing evidence has shown that dipeptides are not merely by-products of protein turn-over, but also can function as bioactive extra-cellular nutrient signalling compounds in host metabolism,[64] as well as mediators of bacterial cross-talk that control biofilm formation.[65] Triethanolamine is likely an exogenous compound, which is widely used as an additive in food packaging, medicines, cosmetics and other industrial products,[66] although it has also been suggested as a potential plant metabolite.[67]

In summary, the untargeted metabolite profiling study presented here provides the first characterization of polar/ionic compounds derived in the sweat from screen-positive CF infants. A preliminary comparison between sweat samples collected from CF affected and non-affected individuals identified several differentiating metabolites associated with CFTR dysfunction and impaired chloride reuptake, including Asn and Gln. These observations are likely due to altered co-transport of these neutral amino acids that is sodium and chloride dependent within the human eccrine sweat gland comprising the secretory coil and dermal duct that are in contact with various epithelial cell types.[47] Poor reuptake of chloride and sodium has long been associated in the sweat of CF patients when using the Gibson and Cooke technique of pilocarpine iontophoresis.[68] Additionally, we demonstrate a potential association between CF status and sweat levels of PA and MEHP that are largely generated *in vivo*

following sweat stimulation by the cholinergenic agent pilocarpine which binds to muscarinic receptors of the eccrine sweat glands. A putative link between these two xenobiotic metabolites and reduced PON enzymes expression and/or activity in CF infants is inferred in this case, indicating lower PON arylesterase/lactonase activity in the serum of affected CF patients and a greater susceptibility to intoxication, oxidative stress and inflammation with age,[69] including chronic lung disease. Additionally, metabolic changes studied in sweat specimens from a teenage CF patient with a gating mutation G551D undergoing nutritional intervention and then subsequent ivacaftor therapy revealed various sweat metabolites that were altered in association with improved growth and lung function, including Arg, Asn, xanthine, uric acid, and MEHP. Many of these sweat metabolites demonstrated a far greater response change than sweat chloride following nutritional and combined therapeutic intervention that can be routinely measured by targeted MS/MS methods. Although our study had a relatively small sample size especially in the case of CF affected infants (n = 18) , we adopted FDR or Bonferroni correction to reduce false discoveries and carefully filtered redundant or artifact signals from the data matrix prior to statistical analysis. Moreover, results were consistent when using different normalization approaches, which generated a similar ranking of the most significant metabolites associated with affected yet asymptomatic CF infants. Although validation using a hold-out sample set was not possible due to limited number of CF samples from infants, an additional comparison was performed between CF affected and non-affected cases within each analytical batch separately, with consistent trends obtained for the top metabolites (PA, Asn, MEHP and Gln). Future work is planned to evaluate sweat metabolites in a larger cohort, including absolute quantification using external calibration to calculate reference levels for sweat metabolites and cut-off limits for potential CF markers. In summary, this study demonstrates the rich information content derived from the sweat metabolome, which can provide new insights into CF pathophysiology and molecular targets for therapy that

complement sweat chloride testing notably for improved CF diagnosis, disease stratification, and treatment monitoring to ensure safe yet efficacious responses to customized interventions that improve both growth and lung function in children.

5.6 Acknowledgements

P.B.-M. wishes to acknowledge funding support from Cystic Fibrosis Canada and the Natural Sciences and Engineering Research Council of Canada. A.N.M. acknowledges generous support from the Province of Ontario in the form of an Ontario Trillium Scholarship. The authors also wish to acknowledge support from McMaster University and Agilent Technologies and especially Dr. Marcus Kim.

5.7 References

(1) Davis, P. B. *Am. J. Respir. Crit. Care Med.* **2006**, *173*, 475–482.

(2) Farrel, P. M.; Lai, H. J.; Li, Z.; Kosorok, M. R.; Laxova, A.; Green, C. G.; Collins, J.; Hoffman, G.; Laessig, R.; Rock, M. J.; Splaingard, M. L. *J. Pediatr.* **2005**, *147*, S30–S36.

(3) Mak, D. Y.; Stephenson, A. L.; Lands, L. C. *J. Cyst. Fibros.* **2016**, *15*, 302–308.

(4) Ross, L. F. *J. Pediatr.* **2008**, *153*, 308–313.

(5) Grosse, S. D.; Boyle, C. A.; Botkin, J. R.; Comeau, A. M.; Kharrazi, M.; Rosenfield, M.; Wilfond, B. S. *MMWR Recomm. Reports* **2004**, *53*, 1–36.

(6) Grosse, S. D. *Healthcare* **2015**, *3*, 1133–1157.

(7) Comeau, A. M.; Accurso, F. J.; White, T. B.; Campbell, P. W.; Hoffman, G.; Parad, R. B.; Wilfond, B. S.; Rosenfeld, M.; Sontag, M. K.; Massie, J.; Farell, P. M.; O'Sullivan, B. P. *Pediatrics* **2007**, *119*, e495–e518.

(8) Newborn Screening Ontario. *Newborn Screening Ontario Annual Public Report*; 2012.

(9) Mccormick, J.; Green, M. W.; Mehta, G.; Culross, F.; Mehta, A. *Eur. J. Hum. Genet.* **2002**, *10*, 583–590.

(10) Gibson, L. E.; Cooke, R. E. *Pediatrics* **1959**, *23*, 545–549.

(11) Munck, A.; Mayell, S. J.; Winters, V.; Shawcross, A.; Derichs, N.; Parad, R.; Barben, J.; Southern, K. W. *J. Cyst. Fibros.* **2015**, *14*, 706–713.

(12) Mishra, A.; Greaves, R.; Massie, J. *Clin. Biochem. Rev.* **2005**, *26*, 135–153.

(13) De Boeck, K.; Wilschanski, M.; Castellani, C.; Taylor, C.; Cuppens, H.; Dodge, J.; Sinaasappel, M. *Thorax* **2006**, *61*, 627–635.

(14) Rowntree, R. K.; Harris, A. *Ann. Hum. Genet.* **2003**, *67*, 471–485.

(15) Patti, G. J.; Yanes, O.; Siuzdak, G. *Nat. Rev. Mol. Cell Biol.* **2012**, *13*, 263–269.

(16) Muhlebach, M. S.; Clancy, J. P.; Heltshe, S. L.; Ziady, A.; Kelley, T.; Accurso, F.; Pilewski, J.; Mayer-Hamblett, N.; Joseloff, E.; Sagel, S. D. *J. Cyst. Fibros.* **2016**, *15*, 714–723.

(17) Ombrone, D.; Giocaliere, E.; Forni, G.; Malvagia, S.; Marca, G. *Mass Spectrom. Rev.* **2016**, *35*, 71–84.

(18) Quinton, P. M. *Physiology* **2007**, *22*, 212–225.

(19) Mena-Bravo, A.; Luque de Castro, M. D. *J. Pharm. Biomed. Anal.* **2014**, *90*, 139–147.

(20) Sato, K.; Kang, W. H.; Saga, K.; Sato, K. T. *J. Am. Acad. Dermatol.* **1989**, *20*, 537–563.

(21) Harker, M.; Coulson, H.; Fairweather, I.; Taylor, D.; Daykin, C. A. *Metabolomics* **2006**, *2*, 105–112.

(22) Kutyshenko, V. P.; Molchanov, M.; Beskaravayny, P.; Uversky, V. N.; Timchenko, M. A. *PLoS One* **2011**, *6*, e28824.

(23) Calderón-Santiago, M.; Priego-Capote, F.; Jurado-Gámez, B.; Luque de Castro, M. D. *J. Chromatogr. A* **2014**, *1333*, 70–78.

(24) Calderón-Santiago, M.; Priego-Capote, F.; Turck, N.; Robin, X.; Jurado-Gámez, B.; Sanchez, J. C.; Luque De Castro, M. D. *Anal. Bioanal. Chem.* **2015**, *407*, 5381–5392.

(25) Delgado-Povedano, M. M.; Calderón-Santigao, M.; Priego-Capote, F.; Luque de Castro, M. D. *Anal. Chim.* **2016**, *905*, 115–125.

(26) Hooton, K.; Han, W.; Li, L. *Anal. Chem.* **2016**, *88*, 7378–7386.

(27) Kuehnbaum, N. L.; Kormendi, A.; Britz-Mckibbin, P. *Anal. Chem.* **2013**, *85*, 10664–10669.

(28) Allen, F.; Pon, A.; Wilson, M.; Greiner, R.; Wishart, D. *Nucleic Acids Res.* **2014**, *42*, 1–6.

(29) Yamamoto, M.; Ly, R.; Gill, B.; Zhu, Y.; Moran-Mirabal, J.; Britz-McKibbin, P. *Anal. Chem.* **2016**, *88*, 10710–10719.

(30) Wehrens, R.; Hageman, J. A.; van Eeuwijk, F.; Kooke, R.; Flood, P. J.; Wijnker, E.; Keurentjes, J. J. B.; Lommen, A.; van Eekelen, H. D. L. M.; Hall, R. D.; Mumm, R.; de Vos, R. C. H. *Metabolomics* **2016**, *12*, 88.

(31) Dieterle, F.; Ross, A.; Schlotterbeck, G.; Senn, H. *Anal. Chem.* **2006**, *78*, 4281–4290.

(32) Xia, J.; Sinelnikov, I. V.; Han, B.; Wishart, D. S. *Nucleic Acids Res.* **2015**, *43*, W251–W257.

(33) Dunn, W. B.; Erban, A.; Weber, R. J. M.; Creek, D. J.; Brown, M.; Breitling, R.; Hankemeier, T.; Goodacre, R.; Neumann, S.; Kopka, J.; Viant, M. R. *Metabolomics* **2013**, *9*, S44–S66.

(34) Johnson, W. E.; Li, C.; Rabinovic, A. *Biostatistics* **2007**, *8*, 118–127.

(35) Hioki, T.; Fukami, T.; Nakajima, M.; Yokoi, T. *Drug Metab. Dispos.* **2011**, *39*, 1345–1352.

(36) Silva, M. J.; Samandar, E.; Preau Jr., J. L.; Needham, L. L.; Calafat, A. M. *Toxicology* **2006**, *219*, 22–32.

(37) Genuis, S. J.; Beesoon, S.; Lobo, R. A.; Birkholz, D. *Sci. World J.* **2012**, *2012*, 615068.

(38) Silva, M. J.; Reidy, J. A.; Herbert, A. R.; Preau, J. L.; Needham, L. L.; Calafat, A. M. *Bull. Environ. Contam. Toxicol.* **2004**, *72*, 1226–1231.

(39) Serrano, S. E.; Braun, J.; Trasande, L.; Dills, R.; Sathyanarayana, S. *Environ. Heal.* **2014**, *13*, 43.

(40) Colacino, J. A.; Harris, T. R.; Schecter, A. *Environ. Health Perspect.* **2010**, *118*, 998–1003.

(41) Ceron, J. J.; Tecles, F.; Tvarijonaviciute, A. *BMC Vet. Res.* **2014**, *10*, 74.

(42) Stoltz, D. A.; Ozer, E. A.; Zabner, J. In *The paraoxonases: Their role in disease development and xenobiotic metabolism*; Mackness, B., Mackness, M., Aviram, M., Paragh, G., Eds.; Springer: Dorcrecht, Netherlands, 2008; pp 307–319.

(43) Griffin, P. E.; Roddam, L. F.; Belessis, Y. C.; Strachan, R.; Beggs, S.; Jaffe, A.; Cooley, M. A. *PLoS One* **2012**, *7*, e42241.

(44) Tsui, L.-C.; Dorfman, R. *Cold Spring Harb. Perspect. Med.* **2013**, *3*, a009472.

(45) D'Eufemia, P.; Finocchiaro, R.; Celli, M.; Tote, J.; Ferrucci, V.; Zambrano, A.; Troiani, P.; Quattrucci, S. *Pediatr. Res.* **2006**, *59*, 13–16.

(46) Forrester, D. L.; Knox, A. J.; Smyth, A. R.; Barr, H. L.; Simms, R.; Pacey, S. J.; Pavord, I. D.; Honeybourne, D.; Dewar, J.; Clayton, A.; Fogarty, A. W. *Pediatr. Pulmonol.* **2016**, *51*, 253–257.

(47) Sonner, Z.; Wilder, E.; Heikenfeld, J.; Kasting, G.; Beyette, F.; Swaile, D.; Sherman, F.; Joyce, J.; Hagen, J.; Kelley-Loughnane, N.; Naik, R. *Biomicrofluidics* **2015**, *9*, 31301.

(48) Sloan, J. L.; Mager, S. *J. Biol. Chem.* **1999**, *274*, 23740–23745.

(49) Pochini, L.; Scalise, M.; Galluccio, M.; Indiveri, C. *Front. Chem.* **2014**, *2*, 61.

(50) Gitlitz, P. H.; Sunderman, F. W.; Hohnadel, D. C. *Clin. Chem.* **1974**, *20*, 1305–1312.

(51) Farrell, P. M.; Kosorok, M. R.; Rock, M. J.; Laxova, A.; Zeng, L.; Lai, H. C.; Hoffman, G.; Laessig, R. H.; Splaingard, M. L.; The Wisconsin Cystic Fibrosis Neonatal Screening Group. *Pediatrics* **2001**, *107*, 1–13.

(52) Jackson, A.; Foley, L.; Daly, L.; Fitzpatrick, P.; Harrington, M.; Zhou, S.; Kelleher, C. *Ir. Med. J.* **2010**, *103*, 113–116.

(53) Dankert-Roelse, J. E.; Mérelle, M. E. *J. Pediatr.* **2005**, *147*, S15–S20.

(54) Grosse, S. D.; Rosenfeld, M.; Devine, O. J.; Lai, H. J.; Farrell, P. M. *J. Pediatr.* **2006**, *149*, 362–366.

(55) DeMarco, M. L.; Dietzen, D. J.; Brown, S. M. *Clin. Biochem.* **2014**, *48*, 443–447.

(56) Kuk, K.; Taylor-Cousar, J. L. *Ther. Adv. Respir. Dis.* **2015**, *9*, 313–326.

(57) Ramsey, B. W.; Davies, J.; McElvaney, G.; Tullis, E.; Bell, S. C.; Drevínnek, P.; Griese, M.; McKone, E. F.; Wainwright, C. E.; Konstan, M. W.; Moss, R.; Ratjen, F.; Sermet-Gaudelus, I.; Rowe, S. M.; Dong, Q.; Rodriguez, S.; Yen, K.; Ordoñez, C.; Elborn, S.; VX09-770-102 Study Group. *N. Engl. J. Med.* **2011**, *365*, 1663–1672.

(58) De Boeck, K.; Munck, A.; Walker, S.; Faro, A.; Hiatt, P.; Gilmartin, G.; Higgins, M. *J. Cyst. Fibros.* **2014**, *13*, 674–680.

(59) Davies, J. C.; Wainwright, C. E.; Canny, G. J.; Chilvers, M. A.; Howenstine, M. S.; Munck, A.; Mainz, J. G.; Rodriguez, S.; Li, H.; Yen, K.; Ordoñez, C. L.; Ahrens, R. *Am. J. Respir. Crit. Care Med.* **2013**, *187*, 1219–1225.

(60) Grasemann, H.; Schwiertz, R.; Matthiesen, S.; Racké, K.; Ratjen, F. *Am. J. Respir. Crit. Care Med.* **2005**, *172*, 1523–1528.

(61) Grasemann, H.; Schwiertz, R.; Grasemann, C.; Vester, U.; Racké, K.; Ratjen, F. *Respiratory Research*. 2006.

(62) Grasemann, H.; Gonska, T.; Avolio, J.; Klingel, M.; Tullis, E.; Ratjen, F. *J. Cyst. Fibros.* **2015**, *14*, 727–732.

(63) Wetmore, D. R.; Joseloff, E.; Pilewski, J.; Lee, D. P.; Lawton, K. A.; Mitchell, M. W.; Milburn, M. V.; Ryals, J. A.; Guo, L. *J. Biol. Chem.* **2010**, *285*, 30516–30522.

(64) Naka, K.; Jomen, Y.; Ishihara, K.; Kim, J.; Ishimoto, T.; Bae, E.-J.; Mohney, R. P.; Stirdivant, S. M.; Oshima, H.; Oshima, M.; Kim, D.-W.; Nakauchi, H.; Takihara, Y.; Kato, Y.; Ooshima, A.; Kim, S.-J. *Nat. Commun.* **2015**, *6*, 8039.

(65) Abraham, W.-R. *Antibiotics* **2016**, *5*, 3.

(66) Knaak, J. B.; Leung, H.-W.; Stott, W. T.; Busch, J.; Bilsky, J. *Rev. Environ. Contam. Toxicol.* **1997**, *149*, 1–86.

(67) Fiehn, O.; Kopka, J.; Dormann, P.; Altmann, T.; Trethewey, R. N.; Willmitzer, L. *Nat. Biotechnol.* **2000**, *18*, 1157–1161.

(68) Hall, S. K.; Stableforth, D. E.; Green, A. *Ann. Clin. Biochem.* **1990**, *27*, 318–320.

(69) Mehdi, M. M.; Rizvi, S. I. *Arch. Med. Res.* **2012**, *43*, 438–443.

5.8 Supporting Information Section

5.8.1 Instrumentation and sweat analysis by MSI-CE-MS

System control and data acquisition were performed using the Mass Hunter Workstation Software (Data Acquisition, version B.07.01, Agilent Technologies, 2014). The CE separation was carried out using uncoated fused-silica capillaries (Polymicro Technologies, Phoenix, AZ, USA) with 50 µm inner diameter and 120 cm total length. The background electrolyte (BGE) used for cationic metabolites (ESI+) was composed of 1 M formic acid and 15% acetonitrile, pH 1.8 [Kuehnbaum, N. L.; Kormendi, A.; Britz-McKibbin, P. Anal. Chem. 2013, 85,

10664-10669], whereas the BGE for anionic species (ESI-) consisted of 50 mM ammonium bicarbonate, pH 8.5 (adjusted with 10% v/v ammonium hydroxide) [Yamamoto, M.; Ly, R.; Gill, B.; Zhu, Y.; Moran-Mirabal, J.; Britz-Mckibbin, P. *Anal. Chem.* **2016**, 88, 10710-10719.]. New capillaries were conditioned by flushing with methanol, water, 1 M sodium hydroxide, water, and formic acid BGE (15 min each). For negative ion mode, this conditioning was followed by 15 min flush with water and 30 min flush with ammonium bicarbonate BGE. The capillary was flushed with BGE for 15 min before each separation, followed by the MSI injection sequence in which seven samples were hydrodynamically injected (5 s, 50 mbar) and interspaced with BGE (40 s, 50 mbar), ending with BGE (5 s, 50 mbar). All separations were performed using normal polarity with an applied voltage of 30 kV and capillary temperature maintained at 25^{o}C. Pressure-assisted separation was used to speed up the analysis of anionic metabolites under high pH and normal polarity by applying a pressure gradient of 1 mbar/min from 10 to 20 min and 3 mbar/min from 20 to 38 min. A standard mixture, a QC sample and a blank (internal standard solution in water) were analyzed at the beginning of each day in order to equilibrate the CE-MS system before analysis of individual sweat samples and confirm absence of background signals for the metabolites being analyzed. For overnight storage, capillaries were flushed with water for 10 min and air dried for 10 min. As preventative maintenance, the electrode was daily cleaned with 50% v/v isopropanol-water and methanol to avoid carry over. The QTOF system was calibrated every morning before analysis using the Agilent tune mixture for 50-1700 *m/z* range. An Agilent 1260 Infinity series isocratic pump equipped a 100:1 splitter was used to deliver sheath liquid to the CE-MS interface at a flow rate of 10 µL/min. The sheath liquid for positive ion mode consisted of 60% v/v methanol in water with 0.1% v/v formic acid, whereas for negative ion mode it was 50% v/v methanol in water. Purine and HP-0921 (API-TOF Reference Mass Solution Kit, Agilent Technologies) were added to the sheath liquid as reference masses for real-time

automatic mass recalibration. The nebulizer gas pressure was kept at 8 psi, while the flow rate for the drying gas was maintained at 16 L/min (300^{o}C), and the sheath gas flow was kept at 3.5 L/min (199^{o}C). The capillary voltage, nozzle voltage, and fragmentor voltage were 2000, 2000 and 380 V, respectively. The instrument was kept in extended dynamic range (EDR, 2 GHz) for positive ion mode experiments to prevent saturation of highly abundant cationic metabolites, whereas negative ion mode experiments were performed under high resolution (Hi Res 4 GHz) to improve detection of anionic metabolites that in general have lower sensitivity. As preventative maintenance, the ion source was daily wiped with lint-free cloth and 50% v/v isopropanol-water in order to avoid accumulation of less volatile compounds.

5.8.2 Preparation of pooled QC sample

A pooled QC sample (n = 10) was prepared by combining equal aliquots of sweat samples collected from 10 children, including five confirmed CF cases and five CF unaffected individuals (19 days to 6 years old). Those samples were not individually analyzed in this study for exceeding the age criteria (≤ 3 months old) or for lacking clinical information from NBS (*e.g.*, siblings of recently diagnosed CF infant, CF affected children who were born before implementation of NBS for CF). In this case, the QC was not prepared from the actual study samples due to restricted volumes in remaining sweat specimens from infants after chloridometer analysis.

5.8.3 Unknown identification by CE-MS/MS

MS/MS experiments were performed using a single long injection in CE-MS/MS to enhance signal response when detecting fragments for low abundance sweat metabolites, with 90 s injection (50 mbar) for cations prepared in 200 mM ammonium acetate buffer, pH 5.0, and 50 s injection (50 mbar) for anions

prepared in water. Data was acquired using the targeted MS/MS function on Mass Hunter, using the EDR 2 GHz mode and collision-induced dissociation experiments using cycling collision energies of 10, 20 and 40 V. MS/MS spectra were extracted using the Find by Targeted MS/MS function on Mass Hunter, generating a individual spectrum per collision energy, except in the case of very low abundance compounds (not detected by Find by Targeted MS/MS), which were manually extracted as an average fragment spectrum for 10, 20 and 40 V. Agilent Mass Hunter Molecular Structure Correlator was used for assignment of molecular formula candidates, with subsequent identification of candidate molecular structures from ChemSpider and Agilent Metlin Personal Metabolite Database/Library. MS and MS/MS search were also performed using open-source databases (HMDB and Metlin) in combination with *in silico* fragmentation prediction using CFM-ID for putative candidates with consistent electromigration behaviour under the CE conditions used. Additionally, literature search and manual tentative MS/MS annotation based on common neutral losses were performed to identify putative metabolite classes. Compound identities were confirmed by comparing RMTs and MS/MS spectra with authentic chemical standards whenever available.

5.8.4 Pilocarpine gel extracts and blanks for sweat collection device

A small piece of one new and two used gel discs (≈ 0.2 g) was transferred to a 1.5 mL centrifuge tube, sonicated for 10 min with 1 mL of water and centrifuged for 10 min at 14,000 g to separate gel debris. Two aliquots of the supernatant were collected and diluted 20 and 40-fold in water containing the internal standards Cl-Tyr and NMS before analysis by MSI-CE-MS in positive and negative ionization modes. A standard solution of pilocarpine was also extracted as a control, indicating a satisfactory mean recovery of 90% for pilocarpine. A blank for the sweat collection device was prepared to evaluate the presence background components in sweat specimens collected using this system. First, a 55-µL aliquot

of water was inserted in the central opening of the coiled microbore tube and collected in the opposite side of the tube in order to capture compounds potentially originated from the plastic material. Then, another 55-µL aliquot of water was placed in the back of the collection device, over the blue dye spot that is located next to the collection tube opening. In this case, the objective was to evaluate if any compounds identified in the sweat samples was potentially coming from the blue dye. The blanks for the collection tube and blue dye were diluted 4, 8, and 16-fold in water containing the internal standards Cl-Tyr and NMS and analyzed by MSI-CE-MS in positive and negative ionization modes.

Table S5.1. Overall variability within sweat samples from CF affected and non-affected infants, as well as pooled sweat QC samples when considering RPAs, batch correction and PQN normalization for samples analyzed in batches 1 and 2.

Response considered / batch	RSD within groups (%)		
	CF	Non-CF	QC
RPA / batch 1	53	58	8
RPA / batch 2	88	95	20
RPA / batches 1 and 2	76	82	25
Batch corrected RPA / batches 1 and 2	76	68	24
PQN normalized RPA / batches 1 and 2	67	67	-

Table S5.2. Top significant metabolites when comparing RPAs for CF affected and non-affected infants.

m/z:RMT:mode	Compound ID	*p*-value[b]	Effect size	Fold-change[c]	*q*-value
225.1245:0.777:n	Pilocarpic acid	9.33E-07**	0.55	0.36	5.04E-05*
133.0608:0.912:p	Asparagine	5.34E-04**	0.41	3.63	1.44E-02*
188.0929:0.860:n	Unknown	4.01E-03	0.34	0.33	6.39E-02
277.1445:0.794:n	MEHP	4.73E-03	0.34	0.58	6.39E-02
147.0764:0.930:p	Glutamine	1.70E-02	0.29	1.34	1.72E-01
151.0402:0.755:n	Methylparaben	1.91E-02	0.28	0.64	1.72E-01
213.0990:0.635:p	Glycylhistidine	2.37E-02	0.27	1.47	1.83E-01
134.0448:0.973:p	Aspartic acid	3.32E-02	0.26	1.39	2.24E-01
168.0770:0.733:p	Amino acid derivative[a]	4.22E-02	0.25	0.83	2.53E-01

[a]*Compounds tentatively identified*
[b]*Two-tailed exact p-values from Mann-Whitney U test*
[c]*Fold-change calculated from median RPAs for CF/non-CF*
***Compounds significantly different after Bonferroni correction (p < 9.26E-04)*
**Compounds significantly different when using FDR (q < 0.05)*

Table S5.3. Top significant metabolites when comparing PQN normalized RPAs for CF affected and unaffected infants.

m/z:RMT:mode	Compound ID	*p*-value[b]	Effect size	Fold-change[c]	*q*-value
225.1245:0.777:n	Pilocarpic acid	1.92E-06**	0.54	0.24	1.04E-04*
133.0608:0.912:p	Asparagine	1.07E-03	0.39	4.67	2.88E-02*
277.1445:0.794:n	MEHP	1.91E-03	0.37	0.37	3.43E-02*
151.0402:0.755:n	Methylparaben	3.48E-03	0.35	0.68	4.70E-02*
188.0929:0.860:n	Unknown	5.52E-03	0.33	0.22	5.87E-02
151.0262:0.938:n	Xanthine	6.97E-03	0.32	0.53	5.87E-02
168.0770:0.733:p	Amino acid derivative[a]	7.61E-03	0.32	0.63	5.87E-02
147.0764:0.930:p	Glutamine	1.03E-02	0.31	1.48	6.95E-02
329.2333:0.739:n	TriHOME[a]	3.09E-02	0.26	0.81	1.85E-01

[a]*Compounds tentatively identified*
[b]*Two-tailed exact p-values from Mann-Whitney U test*
[c]*Fold-change calculated from median PQN normalized RPAs for CF/non-CF*
***Compounds significantly different after Bonferroni correction (p < 9.26E-04)*
**Compounds significantly different when using FDR (q < 0.05)*

Table S5.4. Statistical analysis for pilocarpic acid, MEHP, asparagine and glutamine in the first and second batches separately.

Compound ID	Parameters	Batch 1	Batch 2
Pilocarpic acid	*p*-value	5.03E-05**	7.25E-03
	Effect size	0.59	0.50
	Fold-change	0.33	0.36
	q-value	2.77E-03*	4.43E-02*
MEHP	*p*-value	1.62E-03	2.31E-01
	Effect size	0.48	0.23
	Fold-change	0.43	0.87
	q-value	3.66E-02*	3.43E-01
Asparagine	*p*-value	1.99E-03	7.55E-02
	Effect size	0.47	0.34
	Fold-change	3.46	6.88
	q-value	3.66E-02*	1.66E-01
Glutamine	*p*-value	9.99E-02	3.46E-03
	Effect size	0.26	0.54
	Fold-change	1.30	6.63
	q-value	3.89E-01	3.36E-02*

[a]*Two-tailed exact p-values from Mann-Whitney U test*
[b]*Fold-change calculated from median RPAs for CF/non-CF*
***Compounds significantly different after Bonferroni correction ($p < 9.26E-04$)*
**Compounds significantly different when using FDR ($q < 0.05$)*

Table S5.5. Top-ranked treatment responsive metabolites for a late-diagnosed CF patient undergoing dietary and subsequent ivacaftor therapy. Time points: (1) diagnosis, (2) pre-ivacaftor, and (3) ivacaftor.

Label	Compound ID	*p*-value[b]	*q*-value	Fold-change			Significant contrasts[c]
				1/2	1/3	2/3	
320.1900:0.779:n	*N*-Lauroyl-*N*-methyltaurine[a]	5.61E-11	1.74E-09	0.05	0.0003	0.01	1-3, 2-3
167.0211:0.962:n	Uric acid	1.60E-09	2.48E-08	1.19	0.20	0.17	1-3, 2-3
194.1380:0.802:p	*Unknown*	3.50E-07	2.17E-06	1.97	0.13	0.07	1-3, 2-3
150.1119:0.763:p	Triethanolamine[a]	1.21E-06	6.27E-06	0.89	0.19	0.21	1-3, 2-3
133.0608:0.912:p	Asparagine	1.07E-05	3.89E-05	0.03	0.0005	0.02	1-3, 2-3
151.0262:0.938:n	Xanthine	1.42E-04	3.66E-04	0.91	41.05	45.33	1-3, 2-3
277.1445:0.794:n	MEHP	1.09E-07	7.48E-07	0.44	0.30	0.68	1-2, 1-3, 2-3
213.0990:0.635:p	Glycylhistidine	1.80E-06	8.58E-06	0.30	0.12	0.38	1-2, 1-3, 2-3
175.1190:0.667:p	Arginine	2.10E-05	5.91E-05	0.001	0.0003	0.48	1-2, 1-3, 2-3

[a] *Compounds tentatively identified based on MS/MS without chemical standard and likely exogenous metabolites from use of personal care products*
[b] *One-way ANOVA used to obtain two-tailed p-values*
[c] *Significant contrasts evaluated using Bonferroni correction*

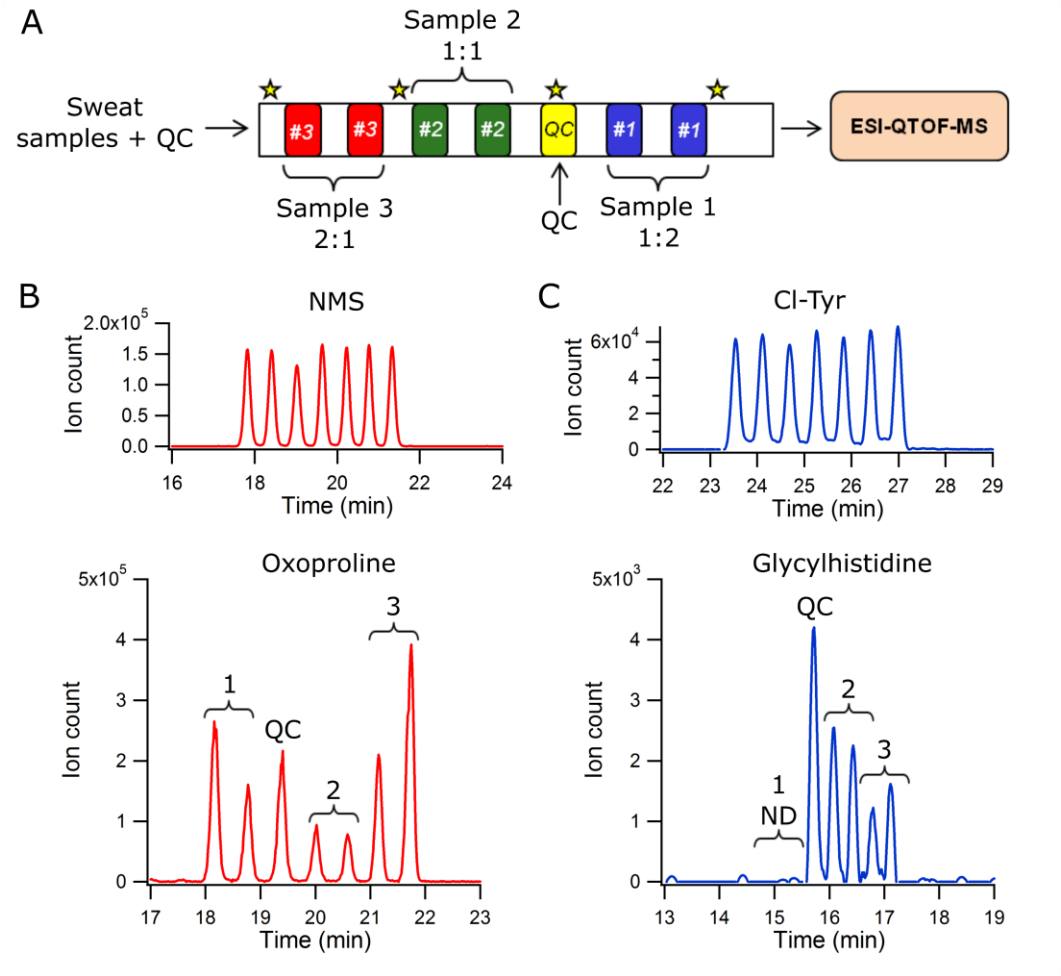

Figure S5.1. (A) Serial injection configuration for temporal signal pattern recognition in MSI-CE-MS for anionic and cationic metabolites, in which three individual sweat samples are prepared in duplicate using different dilution factors and injected in the following sequence: sample #1 (1:2 dilution); sample #2 (1:1 dilution); and sample #3 (2:1 dilution). A pooled QC sample is randomly allocated at position 1, 3, 5 or 7 within each MSI-CE-MS run, as indicated by the stars. In this example, QC was injected in position 3. **(B)** Representative extracted ion electropherogram (EIE) for oxoproline (*m/z* 128.0352, ESI-) showing the peak pattern expected for each sample. **(C)** EIE for glycylhistidine (*m/z* 213.0990, ESI+), where one of the sample pairs (sample #1) was not detected (ND). Ion responses for all sweat metabolites were normalized to an internal standard detected in negative (NMS) and positive (Cl-Tyr) ion mode, which were added to all diluted sweat samples to correct for differences in sample injection volume on-column.

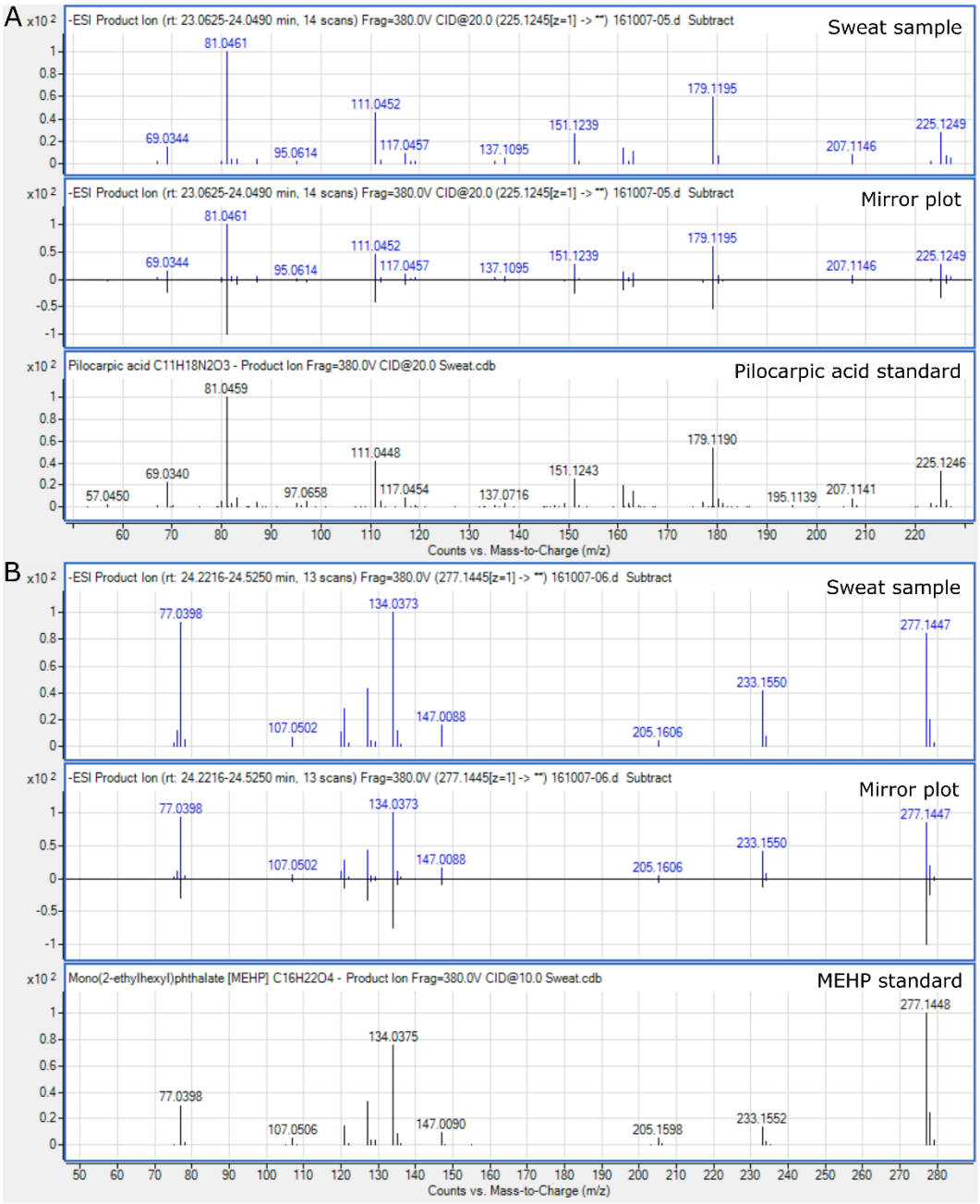

Figure 5S.2. Comparison of MS/MS spectra for (**A**) pilocarpic acid and (**B**) MEHP in sweat samples and authentic standards, with matching scores of 98.25 and 93.33%, respectively.

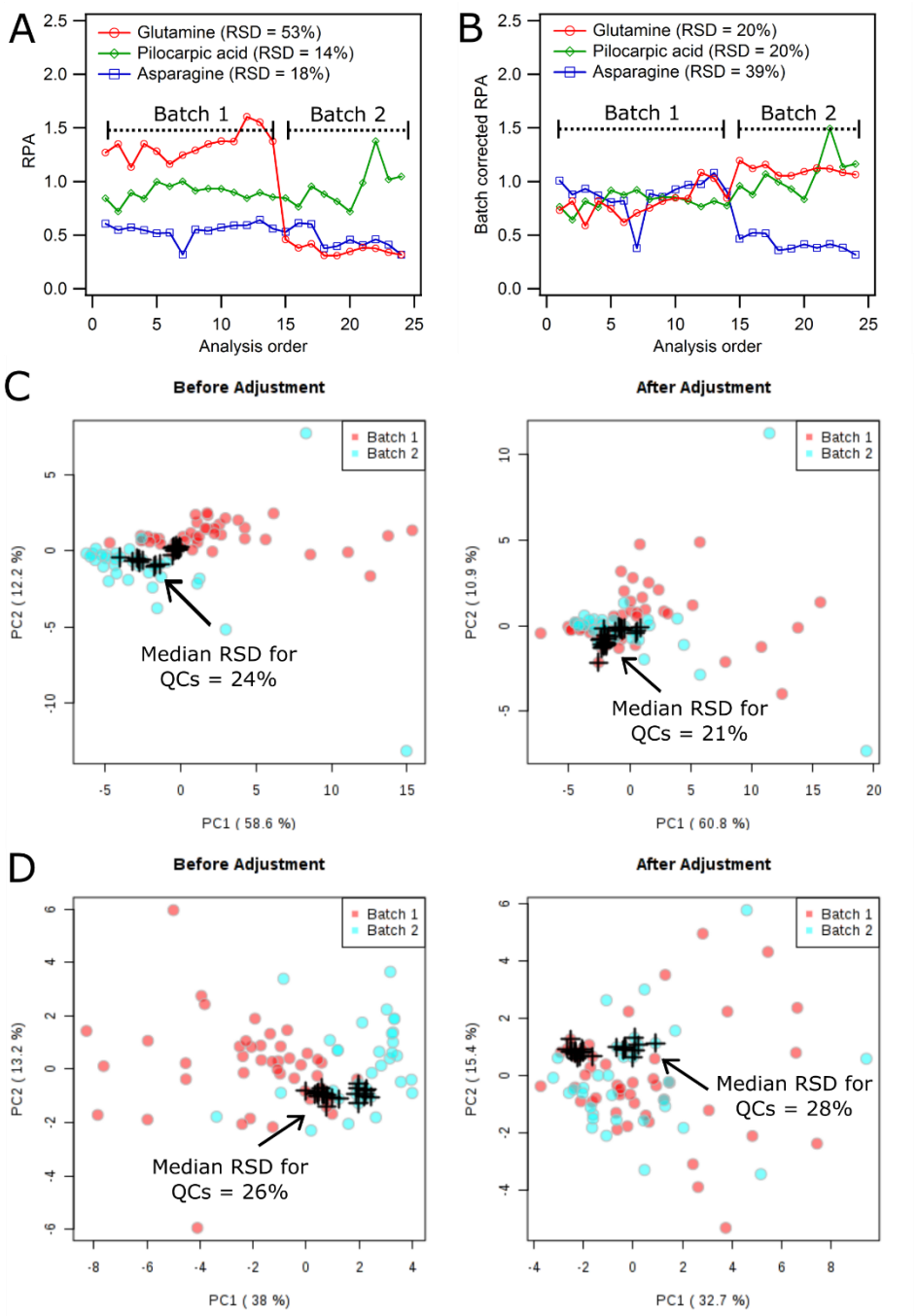

Figure S5.3. QC plots for some example compounds comparing changes in RPAs (**A**) and batch corrected RPAs (**B**). The step-change in RPAs observed for glutamine was corrected by batch effect adjustment. On the other hand, the correction algorithm had a negative impact on some compounds not initially affected by batch effect (*e.g.*, asparagine and pilocarpic acid). PCA plots show overall variability in the responses for anions (**C**) and cations (**D**) before and after batch effect adjustment, respectively.

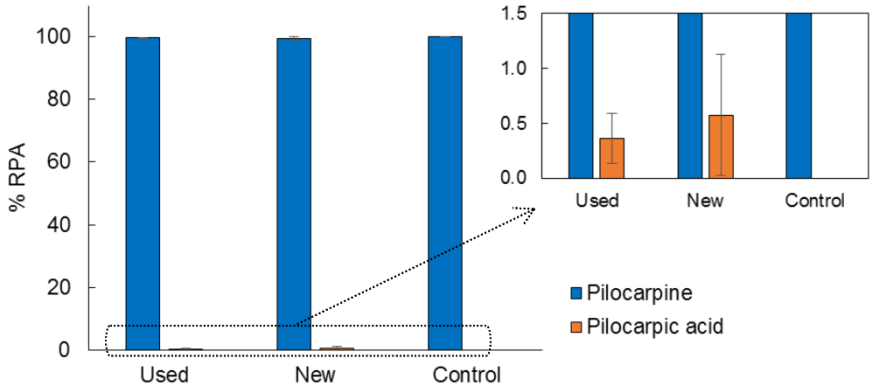

Figure S5.4. Percentage pilocarpine and pilocarpic acid present in new and used gel disc water extracts as compared to a control (pilocarpine solution in water), showing low background fraction of pilocarpic acid (0.1-1.2%).

Chapter VI

Future Directions in Biomarker Discovery and Measurement for Clinical and Epidemiological Applications

Chapter VI: Future Directions in Biomarker Discovery and Measurement for Clinical and Epidemiological Applications

6.1 Overview of major thesis contributions

The work presented in this thesis has contributed two main aspects of biomarker research: (1) providing novel analytical methods for simple and robust routine measurements of targeted inorganic anions in human biofluids with applications in clinical and epidemiological studies; and (2) characterizing the sweat metabolome beyond classical electrolytes in cystic fibrosis (CF) screen-positive infants, which includes a preliminary identification of putative biomarkers associated with CF status and treatment response to nutritional and/or drug therapy. The development of novel analytical methods is crucial to allow reliable measurement of new and well-established biomarkers in support of new advancements in clinical medicine and public health. Methods described in the literature often lack the selectivity and robustness required for routine medical applications in complex biological specimens without interferences, require extensive sample pretreatment prior to analysis, or rely on sophisticated/costly instrumentation that is not amenable to clinical laboratories especially in resource-limited regions. Metabolomics offers a hypothesis-generating approach to identify potential new biomarkers that also provide new insights into disease pathophysiology as related to the complex CF disease spectrum in affected individuals. For example, sweat has provided invaluable information for diagnosis and disease understanding in CF; however, untargeted metabolite profiling in samples from CF screen-positive infants has not been reported in the literature to date. Due to the poor gene-phenotype correlations in CF disease severity that are likely modulated by CF transmembrane conductance regulator (*CFTR*) disease-causing mutations, various gene modifiers, splicing regulation and other unknown environmental factors, metabolomic studies can shed new insight into predicting disease progression and responses to therapy.

Chapter I of this thesis provided an overview of the fundamental roles of biomarkers in medicine, including phases and challenges involved in biomarker discovery. It also discussed the importance of extensive method validation and quality assurance practices for biomarker measurement, required to support decisions in clinical medicine and population health. *Chapter II* introduced a novel assay based on capillary electrophoresis (CE) for strong anion determination in biological fluids that is relevant for clinical applications.[1] In this study, major limitations of currently available methods, which prevent routine analysis of sulfate in most clinical laboratories, were overcome by carefully optimizing a robust and simple CE method with indirect UV detection for selective and rapid quantification of sulfate, sulfite and chloride in urine, plasma and sweat. Additional benefits of the CE assay include interference-free determination of sulfate in presence of excess chloride that requires minimal sample pretreatment while being applicable to volume-restricted biospecimens, such as infant sweat. Rigorous method validation confirmed excellent performance, including assessment of intermediate precision over a 20-day period as required for clinical method validation. A pilot study performed using this CE method indicated lower sulfate levels in single-spot urine samples from kidney stone pediatric patients in comparison to children visiting a nephrology clinic for other disorders. Our results support the hypothesis that sulfate may play a relevant role in kidney stone formation, despite not being an ion comprising stone composition.[2,3] This has potential implications related to current nutritional recommendations and medical treatments[4] that need further investigation in a larger study. Such a study would include analysis of 24 h urine samples together with detailed dietary information on individual patients (*e.g.,* food journal, standardized questionnaire), including their hydration status.

Chapter III described the careful design and validation of a robust analytical method for urinary iodine determination as required for large-scale epidemiological studies.[5] In this case, a novel CE method with direct UV

detection was developed for assessment of iodine nutrition in population-based studies, as an alternative to currently used methods based on inductively coupled plasma-mass spectrometry (ICP-MS) and kinetic spectrophotometric methods, which are prone to interferences, require sample digestion, use toxic reagents or involve high instrumental and operational costs not compatible with many clinical laboratory settings. The CE assay provided adequate sensitivity with high selectivity for sub-micromolar detection and resolution of iodide from over 10^5-fold excess of chloride in human urine. This was achieved by combining sample self-stacking as a simple on-line preconcentration technique with dynamic complexation using α-cyclodextrin (α-CD). However, despite good analytical performance following internal method validation, a significant positive bias was identified when analyzing external reference urine samples. This motivated a subsequent inter-laboratory method comparison for investigating the potential sources of bias in the CE-UV method compared to the gold standard, ICP-MS, which is presented in *Chapter IV*. In this case, the UV-transparent anion and major electrolyte in urine, sulfate was unexpectedly found to be a matrix interference. Sulfate has a similar mobility as iodide that affects the efficacy of sample self-stacking under the CE conditions used in the original method. As a result, an optimized CE method was then further developed and rigorously validated when comparing results acquired by ICP-MS performed independently at two different sites. These sites included the Hamilton General Hospital and the Centers for Disease Control and Prevention (CDC) in support of their worldwide round-robin study Ensuring the Quality of Urinary Iodine Procedures (EQUIP). In this case, it was found that higher α-CD concentrations in the BGE was able to selectively increase the mobility of iodide while completely preventing systematic positive bias due to variable urinary sulfate levels in urine. Therefore, the CE method introduced here represents an affordable and alternative method to support global iodine nutritional monitoring initiatives, which is consistent with the reference method (*i.e.,* ICP-MS) and allows reliable population assessment of

the prevalence of iodine deficiency according to the categories proposed by the World Health Organization (WHO).[6] To the best of our knowledge, this work represents one of first reports to demonstrate the method development, validation and translation of a robust CE assay for large-scale epidemiological studies. This process has required over three years to complete in conjunction with our on-going participation in the EQUIP study.

Chapter V described the non-targeted characterization of polar/ionic compounds derived from sweat samples from screen-positive CF infants following neonatal screening by Newborn Screening Ontario when using multisegment injection-capillary electrophoresis-mass spectrometry (MSI-CE-MS). This work was the first report to characterize the sweat metabolome in CF infants. Prior to this the sweat metabolome had only been characterized in adults in a handful of reports. A pilot study comparing the sweat metabolome in CF affected and unaffected infants (*i.e.*, false positives) identified a panel of differentiating metabolites as related to CF status, including asparagine (Asn), glutamine (Gln), pilocarpic acid (PA) and mono(2-ethylhexyl)phthalic acid (MEHP). Asn and Gln are likely transported by sodium and/or chloride-dependent amino acid transporters that are present in epithelial cells within the sweat gland, although further studies with paired sweat and blood specimens are required to better understand the biological significance of this finding, including the correlation between circulating amino acids in blood from those excreted by the sweat gland following pilocarpine stimulation. Interestingly, PA, a hydrolyzed metabolite from pilocarpine, and MEHP, a hydrolyzed metabolite from the common plasticizer bis(2-ethylhexyl) phthalate (DEHP), were both found to be consistently depleted in sweat in CF affected infants. Although both metabolites are exogenous compounds from drug administration and pre-natal/lifelong environmental exposure, respectively, our work suggests that impaired expression of human paraoxonase (PON) enzymes may be responsible for this unexpected finding. Although never reported in sweat, PONs are non-specific esterases

present in plasma and lung airway epithelial cells that are involved in a number of important biochemical processes, including inhibition of *Pseudomonas aeruginosa* infection, a major cause of pulmonary exacerbation in CF patients.[7] In fact, PON was the first reported gene linkage associated with CF along with other polymorphic biochemical markers prior to the discovery of the CFTR gene in 1989.[8] Further work is needed to better understand the role of PON function in affected CF infants, which may increase their susceptibility to oxidative stress, chronic inflammation and bacterial growth with a reducing capacity for chemical detoxification. *Chapter V* also described metabolic changes in repeated sweat samples collected from a teenage CF patient after nutritional supplementation with subsequent treatment with ivacaftor, which were associated with better growth, improved lung capacity, and a remarkable decrease in sweat chloride levels. Although this study only involved a single teenage patient having a drug-responsive G551D genotype, the results described in this thesis demonstrate that other sweat metabolites can also selectively respond to drug intervention as related to positive clinical outcomes (including Asn and MEHP), which can provide new insights into disease pathophysiology, nutritional status and CFTR function while enabling better treatment monitoring approaches in expanding precision medicine initiatives that complements the classical sweat chloride test.

6.2 Further evaluation of the role of sulfate in kidney stones formation

Although preliminary results reported in *Chapter II* indicated that low intake of sulfate may be related to higher risk of kidney stone formation in a pediatric population, the overall sample size was small (n = 29) and involved only randomly collected single spot urine samples that are susceptible to large variability due to differences in hydration status and diet. In this case, it would be valuable to confirm the findings in a larger patient cohort using 24 h urine samples that allow estimation of sulfate daily excretion. Additionally, in order to provide more insight into the clinical relevance of sulfate, future studies should

involve the measurement of other urinary components as required to calculate supersaturation (*e.g.*, sodium, potassium, citrate, oxalate, etc.), as well as information about dietary protein intake. Although supersaturation is recognized as a vital force for stone formation, questions remain about the real clinical utility of this indicator when applied to disease prognosis, with conflicting results reported in the literature that are likely related to frequent inconsistencies in calculation and terminology (*e.g.*, relative saturation, activity product etc.) derived from different software packages that require a variable number of input variables.[9,10] Therefore, there is a need to further investigate the performance of supersaturation as a risk factor for nephrolithiasis, in which sulfate, a major urinary doubly charged anion, will likely have a great impact. Furthermore, dietary management of kidney stones currently includes the recommendation of restricted protein intake, which still lacks confirmed link with decreased stone recurrence.[11] In this case, future evaluation of urinary sulfate is also important, as a marker of dietary protein intake that reflects ingestion of sulfur-containing amino acids.[12] Therefore, investigation of urinary sulfate in combination with other urinary components relevant for supersaturation, as well as information about dietary protein intake should be performed in a larger cohort with well-characterized description of stone composition in order to improve prognosis and treatment recommendations for kidney stones in children. In fact, comprehensive metabolite profiling of 24 h urine samples that includes known biomarkers of supersaturation offers an exciting approach for better risk assessment and treatment monitoring of pediatric patients suffering from recurrent kidney stones.

6.3 Iodine status determination in Canadian adults

In a upcoming large-scale and multi-centre collaborative initiative, the validated CE-UV method for urinary iodide determination presented in *Chapters III* and *IV* will be used to evaluate iodine nutrition in Canadian participants of the Prospective Urban and Rural Epidemiological (PURE) study.[13] The major

objective of the PURE study is to examine the impact of changes in lifestyle (*e.g.*, physical activity, obesity, smoking, hypertension) on the risk for chronic non-transmissible diseases, such as cardiovascular disease and stroke. In order to assess iodine nutrition in Canadian adults, 800 participants have been randomly selected to have their 24 h urine samples analyzed for iodine, including males and females, 36 to 83 years old, living in four Canadian cities (Hamilton, Ottawa, Vancouver and Quebec). The samples, collected in 2012 and 2013, are accompanied by detailed health and lifestyle information (*e.g.*, chronic diseases, medications, tobacco usage, alcohol consumption), as well as physiological measurements (*i.e.*, body weight, height and blood pressure). In addition, a representative subset of the participants (n = 219) was randomly selected to provide a second 24 h urine sample, which will be used to confirm the consistency of median population iodine levels, despite high day-to-day variability in iodine intake within subjects.[14] This study will provide an estimate of the adequacy of iodine nutrition in Canadians, as well as potential risk factors associated to inadequate iodine levels (deficiency or excess)[15] that can be useful to guide public health policies. For instance, table salt iodization, introduced in the 1920's, has successfully prevented iodine deficiency disorders, including goiter. However, dietary changes over time have resulted in increased consumption of processed foods that are largely derived from non-iodized salt. According to Health Canada, 77% of the salt ingested by Canadians originates from processed food, while only 5% is added during cooking.[16] In this context, table salt iodization is likely no longer effective on a population level, which increases the risk of iodine related disorders and may require new public health policies to adjusting the types of food supplemented with iodine. An anticipated limitation of the PURE study relates to lack of dietary information, which could be useful to investigate main dietary sources of iodine being consumed by the population, although food questionnaires are often unreliable due to self-reporting and recall bias.[17] Additionally, other studies should focus on pregnant/breastfeeding women and

young children, which comprise the most vulnerable population to iodine deficiency.

Future studies in the field of iodine nutrition should also focus on revising the nutritional categories proposed by WHO, which were created based on single spot urinary iodine concentrations in school-age children and simply extended to adults, assuming equivalence.[18] In this case, prevalence of goiter was observed to be < 5% when urinary iodine concentration was > 100 μg/L. Considering that the median urine volume for children is ≈1.0 L/day, it would correspond to a daily excretion of 100 μg/day. Under this assumption, since the median urine volume for adults is ≈1.5 L/day, the corresponding adequate daily excretion would be 150 μg/day.[18,19] As a result of a number of assumptions and approximations, the reliability of the iodine nutrition categories is questionable.[20] However, in the absence of more accurate thresholds, the WHO recommendation is still largely followed. Therefore, future studies to re-evaluate adequate iodine levels in a population are important to avoid over- or underestimation of iodine deficiency. In this case, urinary iodine determination in single spot and 24 h urine samples collected from a large population, including children and adults, would be required in combination with other physiological measurements of thyroid health (*e.g.*, thyroid ultrasound and blood levels of thyroxine).

6.4 Assessment of human paraoxonases in sweat and epithelial tissue

As discussed in *Chapter V*, preliminary results suggest a potential link between CF and human paraononase (PON), which require further confirmation. The first step to verify this hypothesis is to identify the presence of PONs in sweat samples or in the sweat gland, which can be performed by using immunoassays and/or enzyme assays to measure enzyme activity. In this case, the use of freshly collected sweat samples is advisable to decrease the probability of enzyme degradation or unfolding due to freeze-thaw processes and prolonged sample

storage. Alternatively, cell line extracts from skin epithelial tissue can also be used to provide information about enzymes present in cells from the sweat gland that may not necessarily be found in the sweat. Additionally, PON activity in serum samples from affected CF infants can also be compared with non-affected screen-positive cases. Enzyme assays based on CE with UV detection has been recently developed in our group to measure the enzyme activity of *β*-glucocerebrosidase and phenylalanine hydroxylase by simultaneous analysis of a substrate and product.[21] This assay can be adapted in future studies to measure the calcium-dependent activity of PON in volume-restricted biological samples, using, for example, a phenyl ester derivative as substrate, which have been commonly used in other spectrophotometric assays for PONs.[22] Additionally, previously developed immunoassays allow detection and semi-quantification of PONs, including specific antibodies for differentiation of the isoforms PON1, PON2 and PON3. If the presence of PONs is confirmed in sweat samples or epithelial cells, further studies will be required to identify a clear link to the CF dysfunction, with major implications in disease pathophysiology and potential new treatment targets.

6.5 Validation of preliminary findings for CF screen positive infants and response to drug therapy

Future studies to validate the CF-related differential sweat metabolites reported in *Chapter V* are necessary to confirm the findings in a larger and independent cohort, which may require a nation-wide collaboration with other CF centers, as well as a clear protocol for standardized sweat specimen storage and efficient management of patient information. Ideally, sample analysis by MSI-CE-MS should be performed in a single batch, in order to avoid extra data transformation steps to correct for changes in instrumental response over time and allow absolute quantification using external calibration curves acquired as part of the same analytical batch, which will provide metabolite reference ranges in sweat from

infants. In addition, access to paired samples of residual sweat and dried blood spots from newborn screening would provide invaluable information to better interpret the biological significance of differentiating metabolites, including their transport and reuptake during sweat production. Similarly, the exciting pilot study of sweat metabolites reflecting nutritional intervention and importantly drug responsiveness involving a teenage CF patient require confirmation in future studies. In this case, evaluation of a larger cohort may be a difficult task, given that drug treatment is only available for a limited group of patients with G551D mutations who are at least 6 years old.[24] According to Cystic Fibrosis Canada, there are currently 119 CF patient with at least one G551D mutation in the country, including 23 children and 44 adults undergoing ivacaftor therapy.[23] In this case, additional confirmation of preliminary results for a small number of patients can be obtained in future studies by including multiple sample collections before and after treatment, which will give a better estimate of the normal between-day variability. This work can also be applied to evaluate the efficacy of new pharmacological therapies, including ivacaftor (CFTR potentiator) combined with lumacaftor (CFTR corrector), which is under investigation for treatment of CF associated to homozygous DF508 mutations that affect about 45% of all CF patients.[25]

Another major objective in future studies will be the evaluation of screen-positive CF infants with intermediate/borderline sweat chloride levels, classified as CF-screen positive inconclusive diagnosis (CF-SPID).[26] In this case, severity and onset of CF phenotype is very uncertain and may evolve over time or never develop, comprising a spectrum of disorders.[27] For instance, a recent study has reported that about half of the intermediate chloride cases in an Australian pediatric hospital ultimately progressed to a confirmed CF diagnosis.[28] Limited information is currently available to support prognosis or estimate risk of progression to a CF diagnosis,[27] which highlights the need of novel biomarkers to complement the sweat chloride test by providing prognostic information for CF-

SPID patients. In this case, due to delayed diagnosis and onset of symptoms later in life, a longitudinal cohort study is required involving storage of residual sweat and dried-blood spot/plasma samples and periodic monitoring of health outcomes related to disease severity and development (*e.g.*, lung capacity and infections, hospitalizations, pancreatic status, occurrence of CF-related diseases, body height, weight, nasal potential difference, etc.). Important aspects to consider in the study include the number of CF centers to be involved in order to obtain adequate sample size, as well the study duration, which probably should cover most of the childhood (≈ 10 year), when the majority of CF-related symptoms first appear, notably impaired lung function. Anticipated challenges include loss to follow up (*e.g.*, patients who transfer to another CF centre during the study period) and proper implementation of well-defined protocols to ensure consistent sample collection and storage. This study will allow the identification of metabolites associated to the spectrum of phenotypes observed in CF-SPID patients, potentially leading to prognostic/stratifying markers of CF that can overcome one of the main limitations of the sweat chloride test and help clinician to provide better estimates of disease progression and severity.

6.6 General conclusion

In summary, novel CE-based methods have been developed and extensively validated in this thesis to support reliable biomarker measurements for clinical and epidemiological applications, including urinary sulfate that is relevant in the study of kidney stones formation, as well as urinary iodide, utilized to monitor population iodine nutrition in epidemiological studies. Additionally, this thesis presented the first characterization of polar/ionic metabolites in sweat from screen-positive CF infants. Preliminary studies indicated metabolites related to CF status in asymptomatic infants, as well as metabolite changes putatively associated to treatment responsiveness in a teenage CF patient, which constitutes

the first steps towards the identification of potential novel biomarkers for CF diagnosis and treatment monitoring.

6.7 References

(1) Macedo, A. N.; Jiwa, M. I. Y.; Macri, J.; Belostotsky, V.; Hill, S.; Britz-McKibbin, P. *Anal. Chem.* **2013**, *85*, 11112–11120.

(2) van den Born, J. C.; Frenay, A.-R. S.; Bakker, S. J. L.; Pasch, A.; Hillebrands, J.-L.; Lambers Heerspink, H. J.; van Goor, H. *Nitric Oxide* **2016**, *55–56*, 18–24.

(3) van den Berg, E.; Pasch, A.; Westendorp, W. H.; Navis, G.; Brink, E. J.; Gans, R. O. B.; van Goor, H.; Bakker, S. J. L. *J. Am. Soc. Nephrol.* **2014**, *25*, 1303–1312.

(4) Worcester, E. M.; Coe, F. L. *N. Engl. J. Med.* **2010**, *363*, 954–963.

(5) Macedo, A. N.; Teo, K.; Mente, A.; McQueen, M. J.; Zeidler, J.; Poirier, P.; Lear, S. A.; Wielgosz, A.; Britz-McKibbin, P. *Anal. Chem.* **2014**, *86*, 10010–10015.

(6) World Health Organization. *Assessment of iodine deficiency disorders and monitoring their elimination: a guide for programme managers*, 3rd ed.; WHO: Geneva, 2007.

(7) Stoltz, D. A.; Ozer, E. A.; Zabner, J. In *The paraoxonases: Their role in disease development and xenobiotic metabolism*; Mackness, B., Mackness, M., Aviram, M., Paragh, G., Eds.; Springer: Dorcrecht, Netherlands, 2008; pp 307–319.

(8) Tsui, L.-C.; Dorfman, R. *Cold Spring Harb. Perspect. Med.* **2013**, *3*, a009472.

(9) Rodgers, A. L. *BJU Int.* **2014**, *114*, 104–110.

(10) Barbas, C.; García, A.; Saavedra, L.; Muros, M. *J. Chromatogr. B* **2002**, *781*, 433–455.

(11) Sakhaee, K.; Maalouf, N. M.; Sinnott, B. *J. Clin. Endocrinol. Metab.* **2012**, *97* (6), 1847–1860.

(12) Stamler, J.; Elliott, P.; Kesteloot, H.; Nichols, R.; Claeys, G.; Dyer, A. R.; Stamler, R.; Affiliations, A.; Section, N. *Circulation* **1996**, *94*, 1629–1634.

(13) Teo, K.; Chow, C. K.; Vaz, M.; Rangarajan, S.; Yusuf, S. *Am. Heart J.* **2009**, *158*, 1–7.

(14) Rasmussen, L. B.; Ovesen, L.; Christiansen, E. *Eur. J. Clin. Nutr.* **1999**, *53*, 401–407.

(15) Laurberg, P.; Pedersen, I. B.; Knudsen, N.; Ovesen, L.; Andersen, S. *Thyroid* **2001**, *11*, 457–469.

(16) Fischer, P. W. F.; Vigneault, M.; Huang, R.; Arvaniti, K.; Roach, P. *Appl. Physiol. Nutr. Metab.* **2009**, *34*, 884–892.

(17) Kipnis, V.; Midthune, D.; Freedman, L.; Bingham, S.; Day, N. E.; Riboli, E.; Ferrari, P.; Carroll, R. J. *Public Health Nutr.* **2002**, *5*, 915–923.

(18) EFSA Panel on Dietetic Products Nutrition and Allergies. *EFSA J.* **2014**, *12*, 3660.

(19) Laurberg, P.; Andersen, S.; Bjarnadóttir, R. I.; Carlé, A.; Hreidarsson, A.; Knudsen, N.; Ovesen, L.; Pedersen, I.; Rasmussen, L. *Public Health Nutr.* **2007**, *10*, 1547–1552.

(20) Dary, O. *Br. J. Nutr.* **2011**, *106*, 1630–1631.

(21) Shanmuganathan, M.; Britz-Mckibbin, P. *Biochemistry* **2012**, *51*, 7651–7653.

(22) Ceron, J. J.; Tecles, F.; Tvarijonaviciute, A. *BMC Vet. Res.* **2014**, *10*, 74.

(23) Cystic Fibrosis Canada. *The Canadian Cystic Fibrosis Registry 2014 Annual Report*; Toronto (ON), 2016.

(24) Davies, J. C.; Wainwright, C. E.; Canny, G. J.; Chilvers, M. A.; Howenstine, M. S.; Munck, A.; Mainz, J. G.; Rodriguez, S.; Li, H.; Yen, K.; Ordoñez, C. L.; Ahrens, R. *Am. J. Respir. Crit. Care Med.* **2013**, *187*, 1219–1225.

(25) Wainwright, C. E.; Elborn, J. S.; Ramsey, B. W.; Marigowda, G.; Huang, X.; Cipolli, M.; Colombo, C.; Davies, J. C.; De Boeck, K.; Flume, P. A.; Konstan, M. W.; McColley, S. A.; McCoy, K.; McKone, E. F.; Munck, A.; Ratjen, F.; Rowe, S. M.; Waltz, D.; Boyle, M. P. *N. Engl. J. Med.* **2015**, *373*, 220–231.

(26) Munck, A.; Mayell, S. J.; Winters, V.; Shawcross, A.; Derichs, N.; Parad, R.; Barben, J.; Southern, K. W. *J. Cyst. Fibros.* **2015**, *14*, 706–713.

(27) Levy, H.; Farrell, P. M. *J. Pediatr.* **2015**, *166*, 1337–1341.

(28) Groves, T.; Robinson, P.; Wiley, V.; Fitzgerald, D. *J. Pediatr.* **2015**, *166*, 1469–1474.